NORTH-WEST UNIVERSITY
YUNIBESITI YA BOKONE-BOPHIRIMA
NOORDWES-UNIVERSITEIT

Thiocaffeine derivatives as inhibitors of monoamine oxidase

Hermanus Perold Booysen

B. Pharm

Dissertation submitted in partial fulfillment of the requirements for the degree *Magister Scientiae* in Pharmaceutical Chemistry at the North-West University, Potchefstroom Campus

Supervisor: Prof. J.P. Petzer

Co-supervisor: Prof. J.J. Bergh

Potchefstroom

2011

Abstract

Parkinson's disease (PD) is a neurodegenerative disorder which is characterized by selective loss of dopaminergic neurons in the substantia nigra pars compacta (SNpc) of the brain and reduced striatal dopamine (DA). Neuropathologically, PD is characterized by the presence of intraneuronal inclusions called Lewy Bodies (LBs). While the pathogenesis of PD is unknown, it is thought that monoamine oxidase (MAO) may play an important role in the neurodegenerative process. In the basal ganglia DA is oxidized by MAO, a process which is associated with the formation of toxic metabolic by-products. For each mole of DA oxidized by MAO, one mole of hydrogen peroxide and dopaldehyde are formed. Both these products are potentially neurotoxic if not quickly cleared. Inhibitors of MAO reduce the MAO-catalyzed metabolism of DA and as a result, reduce the formation of these toxic by-products. MAO inhibitors are therefore considered useful as a treatment strategy to slow the progression of PD since they may exert a neuroprotective effect in the brain. Since MAO is the principal enzyme for the catabolism of DA in the brain, inhibitors of MAO may conserve the dopamine supply in the brain and therefore exert a symptomatic benefit in PD. MAO inhibitors are frequently combined with L-dopa, the metabolic precursor of DA, in the therapy of PD. MAO inhibitors have been shown to enhance the levels of DA derived from L-dopa, and therefore enhance the therapeutic efficacy of L-dopa.

MAO exists as two isoforms, MAO-A and MAO-B. These enzymes are products of distinct genes and exhibit differing substrate and inhibitor specificities. Both isoforms are present in the brain and utilize DA as substrate. In the brain, the MAO-B isoform exhibits higher activity and density than MAO-A and is therefore considered to play a more important role in DA metabolism than MAO-A. Also MAO-B activity in the brain increases with age while MAO-A activity remains unchanged. In the aged PD brain MAO-B is therefore thought to be the main MAO isozyme responsible for DA catabolism and inhibitors of this enzyme are considered to be useful in the treatment of PD. As mentioned above, MAO-B inhibitors may conserve dopamine in the PD brain and offer a symptomatic effect. MAO-B inhibitors may also protect against further degeneration by reducing potential toxic by-products associated with the oxidative metabolism of DA.

While irreversible inhibitors of MAO-B have been used clinically in the treatment of PD, irreversible inhibition may be associated with certain disadvantages. For example, after terminating treatment with an irreversible MAO inhibitor, recovery of enzyme activity may require several weeks, since the turnover rate for the biosynthesis of MAO in the human brain may be as much as 40 days. In contrast, for reversible inhibitors, following withdrawal of the drug, enzyme activity is recovered quickly upon elimination of the drug from the tissues. This study focuses on the design of new MAO inhibitors that are selective for the MAO-B isoform and which act reversibly with the enzyme.

In this study caffeine served as lead compound for the design of new MAO inhibitors. Although caffeine is a weak MAO-B inhibitor, substitution at the C-8 position with a variety of substituents has been shown to enhance the MAO-B inhibition potency of caffeine to a large degree. In a previous study it was shown that substitution at C-8 of caffeine with alkyloxy substituents yielded particularly potent MAO-B inhibitors with IC_{50} values in the nM range. Based on these promising results, the present study will investigate the possibility that alkylthio substituents at C-8 of caffeine may similarly enhance the MAO-B inhibition potency of caffeine. For this purpose, a series of twelve aryl- and alkylthiocaffeine analogues (**4a**-**l**) were synthesized and evaluated as potential inhibitors of recombinant human MAO-A and ï B. This study was therefore an exploratory study to discover new caffeine derived MAO inhibitors.

Chemistry: The C-8-substituted alkyl- and arylthiocaffeine analogues (**4a-l**) were synthesized by reacting 8-chlorocaffeine with the appropriate alkyl- and arylthiol derivatives in the presence of a base. The structures and purities of the target inhibitors were verified by NMR, MS and HPLC analysis.

MAO inhibition studies: Among the thiocaffeine inhibitors, 8-[4-bromobenzene-methanethiol]caffeine (**4e**) was the most potent MAO-B inhibitor, with an IC_{50} value of 0.16 µM. This inhibitor also exhibited a high degree of selectivity towards MAO-B. The results indicated that extending the length of the C-8 chain of the 8-thiocaffeine analogues yielded MAO-B inhibitors with enhanced inhibition potency. It was also shown that substitution on the phenyl ring of the C-8 substituent with halogens (Cl, Br and F) enhances the MAO-B inhibition potencies. Another potent MAO-B inhibitor was a phenoxyethyl substituted homologue, 8-(2-phenoxyethanethiol)caffeine (**4h**), with an IC_{50} value of 0.332 µM.

Time-dependency and mode of inhibition: This study demonstrates that one selected inhibitor, compound **4e**, does not reduce the catalytic rates of MAO-A and ï B in a time dependent manner. This result shows that the inhibition of MAO-A and ï B is reversible. For the inhibition of MAO-A and ï B by compound **4e**, sets of Lineweaverï Burke plots were constructed. The results showed that the Lineweaver-Burke plots intersected on the y-axis which indicates that this inhibitor is a competitive inhibitor of both MAO-A and ï B and is further proof of the reversible interaction of **4e** with the MAO enzymes.

Future recommendations: Based on the promising MAO-B inhibition potencies of some of the thiocaffeine derivatives, this study recommends that further studies be carried out to optimize the MAO inhibition activities of these compounds. This study specifically recommends that phenylethyl and phenoxyethyl substituted thiocaffeine derivatives, which contain halogens on the phenyl ring, be synthesized and evaluated as MAO inhibitors. Such structures may be particularly potent MAO-B inhibitors.

Conclusions: From the results of this study it may be concluded that thiocaffeine derivatives are promising inhibitors of MAO-A and ï B. These compounds are competitive and reversible inhibitors of MAO.

Opsomming

Parkinson se siekte is 'n neurodegeneratiewe siekte wat gekenmerk word deur die verlies van dopaminergiese neurone in die substantia nigra pars compacta van die brein, met die gevolglike verlies van dopamien (DA) in die striatum. Parkinson se siekte word gekarakteriseer deur intraneuronale komplekse naamlik "Lewy liggame" (LBs). Alhoewel die patogenese steeds onbekend is, speel die ensiem, monoamienoksidase (MAO) moontlik 'n rol in die neurodegeneratiewe proses. In die basale ganglia van die brein word DA geoksideer deur MAO. Hierdie proses word geassosieer met die vorming van toksiese metaboliese neweprodukte. Vir elke mol DA wat deur MAO geoksideer word, word daar een mol waterstofperoksied en dopaldehied gevorm. Albei hierdie neweprodukte is neurotoksies indien dit nie opgeruim word nie. MAO-inhibeerders verlaag die katalitiese afbraak van DA asook die vorming van hierdie neurotoksiese produkte. Om hierdie rede word MAO-inhibeerders gebruik om die verloop van die siekte te vertraag. Hierdie inhibeerders besit ook 'n moontlike neurobeskermde rol in die brein. MAO is hoofsaaklik verantwoordelik vir die afbraak van DA in die brein en daarom kan MAO-inhibeerders die konsentrasie DA in die brein verhoog. Dié verbindings kan dus as simptomatiese behandeling vir Parkinson se siekte aangewend word. MAO-inhibeerders word in kombinasie met L-dopa aan pasiënte toegedien. L-dopa is 'n metaboliese voorloper van DA en word meestal gebruik vir die behandeling van Parkinson se siekte. Daar is bewys dat MAO-inhibeerders DA konsentrasies in die brein kan verhoog. Om dié rede kan MAO inhibeerders dus die terapeutiese effek van L-dopa verbeter.

MAO kom voor as twee verskillende ensieme, MAO-A en MAO-B. Hierdie ensieme is produkte van verskillende gene en het verskillende substraat- en inhibeerderselektiwiteite. Beide ensieme kom in die brein voor en gebruik DA as substraat. Die MAO-B ensiem vertoon hoër aktiwiteit en digtheid in die brein as die MAO-A ensiem. MAO-B speel dus 'n groter rol in die metabolisme van DA in die brein as MAO-A. Die MAO-B aktiwiteit verhoog ook met ouderdom in vergelyking met MAO-A aktiwiteit wat dieselfde bly. MAO-B is dus 'n belangrike ensiem vir die afbraak van DA in bejaarde pasiënte, en MAO-B-inhibeerders word gevolglik gebruik vir die behandeling van Parkinson se siekte. Soos reeds genoem, verhoog MAO-B-inhibeerders DA

konsentrasies in die brein en bied sodoende simptomatiese verligting. Inhibeerders van hierdie ensiem kan ook verdere degenerasie verhoed deur die verlaging van die vorming van toksiese neweprodukte.

Alhoewel onomkeerbare MAO-B-inhibeerders vir die behandeling van Parkinson se siekte gebruik word, hou onomkeerbare inhibeerders sekere nadele in. Dit neem ongeveer 40 dae na behandeling met onomkeerbare inhibeerders, vir MAO-ensiemaktiwiteit om weer na normaal te herstel. Na behandeling met omkeerbare MAO-inhibeerders herstel ensiemaktiwiteit binne ure nadat die inhibeerder uit die weefsel opgeruim is. Hierdie studie fokus dus op die ontwikkeling van selektiewe omkeerbare MAO-B-inhibeerders.

In hierdie studie dien kafeïen as leidraadverbinding. Alhoewel kafeïen 'n swak MAO-B-inhibeerder is, lei substitusie op die C-8 posisie van die kafeïenring tot verhoogde MAO-B-inhiberingspotensie van kafeïen. 'n Vorige studie het getoon dat substitusie met alkieloksiesubstituente op C-8 van kafeïen, verbindings lewer wat potente MAO-B-inhibeerders is met IC_{50} waardes in die nM-gebied. Op grond van hierdie resultate word daar in die huidige studie die moontlikheid ondersoek dat alkieltiosubstituente op C-8 van kafeïen ook kan lei tot óf verhoging van die MAO-B-inhibisiepotensie van kafeïen. Vir hierdie doel is 'n reeks van twaalf ariel- en alkieltiokafeïenanaloë (**4a-l**) gesintetiseer en geëvalueer as moontlike inhibeerders van rekombinante menslike MAO-A en -B. Hierdie studie is 'n verkennende studie met die doel om nuwe kafeïen-afgeleide MAO-remmers te ontdek.

Chemie: Die alkiel- en arieltiokafeïen analoë (**4a-l**) is gesintetiseer deur 8-chlorokafeïen met die toepaslike alkiel- en arieltiolderivate in die teenwoordigheid van 'n basis te reageer. Die strukture en suiwerhede van die teikeninhibeerders is deur KMR, MS en HPLC analise geverifieer.

MAO-inhibisiestudies: Van al die tiokafeïeninhibeerders, is 8-[4-bromobenseen-metaantiol]kafeïen (**4e**) die potentste met 'n IC_{50}-waarde van 0.16 ε M. Hierdie inhibeerder besit ook 'n hoë mate van selektiwiteit vir MAO-B. Die resultate dui aan dat die verlenging van die C-8 syketting van die 8-tiokafeïenanaloog lei tot verbeterde MAO-B-inhibisie. Substitusie met halogene (Cl, Br en F), op die fenielring van die C-8 substituent verhoog ook die MAO-B-inhibisiepotensie. Nog 'n potente MAO-B-inhibeerder is die fenoksietielanaloog, 8-(2-fenoksietaan-tiol)kafeïen (**4h**), met 'n IC_{50} waarde van 0.332 ε M.

Tydsafhanklikheid en meganisme van inhibisie: Hierdie studie toon dat een geselekteerde inhibeerder (**4e**), nie die katalitiese tempo van MAO-A en -B op 'n tydsafhanklike wyse verlaag nie. Hierdie resultaat toon dus dat die inhibisie van MAO-A en B omkeerbaar is. Vir verbinding **4e** is stelle Lineweaver-Burke-grafieke opgestel vir die inhibisie van MAO-A en -B. Die resultate toon dat die Lineweaver-Burke-grafieke op een punt op die y-as sny wat daarop dui dat hierdie inhibeerder 'n kompeterende inhibeerder van MAO-A en -B is. Hierdie resultaat is 'n verdere bewys dat **4e** omkeerbare interaksies met MAO ondergaan.

Aanbevelings: Op grond van die belowende MAO-B-inhibisiepotensies van sommige van die tiokafeïenanaloë, beveel hierdie studie aan dat verdere studies uitgevoer word om hierdie verbindings se MAO-inhibisieaktiwiteite te optimaliseer. Hierdie studie beveel spesifiek aan dat fenieletiel-en fenoksietielgesubstitueerde tiokafeïenanaloë, wat halogene op die fenielring bevat, gesintetiseer en geëvalueer word as MAO-inhibeerders. Sulke strukture kan moontlik potente MAO-B-inhibeerders wees.

Gevolgtrekkings: Uit hierdie studie kan afgelei word dat tiokafeïenanaloë belowende MAO-A en MAO-B inhibeerders is. Hierdie analoë is ook kompeterende en omkeerbare inhibeerders van MAO.

Table of contents

Abbreviations

5-HT	-	Serotonin
6-OHDA	-	6-Hydroxydopamine
AD	-	Alzheimer's disease
ADH	-	Aldehyde dehydrogenase
AOs	-	Amine oxidases
ATP	-	Adenosine-5'-triphosphate
BDNF	-	Brain-derived neurotrophic factor
CNS	-	Central nervous system
COMT	-	Catechol-O-methyl-transferase
COX	-	Cyclooxygenase
CSC	-	(E)-8-(3-Chlrorostyryl)caffeine
DA	-	Dopamine
DDC	-	DOPA decarboxylase
DMDPO	-	Dimethyldecylphosphine oxide
FAD	-	Flavine adenine dinucleotide
GAPDH	-	Glyceraldehyde-3-phosphate dehydrogenase
GDNF	-	Glial-derived neurotrophic factor
GPO	-	Glutathione peroxidase
GSH	-	Glutathione

HNE	-	4-Hydroxy-2-nonenal
JNK	-	c-Jun N-terminal
LBs	-	Lewy Bodies
LDL	-	Low-density lipoprotein
LOX	-	Lipoxygenase
MAO-A	-	Monoamine oxidase A
MAO-B	-	Monoamine oxidase B
$MPDP^+$	-	1-Methyl-4-phenyl-2,3-dihydropyridium
MPP^+	-	1-Methyl-4-phenylpyridinium
MPPP	-	1-Methyl-4-phenyl-4-propionpiperidine
MPTP	-	1-Methyl-4-phenyl-1,2,3,6-tetrahydropyridine
NA	-	Nor-adrenaline
NET	-	Norepinephrine transporters
NGF	-	Nerve growth factor
NSAID	-	Nonsteroidal anti-inflammatory drug
PD	-	Parkisonôs disease
PGE2	-	Prostaglandin E2
PNS	-	Peripheral nervous system
ROS	-	Reactive oxygen species
SET	-	Single electron transfer
SNpc	-	Substantia nigra pars compacta

SSAO	-	Semicarbazide-sensitive amine oxidase
TH	-	Tyrosine hydroxylase
TNFŬ	-	Tumor necrosis factor-Ŭ
TPQ	-	Topa-quinone
UCH-L1	-	Ubiquitin carboxyl-terminal hydrolase L1

Chapter 1

Introduction

1.1 Parkinson's disease

In the early 1800s James Parkinson discovered an unrecognized disorder by studying six patients. Jean Martin Charcot, the father of neurology, proposed that the syndrome should be called *maladie de Parkinson* (Parkinson's disease) (Lees *et al.,* 2009). Parkinson's disease (PD) is a sporadic, neurodegenerative disorder characterized by selective loss of dopaminergic neurons in the substantia nigra pars compacta (SNpc) of the brain and reduced striatal dopamine (DA). A prominent neuropathological feature of PD is the presence of intraneuronal inclusions called Lewy Bodies (LBs) (Przedborski, 2004). An abnormal and aggregated form of the presynaptic protein Ŭ-synuclein is the main component of these LBs (Lees *et al.,* 2009). The clinical manifestations normally encountered with this disease are motor dysfunctions (Lees, 2005). The incidence of this disease rises steeply with age and the disease has a high mortality rate (Lees *et al.,* 2009).

The pathogenesis may occur by at least 3 interrelated mechanisms (Figure 1.1) (Dauer & Przedborski, 2003). The first mechanism proposes that misfolded proteins within the nigrostriatal neurons may aggregate and lead to neurotoxicity by deforming the cell, by interfering with intracellular trafficking and by sequestering proteins that are important for the survival of the neuron (Cumming *et al.,* 1999; Warrick *et al.,* 1999; Cumming *et al.,* 2001; Auluck *et al.,* 2002). The second mechanism proposes that mitochondrial dysfunction within nigrostriatal neurons may lead to the generation of reactive oxygen species (ROS) which in turn leads to neuronal death. The parkinsonian nigrostriatal neuron appears to be a particularly fertile environment for the formation of ROS, since it is reported to contain elevated levels of iron, which is required for the conversion of hydrogen peroxide to the highly reactive and toxic hydroxyl radical. The presence of ROS within the nigrostriatal neuron may in turn lead to the misfolding of proteins. The third mechanism proposes that DA oxidation by monoamine oxidase

(MAO) within the basal ganglia may lead to the formation of toxic products and neurodegeneration (Fernandez & Chen, 2007). For each mole of DA oxidized by MAO, one mole of hydrogen peroxide and dopaldehyde are formed. Both these products are potentially toxic if not quickly cleared. The levels of both aldehyde dehydrogenase (ADH), which metabolises dopaldehyde, and glutathione peroxidise, which metabolises hydrogen peroxide, are reported to be reduced in the basal ganglia of the parkinsonian brain (Yacoubain & Standeart, 2009). MAO therefore plays an important role in the neurodegenerative processes associated with PD and inhibitors of this enzyme have become important drugs for the treatment of this disease.

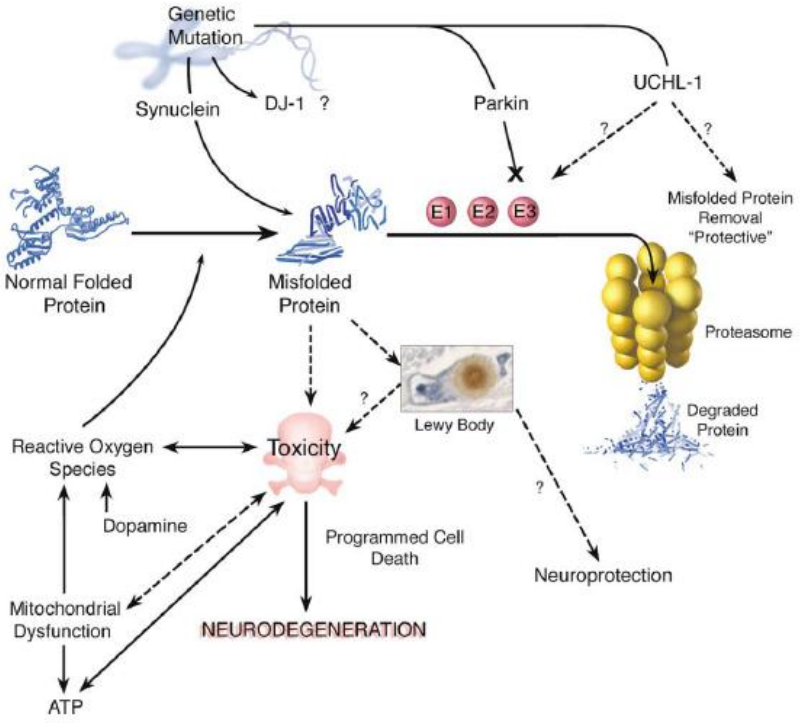

Figure 1.1 Illustration of mechanisms that are implicated in the pathogenesis of PD (Dauer & Przedborski, 2003).

Since MAO inhibitors block DA metabolism and reduce the formation of the toxic by-products, they are considered useful as a treatment strategy to slow the progression of the disease (Burke, 2003). This approach is termed neuroprotection. In the next section MAO will be discussed in more detail. It will be showed that MAO exists as two isoforms in human tissues and that inhibitors of the MAOs are considered useful for the treatment of depression and PD.

Since MAO inhibitors reduce the catabolism of dopamine, they are frequently combined with the dopamime precursor, L-dopa, in the therapy of PD.

1.2 Monoamine oxidase

Monoamine oxidase (MAO) A and B are flavin adenine dinucleotide (FAD) containing enzymes which are tightly anchored to the mitochondrial outer membrane (Binda *et al.,* 2001). Although MAO-A and ï B are encoded by separate genes, they share approximately 70% amino acid sequence identity (Shih *et al.,* 1999). MAO-A preferentially utilizes serotonin and norepinephrine as substrates and is irreversibly inhibited by clorgyline while MAO-B preferentially utilizes benzylamine as substrate and is irreversibly inhibited by (R)-deprenyl. Both isoforms catalyze the oxidative deamination of DA (Youdim *et al.,* 2006). Due to their roles in the metabolism of neurotransmitter amines, inhibitors of MAO-A and ï B have been used in the treatment of neurological disorders. MAO-A inhibitors are used to treat depressive illness (Youdim *et al.,* 2006) while MAO-B inhibitors are useful in the treatment of PD (Fernandez & Chen, 2007). The antidepressant effect of MAO-A inhibitors are dependent on the inhibition of the catabolism of serotonin, norepinephrine and DA in the brain which leads to increased levels of these neurotransmitters. MAO-A inhibitors are particularly effective in the treatment of depression in elderly patients (Youdim *et al.,* 2006). Inhibitors of MAO-B are employed in the treatment of neurodegenerative disorders such as PD. MAO-B appears to be the major DA metabolizing enzyme in the basal ganglia, and inhibitors of this enzyme may conserve the depleted DA stores in the PD brain. This may lead to enhanced dopaminergic neurotransmission and consequently symptomatic relief of PD (Collins *et al.,* 1970). As a consequence, MAO-B inhibitors are employed as adjuvants to L-dopa in the symptomatic treatment of PD (Fernandez & Chen, 2007). MAO-B inhibitors also may exert a neuroprotective effect by reducing the formation of potentially toxic side-products associated with the metabolism of monoamines. These include H_2O_2 and aldehydes that may be neurotoxic if not rapidly metabolized to inactive compounds (Youdim & Bakhle, 2006). Since MAO-B activity as well as density increases in most brain regions with age, MAO-B inhibition may be especially relevant as a treatment strategy in the aged parkinsonian brain (Nicotra *et al.,* 2004).

Based on these observations, this research project will be directed towards the design of new reversible inhibitors of MAO, particularly MAO-B. These inhibitors may find application as both a symptomatic treatment strategy of PD as well as a potential neuroprotective strategy.

1.3 Rationale of this study

In this study caffeine (**1**) served as lead compound for the design of new MAO inhibitors (Figure 1.2). Although caffeine is a weak MAO-B inhibitor, substitution at the C-8 position, with a variety of substituents has been shown to enhance the MAO-B inhibition potency of caffeine to a large degree. For example, substitution with a 3-chlorostyryl substituent at C-8 of caffeine, yields (E)-8-(3-chlorostyryl)caffeine (CSC, **2**) (Figure 1.2) which is a potent MAO-B inhibitor with an IC_{50} value of 146 nM (Pretorius *et al.,* 2008). Also, substitution with a 4-chlorobenzyloxy substituent at C-8 yields 8-(4-chlorobenzyloxy)caffeine (**3d**) (Figure 1.2) which inhibits MAO-B with an IC_{50} value of 65 nM (Strydom *et al.,* 2010). It has been shown that a variety of other benzyloxy substituents also enhance the MAO-B inhibition potency of caffeine. For example, 8-(4-bromobenzyloxy)caffeine (**3e**) (Figure 1.2) inhibits MAO-B with an IC_{50} value of 62 nM (Strydom *et al.,* 2010).

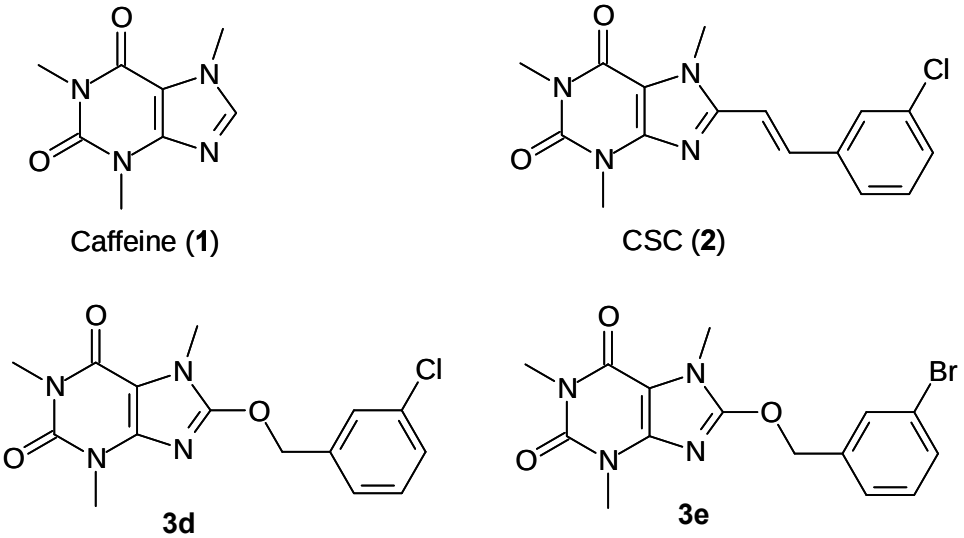

Figure 1.2 The structures of caffeine, CSC, 8-(4-chlorobenzyloxy)caffeine and 8-(4-bromobenzyloxy)caffeine.

In the current study, twelve 8-thiocaffeine analogues (**4a–l**) will be synthesized and evaluated as inhibitors of human MAO-A and ï B. These thiocaffeine derivatives bear close structural resemblance to the 8-oxycaffeine derivatives that were previously shown to be potent MAO inhibitors (Strydom *et al*., 2010) and may therefore have similar biological properties (Table 1.1). This study will determine if C-8 substitution of caffeine with a variety of thiol containing substituents will enhance the MAO-B inhibition activity of caffeine to a similar degree than substitution with an aryl- or alkyloxy substituent (Strydom *et al.,* 2010). Since the 8-oxycaffeines are also reported to be MAO-A inhibitors, the thiocaffeines that will be examined in this study will also be evaluated as inhibitors of MAO-A (Strydom *et al*., 2010).

The structures of the compounds that will be examined in this study are shown in table 1.2. Since this study is an exploratory study, to evaluate the possibility that thiocaffeine derivatives may act as MAO inhibitors, a variety of side chains were selected for substitution at C-8 of the caffeine ring. All side chains will be attached via a thioether linkage at C-8 of the caffeine ring. The side chains selected include phenyl (**4a**), benzyl (**4b**) and phenylethyl (**4c**) substituents. The benzyl substituted thiocaffeines will be further expanded, with the substitution of chlorine (**4d**), bromine (**4e**), fluorine (**4f**) and methoxy (**4g**) on the benzyloxy ring. Also included will be a phenoxyethyl (**4h**) substituent and the saturated cyclohexyl and cyclopentyl rings (**4i** and **4j**). Finaly, two of the thiocaffeines to be examined here, will also contain a naphthalenyl ring (**4k**) and an aliphatic side chain (**4l**).

This study will therefore explore the possibility that 8-thiocaffeine analogues may act as MAO-A and ï B inhibitors. Secondly, the effect of the presence of a thioether functional group at C-8 of the caffeine ring on MAO-A and ï B inhibition activity, will be evaluated. For this purpose the MAO-A and ï B inhibition potencies of the 8-thiocaffeine analogues will be compared to that of the previously studied 8-oxycaffeine analogues (**3a**ï **h**) (Table 1.1). Thirdly this study will examine the effect that a variety of subsituents on C-8 of the caffeine will have on the MAO-A and ï B inhibition potencies of 8-thiocaffeine. The major potential outcomes of this study may be:

1. Identification of new potent reversible 8-thiocaffeine derived MAO-A and ï B inhibitors.

2. The proposal of additional promising 8-thiocaffeine analogues that may be investigated in future studies.

Table 1.1 The structures and IC_{50} values of selected 8-oxycaffeine analogues that were examined as MAO inhibitors in a previous study (Strydom *et al*., 2010).

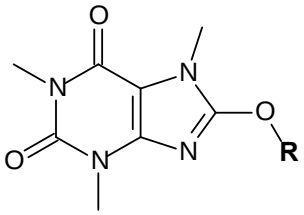

-R		IC_{50} (human) µM		-R		IC_{50} (human) µM	
		MAO-A	**MAO-B**			**MAO-A**	**MAO-B**
3a	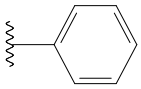	75.19	10.70	**3e**	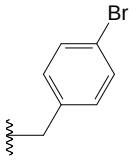	1.304	0.062
3b	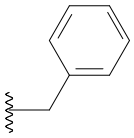	13.755	2.99	**3f**	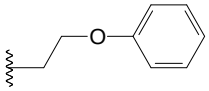	20.35	0.38
3c	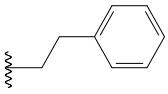	15.925	2.94	**3g**	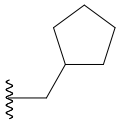	22.81	15.92
3d	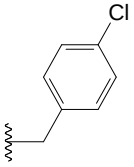	1.337	0.065	**3h**	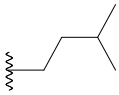	27.34	14.13

Table 1.2 The structures of the 8-thiocaffeine analogues that will be examined in the current study.

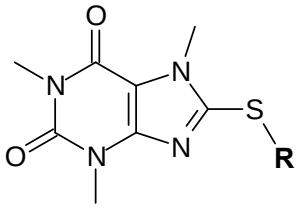

	-R		-R
4a	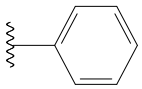	**4g**	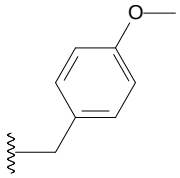
4b	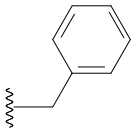	**4h**	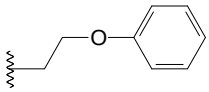
4c	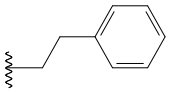	**4i**	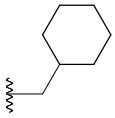
4d	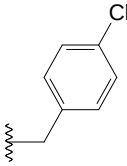	**4j**	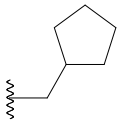
4e	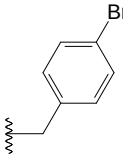	**4k**	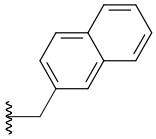
4f	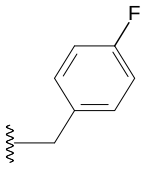	**4l**	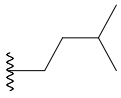

1.4 Objectives of this study

Based on the discussion above the objectives of this study are summarized below:

- Twelve 8-thiocaffeine analogues (**4a–l**) will be synthesized. The starting materials for these syntheses will be 8-chlorocaffeine and a corresponding mercaptan. All the mercaptans required for this study are commercially available. 8-Chlorocaffeine will be synthesized from caffeine and Cl_2 gas.
- The 8-thiocaffeine analogues will be evaluated as inhibitors of MAO-A and ï B. For this purpose the recombinant human enzymes will be used. The inhibition potencies will be expressed as the IC_{50} values (concentration of the inhibitor that produces 50% inhibition). A fluorometric assay will be used to measure the enzyme activities. Certain MAO substrates are oxidized to fluorescent products. For example, kynuramine (which is a substrate for both MAO-A and ï B) is oxidized to 4-hydroxyquinoline (4-HQ). 4-HQ concentrations may be measured with a fluorescence spectrophotometer at an excitation wavelength of 310 nm and an emission wavelength of 400 nm. Fluorescence decreases as the 4-HQ production is decreased by a MAO inhibitor.
- The time-dependency of inhibition of both MAO-A and ï B by selected 8-thiocaffeine analogues will be evaluated. This will be done in order to determine if the inhibitor interacts reversibly or irreversibly with the MAO isozymes. Reversible inhibitors are more desirable than irreversible enzyme inhibitors.
- If the inhibition is found to be reversible, a set of Lineweaver-Burk plots will be generated for selected inhibitors in order to determine if the inhibition mode of the test compound is competitive.

Chapter 2

Literature study

2.1 General background of Parkinson's disease

2.1.1 General background

2.1.1.1 Neurochemical and neuropathological features

PD is primarily the result of the death of dopaminergic neurons in the substantia nigra pars compacta (SNpc) of the brain. This loss of SNpc neurons leads to striatal DA deficiency which is the cause of all major symptoms of PD. DA replacement therapy, through oral administration of levodopa (L-dopa, L-3,4-dihydroxyphenylalanine) (Figure 2.1), can make the symptoms more bearable for the patient. Examples of these symptoms are dyskinesias, tremors at rest, rigidity, slowness or absence of voluntary movement and freezing of gait (Dauer & Przedborski, 2003).

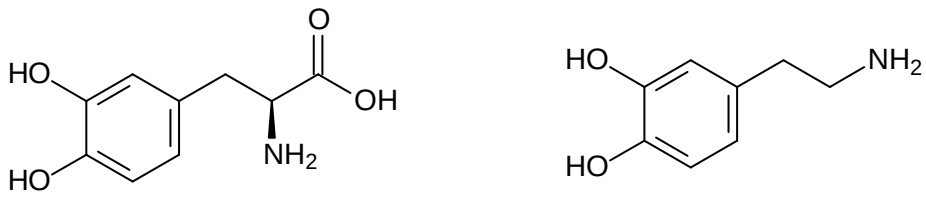

Levodopa Dopamine

Figure 2.1 The chemical structures of L-dopa and dopamine.

The incidence of the disease rises with age, with a mean onset age of 60 years and a duration of the disease from diagnosis of 15 years. Men are 1.5 times more likely than women to develop PD (Twelves *et al.,* 2003).

The principal pathological hallmark of PD is the region-specific selective loss of dopaminergic, neuromelanin-containing neurons from the pars compacta of the substantia nigra (Damier *et al.,*

1999). These neurons exhibit the presence of intraneuronal proteinacious cytoplasmic inclusions termed "Lewy Bodies" (LBs). Terminal loss in the striatum appears to be more distinct than SNpc dopaminergic cell body loss, indicating that the primary target of the degenerative process is the striatal dopaminergic nerve terminals (Bernheimer *et al.,* 1973).

Neurodegeneration and the formation of LBs are also found in noradrenergic, serotonergic and cholinergic systems. Even before the onset of PD symptoms, there may already be damage to other neurochemical systems. This is the reason why some patients develop depression months or years before the onset of PD motor symptoms (Dauer & Przedborski, 2003). A prior hypothesis has also been proposed for the pathogenesis of PD. It is suggested that α-synuclein misfolds or aggregates in one brain region, and triggers other α-synuclein proteins to misfold or aggregate in interconnected neuronal groups. These misfolded proteins are then deposited in the dopaminergic neurons (Hardy, 2005).

2.1.1.2 Aetiology

The cause of sporadic PD is unknown and the environmental toxin hypothesis was dominant for most of the 20th century, because of the discovery of toxin-induced Parkinsonism. The discovery of PD genes has renewed the interest in inherited PD. Both factors may play a role in the aetiology of PD (Dauer & Przedborski, 2003).

Even with the finding that humans, intoxicated with 1-methyl-4-phenyl-1,2,3,6-tetrahydropyridine (MPTP) (Figure 2.2), develop a syndrome nearly identical to PD, there is no convincing data to implicate chronic exposure to a specific toxin in the development of sporadic PD. Another possibility is that an endogenous toxin may be responsible for PD. The normal metabolism of DA leads to the formation of harmful reactive oxygen species (ROS) which may cause PD (Langston *et al.,* 1983). Isoquinoline derivatives, which are derived from DA, have been shown to be toxic to dopaminergic neurons and such derivatives have also been recovered from PD patients (Nagatsu, 1997). This suggests that these derivatives may have been instrumental in causing PD.

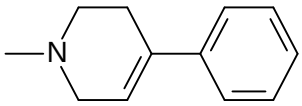

Figure 2.2 The chemical structure of the neurotoxin MPTP.

One of the causes of PD is thought to be gene mutation, especially those leading to mutations of the protein Ŭ-synuclein. LBs contain the Ŭ-synuclein protein, which is essential for the normal function of the nigrostriatal system. Overexpression of human Ŭ-synuclein in nerve cells can lead to an age-dependent loss of dopaminergic neurons (Dauer & Przedborski, 2003). Parkin is another gene of which mutations may lead to PD. This mutated parkin gene was reported in a case of autosomal juvenile Parkinsonism (Kitada *et al*., 1998).

2.1.1.3 Pathogenesis

Although PD is a sporadic disease (Taylor *et al.,* 2005; Dauer & Przedborski, 2003), and its origin is still unknown, a number of environmental causes have been identified. Ageing is thought to be a major risk factor since PD is more prevalent at an advanced age (Taylor *et al.,* 2005). An interesting phenomenon is that non-smokers are twice as likely to develop PD compared to smokers. This has been shown in women, who are not using hormonal replacement therapy as well as in men. A low intake of caffeine has also been correlated to the development of PD (Ascherio *et al.,* 2003). Some reports have also shown that there is a relationship between PD and head injuries, rural living, obesity, minimum exercise and exposure to pesticides or herbicides (Elbaz & Tranchant, 2007). There is further a link between L-dopa responsive parkinsonism and seven genetic mutations that can cause this disease. These mutations are in the proteins, parkin, PINK-1, DJ-1, ATP13A2, Ŭ-synuclein, LRRK-2 and GABA. Parkin mutations are the second most common cause of genetic PD (Healy *et al.,* 2008; Williams *et al.,* 2005).

Dauer & Przedborski (2003) suggested two hypotheses for the pathogenesis of PD. The first proposes that misfolding and aggregation of proteins are instrumental in the death of SNpc dopaminergic neurons and the second proposes that mitochondrial dysfunction, with the consequent oxidative stress and the formation of toxic oxidized DA species, may play a key role in the development of PD. Ŭ-Synuclein, or genetically mutated Ŭ-synuclein misfolds or

aggregates as a result of oxidative damage. This protein may induce cell death by different mechanisms such as deforming the cell or interfering with intracellular trafficking in neurons. Pathogenic mutations may directly induce abnormal protein conformations or may damage the cellûs cellular machinery, which detect and degrade any misfolded proteins (Dauer & Przedborski, 2003).

A prominent neuropathological feature of PD is intraneuronal inclusions, LBs, in the nigral dopaminergic neurons. LBs are composed of a variety of proteins, such as Ŭ-synuclein, parkin, ubiquitin and neurofilaments. They are spherical, eosinophilic, cytoplasmic aggregates (Przedborski, 2004). As already mentioned, an abnormal and aggregated form of Ŭ-synuclein is the main component of LBs (Scherfler *et al.,* 2006). Oxidative modified Ŭ-synuclein exhibits a greater propensity to aggregate *in vitro* than unmodified Ŭ-synuclein (Giasson *et al.,* 2000). Controversy exists about whether LBs promote toxicity or protect the cell from the harmful effects of misfolded proteins (Dauer & Przedborski, 2003).

Over the past few decades a large amount of data has been obtained from clinical studies and *in vitro* and *in vivo* experimental models of PD. Available data suggests that the mechanism of neuronal death in PD begins with a healthy dopaminergic neuron being affected by an etiological factor, for example, mutant Ŭ-synuclein. This neuron will eventually be degenerated as a result of deleterious factors, such as free radicals, mitochondrial dysfunction, excitotoxicity, neuroinflammation and apoptosis that will eventually lead to its death (Lees *et al.,* 2009).

Another cause of a PD syndrome is the parkinsonian inducing neurotoxin, MPTP, which was discovered in the early 1980s (Burns *et al.,* 1985). After systemic administration of MPTP to mice, its active metabolite, 1-methyl-4-phenylpyridinium (MPP^+) (Figure 2.3), is concentrated in the mitochondrial matrix. Here it binds to complex I, which is part of the electron transport chain, of the mitochondria. MPP^+ blocks the flow of electrons along the electron transport chain which leads to an increased production of ROS. This is also associated with a reduction of adenosine-5'-triphosphate (ATP) production (Przedborski *et al.,* 2004). Other parkinsonian inducing toxins are 6-hydroxydopamine (6-OHDA), paraquat and rotenone which may lead to PD via distinctive mechanisms (Dauer & Przedborski, 2003).

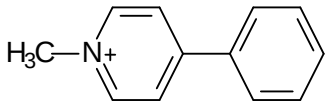

Figure 2.3 The chemical structure of MPTP's active metabolite, MPP^+.

2.1.2 Symptomatic treatment

As mentioned, PD is a neurodegenerative disorder characterized by a loss of dopaminergic neurons in the SNpc region of the brain and a reduction of striatal DA. Clinical manifestations include tremor, slowness of movement, increased muscle tone and postural instability. Most of the drugs used to manage the motor symptoms and other complications are based on restoring striatal DA. This can be done either by increasing the supply of DA or by administering DA agonist drugs (Le & Jankovic, 2001).

2.1.2.1 L-dopa & DOPA decarboxylase inhibitors

PD is still an incurable progressive disease. L-dopa remains the most effective agent for the symptomatic treatment of PD and is usually co-administered with a peripheral decarboxylase inhibitor (such as benserazide or carbidopa) (Figure 2.4), and should be the initial treatment option at any age (Fahn *et al.,* 2004). However, L-dopa does not ameliorate non-motor symptoms, such as dementia. L-dopa is also associated with the long-term development of motor complications, such as dyskinesia and motor fluctuations, which may become more severe as the disease progresses. Also, increased L-dopa dosages are required to maintain the therapeutic effect as the disease progresses (Olanow *et al.,* 2001). As previously stated, L-dopa is administered together with a peripheral decarboxylase inhibitor. These inhibitors inhibit the peripheral decarboxylation of L-dopa and allows for larger amounts of L-dopa to cross the blood-brain barrier into the brain, which results in enhanced DA concentrations in the brain (Fahn *et al.,* 2004).

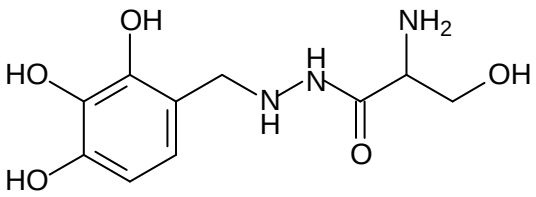

Benserazide

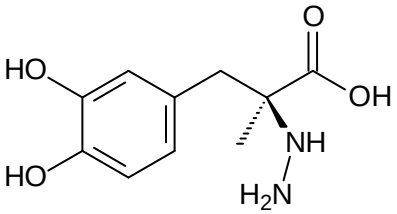

Carbidopa

Figure 2.4 The chemical structures of the two decarboxylase inhibitors, which inhibit the decarboxylation of L-dopa.

2.1.2.2 Dopamine agonists

DA agonists are used in the treatment of PD and act on DA D_2-receptors. Postsynaptic D_2 receptor stimulation is linked to antiparkinsonian activity, while presynaptic D_2 stimulation has been claimed to lead to neuroprotective effects. DA agonists stimulate DA receptors directly. These DA agonists do not require carrier-mediated transport for absorption into the brain, nor do they produce potentially toxic metabolites and free radicals (Deleu *et al.,* 2004). DA agonists provide effective relief of parkinsonian symptoms, either as first-line therapy in early PD, or as an adjunct to L-dopa. DA agonists are less potent than L-dopa, do not target all the PD domains and have significant adverse effects such as nausea and neuropsychiatric effects (Olanow *et al.,* 2001). DA agonists may be divided into ergoline (with an ergot-like structure) and norergoline agonists. Common examples of ergoline agonists are bromocriptine, cabergoline, lisuride and peribedil. Cabergoline, ropinirole and pramipexole (Figure 2.5) have established efficiency for reducing the development of the motor complications in PD and all of these medications have reasonable safety profiles. A recent study showed that the nonergoline DA agonist, rotigotine, was effective and well tolerated when administered to patients via a transdermal patch for 7 months. To extend its efficiency and to decrease motor complications, L-dopa may be augmented with a DA agonist or a catechol-O-methyl-transferase (COMT) inhibitor (Olanow *et al.,* 2001).

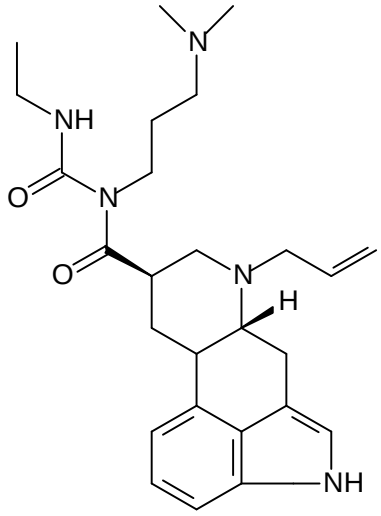

Cabergoline

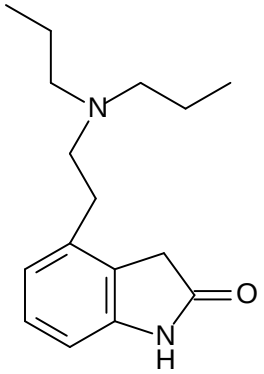

Ropinirole

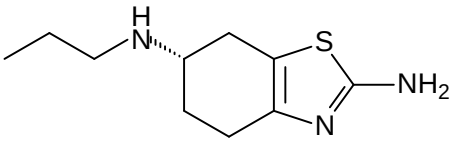

Pramipexole

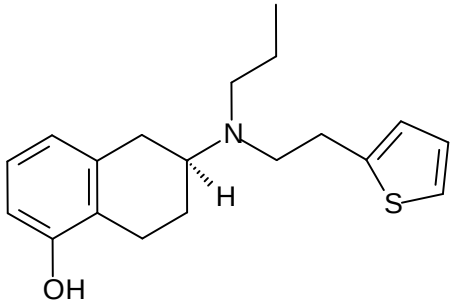

Rotigotine

Figure 2.5 The chemical structures of clinically used DA agonists.

2.1.2.3 Monoamine oxidase B Inhibitors

A crucial discovery in the late 1960s was that of the existence of monoamine oxidase (MAO). It is not a single enzyme but exists in at least two forms that are of great pharmacological significance (Youdim & Bahkle, 2006). Type A MAO is inhibited by clorgyline and metabolizes noradrenaline (NA) and serotonin (5-HT), whereas type B MAO is resistant to clorgyline inhibition and prefers benzylamine as substrate (Johnston, 1968). Tyramine and DA are equally well metabolized by both forms of the enzyme (Youdim *et al.,* 2006). Another important finding was that the isoforms are differently distributed in the mammalian brain and that, in the basal ganglia, MAO-B activity predominates (Collins *et al.,* 1970). MAO-B is involved in the

metabolism of DA to ultimately yield 3,4-dihydroxyphenylacetic acid and homovanillic acid. MAO-B also deaminates ɓ-phenylethylamine, an endogenous amine that stimulates DA release and inhibits neuronal DA uptake (Saura *et al.,* 1990). The development of selective MAO-B inhibitors has made it possible to block only the B isoform of the enzyme, for which DA is the preferred substrate. By inactivating this enzyme, selective MAO-B inhibitors increase the concentrations of both endogenous DA and DA produced from exogenously administered L-dopa (Yamada & Yasuhara, 2004). Progressive deterioration of the dopaminergic neurons in the SNpc results in a depletion of DA along the nigrostriatal pathway. The primary rationale for using selective MAO-B inhibition in PD is that it enhances striatal dopaminergic activity by inhibiting the metabolism of DA, thereby improving PD motor symptoms (Samii *et al.,* 2004).

2.1.2.4 Anti-cholinergic drugs

The anti-cholinergic drugs used in PD are all specific for muscarinic receptors. They are believed to act by correcting the disequilibria between striatal DA and acetylcholine activity. The most commonly used anti-cholinergic drugs in PD are benzhexol, benztropine, orphenadrine and procyclidine (Figure 2.6).

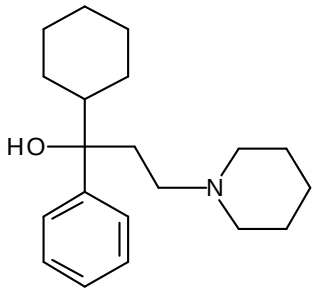

Benzhexol

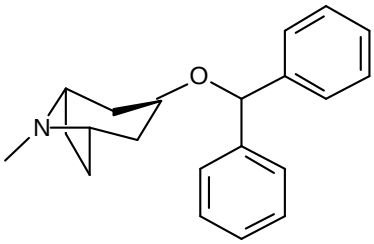

Benztropine

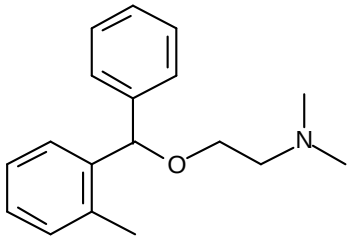

Orphenadrine

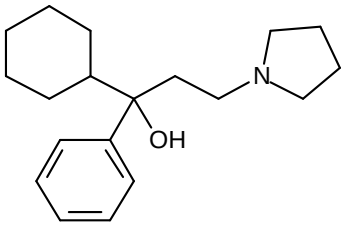

Procyclidine

Figure 2.6 The chemical structures of the most common anti-cholinergic drugs used in PD.

An important factor, limiting the use of these drugs, is the occurrence of anti-cholinergic adverse effects such as impaired neuropsychiatric and cognitive function. Anti-cholinergic drugs have to be used with the utmost caution in these patient groups. These drugs offer mild symptomatic control in PD when used as monotherapy or in combination with other agents. They have been used particularly in tremor-predominant PD, although it is unknown whether their effect on tremor is greater than that of other motor outcome measures (Deleu *et al.,* 2004).

2.1.2.5 Adenosine A_{2a} receptor antagonists

The adenosine A_{2a} receptor has emerged as a possible target for the treatment of PD. Evidence suggests that antagonism of the A_{2a} receptor not only improves the symptoms of the disease but may also protect against the underlying degenerative process. One potent inhibitor among the adenosine A_{2a} antagonists is (E)-8-(3-chlorostyryl)caffeine (CSC) (Ikeda *et al.*, 2002) (Figure2.8).

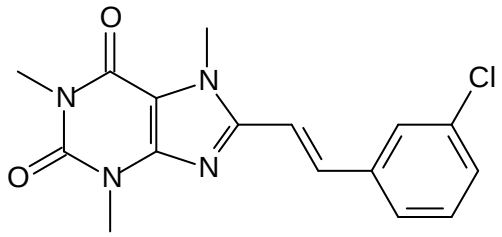

Figure 2.7 The chemical structure of the A_{2a} antagonist, (E)-8-(3-chlorostyryl)caffeine (CSC).

2.1.2.6 Amantadine

Amantadine (Figure 2.8) is another useful drug for the treatment of PD. Amantadine enhances DA release and blocks DA reuptake, has a mild antimuscarinic effect, and is a noncompetitive inhibitor of NMDA glutamate receptors. Interest in this drug has emerged because of its possible usefulness for treating motor fluctuations and dyskinesias in patients requiring chronic L-dopa therapy. Amantadine can also be used with DA agonist therapy. Amantadine appears to be useful in the control of dyskinesias. The fact that amantadine blocks NMDA glutamate receptors suggests that the drug may limit excitotoxic reactions that result from excess glutamatergic stimulation, and may therefore be neuroprotective. Amantadine is useful for

symptomatic control both as monotherapy and as an adjunct to L-dopa and anticholinergic drugs (Deleu *et al.,* 2004).

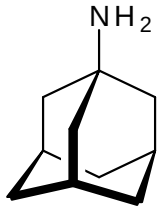

Figure 2.8 The chemical stucture of amantadine.

2.1.3 Drugs for neuroprotection

Current therapies for PD significantly improve the quality of life of patients suffering from this neurodegenerative disease, yet none of the current therapies have convincingly shown to slow or prevent the progression of the disease. According to Yacoubian & Standaert (2009), the definition for ñneuroprotectionò does not include ñneurorestorativeò strategies that aim to replace neuronal elements after they are lost. Treatments with a potential neuroprotective capability for PD have been investigated in randomized controlled clinical trials and other studies since the mid 1980s. Although promising leads have arisen, no therapy has been proven to halt or slow disease progression (LeWitt & Taylor, 2008).

2.1.3.1 MAO-B inhibitors

In the 1980s researchers speculated over two possibilities regarding DA toxicity that may lead to PD. The first of these two possibilities is oxidative stress, resulting from the ability of DA to auto-oxidize to yield oxyradicals. Secondly, the catabolism of DA by MAO is known to generate potentially toxic by-products. At sites within neurons and in nearby glia, the turnover of DA by MAO may yield the hydroxyl radical and other reactive oxygen species (Heikkila *et al.,* 1990).

Several clinical investigations targeting MAO were initiated, and in each instance the compound chosen to inhibit this enzyme was selegiline (Figure 2.9), an irreversible MAO-B inhibitor (LeWitt & Taylor, 2008). The largest of these studies, DATATOP (deprenyl and tocopherol antioxidative therapy of parkinsonism), was initiated in 1987 and was planned to be conducted over 2 years.

The major finding from this study was that selegiline conferred a small but detectable symptomatic anti-parkinsonian effect (Parkinson's Study Group, 1989).

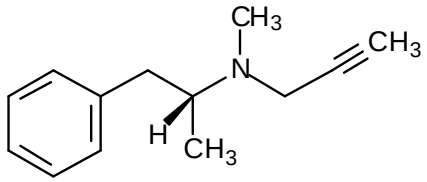

Selegiline (Deprenyl)

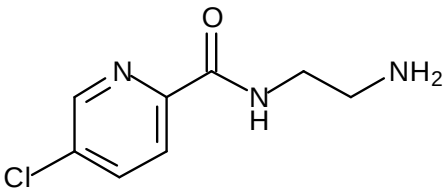

Lazabemide

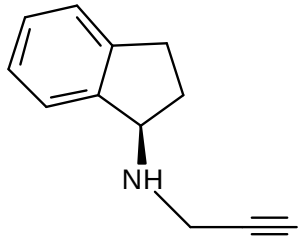

Rasagiline

Figure 2.9 The chemical structures of selected MAO inhibitors.

Lazabemide (Figure 2.9), another MAO-B inhibitor, differs from selegiline in several properties: it is a reversible inhibitor of MAO that has greater selectivity for the type B enzyme *versus* type A and undergoes rapid clearance after discontinuation. Unlike selegiline, it is not a propargylamine derivative and is not metabolized to amphetamine. In untreated PD subjects, lazabemide possesses symptomatic effects similar to that of selegiline. A similar study to the DATATOP study was carried out with lazabemide, only with fewer subjects. After 12 months of lazabemide treatment, the outcome was similar to the findings of the DATATOP study (LeWitt *et al.,* 1993), that is, that lazabemide has a symptomatic anti-parkinsonian effect as well.

Rasagiline (Figure 2.9) is a highly selective MAO-B inhibitor. It shares with selegiline a propargylamine structure and irreversible inhibition. Rasagiline enhances the release of DA in addition to retarding its catabolism, and it antagonizes cellular processes that are involved in the

cascade of events leading to apoptosis. A clinical study was also carried out with rasagiline, the TEMPO trial. The results of the TEMPO trial were in favour of disease-modifying action (Akao *et al.,* 2001). The effectiveness of selegiline, lazabemide and rasagiline as disease-modifying agents provides a focus on their shared property of MAO-B inhibition. Additional potentially protective pharmacological properties of propargylamine compounds, that are unrelated to MAO-B inhibition, however, have also been shown in laboratory models of neurodegeneration and apoptosis studies (Mandel *et al.,* 2003).

2.1.3.2 Dopaminergic drugs

The DA agonists all act on DA D_2-like receptors. Postsynaptic D_2 receptor stimulation is linked to an antiparkinsonian activity and presynaptic D_2 stimulation has been claimed to have neuroprotective effects. Unlike L-dopa, DA agonists stimulate DA receptors, directly. Other theoretical advantages of the DA agonists are that they do not require carrier-mediated transport for absorption into the brain, nor do they produce potentially toxic metabolites and free radicals (Deleu *et al.,* 2004). DA receptor agonists have been hypothesized to be potentially neuroprotective by acting at D_2 autoreceptors found on dopaminergic SN terminals to suppress DA release and thus reduce oxidative stress. Certain agonists, such as pramipexole, may also act as direct antioxidants (Olanow *et al.,* 1998). Although developed for their symptomatic actions in PD, several drugs may also have neuroprotective actions against oxidative stress and may protect dopaminergic neurons against various experimental toxins, including methamphetamine, 3-acetylpyridine, 6-OHDA and MPTP (Ferger *et al.,* 2000). Furthermore, studies investigating a stereoisomer of pramipexole, that is inactive at DA receptors, have shown that it also exerts neuroprotective properties. In mice, the dopaminergic agonist, ropinirole, also enhances mechanisms against oxidative stress and exerts a protective action against 6-OHDA-induced loss of nigrostriatal dopaminergic projections (Tanaka *et al.,* 2001).

2.1.3.3 Antioxidant therapy

Although several compounds with antioxidant properties have been considered for clinical investigation, only Ŭ-tocopherol has undergone evaluation. Ŭ-Tocopherol, a chain breaking antioxidant that enters into lipid-soluble cellular regions such as biological membranes, acts by quenching oxyradical species. There is no evidence for deficiency of Ŭ-tocopherol in PD, and

severe deficiency states do not lead to parkinsonism. Experimental evidence suggest that there is no evidence for a disease-modifying effect (Parkinsonôs Study Group, 1993).

2.1.3.4 Mitochondrial energy enhancement drugs

One of the few systematic markers for PD is altered mitochondrial function. Mitochondria of the SN, platelets and skeletal muscle in PD possess reduced activity of the first step of the mitochondrial electron transport chain, complex I. Coenzyme Q_{10} is an essential cofactor serving as an electron acceptor for mitochondrial complex I. It is also a potent antioxidant in lipid membranes and mitochondria. Creatine serves as a precursor for the conversion to the energy intermediate, phosphocreatine, which in mitochondria transfers phosphoryl groups for ATP synthesis. The effect of increasing creatine intake is an enhancement of phosphocreatine formation. Ultimately the result is the reduction in oxidative stress through the opening of the mitochondrial transition pore. Creatine-treated subjects as well as the coenzyme Q_{10} treated subjects, tended to require less increase of dopaminergic therapy dose over time (Shults ***et al.,*** 1999).

2.1.3.5 Anti-inflammatory drugs

The role of inflammation in PD has become more recognized recently. Activation of microglia, increased cytokine production and increased complement protein levels, have been demonstrated in PD. As a means to slow disease progression, anti-inflammatory agents, including nonsteroidal anti-inflammatory drugs (NSAIDs) and minocycline, have been pursued as potential disease-modifying treatments for PD. Several studies in culture and in animal models have shown that certain NSAIDs, such as aspirin, have neuroprotective qualities (Tansey ***et al.***, 2007; Esposito ***et al.,*** 2007). An example of an alternative approach to targeting neuroinflammation may be the use of statins (3-hydroxy-3-mythylglutaryl-coenzyme A reductase inhibitors). In addition to lowering cholesterol, these drugs have anti-inflammatory effects, including the reduction of tumor necrosis factor-Ŭ (TNFŬ), nitric oxide and superoxide production by microglia. Simvastatin has been shown to reduce DA loss in MPTP animal models. Recent epidemiological studies showed that statin use, particularly simvastatin, is associated with reduced PD incidence (Selley, 2005).

2.1.3.6 Anti-apoptotic drugs

Apoptosis is a mechanism that participates in neural development and plays a role in some forms of neural injury. Activation of these cell death pathways most likely represents end-stage processes in PD neurodegeneration. Therefore, inhibitors of these cell death pathways have been proposed as potential neuroprotective agents regardless of the initial causes for neurodegeration in PD (Yacoubian & Standaert, 2009). Several lines of evidence have pointed to the activation of apoptosis as a possible mechanism for neurodegeneration in PD. On this basis, the search of anti-apoptotic interventions led to proposals for the study of three different compounds and how they interact with pro-apoptotic mechanisms (Waldmeier *et al.,* 2006).

The propargylamine, TCH346, is an anti-apoptotic compound that inhibits the glycolytic enzyme, glyceraldehyde-3-phosphate dehydrogenase (GAPDH), which can initiate apoptosis (Yacoubian & Standaert, 2009). TCH346 was developed because of its shared structural similarities with selegiline. TCH346 does not inhibit MAO-B, however, and unlike selegiline, it is not metabolized to amphetamine metabolites. In rhesus monkeys, exposed to MPTP, near-complete protection against the development of motor impairment was achieved. Unfortunately it did not reveal any evidence for a neuroprotective effect in clinical trials (Olanow *et al.,* 2006).

CEP-1347, an inhibitor of mixed lineage kinases, that can activate the c-Jun N-terminal (JNK) pathway, that is involved in cell death, is another anti-apoptotic agent that showed promise in preclinical studies (Maroney *et al.,* 1998).

Minocycline (Figure 2.10) has been extensively studied because of its promise in treating neurodegenerative diseases. In rodent models of parkinsonism induced by 6-OHDA and MPTP, pre-treatment with minocycline improved survival of dopaminergic SN neurons. Minocycline inhibits the activation of microglia, which is a prominent feature in the brain of PD patients and in experimental neurotoxin models. Although these properties seem to be in favour of minocycline providing a possible neuroprotective effect in PD, preclinical results have not supported this possibility (Wu *et al.,* 2002).

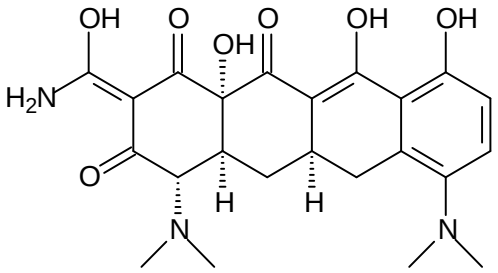

Figure 2.10 The chemical structure of the anti-apoptotic drug, minocycline.

2.1.3.7 Anti-glutamatergic drugs

Because glutamate can act as an excitotoxin, contributing to neural damage, one rationale for PD neuroprotection has been to block glutamate neurotransmission in the SN. Riluzole (Figure 2.11) demonstrates limited but definite effectiveness in slowing the deterioration of amyotrophic lateral sclerosis and has been FDA-approved for this use. Riluzole acts by blocking the presynaptic release of glutamate. Unlike other compounds, that are potent glutamate blockers and that can cause significant CNS toxicity, riluzole is well tolerated (Rascol ***et al.,*** 2002).

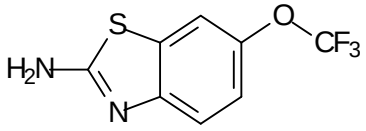

Figure 2.11 The chemical structure of an anti-glutamatergic drug, riluzole

2.1.3.8 Adenosine A_{2A} receptor antagonists

Epidemiological studies have indicated that caffeine may reduce the incidence of PD, at least in men. As caffeine (Figure 2.12) mediates its action by antagonizing adenosine receptors, this finding has led to interest in evaluating adenosine receptor antagonists as potential neuroprotective agents. In the striatum, the A_{2A} receptors can heterodimerize with the D_2 receptor to inhibit DA signalling. Antagonism of the A_{2A} receptor therefore may promote DA function. Two small clinical trials of the A_{2A} antagonist, istradefylline (Figure 2.12), has demonstrated potential symptomatic effects in advanced PD. More recent research has suggested that A_{2A} antagonists not only improve symptomatic function in PD but may also be

neuroprotective (Yacoubian & Standaert, 2009). Caffeine and istradefylline are both neuroprotective in the MPTP animal model of PD (Ikeda *et al.,* 2002).

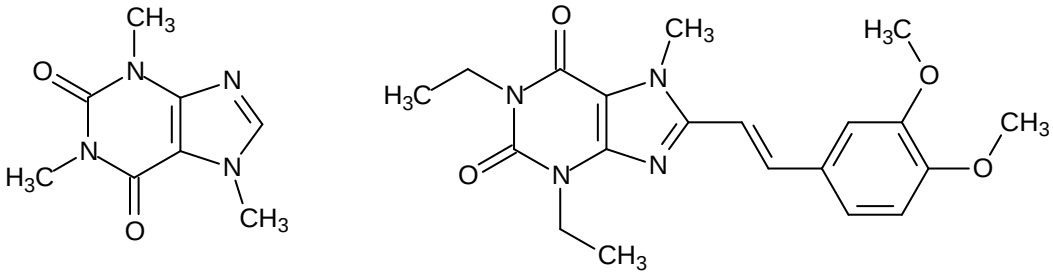

Caffeine Istradefylline

Figure 2.12 The chemical structures of selected adenosine receptor antagonists.

2.1.4 Mechanisms of neurodegeneration

Several mechanisms have been implicated in PD pathogenesis. No one mechanism appears to be primary in all cases of PD, and these pathogenic mechanisms likely act synergistically through complex interactions to promote neurodegeneration (Yacoubian & Standaert, 2009).

2.1.4.1 Oxidative stress and mitochondrial dysfunction

Oxidative stress results from an overabundance of reactive free radicals secondary to either an overproduction of reactive species or a failure of cell buffering mechanisms that normally limit their accumulation. DA metabolism promotes oxidative stress through the production of quinones, peroxides, and other ROS. Mitochondrial dysfunction is another source for the production of ROS, which can further damage mitochondria. For example, Complex I inhibitors, such as MPP^+ and rotenone, cause a parkinsonian syndrome in animals. Increased iron levels, seen in the SN of PD patients, also promote free radical damage, particularly in the presence of neuromelanin. Several different strategies have been proposed to limit oxidative stress in PD. These strategies include inhibitors of MAO, a key enzyme involved in DA catabolism, and enhancers of mitochondrial electron transport, such as coenzyme Q_{10}. Other strategies include compounds that can directly quench free radicals, such as vitamin E, and molecules that can

promote endogenous mechanisms that buffer free radicals, such as selenium (Hastings & Lewis, 1996).

Iron appears to play a particularly important role in neurodegenerative processes. Over the years, several links between iron and central nervous system (CNS) dysfunction have been uncovered. In many neurodegenerative diseases, the site of neural death in the brain, are also sites at which iron accumulated (Zecca *et al.,* 2004). The link between MAO, iron and neuronal damage appears to be an increase in oxidative stress. A normal product of MAO is hydrogen peroxide (H_2O_2). This is inactivated in the brain, mainly by glutathione peroxidase (GPO), which uses glutathione (GSH) as a cofactor. When brain GSH levels are low, as in PD, H_2O_2 could accumulate and then be available for the Fenton reaction. In this reaction, iron, as the ferrous ion Fe^{2+}, generates a highly active free radical, the hydroxyl radical, from H_2O_2. The hydroxyl radical depletes cellular anti-oxidants and react with and damages lipids, proteins and DNA (Riederer *et al.,* 1989) (Figure 2.13).

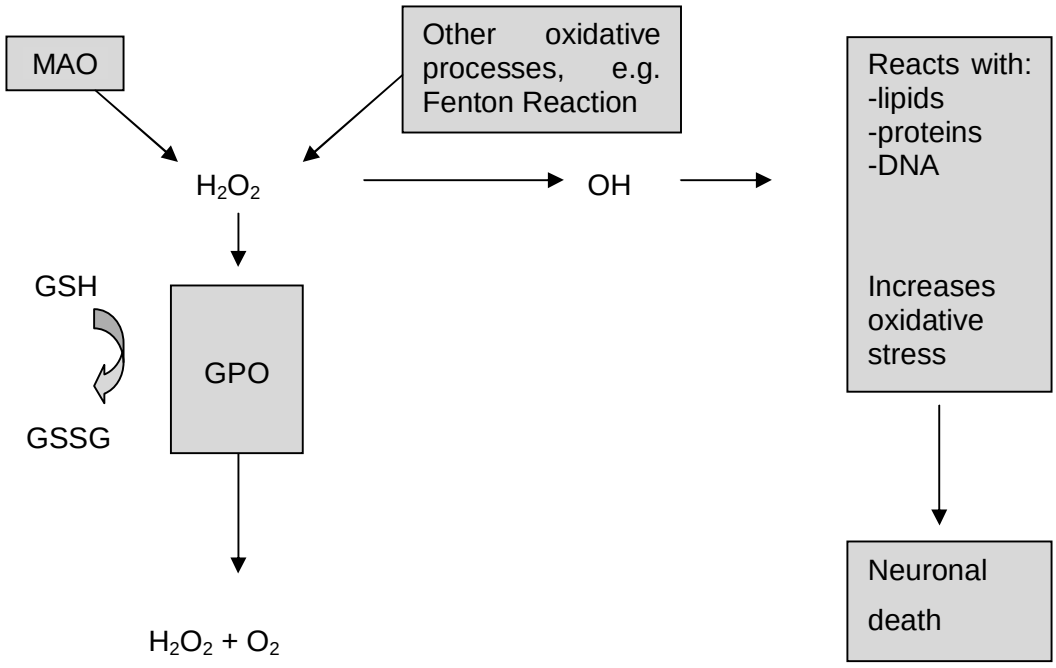

Figure 2.13 The mechanism of neurotoxicity induced by iron and hydrogen peroxide.

With increasing age, brain iron and brain MAO increase, thus increasing both components of the Fenton reaction and the potential for hydroxyl radical generation. Another approach to

protect against the degenerative processes in PD is to remove the Fe^{2+} ions. Thus, the intraventricular injection of a well-known iron chelator, deferal, protects against lesions of nigrostriatal DA neurons induced by 6-hydroxydopamine (6-OHDA) or MPTP (Youdim & Bakhle, 2006).

2.1.4.2 Protein aggregation and misfolding

Protein aggregation and misfolding have emerged as important mechanisms in many neurodegenerative disorders, including PD. In PD, the primary aggregating protein is Ŭ-synuclein, whose link to PD was first identified through rare families with autosomal dominant PD caused by mutations in this protein. While mutations in Ŭ-synuclein are found in a small number of inherited PD cases, Ŭ-synuclein is the major component of LBs and Lewy neurites found in sporadic PD (Athanassiadou *et al.,* 1999; Spillantini *et al.,* 1997). Recent studies, implicating parkin and ubiquitin carboxyl-terminal hydrolase L1 (UCH-L1) in genetic forms of PD, reinforce the connection between protein aggregation and PD pathogenesis. Parkin is an E3 ubiquitin ligase involved in targeting misfolded proteins for degradation. Mutations of parkin found in genetic forms of PD, disrupt its E3 ubiquitin ligase activity (Kitada *et al.,* 1998). Overproduction or impaired clearance of Ŭ-synuclein results in aggregation and may be a central mechanism for PD. Therefore, therapeutic strategies to prevent protein aggregation or to enhance the clearance of misfolded proteins are the subject of intensive study. Inhibitors of Ŭ-synuclein aggregation could serve as potential neuroprotective therapies, although a clearer understanding of the toxicity form of Ŭ-synuclein is important (Yacoubian & Standaert, 2009).

2.1.4.3 Neuroinflammation

Neuroinflammation is likely to contribute to neuronal dysfunction and eventual death of vulnerable neuronal populations. While acute inflammation in the CNS is often accompanied by secretion of microglial-derived neuroprotective factors, which promote repair, chronic neuroinflammation is more likely to increase susceptibility of vulnerable neurons to toxic injury, because it can induce oxidative stress. The two mechanisms by which neuroinflammation induces oxidative stress, are via the production of high levels of ROS by activated glia, such as microglia and astrocytes, and via arachidonic acid signalling, through the activation of cyclooxygenase (COX) and lipoxygenase (LOX) pathways. Prostaglandin E2 (PGE2), produced

by COX-2, can induce an intraneuronal toxic effect directly on DA neurons. Prostaglandins of the J2 series also induce oxidative stress by causing a decrease in glutathione and glutathione peroxidase activity, by decreasing the mitochondrial membrane potential and by over production of protein-bound lipid peroxidation products, including acrolein and 4-hydroxy-2-nonenal (HNE). These effects suggest that prostaglandins of the J2 series may be a source of increased ROS generation (Tansey *et al.,* 2007).

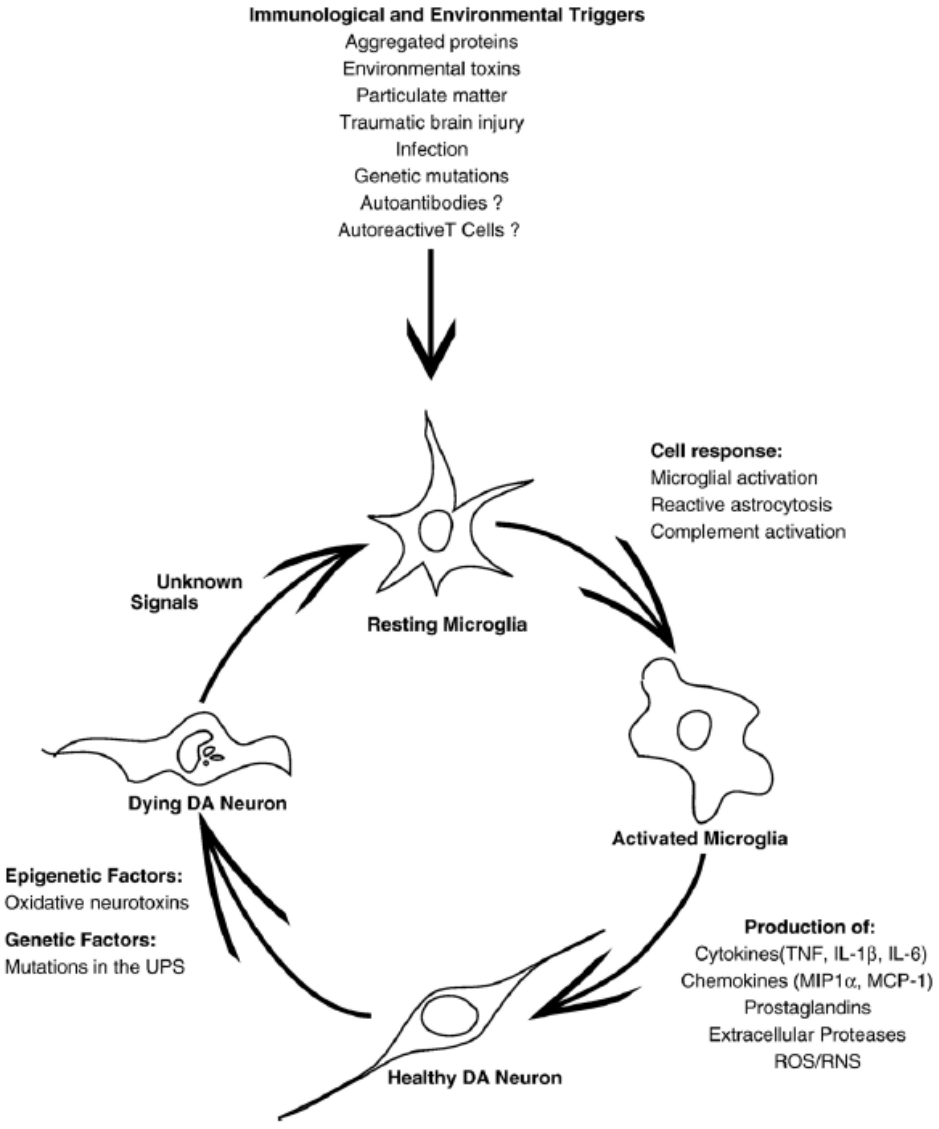

Figure 2.14 Mechanisms and triggers that initiate and sustain microglia activation and contribute to dopaminergic neuron degeneration (Tansey *et al.,* 2007)

2.1.4.4 Excitotoxicity

Excitotoxicity has been implicated as a pathogenic mechanism in several neurodegenerative disorders, including PD. Glutamate is the primary excitatory transmitter in the mammalian central nervous system and a primary driver of the excitotoxicity process. Dopaminergic neurons in the SN have high levels of glutamate receptors and receive glutamatergic innervations from the subthalamic nucleus and cortex. Excessive NMDA receptor activation by glutamate could increase intracellular calcium levels that then activate cell death pathways. Calcium influx produced by excessive glutamate receptor activation can also promote peroxynitrite production through the activation of nitric oxide synthase**.** NMDA receptor antagonists protect against dopaminergic cell loss in MPTP models (Yacoubian & Standaert, 2009).

2.1.4.5 Apoptosis

Apoptosis is a mechanism that has been demonstrated to participate in neural development and to play a role in some forms of neural injury. There has been controversy as to whether apoptosis is directly involved in PD. Several pathological studies have revealed signs of both apoptotic and autophagic cell death in the SN of PD brains, although the extent is limited because of the slow process of cell death which underlies PD. Alterations in cell death pathways are unlikely to be the primary cause of PD, but both apoptotic and autophagic cell death pathways are hypothesized to become activated in PD through oxidative stress, protein aggregation, excitotoxicity or inflammatory processes. Activation of these cell death pathways most likely represents end-stage processes in PD neurodegeneration (Tatton ***et al.,*** 2003).

2.1.4.6 Loss of trophic factors

The loss of neurotrophic factors has been implicated as a potential contributor to cell death observed in PD. The neurotrophic factors, brain-derived neurotrophic factor (BDNF), glial-derived neurotrophic factor (GDNF) and nerve growth factor (NGF) have all been demonstrated to be reduced in the nigra in PD. As a result, treatment with growth factors have been proposed as a potential neuroprotective therapy in PD. Indeed, the potent ability of these agents to stimulate growth of dopaminergic neurons suggest that they may be useful neuroprotective

treatments, even if deficiency of the factor is not the primary cause of the disease process (Howells *et al.,* 2000).

2.2 The monoamine oxidases

2.2.1 General background and tissue distribution of MAO

It is about 50 years since the MAO inhibitors were first developed as antidepressants. Some inhibitors of these enzymes have been shown to have potential uses in the treatment of several neurodegenerative conditions, including PD and Alzheimerôs disease (AD) (Youdim *et al*., 2006). In 1928 an enzyme, catalyzing the oxidative deamination of tyramine was described which was called tyramine oxidase. A few years later, it was found that tyramine oxidase, noradrenaline oxidase and aliphatic oxidase was the same enzyme, capable of metabolizing primary, secondary and tertiary amines. Early inhibitors of MAO were anti-tuberculosis drugs such as isoniazid (Figure 2.15), a potent inhibitor of MAO. A related compound, iproniazid (Figure 2.15), became the first MAO inhibitor to be used successfully in the treatment of depressive illness (Youdim *et al.,* 1988).

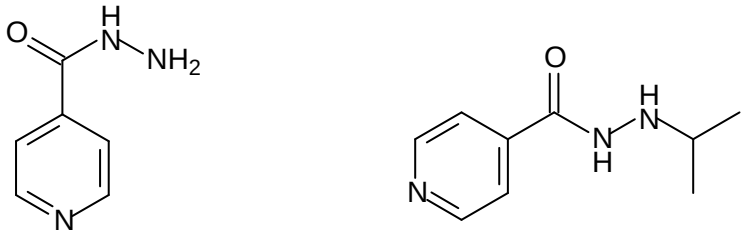

Isoniazid Iproniazid

Figure 2.15 The chemical structures of selected anti-tuberculosis drugs.

The reaction mechanism of MAO involves oxidative deamination of primary, secondary and tertiary amines to the corresponding aldehyde, with the generation of hydrogen peroxide. The aldehyde is rapidly metabolized by aldehyde dehydrogenase to acidic metabolites (Figure 2.16). It is these acidic metabolites that are commonly used as the measure of MAO activity *in vitro* or *in vivo* (Grunblatt *et al.,* 2004).

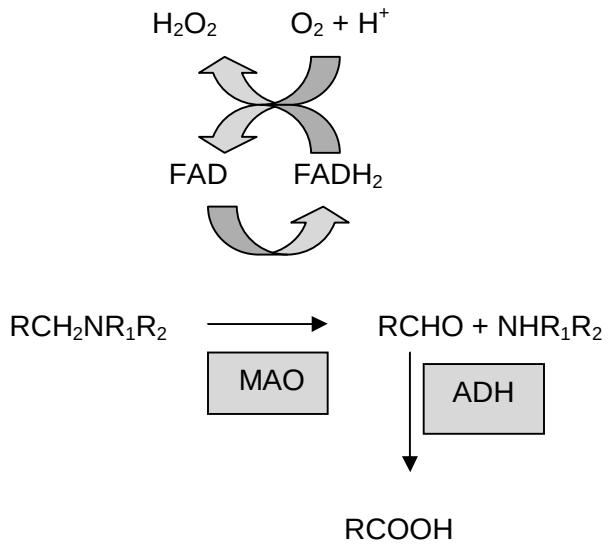

Figure 2.16 Reaction pathway of monoamine metabolism by oxidative deamination by mitochondrial MAO.

Gene profiling of post-mortem samples of SN from PD patients disclosed a deficiency in aldehyde dehydrogenase (ADH) that could allow a build-up of neurotoxic aldehydes derived from DA by MAO (Grunblatt ***et al.,*** 2004). A crucial finding in the late 1960s was that MAO was not a single enzyme but could exist in at least two forms (type A and type B) that had different pH optima and sensitivity to heat inactivation. Type A MAO was inhibited by clorgyline and metabolized NA and 5-HT, where type B MAO was inhibited by selegiline and metabolizes benzylamine. Tyramine and DA were equally well metabolized by both forms of the enzyme (Johnston, 1968).

MAO-A and -B are tightly associated with the mitochondrial outer membrane, although a small proportion of each enzyme is associated with the microsomal fraction. During development, MAO-A appears before MAO-B, with the level of the latter increasing dramatically in the brain after birth. MAO is present in most mammalian tissues, but the proportion of the two iso-enzymes varies from tissue to tissue. Microvessels in the blood-brain barrier are rich in MAO-B. In the human brain, there are regional differences in MAO activity: the basal ganglia (striatum) and hypothalamus show the highest activities, whereas low levels of activity are observed in the cerebellum and neocortex. The two iso-enzymes are not evenly distributed in the human brain, and the main form in the basal ganglia is MAO-B. Both MAO-A and -B can contribute to DA metabolism in the human brain (Youdim ***et al.,*** 2006).

2.2.2 Biological function of MAO-B

MAO in peripheral tissues, such as the intestine, liver, lungs and placenta, seems to protect the body by oxidizing amines from the blood or by preventing their entry into the circulation. MAO-B in the microvessels of the blood-brain barrier presumably has a similar protective function, acting as a metabolic barrier. It has been suggested that in the peripheral nervous system (PNS) and CNS, intraneuronal MAO-A and -B protect neurons from exogenous amines, terminate the actions of amine neurotransmitters and regulate the contents of intracellular amine stores.

Hydrogen peroxide formed during the MAO catalytic reaction might have important metabolic and signalling functions in the brain, and the aldehydes derived from 5-HT and NA deamination might be involved in the regulation of sleep. At higher concentrations, the products, ammonia and hydrogen peroxide, are toxic. The aldehyde derived from DA is known to be cytotoxic. This is important in PD because, as mentioned, the levels of ADH in the SN are greatly reduced. Such aldehydes might also form adducts with amine groups to yield toxic compounds such as tetrahydropapaveroline that have been associated with parkinsonism and with alcohol-related abnormalities (Shin *et al.,* 2004).

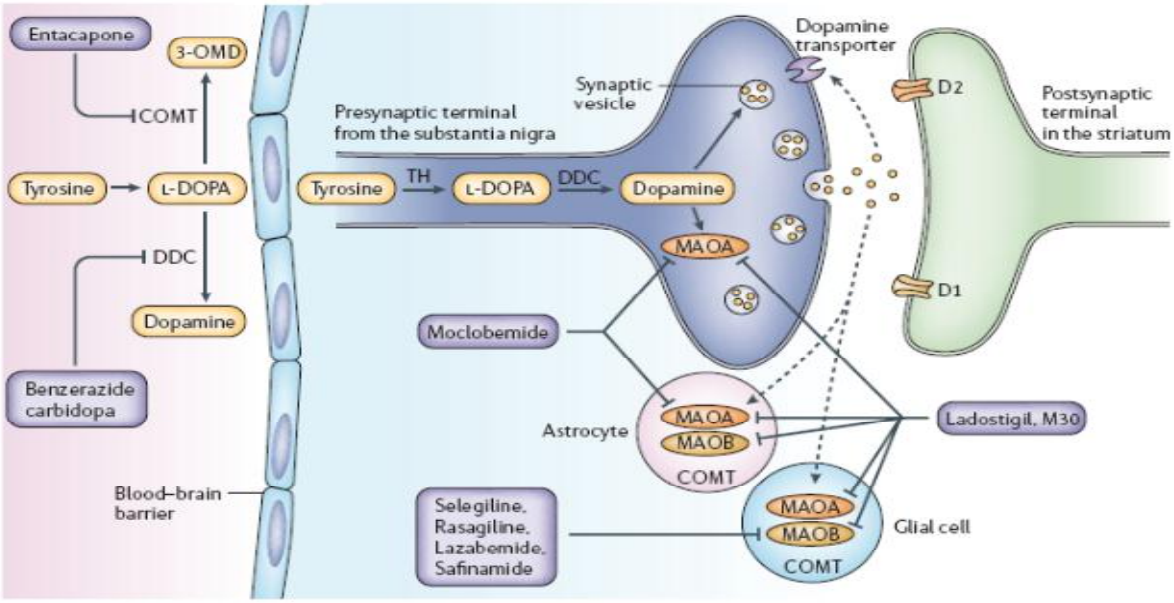

Figure 2.17 DA synthesis and its metabolism by MAO-A and MAO-B (Youdim *et al.,* 2006).

2.2.2.1 Genes and MAO

MAO-A and -B proteins have ~70% amino acid identity and are encoded by separate genes located on the X chromosome. Differences in the core promoter regions might account for the varying effects of some hormones on MAO expression and the differential expression of the MAO-A and -B genes (Zhu *et al.,* 1994). Progesterone, testosterone, corticosterone and the glucocorticoids increase the levels of MAO-A, but have little effect on MAO-B in fibroblasts and capillary endothelial cells. Likewise, MAO-A but not MAO-B is elevated in the endometrium, reproductive tissue and the brain, when levels of progesterone are high during the oestrous cycle. Following several studies, it was shown that MAO is not essential for survival (Youdim *et al.,* 1989). Gene deletion has shown that MAO-A activity is important during development. A compulsive-aggression phenotype results from lack of MAO-A function in humans and mice. Low platelet MAO-B activity might be associated with personality traits such as sensation seeking, impulsiveness and extraversion. These traits have also been linked to vulnerability to substance abuse, for example, tobacco smoking, early-onset or type 2 alcoholism and gambling. Cigarette smoke contains MAO inhibitors, so it is not clear whether people tend to smoke because they have low MAO-B activity, or whether they have low platelet MAO-B activity because they smoke. Lowered MAO-B activity might be associated with the reduced risk of PD in smokers. It is becoming increasingly clear that the MAOs have important roles in brain development and function (Youdim *et al.,* 2006).

2.2.3 Biological function of MAO-A

2.2.3.1 The cheese reaction

In the late 1950s and 1960s, MAO inhibitors demonstrated remarkable antidepressant actions, but their clinical value was seriously compromised by side effects. Iproniazid for example, caused liver toxicity, which is associated with its hydrazine structure. Although this problem was resolved by the development of other, non-hydrazine MAO inhibitors, these, notably tranylcypromine, induced another important side effect, the ócheese reactionô (Youdim *et al.,* 1988).

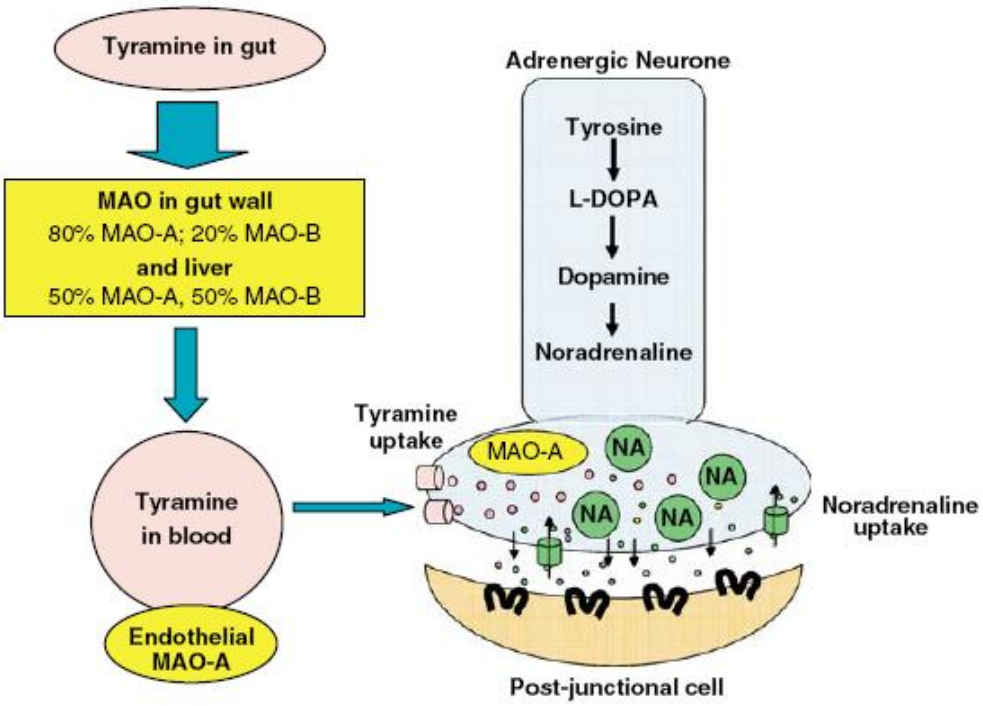

Figure 2.18 The mechanism of potentiation of cardiovascular effects of tyramine: the cheese reaction (Youdim & Bakhle, 2006).

The cheese reaction (Figure 2.18) is induced by tyramine and other indirectly acting sympathomimetic amines present in food and fermented drinks, such as beer and wine. Under normal circumstances, such dietary amines are extensively metabolized by MAO in the gut wall and in the liver and they are thus prevented from entering the systemic circulation. In the presence of a MAO inhibitor, this protective system is inactivated and tyramine or other monoamines present in ingested food are not metabolized and enter the circulation. From here they have access to the brain, and induce a significant release of NA from peripheral adrenergic neurons. The consequence of this release is a severe hypertensive response which, in some cases, can be fatal. These serious side effects stimulated a search for antidepressants that are not MAO inhibitors, and led to their eventual replacement by the neurotransmitter uptake inhibitors, the tricyclic antidepressants, and more recently the 5-HT selective re-uptake inhibitors (SSRI) such as fluoxetine (Finberg *et al.,* 1981).

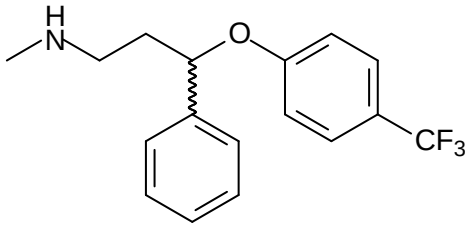

Figure 2.19 The chemical structure of the SSRI Fluoxetine.

Selective, irreversible MAO-B inhibitors have no such effects, because the intestine contains little MAO-B and tyramine is effectively metabolized by intestinal MAO-A. The development of reversible MAO-A inhibitors, such as moclobemide, also avoided this problem because reversible inhibitors can sufficiently block MAO-A in the CNS to obtain an antidepressant effect, while dietary tyramine is able to displace the inhibitor from peripheral MAO-A, allowing for its metabolism. A recent developed brain-selective MAO-A/B inhibitor, ladostigil, does not cause the cheese reaction (Youdim *et al.,* 2006).

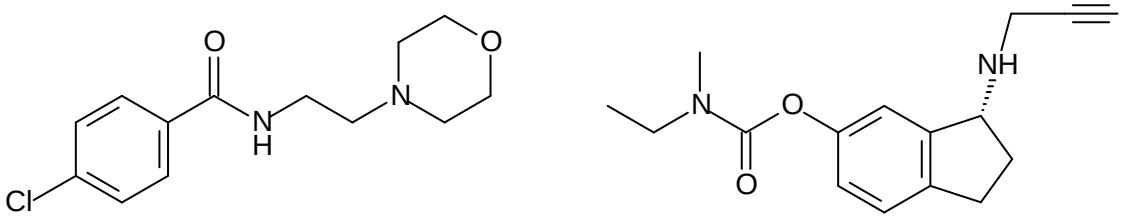

Moclobemide Ladostigil

Figure 2.20 The chemical structures of selected MAO-A inhibitors.

2.2.3.2 MAO-A in depression

MAO inhibitors have been used for decades in the treatment of depression. The antidepressant properties of MAO inhibitors result from selective MAO-A inhibition in the CNS, which leads to increased brain levels of DA, NA and 5-HT (Zisook, 1985). When one isoform of MAO is fully inhibited, the other isoform metabolize DA adequately. Thus, with selective inhibition of MAO-A or -B, the level of DA will not change drastically in the human striatum (Riederer & Youdim, 1986). The two monoamines implicated in depressive illness are NA and 5-HT, both substrates

for MAO-A. The antidepressant effects of MAO-A inhibition with the earlier, non-selective, irreversible inhibitors had been already established. The major disadvantage was the incidence of the cheese reaction with those early inhibitors. Because the selective reversible inhibitors did not provoke this reaction, moclobemide was assessed as an antidepressant and found to be effective in improving vigilance, psychomotor speed and long-term memory (Youdim & Bakhle, 2006).

In the treatment of therapy-resistant depression, MAO-inhibitors provide an important option and a combination of reversible MAO-A and reversible MAO-B inhibitors may be worth considering. However, combination of MAO-inhibitors with uptake inhibitors, such as the tricyclic antidepressants and SSRI`s, should be avoided as such combinations may provoke the 5-HT syndrome, a serious adverse reaction. Moclobemide shows a useful antidepressant action and is well tolerated with standard PD therapies. Furthermore, in PD patients who are not depressed, moclobemide does not significantly influence cognitive measures of mood (Youdim & Weinstock, 2004).

2.2.4 The role of MAO-B in PD

2.2.4.1 Metabolism of DA

Tyrosine passes through the blood-brain barrier and is hydroxylated by tyrosine hydroxylase (TH) to L-dopa, which is then decarboxylated by DOPA decarboxylase (DDC) to DA within the neuron. DA is taken up into synaptic vesicles or is metabolized by MAO-A at neuronal mitochondria. After release from the terminal, extracellular DA is cleared by uptake into astrocytes and glia which contain both MAO-A and ï B (Figure 2.21). Selective inhibition of one MAO isoform allows the other to metabolize DA effectively and does not alter the steady state levels of striatal DA. On the other hand, non-selective inhibition of both isoforms induces highly significant increases in striatal DA and in other regions (Youdim & Bakhle, 2006).

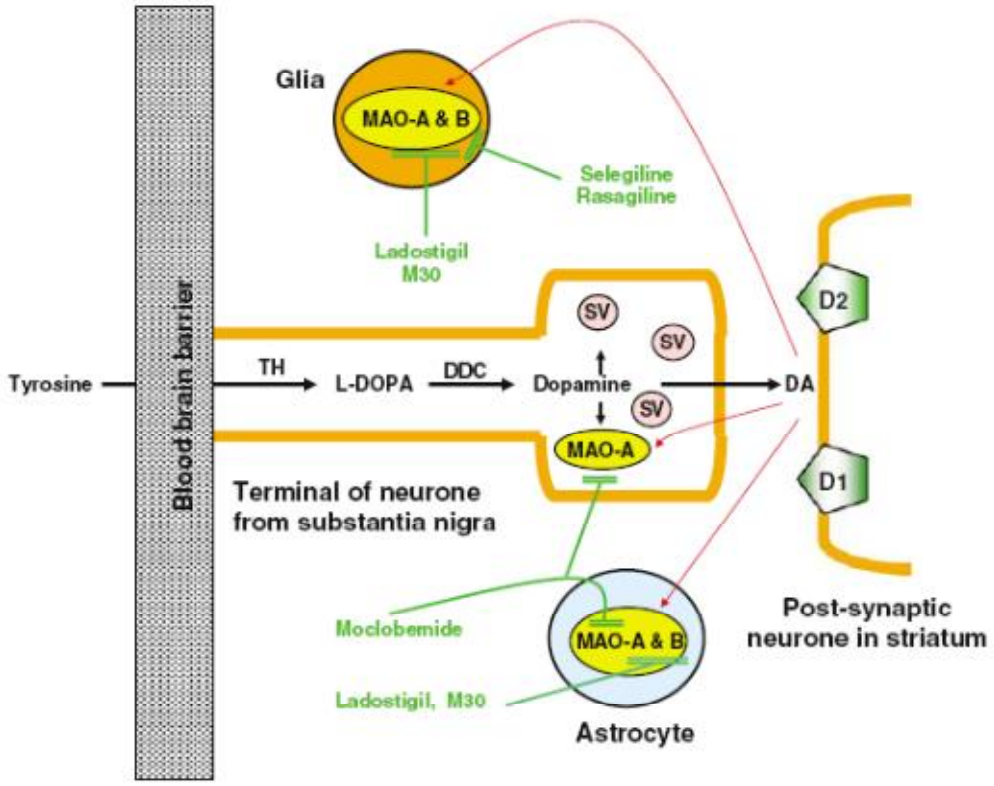

Figure 2.21 Pathways of DA synthesis in dopaminergic neurons and metabolism by MAO-A and ï B in the brain (Youdim & Bakhle, 2006).

DA is thought to produce ROS via both enzymatic and non-enzymatic catabolism. DA oxidation can occur either spontaneously in the presence of transition metal ions or via an enzyme-catalyzed reaction. The metabolism of DA by MAO generates a spectrum of toxic species, namely H_2O_2, oxygen radicals, semiquinones, and quinones. Conditions that increase brain concentration and/or turnover of DA could potentially increase the formation of reactive metabolites, especially under conditions in which the ratio of available DA to antioxidant capacity is high. Administration of DA under conditions of decreased antioxidant protection (e.g. when GSH levels are compromised) has been found to increase oxidative stress, because DA rapidly oxidizes to form ROS (Cantuti-Castelvetri *et al.,* 2003).

2.2.5 The potential role of MAO-A in PD

In rodents, MAO-A is present in the extraneuronal compartment and within the dopaminergic terminals, were it is involved in the metabolism of both intraneuronal and released DA, respectively. The intraneuronal enzyme ensures a low level of the neurotransmitter monoamines within the neuron (Youdim *et al.,* 1988). Little attention had been paid to MAO-A inhibition as a practical means of controlling DA levels in the brain, even though it had clearly been established that DA is as well metabolized by MAO-A, as by MAO-B, and that the striatum contains MAO-A (Green *et al.,* 1977). It is therefore plausible that mixed MAO-A/B inhibitors may be more effective in enhancing central DA levels and may present a more effective therapeutic strategy than selective MAO inhibitors (Youdim & Bakhle, 2006).

2.2.6 Irreversible inhibitors of MAO-B

2.2.6.1 (R)-Deprenyl

Deprenyl (selegiline) irreversibly inhibits MAO-B and its (-)-isomer is a more potent inhibitor, than its (+)-enantiomer. The neuroprotective action of selegiline is also multi-fold in nature. There are at least six accepted mechanisms by which selegiline could prevent neurodegeneration:

1. It may decrease the free radical formation from the normal metabolism of the biogenic amines, mainly DA, by inhibition of MAO-B in the CNS. Further reaction between endogenous amines and aldehydes formed by MAO-B, can also play a role in neurodegeneration.
2. The inhibitor may increase the free radical scavenging capacity of the brain.
3. Due to MAO-B inhibition, selegiline may prevent the activation of the environmental pre-toxins.
4. Oral administration of selegiline inhibits the oxidation of low-density lipoprotein (LDL) isolated from healthy men and post-menopausal women.
5. Selegiline exhibits protective effects against neuronal apoptosis in cell culture.
6. Due to the uptake inhibitory properties at the nerve endings, selegiline may reduce neuronal damage (Riederer *et al.,* 2004).

Studies have shown that treatment with selegiline slows the progression of PD (Riederer *et al.,* 2004). In other studies, statistically significant effects of selegiline on memory and attention was shown, that seem to be due to an improved function of the monoaminergic systems involved in the process of neuronal degeneration (Riederer *et al.,* 2004). Selegiline at low doses inhibits the oxidative deamination of DA, phenylethylamine and benzylamine, but not of NA or 5-HT. At higher doses the selectivity is lost. Selegiline is free from the cheese reaction and suitable for use as an adjunct in PD patients already treated with L-dopa, since the basal ganglia from human brain contains MAO-B. A preliminary analysis of the clinical response and survival of these patients indicated that those receiving selegiline plus L-dopa had a better survival rate than those treated with L-dopa alone. These results suggested that selegiline may slow the rate of degeneration of dopaminergic neurons (Youdim & Bakhle, 2006).

2.2.6.2 Rasagiline

Rasagiline is a propargylamine-containing compound that possesses a selective irreversible inhibitory effect on MAO-B. It has structural similarity to selegiline, but unlike the latter, is not a sympathomimetic drug and is not metabolized to amphetamine. *In vivo* studies demonstrated that rasagiline is up to 10 times more active than selegiline as a MAO-B inhibitor. Its neuroprotective activity has been examined in several *in vitro, in vivo* and cell culture studies. It was found to also prevent the cell death caused by apoptosis (Finberg *et al.,* 1999).

For a MAO inhibitor to be effective in PD, it must raise the levels of DA at its receptor sites in the striatum. Using microdialysis techniques in rat striatum, chronic treatment with rasagiline and selegiline was shown to increase, by a similar extent, DA levels in the microdialysate. In primates, which have a larger proportion of MAO-B in the brain than rodents, extracellular DA levels in the striatum were studied, following local infusion of L-dopa via a microdialysis probe. Rasagiline, administered systemically, enhanced DA levels in microdialysate following L-dopa treatment. This MAO-B inhibitor appears to have the appropriate activities to alleviate the symptoms of PD (Finberg *et al.,* 1998). As for neuroprotection, rasagiline possesses activity superior to that of selegiline in neuronal cultures. The neuroprotective activity of rasagiline is dependent of its stereochemistry, however it is independent of stereochemistry, since the S-enantiomer of rasagiline, TVP1022 exhibits similar activity. Studies also claim that the clinical

benefits of rasagiline are not entirely symptomatic in nature and that rasagiline may have an added neuroprotective effect (Mandell *et al.,* 2005).

2.2.7 Reversible inhibitors of MAO-B

2.2.7.1 Lazabemide

Lazabemide is a short-acting, reversible, highly selective inhibitor of MAO-B, which unlike deprenyl, is not metabolized to pharmacologically active metabolites. Previously, lazabemide was found to be safe and well tolerated at dosages of up to 400 mg per day during a 6-week study of patients with early-untreated PD. At dosages raging from 25 to 200 mg per day, lazabemide was well tolerated and delayed the need for L-dopa in early, otherwise untreated PD. The antioxidant activity of lazabemide was significantly higher than that of either vitamin E or the MAO-B inhibitor, selegiline. The ability of lazabemide to inhibit oxidative damage may be attributed to physico-chemical interactions with the membrane lipid bilayer, as determined by small angle X-ray diffraction methods (Mason *et al.,* 2000).

Lazabemide differs from selegiline in several properties: it is a reversible inhibitor of MAO that has greater selectivity for the type B enzyme *versus* type A and undergoes rapid clearance after discontinuation. Lazabemide is not a propargylamine derivative and is not metabolized to amphetamine (Parkinsonôs Study Group, 1994). Some studies showed that the symptomatic effects of lazabemide are similar to those of selegiline. It is reported that lazabemide reduces the need for L-dopa treatment by 51% (Parkinsonôs Study Group, 1996).

2.2.7.2 Safinamide

Safinamide is an Ŭ-aminoamide derivative that may combine MAO-B inhibition with DA reuptake inhibition. Treatment with safinamide is associated with improvements in measures of cognitive function, strategic target detection and auditory number sequencing. Safinamide may represent an alternative to currently available therapies as an adjunct to L-dopa or DA agonists in patients with PD (Fernandez & Chen, 2007).

2.2.8 Inhibitors of MAO-A

The studies with selegiline and rasagiline on MAO-B provided encouragement for others to continue with the development of selective, but reversible, inhibitors of MAO-A, lacking the cheese reaction. In rodents, MAO-A is present in the extraneuronal compartment and within the dopaminergic terminals, where it is involved in the metabolism of both intraneuronal and released DA, respectively (Youdim *et al.,* 1988). MAO-A inhibition as a practical means of controlling DA levels in brain, received little attention even though it had been clearly established that DA is as well metabolized by MAO-A, as by MAO-B, and that the striatum contains MAO-A. This was partly because MAO-A inhibition was known to induce the cheese reaction and partly because there was little evidence of the effect of MAO-A inhibition on DA levels in humans. In brains, obtained at autopsy from patients after treatment with either selegiline or clorgyline, the increase in DA was not as marked as the increase in phenylethylamine, NA and 5-HT (Youdim *et al.,* 1972). Clorgyline does not alter DA levels in the rat brain. The results of laboratory experiments indicated that when one isoform of MAO was fully inhibited, the other isoform would metabolize DA adequately. Thus, with selective inhibition of MAO-A or -B, the levels of DA will not change drastically in the human striatum (Youdim & Bakhle, 2006).

The risk of producing the cheese reaction was abolished by the advent of the reversible MAO-A inhibitors such as moclobemide. This is because reversibility allows competition, so that ingested tyramine is able to displace the inhibitor from the enzyme and can be metabolized in the normal way, in the gut and liver. It had also become possible to show dynamic changes in striatal DA by microdialysis studies in rodents and these showed a clear increase of DA release after moclobemide, clorgyline or rasagiline treatment (Haefely *et al.,* 1992). Although selective inhibition of MAO-A or -B did not affect the steady state levels of DA in the brain, such inhibition did affect its release. Such action could explain the anti-symptomatic effects of these drugs in PD patients. Clinical studies of moclobemide in PD were carried out as an addition to therapy with L-dopa and dopaminergic agonists. Moclobemide has a mild symptomatic benefit, mostly on motor functions. This inhibitor is also safe and effective in patients treated with L-dopa and a peripheral decarboxylase inhibitor (Youdim & Weinstock, 2004).

Microdialysis studies showed that moclobemide can be displaced from its binding site on MAO-A by DA and dis-inhibition of the enzyme would result (Colzi *et al.,* 1993). This would allow DA to be metabolized and decrease the amounts available for binding to receptors. Clinical evaluation of other reversible selective MAO-A inhibitors, such as brofaromine and befloxatone, which have greater affinity for MAO-A, are underway (Davidson, 2003).

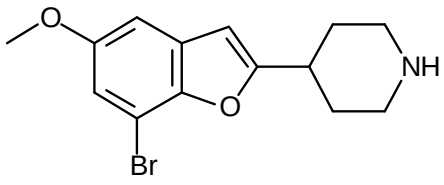

Brofaromine

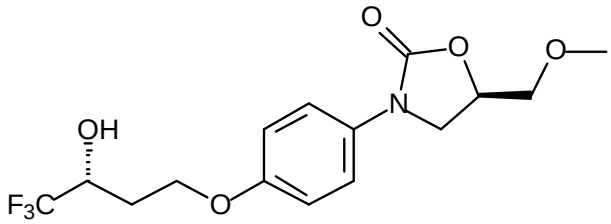

Befloxatone

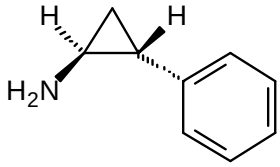

Tranylcypromine

Figure 2.22 The chemical structures of selected MAO-A inhibitors.

MAO inhibitors have a range of potential therapeutic uses. As previously discussed, the first MAO inhibitory antidepressant to be discovered was iproniazid. This compound was initially developed for the treatment of tuberculosis. Although it proved to be ineffective, it was observed to have ópsychoenergizingô effects in patients and was also shown to inhibit MAO. This was followed by the development of other hydrazine derived MAO inhibitors, such as phenelzine, as antidepressants. Reports of liver toxicity, hypertensive crises, haemorrhage, and in some cases, death, resulted in the withdrawal of most hydrazine type MAO inhibitors (Youdim *et al.,* 2006).

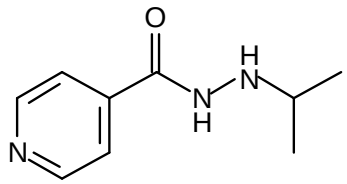

Iproniazid

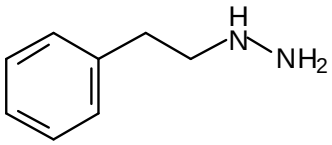

Phenelzine

Figure 2.23 The chemical structures of selected antidepressant MAO-A inhibitors.

2.2.9 Mechanism of action of MAO-B

2.2.9.1 General background

Monoamine oxidase A and B are mitochondrial bound flavoproteins that catalyze the oxidative deamination of neurotransmitters and biogenic amines. A number of mechanism-based inhibitors have been developed for clinical use as antidepressants and as neuroprotective drugs. The binding of substrates or inhibitors to MAO-B involves an initial negotiation of a protein loop, occurring near the surface of the membrane and two hydrophobic cavities, an éentranceôcavity and an éactive siteôcavity. These two cavities can either be separate or in a fused state, depending on the conformation of the Ile-199 side chain, which appears to function as a gate. The amine functional groups of the bound substrate approaches the *re* face of the bent and épuckeredôcovalent FAD through an éaromatic cageôformed by two tyrosine residues that are perpendicular to the plane of the flavin ring. No amino acid residues that may function as acids or bases are found near the catalytic site (Edmondson *et al*., 2004).

A breakthrough to our understanding of the molecular properties of MAO-A and -B was the cloning and sequencing of the respective genes for these two enzymes, which convincingly demonstrated that MAO-A and -B are two separate enzymes that share many similar properties such as the same type of covalent flavin, an 8Ŭ-S-cysteinyl FAD and a 70% sequence identity (Bach *et al.,* 1988).

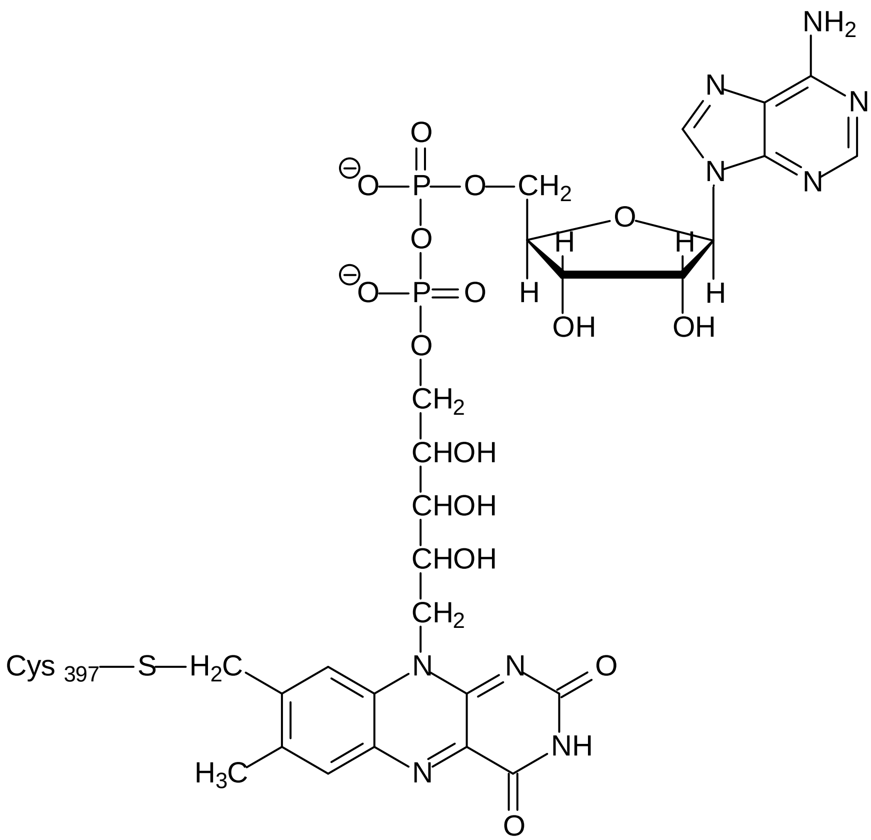

Figure 2.24 The chemical structure of covalent FAD in MAO

Both MAO-A and ï B contain covalently bound FAD as their only redox cofactor that is absolutely required for catalysis. The site of covalent attachment of the flavin to either enzyme, is via a thioether linkage between a cysteinyl residue and the 8Ŭ-methylene of the isoalloxazine ring (Kearney *et al.,* 1971). In MAO-B, the cysteine linkage is to Cys397 while in MAO-A, Cys406 is the residue involved (Bach *et al.,* 1988). In both enzymes, the site for covalent linkage is toward the C-terminal portion of the molecule. In the case of MAO-A, a Cys406Ala mutant shows that the enzyme can function with a non-covalently bound FAD. Additional post-translational modifications of MAO-A and -B include acetylation of their respective N-termini. In the case of MAO-A, the amino-terminal methionine residue, remains with the protein and is N-acetylated. For MAO-B, the amino terminal methionine residue is cleaved from the protein on processing the nascent polypeptide chain and the resulting N-terminal serine is acetylated both in the recombinant human and in the bovine enzymes. No other post-translational modifications such as glycosylation or covalent lipid attachments are observed (Newton-Vinson *et al.,* 2000).

2.2.9.2 The Singel electron transfer (SET) and polar-nucleophilic pathway

The reaction catalyzed by MAO-A or -B is the oxidative deamination of primary, secondary and tertiary amines as depicted in the following reaction:

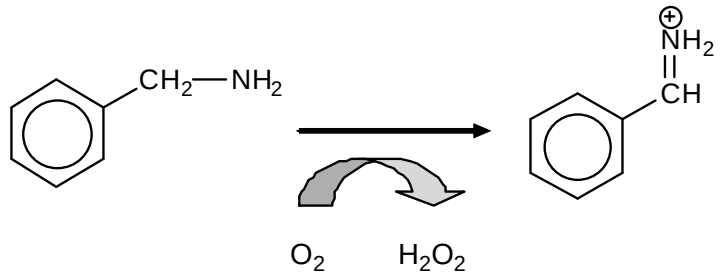

Figure 2.25 The oxidation of benzylamine by MAO.

The catalytic pathway for MAO-B catalysis has been demonstrated to be dependent on the nature of the substrate. For benzylamine and its analogues, the lower loop of the pathway in figure 2.26 is operative. When phenylethylamine is the substrate, kinetic studies show the imine product dissociates from the reduced enzyme, leaving the free reduced enzyme to react with O_2 in the rate limiting step (the top loop of the pathway in figure 2.26). Kinetic studies with MAO-A show that catalysis occurs via the lower loop for the substrates tested. A major difference in steady state catalytic properties on comparison of MAO-A with MAO-B is their respective K_m (O_2) values. MAO-A exhibit a K_m (O_2) of 6 ε M while the corresponding value for MAO-B is 250 ε M. Therefore, at saturating concentration of the amine substrate, MAO-A is operating at a maximal velocity while MAO-B is operating at approximately half-maximal velocity under physiological conditions (Ramsay, 1991).

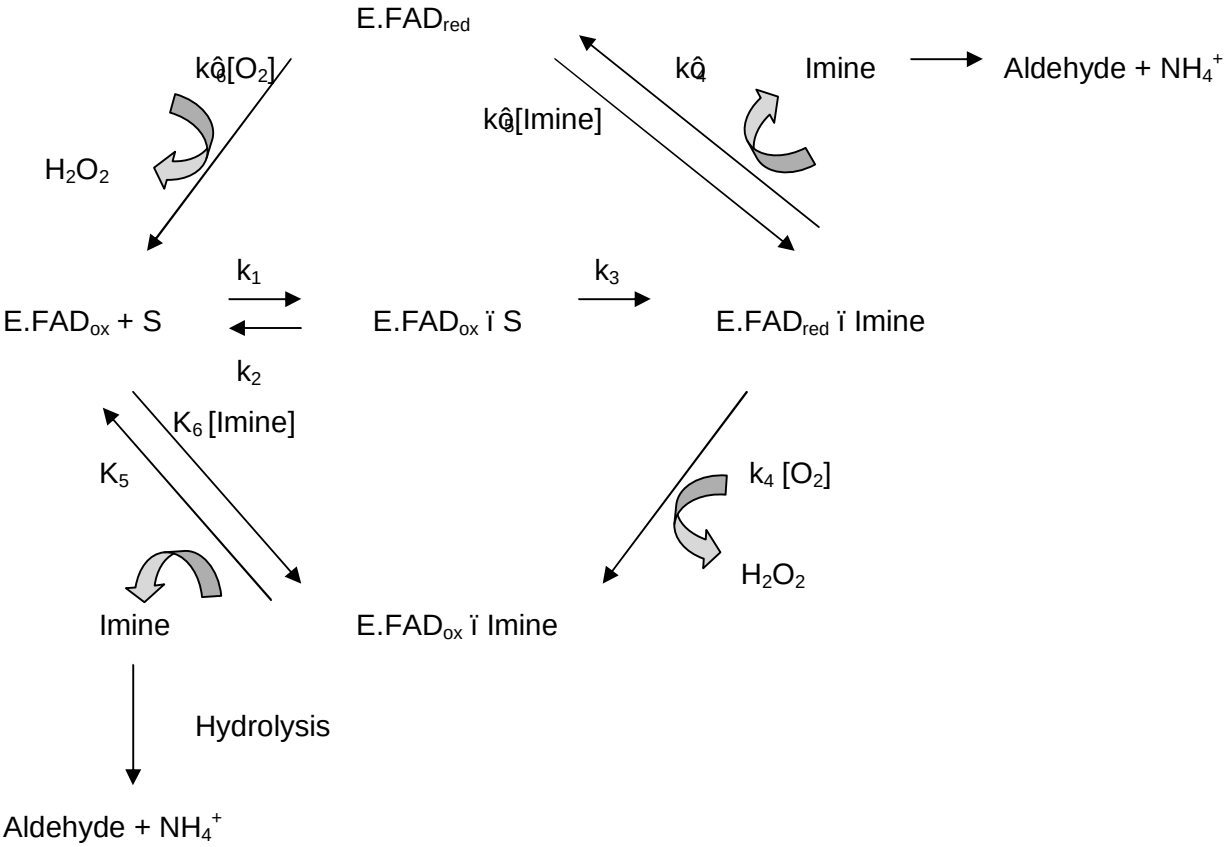

Figure 2.26 Reaction pathway for MAO catalysis.

Two proposals have been suggested for the detailed mechanism of electron transfer from the amine to the flavin in MAO catalysis. The following discussion will assume that MAO-A and MAO-B operate by similar mechanisms for C-H bond cleavage and flavin reduction. A single electron transfer (SET) mechanism has been proposed by Silverman (1992) based on a large number of studies using cyclopropylamines and other amine analogues (Silverman, 1992). This mechanism is shown in figure 2.27. The first step in the reaction is a one-electron oxidation of the lone pair on the amine nitrogen to form an aminium cation radical and a flavin radical. Formation of the aminium radical results in a lowered pKa of the Ŭ-C-H, which is proposed to permit H^+ abstraction by an active site base in the catalytic site. The structural data on MAO-B shows no amino acid residue in the catalytic site that could perform this role. Other experimental probes for a radical pair, such as magnetic field dependence of the rate of flavin reduction or spectral monitoring for any intermediate flavin radical anion or neutral species

during stopped-flow experiments, have also failed to provide any support for an SET mechanism as dipicted in figure 2.27 (Miller *et al.,* 1995).

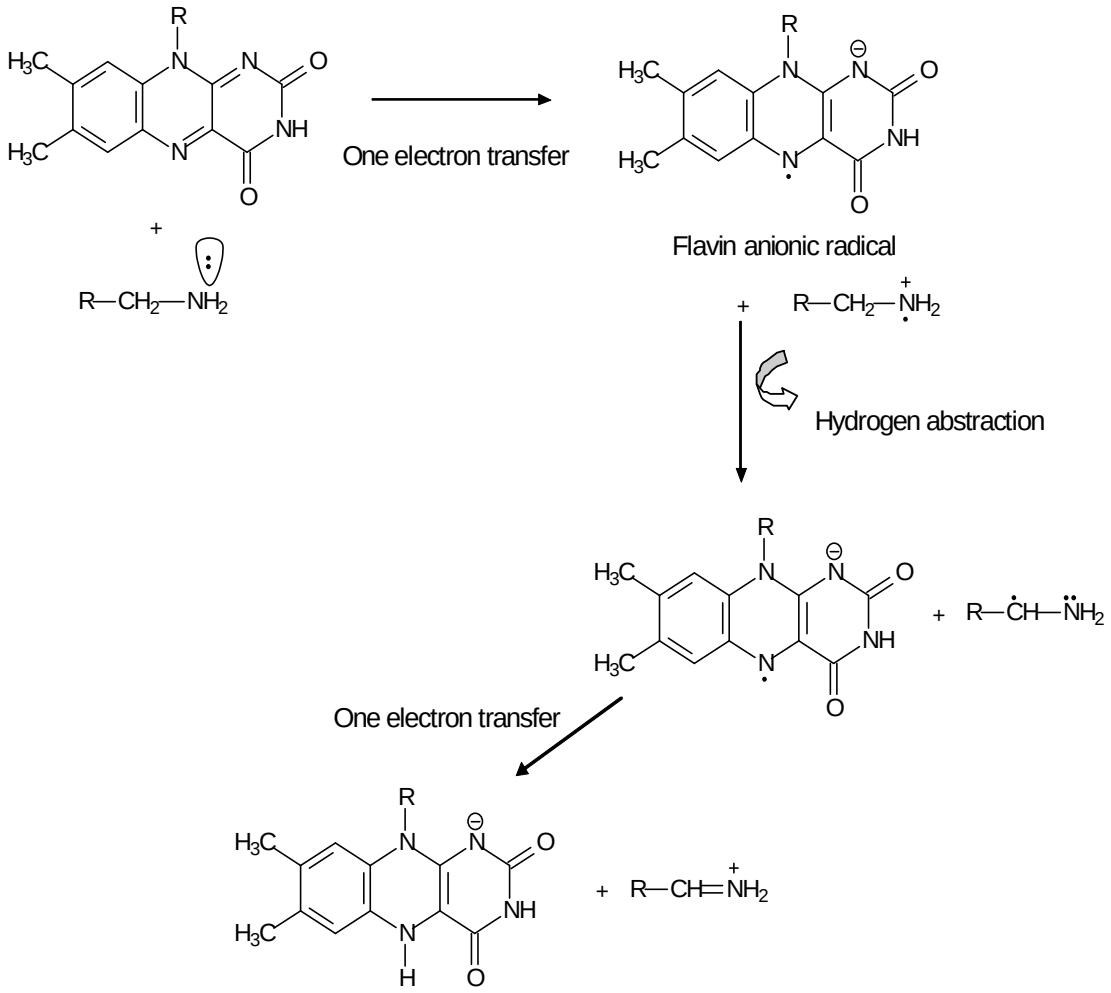

Figure 2.27 Single electron transfer (SET) mechanism proposed for MAO catalysis.

In the polar nucleophilic mechanism (Figure 2.28), the deprotonated amine attacks the flavin at the C-(4a) position as the initial step in catalysis. Flavin C-(4a)-nucleophile adducts have been identified in both model systems and in other flavoenzyme systems. Structural data show that the tranylcypromine complex with MAO-B is a flavin C-(4a) adduct. On formation of such an adduct, the N-(5) position of the flavin becomes a strong base, which would exhibit sufficient basicity to abstract the Ŭ-pro-R-H from the substrate. This proton-transfer step probably occurs as a concerted reaction, however, this designation still requires experimental verification. The

proximity of the benzyl C-H bond with the N-(5) of the flavin, is consistent with the absolute stereochemistry exhibited for C-H transfer (Edmondson *et al*., 2004).

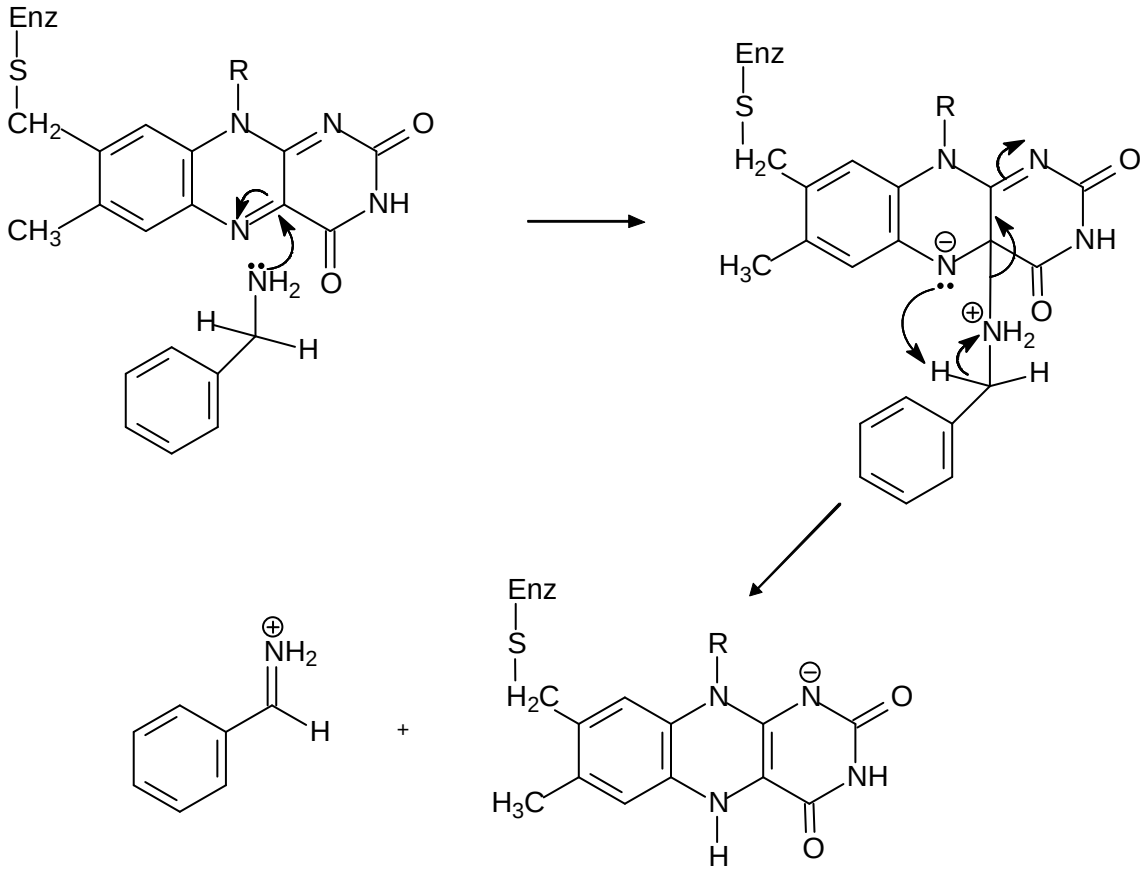

Figure 2.28 Polar nucleophilic mechanism proposed for MAO catalysis.

2.2.10 Three-dimensional structure of MAO-B

MAO-B is a mitochondrial outer membrane flavoenzyme that is a well-known target for antidepressant and neuroprotective drugs. The enzyme binds to the membrane through a C-terminal transmembrane helix and apolar loops, located at various positions in the sequence. The electron density shows that pargyline, a co-crystallized ligand and an analogue of the clinically used MAO-B inhibitor selegiline, binds covalently to the flavin N5 atom. The active site of MAO-B consists of a 420 Å^3-hydrophobic substrate cavity interconnected to an entrance cavity of 290 Å^3. The recognition site for the substrate amino group is an aromatic cage formed by Tyr-398 and Tyr-435. The structure provides a framework for probing the catalytic

mechanism, understanding the differences between the MAO-A and -B isoforms and designing specific inhibitors. The human MAO-B structure was solved by the single isomorphous replacement method combined with multicrystal 12-fold averaging. These results reveal the architecture of the catalytic centre and of sites on the protein that are important for its binding to the outer membrane of the mitochondrion (Binda *et al.,* 2001).

The 520 amino acids of MAO-B fold into a compact structure that exhibit a topology initially found in *p*-hydroxybensoate hydroxylase and then observed in several other flavoproteins. The crystal structure shows that the enzyme is dimeric, which is unlikely to be a crystal packing artifact because the dimer is present in the two crystal forms (orthorhombic and triclinic) employed in the structure determination. The monomer-monomer interactions are indeed extensive (Binda *et al.,* 2001), with each monomer consisting of a globular domain anchored to the membrane through a C-terminal helix. The MAO-B active site consists of two cavities, the substrate cavity in front of the flavin and the entrance cavity located underneath the protein surface and closed by the loop formed by residues 99-112 (Binda *et al.,* 2007). MAO-B is tightly bound to the outer mitochondrial membrane, as evidenced by the need for digestion of phospholipids for its efficient detergent extraction. The protein region responsible for membrane attachment is formed by the C-terminal amino acids, 461-520. Analysis of the MAO-B amino acid sequence, predicts that residues 489-515 form a transmembrane helix, 27 amino acids long, which is well within the range of values observed for transmembrane helices in membrane proteins of known three-dimensional structures (Binda *et al.,* 2001).

The crystal structure reveals that the C-terminal residues form an extended polypeptide chain, that traverses the monomer surface. This extended chain is followed by a Ŭ-helix that initiates at Val-489, forming the predicted transmembrane helical segment. The helix of each monomer protrudes from the basal face of the dimer, with each helical axis approximately parallel to the molecular two-fold axis. This observation suggests that the dimer binds to the membrane with its two-fold axis perpendicular to the membrane plane and the C-terminal helices inserted in the lipid bilayer. In addition to the C-terminal helical segment, the structure shows that other protein regions may be involved in membrane binding (Ulmschneider & Sansom, 2001).

A B

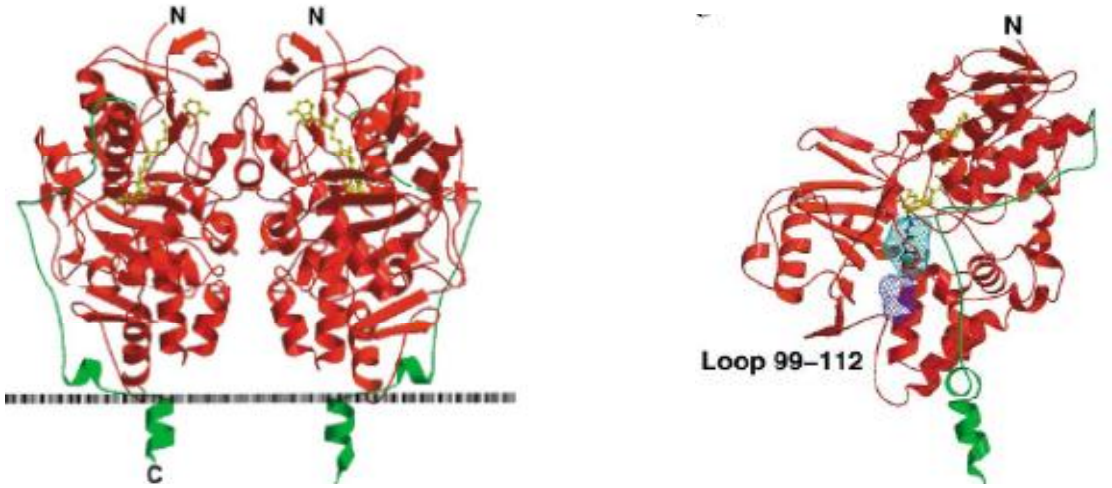

Figure 2.29 Panel A shows a ribbon diagram of the MAO-B dimer with the two-fold axis vertical in the plane of the paper. Panel B shows the cavities constituting the substrate path from the protein surface to the flavin in the MAO-B monomer (Binda *et al.,* 2001).

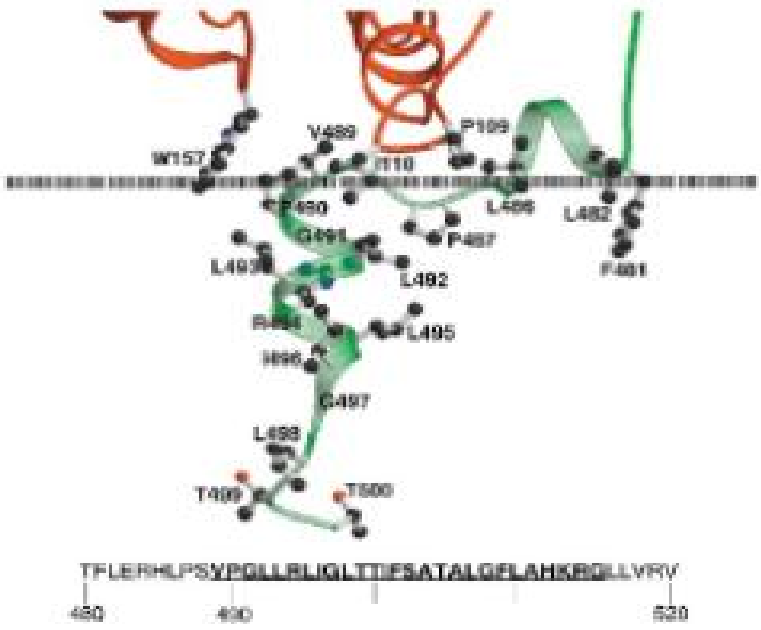

Figure 2.30 The membrane binding region in the structure of human MAO-B (Binda *et al*., 2001).

The electron density map shows that pargyline covalently binds to the N-5 atom at the *re* side of the flavin in a solvent inaccessible environment. The substrate binding site is formed by a flat cavity with a volume of 420 Ù^3. This cavity is lined by a number of aromatic and aliphatic amino acids, providing the highly hydrophobic environment, predicted by substrate specificity and quantitative structure-activity relationship studies. Adjacent to the substrate cavity is a separate, smaller hydrophobic cavity lined by residues Phe-103, Pro-104, Trp-119, Leu-164, Leu-167, Phe-168, Leu-171, Ile-199, Ile-316 and Tyr-326. This second cavity is situated between the active site and the protein surface, and is shielded from solvent by loop 99-112. Residues Tyr-326, Ile-199, Leu-171 and Phe-168 are the side chains that separate the two cavities. After a substrate reaches the ócentrance cavityô a transient movement of the four residues separating the entrance from the substrate cavities must occur to allow its diffusion into the active site (Walker & Edmondson, 1994).

Safinamide and the related coumarin derivatives (Figure 2.31), respresent new MAO inhibitors with promising therapeutic properties. On comparison of their interaction with purified recombinant human MAO-A and -B, it was found that safinamide exhibits a >700-fold selectivity for human MAO-B. 7-(3-Chlorobenzyloxy)-4-(methylamino)methyl-coumarin and 7-(3-chlorobenzyloxy)-4-carbox-aldehyde-coumarin showed tighter binding to human MAO-B than to human MAO-A, although their isoform selectivity is less pronounced than that of safinamide. The crystal structures of human MAO-B in complex with the three inhibitors revealed that they all bind noncovalently to the enzyme, which represents a desirable property to minimize toxic side effects since *de novo* protein synthesis is not required for the recovery of enzymatic activity. Safinamide and the coumarin derivatives bind to human MAO-B by traversing the active site cavities in their entire length. This contributes to the high selectivity of these inhibitors because the active site of human MAO-A does not have this bipartite cavity (De Colibus *et al.,* 2005).

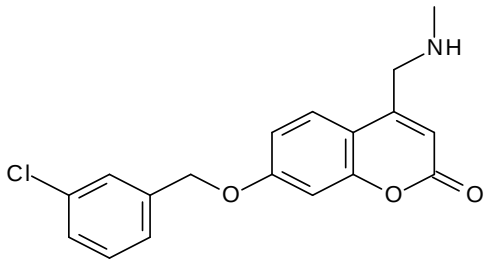

7-(3-Chlorobenzyloxy)-4-(methylamino)methyl-coumarin

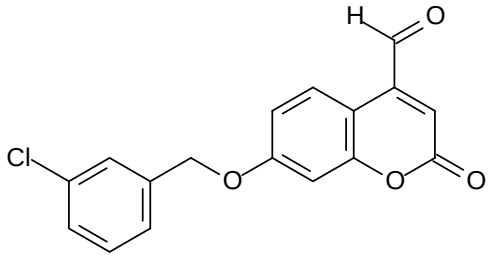

7-(3-Chlorobenzyloxy)-4-carboxaldehyde-coumarin

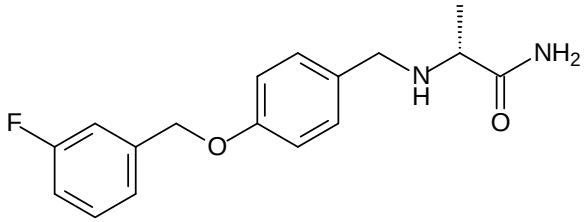

Safinamide

Figure 2.31 The chemical structures of the related coumarin derivatives and safinamide

These inhibitors have polar substituents that orient their binding mode to the hydrophilic space in front of the flavin to establish H-bond interactions both with conserved water molecules and with protein residues. These H-bond interactions were not found in the structures of other MAO-B complexes with reversible inhibitors, where binding interactions were generally Van der Waals or hydrophobic contacts. Inspection of the structures reveals that a niche of the substrate cavity, lined by Tyr-60, Tyr-326 and Gln-206 remains unoccupied in the safinamide complex, whereas it is filled by the pyran ring of the coumarin derivatives. Conversely, safinamide occupies the hydrophilic part of the cavity with its propionamide group extending more toward the flavin and replacing two water molecules found in the complexes with the coumarin compounds (Binda *et al.,* 2007).

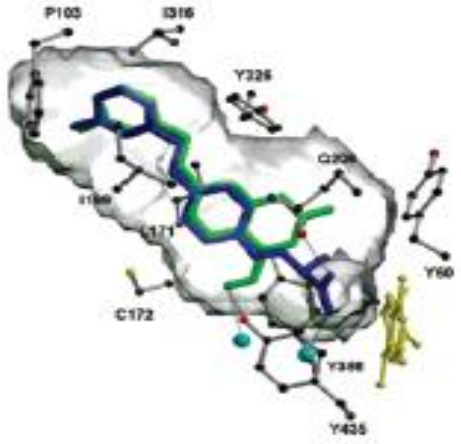

Fig 2.32 Safinamide (blue) and 7-(3-chlorobenzyloxy)-4-carboxaldehyde-coumarin (green) bound in the MAO B cavity. The active site residues and the flavin are drawn in gray and yellow, respectively. Hydrogen bonds established by the two inhibitors with protein residues and water molecules (cyan spheres) are shown as dashed lines (Binda *et al.,* 2007).

2.2.11 Three-dimensional structure of MAO-A

To understand the relationship between structure and function of MAO-A, the low-resolution rat MAO-A structure was extended to the high-resolution wild-type human MAO-A structure at 2.2 Ù. This high-resolution structure is similar to that of rat MAO-A and human MAO-B, but different from the known structure of human MAO-A, specifically regarding residues 108-118 and 210-216, which surround the substrate/inhibitor cavity. These structures show that the inhibitor selectivity of MAO-A and -B is caused by the structural differences arising from Ile-335 in MAO-A versus Tyr-326 in MAO-B. It has also been shown that the flexibility of loops 108-118 is essential for MAO-A activity. Since the flexibility of loop 108-118 is facilitated by anchoring of the enzyme into the membrane, attachment of the enzyme to the mitochondrial membrane is critical for the function of the enzyme. Studies showed that the 29 C-terminal residues in MAO-B are responsible for targeting and anchoring the protein to the mitochondrial outer membrane. A C-terminal truncation leads to a significant decrease in MAO-B catalytic activity, but does not produce any significant change in inhibitor specificity. This result further demonstrates that C-terminal anchoring for MAO-A and ï B must be important for their biological functions.

Interestingly, the human MAO-As are monomers rather than dimers, as in the case of MAO-B (Son *et al.,* 2008).

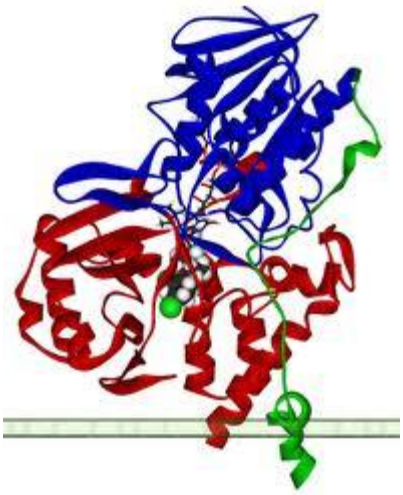

Figure 2.33 The structure of human MAO-A (Son *et al.,* 2008).

Dimethyldecylphosphine oxide (DMDPO), the detergent used in crystallizing the protein, was found to be present in the MAO-A crystal structure. The molecules were surrounded by three aromatic residues and a proline: Trp-116, Trp-491, Tyr-121 and Pro-118. *In vivo*, the DMDPO site is likely occupied by phospholipid in the mitochondrial outer membrane. In addition, the horizontal arrangement of the positively charged residues (Arg-129, His-148, Lys-151, Lys-163, Arg-493, Lys-503, Lys-520 and Lys-522) that may interact with the phospholipid hydrophilic head groups, indicates the location of the outermembrane surface, as shown in figure 2.34. A one-turn helix, parallel to the membrane surface, is thought to be buried in the membrane (Ma *et al.,* 2004).

Sixteen residues surround the substrate/inhibitor cavity of MAO-A, and six of the 16 residues differ between MAO-A and -B. Harmine, a reversible inhibitor, was co-crystallized in the active site cavity of the enzyme. It interacts with Tyr-69, Asn-181, Phe-208, Val-210, Gln-215, Cys-323, Ile-325, Ile-335, Leu-337, Phe-352, Tyr-407, Tyr-444 and FAD. Seven water molecules occupy the space between the inhibitor and these groups. The inhibitor and the FAD are bridged through two water molecules by hydrogen bonds. The amide group of the Gln-215 side chain interacts tightly with harmine by a ´ - ´ interaction (Ma *et al.,* 2004).

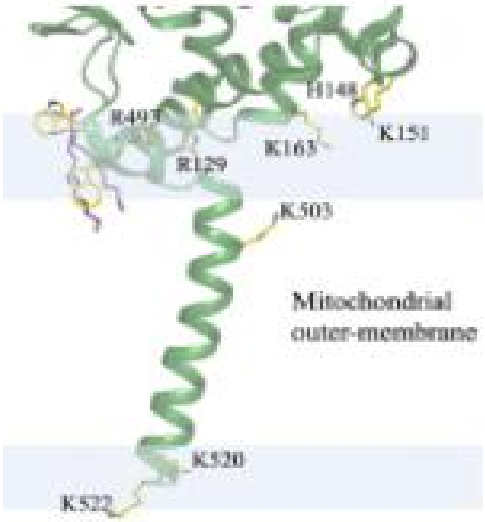

Figure 2.34 Binding model of MAO-A into the mitochondrial outer membrane (Son *et al.,* 2008).

2.2.12 Animal models of PD

2.2.12.1 MPTP

In the early 1980s several drug users from northern California developed an acute state of akinesia following the intravenous injection of a street preparation of 1-methyl-4-phenyl-4-propionpiperidine (MPPP) (Figure 2.35), an analog of the narcotic meperidine. It was found that MPTP, which was inadvertently produced during the illicit synthesis of MPPP, was responsible for this clinical picture (Bové *et al.,* 2005).

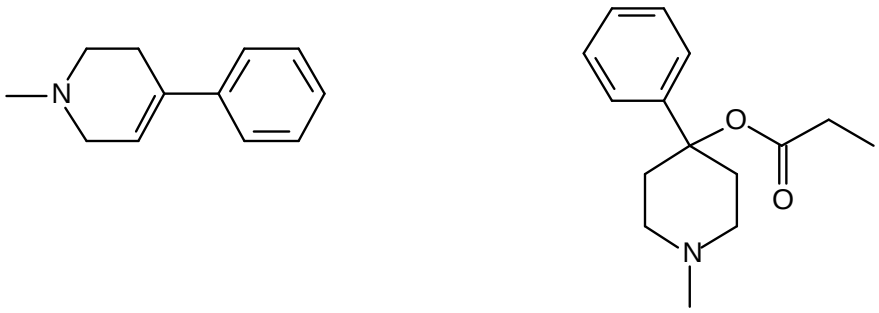

MPTP MPPP

Figure 2.35 The chemical structures of MPPP and MPTP.

It is widely believed that the nigrostriatal toxicity of MPTP is due to its oxidation by brain MAO, first to 1-methyl-4-phenyl-2,3-dihydropyridium ($MPDP^+$), and eventually to 1-methyl-4-phenylpyridinium (MPP^+). Following uptake by the synaptic DA reuptake system, it is concentrated in the matrix of striatal mitochondria by an energy-dependent carrier, energized by the electrical gradient of the membrane. At the very high intramitochondrial concentrations thus reached, MPP^+ inhibits NADH dehydrogenase. This leads to cessation of oxidative phosphorylation, ATP depletion, and cell death. The reports that MPTP causes acute parkinsonian symptoms, DA depletion, and nigrostriatal degeneration in man, monkeys and some other susceptible species, offer an animal model for PD. It was discovered that brain MAO, particularly the B type, has to oxidize MPTP to neurotoxic products and that MAO-B inhibitors block the neurotoxicity *in vivo.* Although both forms of MAO oxidize MPTP sufficiently and rapidly *in vitro* to give rise to toxic concentrations of MPP^+, *in vivo* only the B type plays a role, as judged by the complete prevention of the toxicity of MPTP by MAO-B inhibition. This is so because product inhibition of MAO-A rapidly halts its action while MAO-B is much less sensitive to inactivation by $MPDP^+$ and MPP^+ (Singer ***et al.,*** 1988).

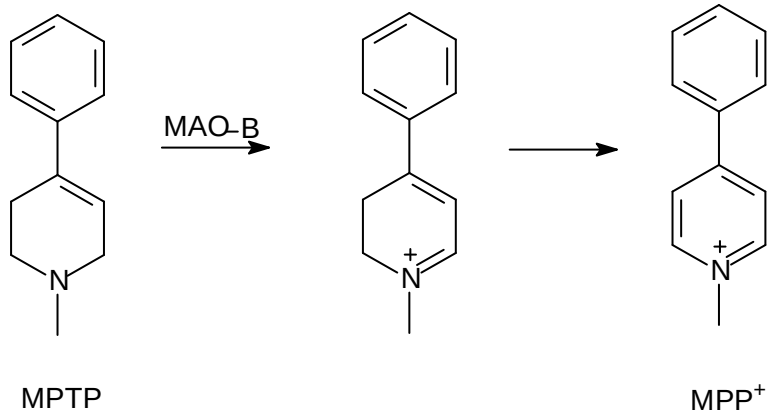

MPTP MPP^+

Figure 2.36 The chemical reaction of MPTP to MPP^+.

Endothelial cells in the microvasculature, that make up the BBB, contain MAO and several studies have correlated levels of MAO with MPTP-induced neuronal loss. Since MPP^+ cannot be transported through the BBB, this level of toxification/detoxification can provide a first line of defense against exogenous agents (Smeyne & Jackson-Lewis, 2005).

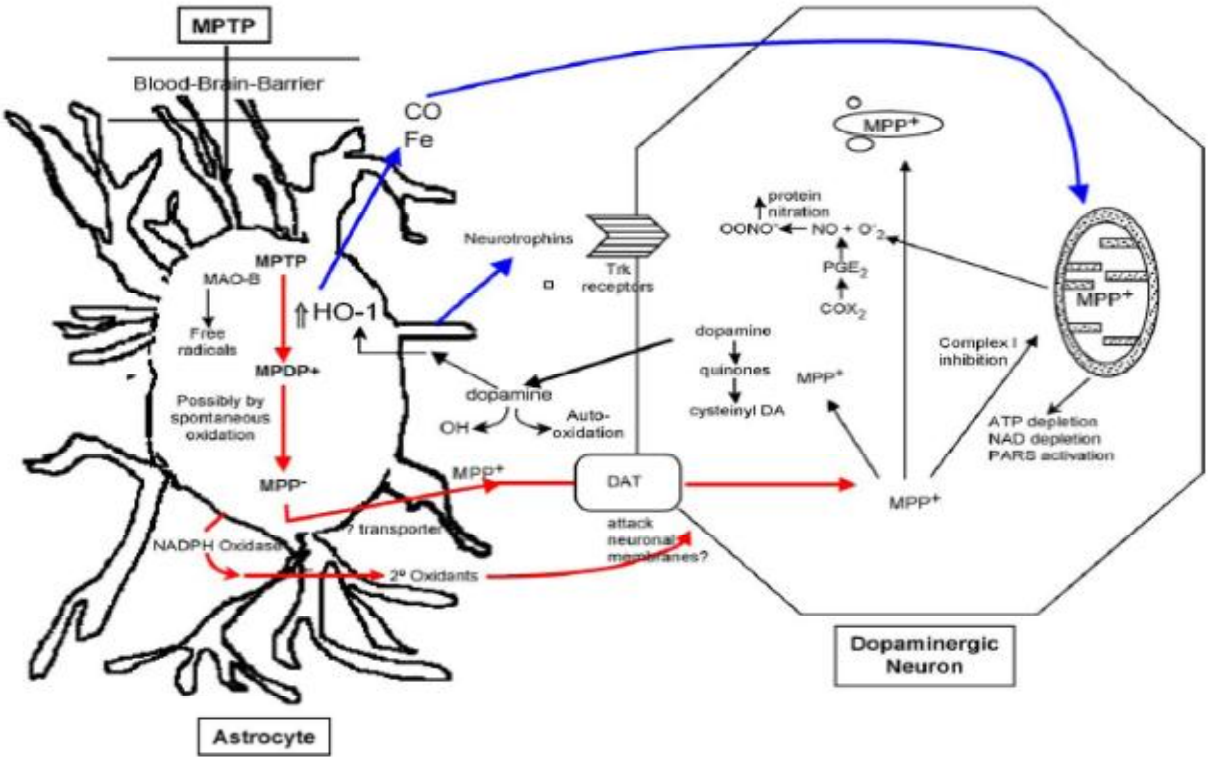

Figure 2.37 Schematic representation of the mechanism of MPTP action in the nigrostriatal system (Smeyne & Jackson-Lewis, 2005).

MPTP, that is not converted to MPP^+ in the periphery, rapidly enters the brain, where it is taken into glial cells by a number of mechanisms, including monoamine and glutamate transporters or pH-dependent antiporters (Brooks *et al.,* 1989). Glial cells also contain large pools of MAO, and also convert MPTP from its protoxin form to MPP^+ (Ransom *et al.,* 1987). Once MPP^+ is released into the extracellular space, MPP^+ is taken up into dopaminergic cells by the DA transporter (DAT). Once in the neuronal cell, MPP^+ can move through several cellular compartments: it can enter into mitochondria where it interferes with complex I of the electron transport chain or it can be sequestered into cytoplasmic vesicles via the vesicular monoamine transporter (Brooks *et al.,* 1989).

Whether MPP^+, taken up at the terminals in the striatum, exerts its destructive effect locally or is first transported to the cell body in the SN, remains unresolved. It is significant that mazindol, a reuptake inhibitor, protects mice against MPTP toxicity. Though the inhibition by MPP^+, as that

caused by barbiturates and rotenone, is non-covalent and hence reversible, the damage caused by MPP^+ is permanent, for once the ATP supply is cut off, the cell dies and nigrostriatal cells do not regenerate (Singer *et al.,* 1988).

Although complex I inhibition by MPP^+ (Figure 2.38) reduces energy production within dopaminergic neurons, it is likely that this is not the immediate cause of the SNpc neuronal death. The damage done within these dopaminergic neurons is likely to result from compounds generated in the cell, secondary to energy depletion. The formation of the superoxide radical is one example of this process. Cleeter *et al.* (1992) showed that MPP^+, following inhibition of mitochondrial complex I activity, results in an excessive amount of superoxide radicals within the neuronal cytosol. Further support for the role of superoxide radicals came from Przedborski *et al.* (1992), who demonstrated that over expression of the copper-zinc form of superoxide dismutase in mice is neuroprotective against the damaging effect of MPTP.

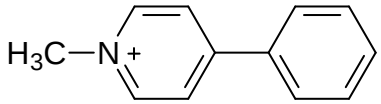

MPP+

Figure 2.38 The chemical structure of MPP^+.

2.2.13 6-Hydroxydopamine (6-OHDA).

6-OHDA, the first toxin used to create animal models of PD, was introduced more than 30 years ago. Although 6-OHDA-induced pathology differs from PD, it is still extensively used. 6-OHDA-induced toxicity is relatively selective for monoaminergic neurons, as a result of preferential uptake by DA and noradrenergic transporters (Luthman *et al.,* 1989). Inside neurons, 6-OHDA accumulates in the cytosol, and generates quinones that attack nucleophilic groups. Because 6-OHDA cannot cross the blood-brain barrier, it must be administered by local stereotaxic injection into the SN, median forebrain bundle, or striatum, to target the nigrostriatal dopaminergic pathway (Javoy *et al.,* 1976). So far, however, none of the modes of 6-OHDA intoxication have led to the formation of LB-like inclusions. For striatal stereotaxic lesions, 6-OHDA is injected unilaterally, with the contralateral side serving as control (Ungerstedt, 1971).

6-OHDA shares some structural similarities with DA and NA, exhibiting a high affinity for several catecholaminergic plasma membrane transporters such as the DAT and norepinephrine transporters (NET). With respect to its mode of action, it is well accepted that 6-OHDA destroys catecholaminergic structures by a combined effect of ROS and quinones. This view stems primarily from the demonstration that 6-OHDA, once dissolved in an aerobic and alkaline milieu, readily oxidizes, yielding H_2O_2 and *para*-quinone (Bové *et al.,* 2005).

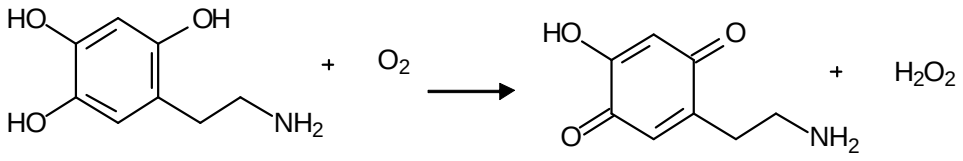

Figure 2.39 The oxidation of 6-OHDA.

Like other parkinsonian neurotoxins to be discussed here, 6-OHDA can be administered by systemic injection. However, contrary to MPTP, rotenone or paraquat, this route of administration will not produce the desired nigrostriatal lesion. Instead, this route of 6-OHDA administration will lead to damage of the peripheral nervous system. After 6-OHDA injections into the substantia nigra or the medial forebrain bundle, dopaminergic neurons start to die within the first 24 hours and show a nonapoptotic morphology. Maximal reduction of striatal DA levels are reached within 3-4 days after lesion, and in most studies, residual striatal DA content is less than 20% of controls (Faull & Laverty, 1969). In contrast, unilateral injections cause a typical asymmetric circling motor behaviour whose magnitude in rodents depends on the degree of the nigrostriatal lesion. This specific behavioural abnormality is most prominent after administration of drugs that stimulate dopaminergic receptors, such as apomorphine. Quantification of this turning behaviour has been used extensively to assess the antiparkinsonian potency of new drugs, transplantation, and gene therapies and to study the motor fluctuations after the chronic treatment with L-dopa (Bové *et al.,* 2002).

2.2.14 Rotenone

Among the animal models of PD, rotenone represents one of the most recently used approaches. Rotenone is a member of the rotenoids, a family of natural cytotoxic compounds

extracted from various parts of *Leguminosa* plants. Rotenone is widely used as an insecticide and fish poison. Like MPTP, retonone is highly lipophilic and thus readily gains access to all organs, including the brain. After a single intravenous injection, rotenone reaches maximal concentration in the CNS within 15 min and decays to about half of this level in less than 2 hours. Its brain distribution is heterogeneous. In mitochondria, rotenone impairs oxidative phosphorylation by inhibiting complex I of the electron transport chain (Schuler & Casida, 2001).

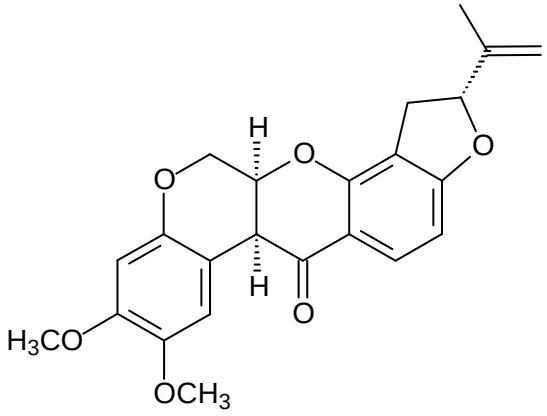

Figure 2.40 The chemical structure of rotenone.

Oral delivery of rotenone appears to cause little neurotoxicity in animals. Systemic administration, on the other hand, often causes toxicity and lethality, the degree of which is related to the dose used. Stereotaxic injection of rotenone into the median forebrain bundle depletes striatal DA and 5-HT. Rats treated for a week with 10-18 mg/kg-day of rotenone by intravenous infusion show bilateral lesions of the striatum and the globus pallidus, characterized by neuronal loss and gliosis. Greenamyre and collaborators have found that intravenous and subcutaneous infusion of 2-3 mg/kg-day of rotenone, for about 3 weeks to rats, does produce nigrostriatal dopaminergic neurodegeneration (Betarbet *et al*., 2000).

2.2.15 Paraquat

The herbicide paraquat (N,Nôdimethyl-4-4ôbipyridinium) also induces parkinsonism in animals. Paraquat also shows structural similarity to MPP^+ and is present in the environment (Liou *et al.,* 1997). Paraquat toxicity is mediated by redox cycling with a cellular diaphorase, such as nitric oxidase synthase, yielding ROS (Day *et al.,* 1999). Paraquat does not easily penetrate the

blood brain barrier (BBB), and its CNS distribution does not parallel any known enzymatic or neuroanatomic distribution (Shimizu *et al.,* 2001). However, paraquat enters the brain via the assistance of L-neutral amino acid transports, since pretreatment of animals with L-valine or L-phenylalanine completely prevents neurodegeneration. Investigators also found selective nigral dopaminergic cell loss in mice injected with paraquat (Bové *et al*., 2005). The toxicity of paraquat appears to be mediated by the formation of superoxide radicals. Systemic administration of paraquat to mice, leads to SNpc dopaminergic neuron degeneration accompanied by Ŭ-synuclein immunostaining in the frontal cortex (Manning-Bog *et al.,* 2002).

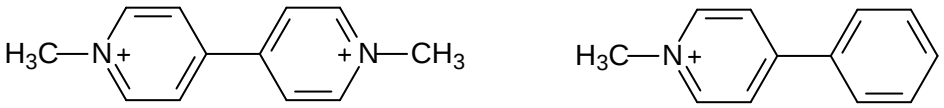

Paraquat MPP^+

Figure 2.41 Comparison of the chemical structures of MPP^+ and paraquat.

2.2.16 Copper-containing amine oxidases

A distinct class of copper-containing, semicarbazide-sensitive amine oxidases (SSAOs), expressed on the cell surface and in soluble forms, oxidatively deaminate primary amines. Via transient covalent enzyme-substrate intermediates, this reaction results in production of aldehydes, hydrogen peroxide and ammonium, which are all biologically active substances (Jalkanen & Salmi, 2001).

Amine oxidases (AOs) have been traditionally divided into two main groups, based on the chemical nature of the attached cofactor as can be seen in figure 2.42. The FAD-containing enzymes are intracellular enzymes (Shih *et al.,* 1999). The other class of AOs contains a cofactor, which is topa-quinone (TPQ) in most cases (Klinman & Mu, 1994). These enzymes include diamine oxidases, lysyl oxidase and the plasma membrane and soluble AOs. These enzymes are collectively designated as SSAOs due to their characteristic sensitivity of inhibition by a carbonyl-reactive compound, semicarbazide (Jalkanen & Salmi, 2001).

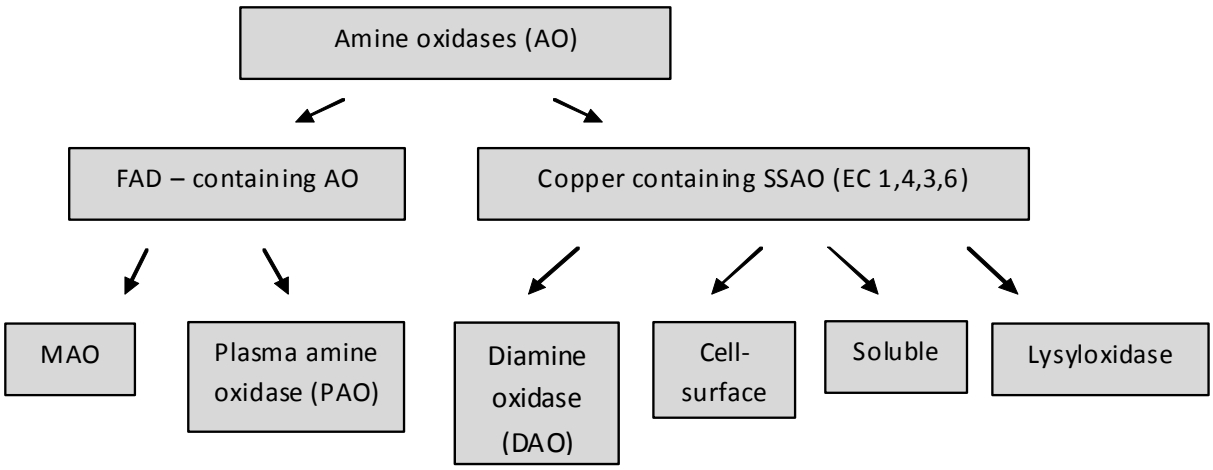

Figure 2.42 The classification of AOs.

The TPQ-containing semicarbazide-sensitive amine oxidases (SSAOs) are mostly soluble or expressed on the cell surface, and have different preferred substrates and are insensitive or only weakly sensitive to classical MAO inhibitors (Lyles, 1996). SSAOs have been historically defined by their inhibition with carbonyl-reactive compounds like semicarbazide. Various other compounds, including propargylamine, aminoguanidine, carbidopa and procarbazine are also inhibitors of SSAOs (Tabor *et al.,* 1954).

Most SSAOs are dimeric glycoproteins with molecular masses of 140-180 kDa. SSAOs contain two atoms of copper per dimer (Klinman & Mu, 1994). TPQ is generated from an intrinsic tyrosine of the molecule by a self-processing event that only requires the bound copper ion and molecular oxygen (Mu *et al.,* 1992). There are three conserved histidines in SSAOs, which coordinate the copper atoms. One His-X-His motif is approximately 50 residues towards the C-terminal from the cofactor and the other histidine is approximately 20-30 residues toward the N-terminus from the cofactor. A conserved Asp residue, ~100 residues towards the N-terminal from the TPQ, is important since it serves as a catalytic base in the reductive half-reaction (Jalkanen & Salmi, 2001).

SSAOs exist in soluble forms, as well as in a membrane-bound form (Lyles, 1996). There has been considerable disagreement as to whether the soluble form is a product of a different gene or a cleavage product of the transmembrane form of SSAO (Jalkanen & Salmi, 2001). All

SSAOs catalyse the oxidative deamination of primary amines in a reaction (Klinman & Mu, 1994):

$$R{-}CH_2{-}NH_2 + O_2 + H_2O \longrightarrow R{-}CHO + H_2O_2 + NH_3$$

The kinetic reaction consists of two half-reactions. First, the enzyme is reduced by the substrate with simultaneous release of the corresponding aldehyde. In the second part, the enzyme is reoxidated by molecular oxygen with concomitant release of H_2O_2 and ammonium (Jalkanen & Salmi, 2001). In bacteria and yeast, the SSAO reaction provides these microbes with a source of nitrogen when growing in the presence of various amines. In plants, on the other hand, the H_2O_2 released from the SSAO-catalysed reaction is used for wound healing (Klinman & Mu, 1994). Lysyl oxidase is unique amongst the SSAO family of enzymes. Although it is sensitive to SSAO inhibitors, it is considerably smaller than the other SSAOs, its primary sequence lacks certain critical motifs (e.g. the copper-coordinating histidines) and its cofactor appears to be lysine tyrosylquinone rather than TPQ (Wang *et al.,* 1997).

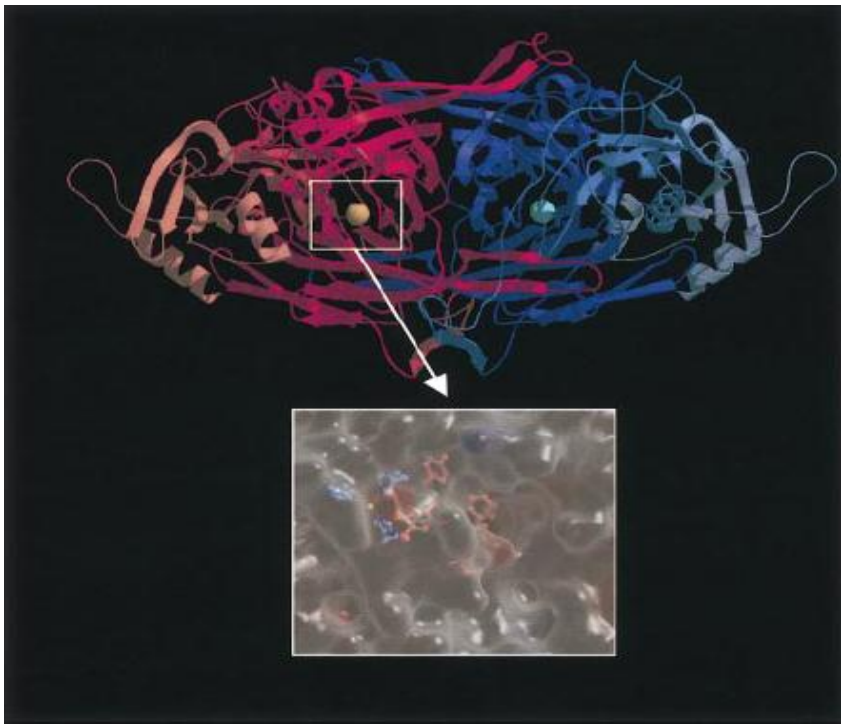

Figure 2.43 An overall fold of the catalytically active domain of an SSAO (Jalkanen & Salmi, 2001).

2.2.17 Enzyme kinetics

Enzyme kinetics play a role in the determination of inhibitor potency. The K_i value is the inhibitor constant. This constant expresses the inhibitorôs potency. The lower the value of K_i, the higher the inhibitorôs potency while the higher the value of K_i, the lower the inhibitorôs potency. A general equation for a chemical reaction between a substrate and enzyme can be illustrated as:

$$S + E \xrightarrow[V_i]{} SE$$

Where S is the substrate and E the enzyme, V_i is the velocity of the forward reaction. If the substrate is in excess compared to the enzyme, V_i will be directly proportionate to the enzyme concentration (V_i Ŭ [E]). When the substrate concentration increases, V_i will increase until V_{max} is reached where a further increase in substrate will have no effect on V_i. The enzyme is thus saturated. V_i is dependant on how quickly the substrate is released from the enzyme for another reaction. The Michaelis-Menten equation illustrates the relationship between initial reaction velocity V_i and substrate concentration [S], as shown graphically below:

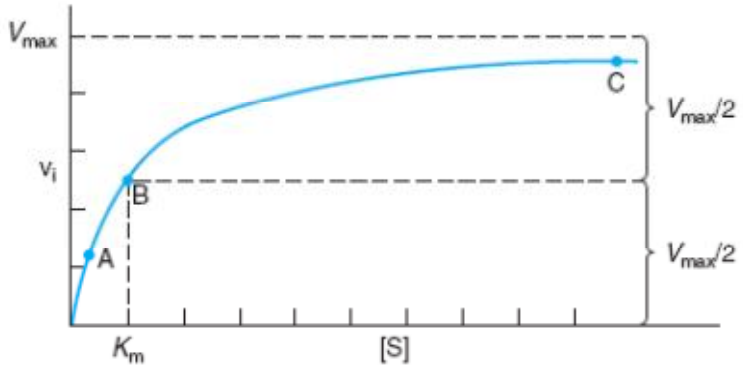

Figure 2.44 Effect of substrate concentration on the initial velocity of an enzyme-catalyzed reaction.

$$V_i = \frac{V_{\max}[S]}{K_m + [S]} \qquad 1)$$

The Michaelis constant K_m is the substrate concentration at which V_i is half the maximal velocity attainable at a particular concentration of enzyme. When [S] is much less than K_m, the term K_m + [S] is essentially equal to K_m. Replacing K_m + [S] with K_m reduces equation 1 to

$$V_i = \frac{V_{\max}[S]}{K_m + [S]} \qquad V_i \approx \frac{V_{\max}[S]}{K_m} \approx \left(\frac{V_{\max}}{K_m}\right)[S] \qquad 2)$$

When [S] is much greater than K_m, the term K_m + [S] is essentially equal to [S]. Replacing K_m + [S] with [S] reduces equation 2 to

$$V_i = \frac{V_{\max}[S]}{K_m + [S]} \qquad V_i \approx \frac{V_{\max}[S]}{[S]} \approx V_{\max} \qquad 3)$$

When [S]=K_m, the initial velocity is half-maximal

$$V_i = \frac{V_{\max}[S]}{K_m + [S]} = \frac{V_{\max}[S]}{2[S]} = \frac{V_{\max}}{2} \qquad 4)$$

Rearranging the Michealis-Menten equation into an equation for a straight line results in the equation:

$$\frac{1}{V_i} = \left(\frac{K_m}{V_{\max}}\right)\frac{1}{[S]} + \frac{1}{V_{\max}} \qquad 5)$$

This equation can now be used to create a graph which is called a double reciporcal or Lineweaver-Burk plot. K_m is thus most easily calculated from the x intercept, where x = -1/K_m

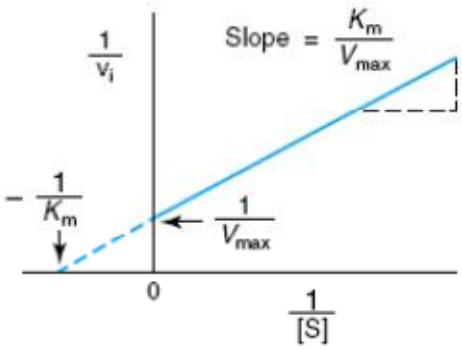

Figure 2.45 Double reciprocal or Lineweaver-Burk plot.

Double reciprocal plots distinguish between competitive and noncompetitive inhibitors and simplify evaluation of the inhibition constant, K_i. To construct the Lineweaver-Burk plot V_i is determined at several substrate concentrations both in the presence and in the absence of the inhibitor.

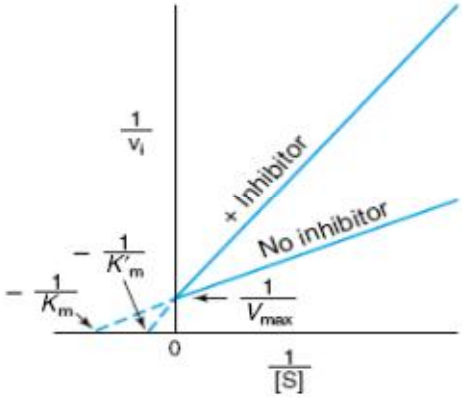

Figure 2.46 Lineweaver-Burk plots of competitive inhibition.

Thus, a competitive inhibitor has no effect on V_{max} but raises K_m, the apparent K_m for the substrate. For simple competitive inhibition, the intercept on the x axis is

$$x = \frac{-1}{K_m}\left(1 + \frac{[I]}{K_i}\right) \qquad 6)$$

Lineweaver-Burk plots of non-competitive inhibition typically exhibits a constant K_m value, while V_{max} decreases

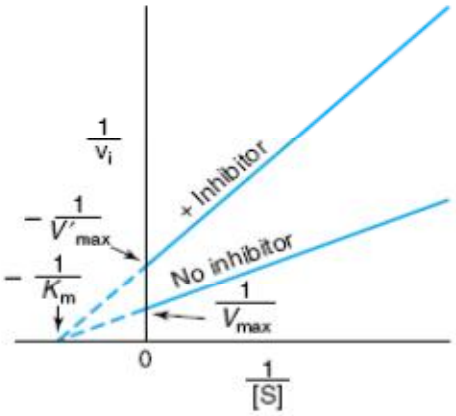

Figure 2.47 Lineweaver-Burk plots for simple non-competitive inhibition.

2.2.18 Conclusion

This chapter showed that PD is a neurodegenerative disease with a complex pathogenis. It further showed that the MAO enzyme is important in the neurodegeneration processes associated with PD and that inhibitors of those enzymes are important targets for the therapy of PD. This chapter discussed various aspects related to the MAO enzymes, such as the three-dimensional structures, possible mechanisms of catalysis and inhibition of those enzymes. It was also shown that MAO plays an important role in the generation of PD in animal models. Another class of enzymes, the SSAOs were also discussed, since they catalyse similar reactions than the MAOs. A brief introduction into enzyme kinetics was provided (Rodwell & Kennely, 2009).

Chapter 3

Synthesis

3.1 Introduction

As mentioned in the introduction chapter, the current study aims to synthesize twelve 8-thiocaffeine analogues (**4a–l**) and evaluate them as inhibitors of MAO-A and ï B. Although caffeine is a weak MAO-B inhibitor, substitution at C-8 with a variety of side chains have been shown to enhance the MAO-B inhibition potency of caffeine by several orders of a magnitude. The (E)-8-(3-chlorostyryl) substituent of CSC, for example, is an illustration of a substituent that enhances the MAO-B inhibition potency of caffeine to a large extent (Ikeda *et al.*, 2002). It has also been found that substitution of caffeine at C-8, with a benzyloxy side-chain, dramatically enhances the MAO-B inhibition potency of caffeine (Strydom *et al.,* 2010). In this study, caffeine will be substituted with a variety of substituents at C-8 of caffeine via a thioether linkage. One of the aims of this study is therefore to compare the MAO-B inhibition potencies of the 8-thiocaffeine analogues with the previously studied oxycaffeine analogues. Since the 8-substituted oxycaffeine are also reported to be MAO-A inhibitors, the 8-thiocaffeine analogues that will be synthesized here will also be evaluated as human MAO-A inhibitors. Table 3.1 illustrates the 8-thiocaffeine analogues that will be synthesized in this study.

Table 3.1. The structures of the 8-thiocaffeine analogues that will be examined in the current study.

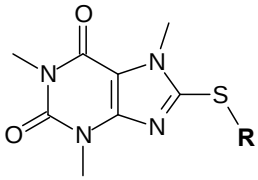

Compound	R	Compound	R
4a	C_6H_5	**4g**	$-CH_2-(4-OCH_3-C_6H_4)$
4b	$-CH_2-C_6H_5$	**4h**	$-(CH_2)_2-O-C_6H_5$
4c	$-(CH_2)_2-C_6H_5$	**4i**	$-C_6H_{11}$
4d	$-CH_2-(4-Cl-C_6H_4)$	**4j**	$-C_5H_9$
4e	$-CH_2-(4-Br-C_6H_4)$	**4k**	-2-Naphthalenyl
4f	$-CH_2-(4-F-C_6H_4)$	**4l**	$-(CH_2)_2-CH(CH_3)_2$

3.2 General synthetic approach for the synthesis of 8-thiocaffeine analogues (4a–l) and 8-chlorocaffeine.

8-Thiocaffeine analogues: A general synthetic route used for the preparation of 8-thiocaffeine analogues, makes use of 8-chlorocaffeine (**A**) as starting material (Figure 3.1) (Long, 1947). 8-Chlorocaffeine is reacted with an appropriate mercaptan (**B**), which is commercially available, to yield the desired thioether (**C**). This reaction occurs in the presence of sodium hydroxide and a waterï ethanol mixture serves as the solvent (Long, 1947).

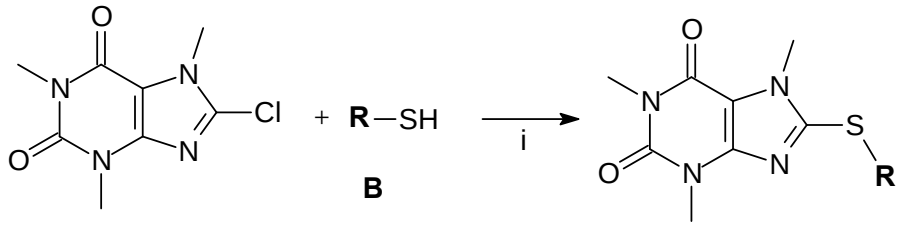

A **B** **C**

Figure 3.1 Reaction scheme for the synthesis of 8-thiocaffeine analogues. Key: (i) NaOH, waterï ethanol.

8-Chlorocaffeine: The method for the synthesis of 8-chlorocaffeine is essentially that of Fischer and Reese (1883). A mixture of dry caffeine (**D**) and chloroform is prepared in a flask fitted with

an inlet tube and a reflux condenser and heated to reflux until the caffeine is dissolved. In a separate flask, hydrochloric acid is carefully added to potassium permanganate to produce chlorine gas (Cl_2). The Cl_2 gas is subsequently passed through the inlet tube and reacts with the dissolved caffeine at room temperature. After the solvent is removed by distillation *in vacuo*, 8-chlorocaffeine (**A**) is obtained in high yields.

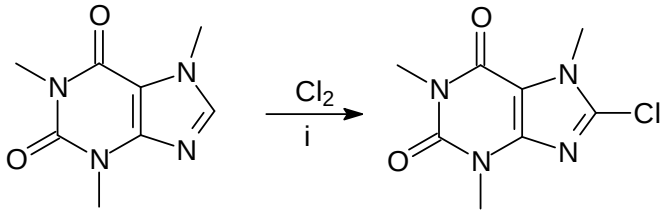

D **A**

Figure 3.2 Reaction scheme for the synthesisis of 8-chlorocaffeine. Key: (i) $CHCl_3$, room temperature.

3.3 Detailed synthetic methods for the synthesis of 8-thiocaffeine analogues (4a–l) and 8-chlorocaffeine.

8-Thiocaffeine analogues (**4a-l**): Sodium hydroxide (0.12 g, 3 mmol) was dissolved in 3.5 ml water at room temperature. Ethanol (3.5 ml) was added to the mixture. The reaction was cooled in an ice-bath for 5 minutes and the appropriate thiol (3 mmol) (Table 3.2) was subsequently added to the reaction. 8-Chlorocaffeine (0.701 g, 3 mmol) was added rapidly in a single portion to the mixture to yield a white suspension. The reaction was heated under reflux at the temperature that corresponds to the boiling point of the thiol reagent. These boiling points were obtained from literature and are given in table 3.2. The reaction mixture was stirred and heated for 60 minutes.

Thin layer chromatography was used to determine whether the thiol and the 8-chlorocaffeine reacted completely in the respective reactions. If the reaction was not complete after 60 minutes of heating, the solution was reheated to the same temperature and refluxed for another 60 minutes. The product was collected by filtration and allowed to dry at room temperature. The product was recrystalized from 30 ml ethanol and again allowed to dry at room temperature

overnight. The product was weighed and the percentage yield and the melting point were determined.

Table 3.2 The boiling points of the thiol starting materials that were used for the synthesis of the 8-thiocaffeine analogues **4a**ï **l**. The melting points of the 8-thiocaffeine analogues **4a**ï **l** that were recorded are also given.

Thiol starting material	Boiling Point (˚C)	Product	Melting Point (˚C)
Phenyl mercaptan	169	**4a**	149
Benzyl mercaptan	75-77	**4b**	149
Phenylethyl mercaptan	217-218	**4c**	95
4-Chlorobenzyl mercaptan	75	**4d**	169
4-Bromobenzyl mercaptan	265	**4e**	166
4-Fluorobenzyl mercaptan	72-74	**4f**	175
4-Methoxybenzyl mercaptan	90-95	**4g**	159
2-Phenoxyethanethiolin	201	**4h**	114
Cyclohexanethiol	132	**4i**	135
Cyclopentanethiol	157-158	**4j**	133
2-Naphthalenethiol	286	**4k**	175
3-Methyl-1-butanethiol	120	**4l**	79

8-Chlorocaffeine: As shown in figure 3.3 the hydrochloric acid (160 ml) (1) was slowly added to 26 g (0.17 mol) potassium permanganate (2) at room temperature (Figure 3.3). The chlorine gas (Cl_2), which is the product from this reaction, was then passed through three consecutive flasks (3, 4 and 5). The first flask (3) contained 200 ml water, the second flask (4) contained 100 ml of sulphuric acid and the third flask (5) was left empty. The water was used to remove any residual HCl from the generated Cl_2 gas. The sulphuric acid acted to dry the Cl_2 gas while the empty flask served as safety trap between the Cl_2 generating source and the reaction. The Cl_2 was then passed through a solution of caffeine (5 g, 0.03 mol) (6) in 40 ml chloroform at 85 ęC. After several minutes, a white precipitate, the hydrochloric acid salt of chlorocaffeine formed in (6). At this point the reaction mixture took on a light yellow appearance. The chloroform

solvent was removed with the aid of a rotary evaporator, to yield 8-chlorocaffeine as a white solid.

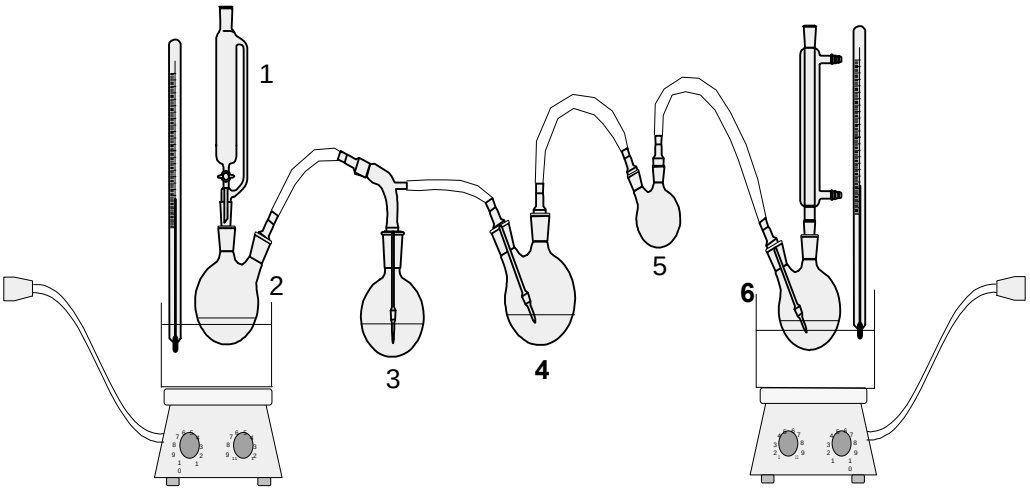

Figure 3.3 Illustration of the glassware and apparatus required for the synthesis of 8-chlorocaffeine.

3.4 Chemicals and instrumentation

Unless otherwise noted, all starting materials were obtained from Sigma-Aldrich® and were used without purification.

- Proton (^{1}H) and carbon (^{13}C) NMR spectra were recorded on a Bruker® Avance III 600 spectrometer at frequencies of 600 MHz and 150 MHz, respectively. All NMR measurements were conducted in $CDCl_3$ and the chemical shifts are reported in parts per million (ŭ) downfield from the signal of tetramethylsilane added to the deuterated solvent. Spin multiplicities are given as s (singlet), brs (broad singlet), d (doublet), dd (doublet of doublets), t (triplet), m (multiplet) or sept (septet).
- Direct insertion electron impact ionization (EIMS) and high resolution mass spectra (HRMS) were obtained on a DFS high resolution magnetic sector mass spectrometer (Thermo Electron Corporation).
- Melting points (mp) were determined on a Stuart® SMP10 melting point apparatus and are uncorrected.
- Thin layer chromatography (TLC) was carried out using silica gel 60 (Merck®) with UV_{254} fluorescent indicator.

- To determine the purity of the synthesized compounds, HPLC analyses were conducted with an Agilent® 1100 HPLC system equipped with a quaternary pump and an Agilent® 1100 series diode array detector. HPLC grade acetonitrile (Merck®) and Milli-Q water (Millipore®) was used for the chromatography.

3.5 Physical characterization

The structures of the 8-thiocaffeine analogues were verified by ^{1}H-NMR and ^{13}C-NMR, as well as by high resolution mass spectrometry. The purities of the target compounds were verified by HPLC analysis. For the purpose of the HPLC analysis, strong eluting conditions (up to 85% acetonitrile) were employed and the eluent was monitored at 210 nm, a wavelength where most organic compounds absorb UV light. It is therefore likely that impurities, if present, will elute and be detected under these conditions. The HPLC conditions and chromatograms obtained, are given in the addendum.

3.6 Results

3.6.1 The physical data for the 8-thiocaffeine derivatives

8-(Phenylsulfanyl)caffeine (4a)

The title compound was prepared from phenyl mercaptan in a yield of 64.3%: mp 149 °C (ethanol). ^{1}H NMR (Bruker Avance III 600, $CDCl_3$) ŭ 3.37 (s, 3H), 3.53 (s, 3H), 3.90 (s, 3H), 7.32 (m, 5H); ^{13}C NMR (Bruker Avance III 600, $CDCl_3$) ŭ 28.0, 29.9, 33.1, 109.6, 128.2, 129.6, 130.5, 130.9, 146.4, 148.0, 151.4, 154.9; EI-HRMS *m*/*z*: calcd for $C_{14}H_{15}N_4O_2S$ (MH^+), 303.0916, found 303.0912; Purity (HPLC): 98%.

8-(Benzylsulfanyl)caffeine (4b)

The title compound was prepared from benzyl mercaptan in a yield of 59.0%: mp 149 °C (ethanol). ^{1}H NMR (Bruker Avance III 600, $CDCl_3$) *δ* 3.35 (s, 3H), 3.57 (s, 3H), 3.69 (s, 3H), 4.42 (s, 2H), 7.27 (m, 3H), 7.31 (m, 2H); ^{13}C NMR (Bruker Avance III 600, $CDCl_3$) *δ* 27.8, 29.7, 32.2, 37.4, 108.7, 127.9, 128.7, 128.9, 136.6, 148.3, 150.0, 151.5, 154.6; EI-HRMS *m*/*z*: calcd for $C_{15}H_{17}O_2N_4S$ (MH^+), 317.1072, found 317.1073; Purity (HPLC): 99%.

8-[(2-Phenylethyl)sulfanyl]caffeine (4c)

The title compound was prepared from phenylethyl mercaptan in a yield of 22.9%: mp 95 °C (ethanol). ^{1}H NMR (Bruker Avance III 600, $CDCl_3$) *δ* 3.04 (t, 2H, J = 7.9 Hz), 3.36 (s, 3H), 3.49 (t, 2H, J = 7.9 Hz), 3.55 (s, 3H), 3.78 (s, 3H), 7.21 (m, 3H), 7.29 (m, 2H); ^{13}C NMR (Bruker Avance III 600, $CDCl_3$) *δ* 27.8, 29.7, 32.1, 33.8, 36.0, 108.5, 126.7, 128.5, 139.3, 148.5, 150.9, 151.5, 154.5; EI-HRMS *m*/*z*: calcd for $C_{16}H_{19}N_4O_2S$ (MH^+), 331.1229, found 331.1229; Purity (HPLC): 99%.

8-{[(4-Chlorophenyl)methyl]sulfanyl}caffeine (*4d*)

The title compound was prepared from 4-chlorobenzyl-methanethiol in a yield of 85.6%: mp 169 °C (ethanol). ^{1}H NMR (Bruker Avance III 600, $CDCl_3$) ŭ 3.35 (s, 3H), 3.55 (s, 3H), 3.72 (s, 3H), 4.39 (s, 2H), 7.26 (m, 4H); ^{13}C NMR (Bruker Avance III 600, $CDCl_3$) ŭ 27.8, 29.7, 32.2, 36.4, 108.7, 128.8, 130.3, 133.7, 135.2, 148.3, 149.7, 151.4, 154.5; EI-HRMS m/z: calcd for $C_{15}H_{16}ClN_4O_2S$ (MH^+), 351.0682, found 351.0679; Purity (HPLC): 97%.

8-{[(4-Bromophenyl)methyl]sulfanyl}caffeine (4e)

The title compound was prepared from 4-bromobenzyl mercaptan in a yield of 82.0%: mp 166 °C (ethanol). ^{1}H NMR (Bruker Avance III 600, $CDCl_3$) ŭ 3.35 (s, 3H), 3.55 (s, 3H), 3.72 (s, 3H), 4.38 (s, 2H), 7.22 (d, 2H, J = 8.3 Hz), 7.39 (d, 2H, J = 8.3 Hz); ^{13}C NMR (Bruker Avance III 600, $CDCl_3$) ŭ 27.8, 29.7, 32.2, 36.4, 108.2, 121.8, 130.6, 131.8, 135.8, 148.3, 149.7, 151.4, 154.5; EI-HRMS m/z: calcd for $C_{15}H_{16}BrN_4O_2S$ (MH^+), 395.0177, found 395.0178; Purity (HPLC): 98%.

8-{[(4-Fluorophenyl)methyl]sulfanyl}caffeine (*4f*)

The title compound was prepared from 4-fluorobenzyl mercaptan in a yield of 75.3%: mp 175 °C (ethanol). ^{1}H NMR (Bruker Avance III 600, $CDCl_3$) ŭ 3.35 (s, 3H), 3.55 (s, 3H), 3.72 (s, 3H), 4.40 (s, 2H), 6.96 (t, 2H, J = 8.4 Hz), 7.30 (q, 2H, J = 5.3 Hz); ^{13}C NMR (Bruker Avance III 600, $CDCl_3$) ŭ 27.8, 29.7, 32.1, 36.4, 108.7, 115.5, 130.6, 132.4, 148.3, 149.8, 151.4, 154.5, 161.4, 163.1; EI-HRMS m/z: calcd for $C_{15}H_{16}FN_4O_2S$ (MH^+), 335.0976, found 335.0972; Purity (HPLC): 95%.

8-{[(4-Methoxyphenyl)methyl]sulfanyl}caffeine (*4g*)

The title compound was prepared from 4-methoxybenzyl mercaptan in a yield of 94.3%: mp 159 °C (ethanol). ^{1}H NMR (Bruker Avance III 600, $CDCl_3$) ŭ 3.36 (s, 3H), 3.58 (s, 3H), 3.71 (s, 3H),

3.76 (s, 3H), 4.39 (s, 2H), 6.81 (d, 2H, J = 8.7 Hz), 7.23 (t, 2H, J = 8.7 Hz); ^{13}C NMR (Bruker Avance III 600, $CDCl_3$) ŭ 27.9, 29.7, 32.2, 37.0, 55.3, 108.6, 114.1, 128.4, 130.2, 148.4, 150.3, 151.5, 154.6, 159.2; EI-HRMS *m*/*z*: calcd for $C_{15}H_{19}N_4O_3S$ (MH^+), 347.1176, found 347.1171; Purity (HPLC): 94%.

8-[(2-Phenoxyethyl)sulfanyl]caffeine (4h)

The title compound was prepared from 2-phenoxyethanethiol in in a yield of 43.9%: mp 114 °C (ethanol). ^{1}H NMR (Bruker Avance III 600, $CDCl_3$) ŭ 3.37 (s, 3H), 3.53 (s, 3H), 3.63 (t, 2H, J = 6.2 Hz), 3.83 (s, 3H), 4.30 (t, 2H, J = 6.4 Hz), 6.91 (d, 2H, J = 8.3 Hz), 6.94 (t, 1H, J = 7.2 Hz), 7.25 (t, 2H, J = 8.3 Hz); ^{13}C NMR (Bruker Avance III 600, $CDCl_3$) ŭ 27.8, 29.7, 31.5, 32.2, 66.3, 108.7, 114.5, 121.3, 129.5, 148.4, 150.3, 151.5, 154.5, 158.1; EI-HRMS *m*/*z*: calcd for $C_{16}H_{19}N_4O_3S$ (MH^+), 347.1176, found 347.1173; Purity (HPLC): 95%.

8-(Cyclohexylsulfanyl)caffeine (*4i*)

The title compound was prepared from cyclohexanethiol in a yield of 37.2%: mp 133 °C (ethanol). ^{1}H NMR (Bruker Avance III 600, $CDCl_3$) *δ* 1.28 (m, 1H), 1.39 (m, 2H), 1.47 (m, 2H), 1.58 (m, 1H), 1.73 (m, 2H), 2.03 (m, 2H), 3.34 (s, 3H), 3.52 (s, 3H), 3.71 (m, 1H), 3.82 (s,3H); ^{13}C NMR (Bruker Avance III 600, $CDCl_3$) *δ* 25.4, 25.8, 27.8, 29.7, 32.3, 33.4, 47.2, 108.4, 148.5, 150.3, 151.5, 154.6; EI-HRMS *m*/*z*: calcd for $C_{14}H_{21}N_4O_2S$ (MH^+), 309.1385, found 309.1385; Purity (HPLC): 99%.

8-(Cyclopentylsulfanyl)caffeine (4j)

The title compound was prepared from cyclopentanethiol in a yield of 60.9%: mp 135 °C (ethanol). ^{1}H NMR (Bruker Avance III 600, $CDCl_3$) *δ* 1.63 (m, 4H), 1.76 (m, 2H), 2.15 (m, 2H), 3.34 (s, 3H), 3.51 (s, 3H), 3.80 (s, 3H), 3.99 (pent, 1H, J = 7.2 Hz); ^{13}C NMR (Bruker Avance III 600, $CDCl_3$) *δ* 24.6, 27.8, 29.7, 32.2, 33.8, 46.4, 108.3, 148.5, 151.3, 151.5, 154.6; EI-HRMS m/z: calcd for $C_{13}H_{19}N_4O_2S$ (MH^+), 295.1229, found 295.1233; Purity (HPLC): 95%.

8-(Naphthalen-2-ylsulfanyl)caffeine (*4k*)

The title compound was prepared from 2-naphthalenethiol in a yield of 87.7%: mp 175 °C (ethanol). ^{1}H NMR (Bruker Avance III 600, $CDCl_3$) ŭ 3.37 (s, 3H), 3.53 (s, 3H), 3.91 (s, 3H), 7.36 (dd, 1H, J = 1.6, 9.4 Hz), 7.48 (m, 2H), 7.73 (m, 1H), 7.78 (m, 2H), 7.84 (s, 1H); ^{13}C NMR (Bruker Avance III 600, $CDCl_3$) ŭ 27.9, 29.8, 33.1, 109.5, 126.9, 127.0 127.5, 127.8, 129.4,

129.7, 132.6, 133.6, 146.4, 148.0, 151.4, 154.9; EI-HRMS m/z: calcd for $C_{18}H_{17}N_4O_2S$ (MH^+), 353.1072, found 353.1074; Purity (HPLC): 94%.

8-[(3-Methylbutyl)sulfanyl]caffeine (4l)

The title compound was prepared from 3-methyl-1-butanethiol in a yield of 35.3%: mp 79 °C (ethanol). ^{1}H NMR (Bruker Avance III 600, $CDCl_3$) δ 0.92 (d, 6H, J = 6.7 Hz), 1.59 (q, 2H, J = 7.9 Hz), 1.69 (sept, 1H, J = 6.7 Hz), 3.23 (t, 2H, J = 7.5 Hz), 3.34 (s, 3H), 3.51 (s, 3H), 3.79 (s, 3H); ^{13}C NMR (Bruker Avance III 600, $CDCl_3$) δ 22.1, 27.4, 27.8, 29.6, 30.8, 32.1, 38.5, 108.4, 148.4, 151.3, 151.5, 154.5; EI-HRMS *m*/*z*: calcd for $C_{13}H_{21}N_4O_2S$ (MH^+), 297.1385, found 297.1382; Purity (HPLC): 97%.

3.6.2 Interpretation of the NMR spectra

In Table 3.3 the structures of the thiocaffeine analogues are given and correlated with the ^{1}H NMR data. All of the appropriate signals were observed for each compound **4a**ï **l**. These include the 3 singlets for the caffeine methyl groups, the signals of the aliphatic protons present in the C-8 side chain and the signals for the aromatic protons present on the ring systems of the C-8 side chains. For those compounds which did not have aromatic ring systems in the C-8 side chain (**4i**, **4j** and **4l**) no signals for aromatic protons were observed. The singlet of the methoxy groups (substituted on the phenyl ring) of compound **4g** is also observed. The appropriate integration values and chemical shifts were also observed for all signals. In addition, the ^{13}C NMR data (not tabulated) also corresponded to each of the target structures in terms of the number of ^{13}C signals and their expected chemical shifts.

Table 3.3 Correlation of the ^{1}H NMR data with the structures of the 8-thiocaffeine derivatives.

	Structure	**NMR signal assignment**
4a	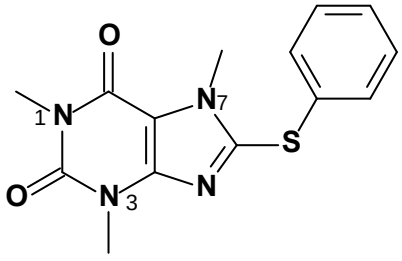	• Methyl groups at N-1, N-3 and N-7 ï singlets at 3.37 (3H), 3.53 (3H) and 3.90 (3H) ppm. • Aromatic protons ï signals at 7.32 (5H) ppm.

4b	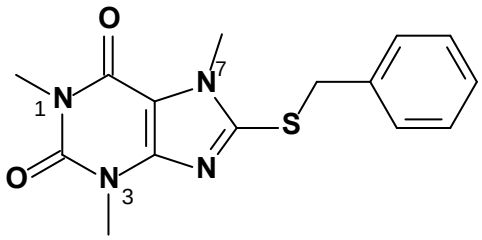	• Methyl groups at N-1, N-3 and N-7 ï singlets at 3.35 (3H), 3.57 (3H) and 3.69 (3H) ppm. • CH_2ï singlet at 4.42 (2H) ppm • Aromatic protons ï signals at 7.27 (3H) and 7.31 (2H) ppm.
4c	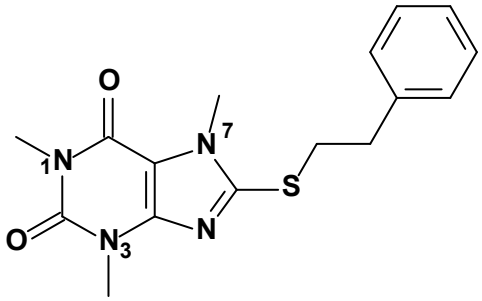	• Methyl groups at N-1, N-3 and N-7 ï singlets at 3.36 (3H), 3.55 (3H) and 3.78 (3H) ppm. • CH_2ï CH_2ï triplets at 3.04 (2H) and 3.49 (2H) ppm • Aromatic protons ï signals at 7.21 (3H) and 7.29 (2H) ppm.
4d	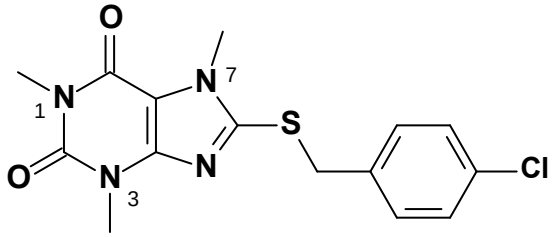	• Methyl groups at N-1, N-3 and N-7 ï singlets at 3.35 (3H), 3.55 (3H) and 3.72 (3H) ppm. • CH_2ï singlet 4.39 (2H) ppm. • Aromatic protons ï signal at 7.26 (4H) ppm.
4e	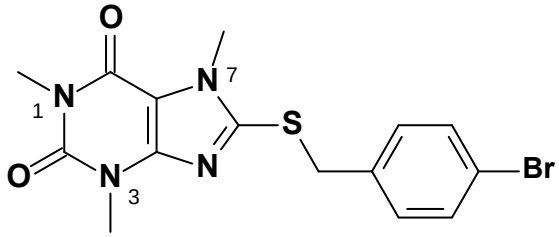	• Methyl groups at N-1, N-3 and N-7 ï singlets at 3.35 (3H), 3.55 (3H) and 3.72 (3H) ppm. • CH_2ï singlet at 4.38 (2H) ppm. • Aromatic protons ï signals at 7.22 (2H) and 7.39 (2H) ppm.
4f	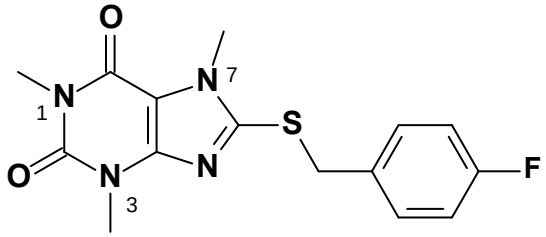	• Methyl groups at N-1, N-3 and N-7 ï singlets at 3.35 (3H), 3.55 (3H) and 3.72 (3H) ppm. • CH_2ï singlet at 4.40 (2H) ppm. • Aromatic protons ï triplet at 6.96 (2H) and quartet at 7.30 (2H) ppm.

4g	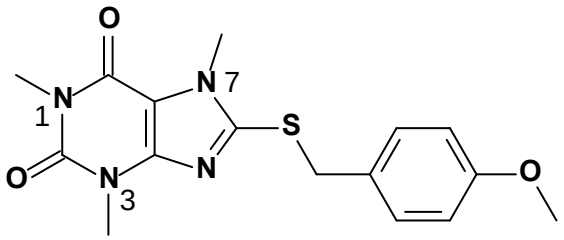	• Methyl groups at N-1, N-3 N-7 and the methoxy CH_3 ï singlets at 3.36 (3H), 3.58 (3H), 3.71 (3H) and 3.76 (3H) ppm. • b. CH_2ï singlet at 4.39 (2H) ppm. • Aromatic protons ï doublet at 6.81 (2H) and triplet at 7.23 (2H) ppm.
4h	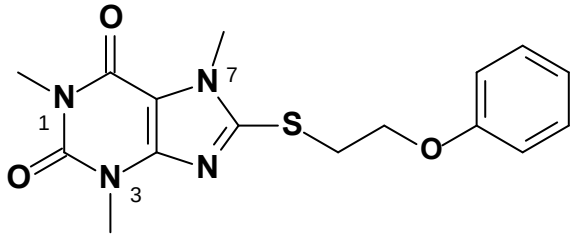	• Methyl groups at N-1, N-3 and N-7 ï singlets at 3.37 (3H), 3.53 (3H) and 3.83 (3H) ppm. • CH_2ï triplets at 3.63 (2H) and 4.30 (2H) ppm. • Aromatic protons ï doublet at 6.91 (2H), triplets at 6.94 (1H) and 7.25 (2H) ppm.
4i	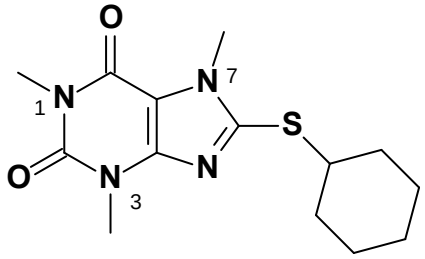	• Methyl groups at N-1, N-3 and N-7 ï singlets at 3.34 (3H), 3.52 (3H), 3.82 (3H) ppm. • Cyclohexyl protons ï signals at 1.28 (1H), 1.39 (2H), 1.47 (2H), 1.58 (1H), 1.73 (2H), 2.03 (2H) and 3.71 (1H) ppm.
4j	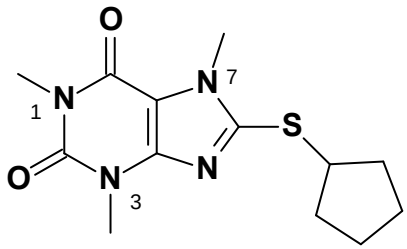	• Methyl groups at N-1, N-3 and N-7 ï singlets at 3.34 (3H), 3.51 (3H) and 3.80 (3H) ppm. • Cyclopentyl protons ï signals at 1.63 (4H), 1.76 (2H), 2.15 (2H), 3.99 (1H) ppm.
4k	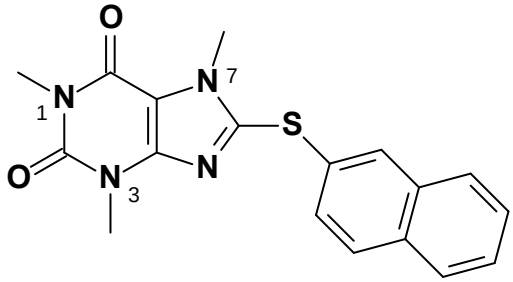	• Methyl groups at N-1, N-3 and N-7 ï singlets at 3.37 (3H), 3.53 (3H) and 3.91 (3H) ppm. • Aromatic protons ï signals at 7.36 (1H), 7.48 (2H), 7.73 (1H), 7.78 (2H) and 7.84 (1H) ppm.

4l	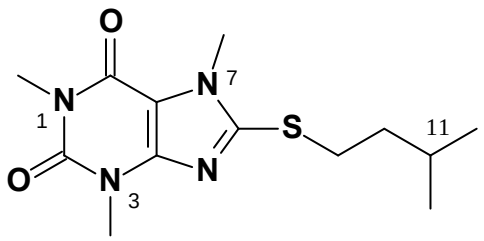	• Methyl groups at N-1, N-3 and N-7 ï singlets at 3.34 (3H), 3.51 (3H) and 3.79 (3H) ppm. • Aliphatic side chain ï doublet at 0.92 (6H), quartet at 1.59 (2H), septet at 1.69 (1H) and triplet at 3.23 (2H) ppm.

3.6.3 Interpretation of the mass spectra

As shown in table 3.4, the high resolution masses that were obtained for each of the 8-tiocaffeine analogues very closely corresponded to the calculated values. This is further confirmation of the structures of these compounds.

Table 3.4 Correlation of the calculated exact masses with the experimentally obtained masses of the 8-thiocaffeine derivatives. All masses are given as MH^+.

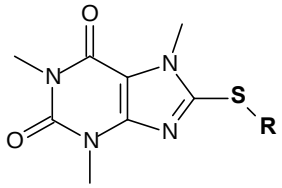

Compound	R	Mass Spectrometry			
		Calcd.	Found	Formula	ppm[a]
4a	$-C_6H_5$	303.0916	303.0912	$C_{14}H_{15}N_4O_2S$	1.3
4b	$-CH_2-C_6H_5$	317.1072	317.1073	$C_{15}H_{17}O_2N_4S$	0.3
4c	$-(CH_2)_2-C_6H_5$	331.1229	331.1229	$C_{16}H_{19}N_4O_2S$	0
4d	$-CH_2-(4-Cl-C_6H_4)$	351.0682	351.0679	$C_{15}H_{16}ClN_4O_2S$	0.9
4e	$-CH_2-(4-Br-C_6H_4)$	395.0177	395.0178	$C_{15}H_{16}BrN_4O_2S$	0.3
4f	$-CH_2-(4-F-C_6H_4)$	335.0978	335.0972	$C_{15}H_{16}FN_4O_2S$	1.8
4g	$-CH_2-(4-OCH_3-C_6H_4)$	347.1178	347.1171	$C_{15}H_{19}N_4O_3S$	2.0
4h	$-(CH_2)_2-O-C_6H_5$	347.1178	347.1173	$C_{16}H_{19}N_4O_3S$	1.4
4i	$-C_6H_{11}$	309.1385	309.1385	$C_{14}H_{21}N_4O_2S$	0
4j	$-C_5H_9$	295.1229	295.1233	$C_{13}H_{19}N_4O_2S$	1.4
4k	-2-Naphthalenyl	353.1072	353.1074	$C_{18}H_{17}N_4O_2S$	0.6
4l	$-(CH_2)_2-CH(CH_3)_2$	297.1385	297.1382	$C_{13}H_{21}N_4O_2S$	1.0

[a]ppm = (found ï calcd.)/calcd. X 1 000 000. In general a ppm difference smaller than 5 is considered to be in good agreement.

3.7 Conclusion

This chapter described the successful synthesis of the target 8-thiocaffeine derivatives (**4a-l**). All the structures were confirmed by NMR and MS and the purities were established by HPLC analysis. Both the ^{1}H NMR and ^{13}C NMR spectra corresponded with the proposed structures and the expected exact masses were also recorded for each compound. In addition, HPLC analysis revealed a single peak for each compound analysed.

Chapter 4

Enzymology

4.1 Introduction

In this chapter, the 8-thiocaffeine analogues (**4a-l**) that were synthesized in the previous chapter, were investigated as inhibitors of MAO-A and ï B and compared to the 8-benzyloxycaffeine analogues examined previously (Strydom *et al*., 2010). Compounds acting as inhibitors may be considered as potential lead compounds for the development of drugs for the treatment of PD. These investigations should establish if the goal of this study was achieved, namely the design of new potent, reversible and competitive inhibitors of the MAOs. As outlined in the Introduction, the objectives of this chapter were as follows:

- The 8-thiocaffeine analogues (**4a-l**) that were synthesized in the previous chapter were evaluated as inhibitors of MAO-A and ï B. The inhibition potencies were expressed as the IC_{50} values for the inhibition of the MAOs. For this purpose, the recombinant human enzymes (which are commercially available) were employed. A fluorometric assay was used to measure the enzyme activities. The MAO activity measurements were based on measuring the amount of 4-hydroxyquinoline (4-HQ) that is produced in the oxidation process. Certain MAO substrates, such as kynuramine, are oxidized to fluorescent products. Kynuramine is the substrate for both MAO-A and ï B and is oxidized to 4-HQ as shown in figure 4.1. The concentrations of the generated 4-HQ are measured with a fluorescence spectrophotometer at an excitation wavelength of 310 nm and an emission wavelength of 400 nm. Fluorescence decreases as 4-HQ production is reduced by a MAO inhibitor such as the compounds (**4a-l**) that were synthesized in this study.
- In order to determine if the inhibitors interact reversibly or irreversibly with MAO-A and ï B, the time-dependency of inhibition of both human MAO-A and ï B by selected 8-thiocaffeine analogues was evaluated.
- Lineweaver-Burk plots were generated for a selected reversible inhibitor to determine if the mode of inhibition was competitive.

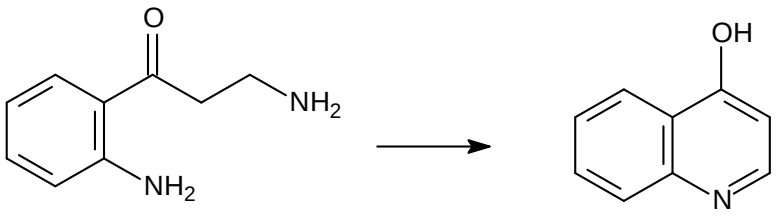

Figure 4.1 The oxidation of kynuramine by MAO-A or ï B to yield 4-hydroxyquinoline.

4.2 Chemicals and instrumentation

For fluorescence spectrophotometry, a Varian® Cary Eclipse fluorescence spectrophotometer was employed. Microsomes from insect cells containing recombinant human MAO-A and ï B (5 mg/ml) and kynuramine.2HBr were obtained from Sigma-Aldrich®.

4.3 Biological evaluation to determine the IC_{50} values

4.3.1 Introduction

For these studies a fluorometric method was used to determine the activities of MAO-A and ï B. This protocol measures the amount of 4-HQ produced when kynuramine is oxidized by the MAO enzymes. Since kynuramine is a mixed MAO-A/B substrate it may be used to determine the activities of both enzymes. These enzymes catalyze the oxidative deamination of kynuramine to produce the product, 4-HQ. 4-HQ can be readily measured with fluorescence spectrofluorometry. For this purpose the concentration of 4-HQ is measured at an excitation wavelength of 310 nm and at an emission wavelength of 400 nm (Strydom ***et al.,*** 2010).

4.3.2 Method

Recombinant human MAO-A and -B (5 mg/mL) were obtained from Sigmaï Aldrich®, pre-aliquoted and stored at ï 70 ºC. Potassium phosphate buffer (100 mM, pH 7.4, made isotonic with KCl) was used for all the enzymatic reactions. The reactions contained MAO-A and ï B (0.0075 mg/mL), various concentrations of the test inhibitor (0ï 100 ε M) and kynuramine, The final concentrations of kynuramine in the reactions were 30 ε M and 45 ε M for MAO-B and -A, respectively. The final volume of the reactions was 500 ε l and were made up of 50 µl kynuramine (substrate), 20 µl test inhibitor, 380 µl potassium phosphate (buffer) and 50 µl

enzyme (0.075 mg/ml). Stock solutions of the test inhibitors were prepared in DMSO and added to the reactions to yield a final concentration of 4% (v/v) DMSO. The reactions were incubated for 20 min at 37 ºC and terminated with the addition of 400 εl of sodium hydroxide for both MAO-A and -B. Distilled water (1000 εl) was added to each reaction before it was centrifuged for 10 min at 16,000 *g*. The different concentrations of the MAO generated 4-HQ in the reactions, were determined by measuring the fluorescence of the supernatant at an excitation wavelength of 310 nm and an emission wavelength of 400 nm (Zhou *et al.*, 1997). Quantitative estimations of 4-HQ were made with the aid of a linear calibration curve ranging from 0.047ï 1.56 µM of the reference standard. Each calibration standard was prepared to a final volume of 500 εl in potassium phosphate buffer (100 mM, pH 7.4) and contained 4% DMSO. To each standard was added 400 εl of sodium hydroxide and 1000 εl distilled water. The IC_{50} values were determined by plotting the initial rate of oxidation versus the logarithm of the inhibitor concentration to obtain a sigmoidal doseï response curve.

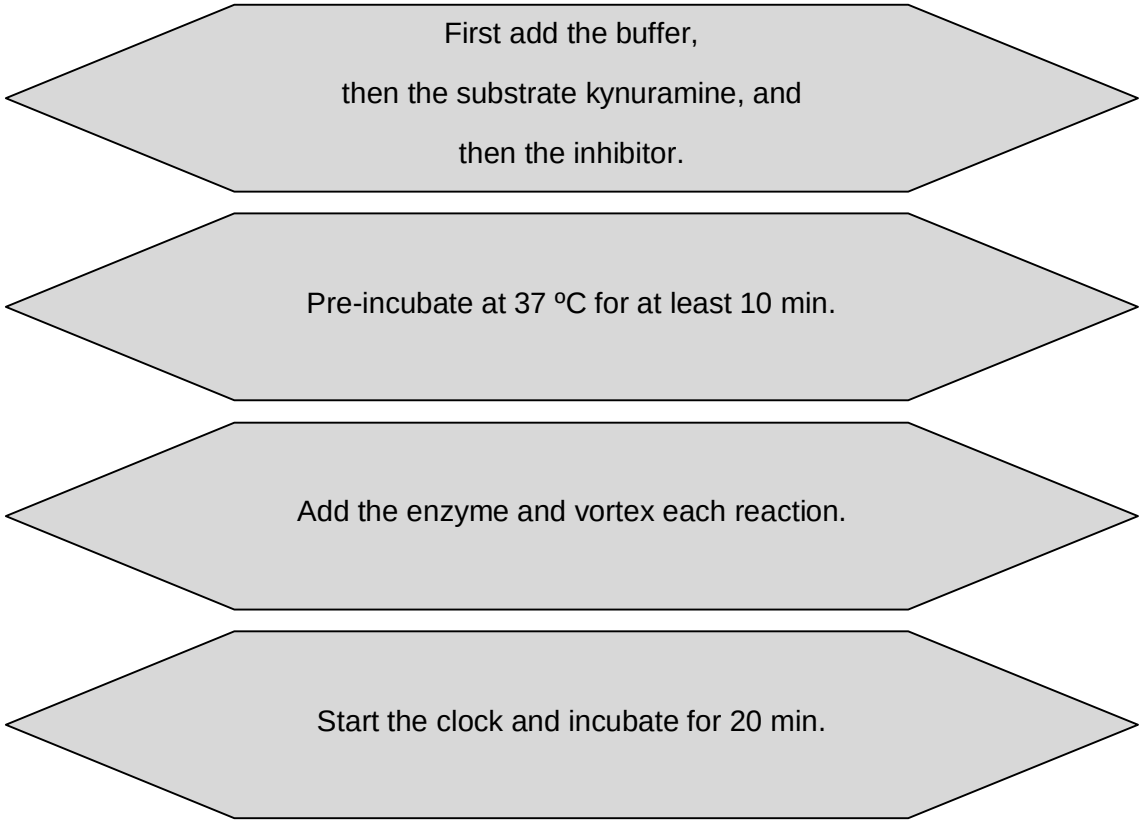

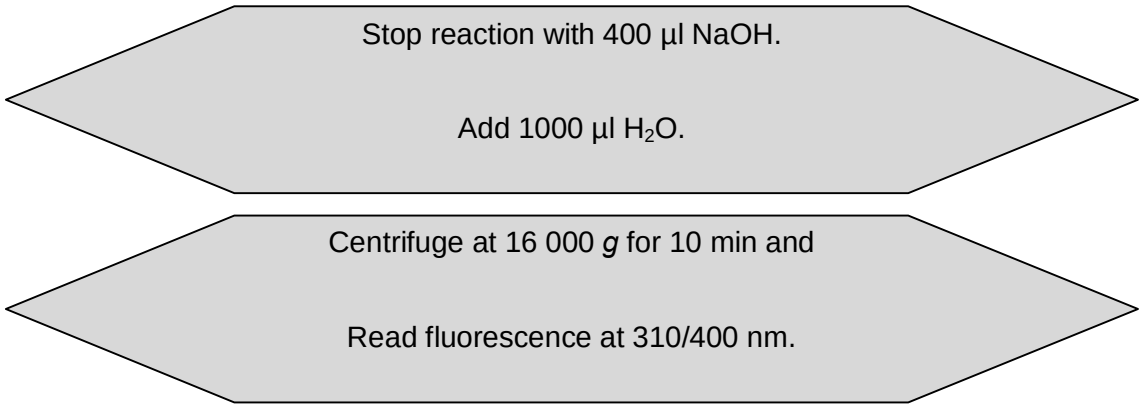

Figure 4.2 An overview of MAO activity measurements in the presence of an inhibitor.

4.3.3 Results – Sigmoidal curves obtained for the IC_{50} determinations

The IC_{50} of an inhibitor represents the concentration of a drug that is needed for 50% inhibition *in vitro*. The logarithms of die different concentrations of the inhibitor are plotted graphically against the rate of the MAO catalyzed oxidation of kynuramine and the concentration of the inhibitor, which reduces the rate to half of the maximal value is the IC_{50}. As an example, the sigmoidal curve for the determination of the IC_{50} value towards human MAO-B of the most potent compound (**4e**) is given in figure 4.3.

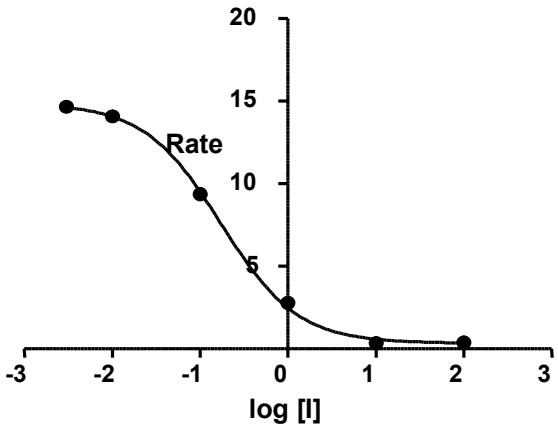

Figure 4.3 The sigmoidal dose-response curve of the initial rates of oxidation of kynuramine by recombinant human MAO-B vs. the logarithm of concentration of inhibitor **4e** (expressed in µM). The determinations were carried out in triplicate and the values are expressed as the mean ±

standard deviation. The concentration of kynuramine used was 30 µM and the rate data are expressed as nmoles 4-hydroxyquinoline formed/min/mg protein.

4.3.4 Results – IC_{50} values

Presented in table 4.1 are the IC_{50} values that were measured for the inhibition of both recombinant human MAO-A and ï B by the 8-thiocaffeine analogues **4a-l**. Lower IC_{50} values indicate that an inhibitor has a higher binding affinity for the enzyme and is therefore a more potent inhibitor. Also given is the selectivity index of each inhibitor. The selectivity index (SI) is the selectivity of the inhibitor for the MAO-B isoform and is given as the ratio of the IC_{50} value for the inhibition of MAO-A devided by the IC_{50} value for the inhibition of MAO- B. A higher selectivity index value indicates that an inhibitor is selective for the MAO-B isoenzyme.

As shown in table 4.1, the 8-thiocaffeine analogues (**4a-l**) evaluated in this study were inhibitors of both human MAO-A and -B. The only exception was compound **4g,** which was found not to be a MAO-A and ï B inhibitor. The following general observations can be made from the IC_{50} values given in table 4.1:

- **4g** did not inhibit MAO-A and ï B.
- **4e** is the most potent MAO-A and ï B inhibitor with IC_{50} values of 2.61 µM and 0.16 µM, respectively. This compound also shows a relative high degree of isoform selectivity (16 fold) and may therefore be considered to be a MAO-B selective inhibitor.
- The second most potent MAO-B inhibitor was compound **4d** with IC_{50} values of 2.76 µM and 0.192 µM for MAO-A and ï B, respectively. Compound **4d** was also found to be selective for the MAO-B isoform (14 fold).
- **4a** was found to be the weakest inhibitor of both MAO-A and ï B among the compounds evaluated with IC_{50} values of 215.29 µM and 33.207 µM for the two isoforms, respectively.
- Compound **4c** was found to have the highest degree of isoform selectivity (92 fold for MAO-B) among the thiocaffeines. This compound shows weak inhibition of MAO-A, but potent inhibition of MAO-B with IC_{50} values of 20.537 µM and 0.223 µM for the two isozymes, respectively.

Table 4.1 The IC_{50} values for the inhibition of recombinant human MAO-A and ï B by 8-thiocaffeine compounds **4e-l**[a]

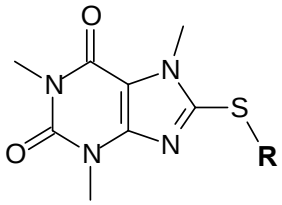

Compound	R	MAO-A IC_{50} (µM)	MAO-B IC_{50} (µM)	SI[b]
4a	$-C_6H_5$	215.290 ± 284.268	33.207 ± 3.405	6.5
4b	$-CH_2-C_6H_5$	8.224 ± 1.131	1.863 ± 0.034	4.4
4c	$-(CH_2)_2-C_6H_5$	20.537 ± 4.490	0.223 ± 0.010	92.1
4d	$-CH_2-(4-Cl-C_6H_4)$	2.76 ± 0.57	0.192 ± 0.025	14.4
4e	$-CH_2-(4-Br-C_6H_4)$	2.61 ± 0.10	0.16 ± 0.02	16.3
4f	$-CH_2-(4-F-C_6H_4)$	4.79 ± 0.58	0.34 ± 0.03	14.1
4g	$-CH_2-(4-OCH_3-C_6H_4)$	N/A[c]	N/A	N/A
4h	$-(CH_2)_2-O-C_6H_5$	15.493 ± 2.169	0.332 ± 0.033	46.7
4i	$-C_6H_{11}$	24.427 ± 8.757	13.100 ± 3.491	1.9
4j	$-C_5H_9$	9.40 ± 0.57	20.863 ± 3.107	0.01
4k	-2-Naphthalenyl	3.60 ± 0.29	3.596 ± 1.104	1.0
4l	$-(CH_2)_2-CH(CH_3)_2$	15.163 ± 4.091	2.620 ± 0.546	5.8

[a] All values are expressed as the mean ± SD of triplicate determinations.

[b] The selectivity index is the selectivity for the MAO-B isoform and is given as the ratio of IC_{50}(MAO-A)/IC_{50}(MAO-B).

[c] N/A is no activity.

- Compound **4h** also exhibited a high degree of isoform selectivity (47 fold for MAO-B).
- The potency of **4e** for the MAO-B isoform may be better judged by considering that **4e** is only 2 fold weaker as a MAO-B inhibitor compared to safinamide (IC_{50} = 0.08 µM), a MAO-B inhibitor that has entered clinical trials for the treatment of PD (Strydom *et al*., 2010). This makes compound **4e** a promising lead for the design of MAO-B inhibitors.
- Of importance is the observation that the thiocaffeines bearing the halogens, ï Cl and ï Br (**4d** and **4e**), are the most potent MAO-B inhibitors among the compounds studied, while the ï F containing analogue, **4f**, also exhibited potent MAO-B inhibition. These

findings suggest that substitution on the phenyl ring of the 8-thiocaffeine analogues with halogens (Cl, Br and F) enhances the MAO-B inhibition potencies.

- Interestingly, extending the length of the aliphatic chain between the 8-thiocaffeine and the phenyl ring of the C-8 side chain is associated with an increase in MAO-B inhibition potency. For example, the phenylethyl substituted homologue (**4c**, IC_{50} = 0.223 µM) is a more potent inhibitor than the benzyl substituted homologue (**4b**, IC_{50} = 1.863 µM) which is, in turn, a better MAO-B inhibitor than the phenyl substituted homologue (**4a**, IC_{50} = 33.2 µM).

Based on the discussed above, the following comparisons between the MAO inhibition potencies of the 8-thiocaffeines analogues (**4a-l**) may be made:

Table 4.2 A comparison of the IC_{50} values for the inhibition of MAO-B of the 8-thiocaffeine analogues with different chain lengths between the caffeine and the phenyl ring.

Compound	R	MAO-B IC_{50} (µM)	Ratio C_6H_5/X[a]
4a	$-C_6H_5$	33.207	-
4b	$-CH_2-C_6H_5$	1.863	17.8
4c	$-(CH_2)_2-C_6H_5$	0.223	148.9

[a]The ratio of $IC_{50}(-C_6H_5)/IC_{50}(-CH_2-C_6H_5$ and $-(CH_2)_2-C_6H_5)$

As can be seen in table 4.2, increasing the chain length of the C-8 side chain enhances the MAO-B inhibition potency of the 8-thiocaffeine analogues. For example, the phenylethyl substituted analogue (**4c**) is a more potent inhibitor than the benzyl substituted analogue (**4b**) which is, in turn, a better MAO-B inhibitor than the phenyl substituted analogue (**4a**). In fact compound **4c** is 148 fold more potent as an MAO-B inhibitor than **4a** while **4b** is 17 fold more potent as a MAO-B inhibitor than **4a**.

The results in table 4.3 suggest that the phenyl ring may not be most optimal ring system for the design of C-8 substituted thiocaffeine analogues as MAO-B inhibitors. The naphthalenyl substituted homologue (**4k**) is approximately 9 fold more potent than the phenyl substituted homologue (**4a**), while the homologue containing an aliphatic C-8 side chain (**4l**) is approximately 12 fold more potent than the phenyl substituted homologue (**4a**).

Table 4.3 A comparison of the IC_{50} values for the inhibition of MAO-B of the 8-thiocaffeine analogues, bearing naphthalyl and aliphatic side chains with the homologue bearing a phenyl ring on the C-8 substituent.

Compound	R	MAO-B IC_{50} (µM)	Ratio C_6H_5/X[a]
4a	$-C_6H_5$	33.207	-
4k	-2-Naphthalenyl	3.596	9.2
4l	$-(CH_2)_2-CH(CH_3)_2$	2.620	12.7

[a]The ratio of $IC_{50}(C_6H_5)/IC_{50}$(-2-Naphthalenyl and $-(CH_2)_2-CH(CH_3)_2$)

Table 4.4 A comparison of the IC_{50} values for the inhibition of MAO-B of the 8-thiocaffeine analogues bearing Cl, Br and F substituents on the phenyl ring with the homologue bearing an unsubstituted benzyl moiety.

Compound	R	MAO-B IC_{50} (µM)	Ratio $CH_2-C_6H_5/X$[a]
4b	$-CH_2-C_6H_5$	1.863	-
4d	$-CH_2-(4-Cl-C_6H_4)$	0.192	9.7
4e	$-CH_2-(4-Br-C_6H_4)$	0.16	11.6
4f	$-CH_2-(4-F-C_6H_4)$	0.34	5.5

[a]The ratio of $IC_{50}(CH_2-C_6H_5)/IC_{50}$(Cl, Br and F)

As shown in table 4.4, thiocaffeines bearing halogens exhibited enhanced MAO-B inhibition potencies compared to the unsubstituted homologue. For example, the chlorine (**4d**, IC_{50} = 0.192 µM), bromine (**4e**, IC_{50} = 0.16 µM) and fluorine (**4f**, IC_{50} = 0. 43 µM) substituted homologues were approximately 5-11 fold more potent as MAO-B inhibitors, than the unsubstituted homologue **4b** (IC_{50} = 1.863 µM). This suggests that substitution on the phenyl ring of the 8-thiocaffeine analogues with halogens (Cl, Br and F) enhances the MAO-B inhibition potencies.

Table 4.5 A comparison of the IC_{50} values for the inhibition of MAO-B by the 8-thiocaffeine analogues bearing different cycloalkane rings on the C-8 substituent, with the homologue bearing a phenyl ring.

Compound	R	MAO-B IC_{50} (µM)	Ratio X/-C_6H_5[a]
4a	-C_6H_5	33.207	-
4i	-C_6H_{11}	13.100	2.5
4j	-C_5H_9	20.863	1.6

[a]The ratio of IC_{50}(-C_6H_{11} and -C_5H_9)/IC_{50}(-C_6H_5)

As shown in table 4.5, substitution with saturated moieties at C-8 of thiocaffeine, **4i** and **4j**, yielded compounds with improved MAO-B inhibition potencies compared to the corresponding phenyl substituted homologue (**4a**). These homologues, containing a cyclohexyl (**4i**) and cyclopentyl (**4j**) side chain at C-8 of thiocaffeine were 1.6 - 2.5 fold better MAO-B inhibitors than the corresponding phenyl substituted homologue (**4a**). This suggests that substitution at C-8 of the thiocaffeine ring with a cyclohexyl and cyclopentyl group should enhance MAO-B inhibition.

Another interesting finding of the present study is that the phenoxyethyl substituted homologue (**4h**), with an IC_{50} value of 0.332 µM (table 4.1), is a more potent MAO-B inhibitor than both the phenyl substituted analogue (**4a**) and the benzyl substituted analogue (**4b**). This finding further supports the observation made in the case of **4c**, indicating that an increase in the chain length of the C-8 side chain, enhances the MAO-B inhibition potency of the 8-thiocaffeine analogues.

The following three observations above may be considered particularly important and may be applied in the design of even more potent thiocaffeine derived MAO-B inhibitors:

- The phenylethyl substituted analogue (**4c**) is a potent MAO-B inhibitor with an IC_{50} value of 0.223 µM.
- The phenoxyethyl substituted homologue (**4h**) is also a potent MAO-B inhibitor with an IC_{50} value of 0.332 µM.
- Substitution on the phenyl ring of the C-8 side chain of 8-thiocaffeine analogues with halogens (Cl, Br and F) enhances the MAO-B inhibition potencies.

From these observations the design of phenylethyl and phenoxyethyl substituted thiocaffeine derivatives which contain halogens, especially chlorine and bromine on the phenyl ring, may yield structures with particularly potent MAO-B inhibition properties. Examples of such structures are illustrated in table 4.6 below. It is the recommendation of this study that these structures be synthesized in future studies and evaluated as potential MAO inhibitors.

Table 4.6 The structures of 8-thiocaffeines that may be synthesized in future studies and evaluated as potential MAO inhibitors.

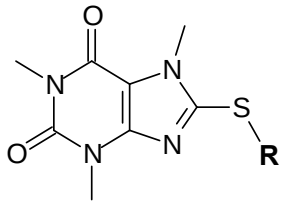

Compound	R
5a	$-(CH_2)_2-(Cl-C_6H_5)$
5b	$-(CH_2)_2-(Br-C_6H_5)$
5c	$-(CH_2)_2-O-(Cl-C_6H_5)$
5d	$-(CH_2)_2-O-(Br-C_6H_5)$

4.3.5 Comparison of the MAO inhibition properties of the 8-thiocaffeines with those of the 8-benzyloxycaffeines.

As mentioned in the objectives, one aim of the current study is to compare the MAO inhibition potencies of the 8-thiocaffeine analogues to those obtained previously for a series of 8-benzyloxycaffeine analogues (Strydom ***et al***., 2010). Shown below (Table 4.7) are the IC_{50} values of the 8-benzyloxycaffeine analogues for the inhibition of recombinant human MAO-A and -B. Table 4.8 and 4.9 compares the 8-benzyloxycafeines and the corresponding 8-thiocaffeine analogues with regards to their potency towards MAO-A and MAO-B inhibition respectively.

Table 4.7 The IC_{50} values for the inhibition of recombinant human MAO-A and ï B by 8-benzyloxycaffeine analogues (Strydom *et al.,* 2010).

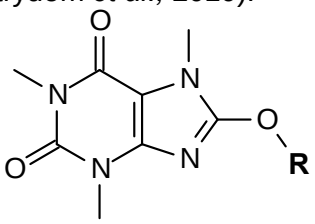

Compound	R	MAO-A IC_{50} (µM)	MAO-B IC_{50} (µM)	SI[a]
3a	C_6H_5	75.19	10.705	7.0
3b	$-CH_2-C_6H_9$	13.755	2.99	4.6
3c	$-(CH_2)_2-C_6H_5$	15.925	2.943	5.4
3d	$-CH_2-(4-Cl-C_6H_4)$	1.337	0.065	20.6
3e	$-CH_2-(4-Br-C_6H_4)$	1.304	0.062	21.0
3f	$-(CH_2)_2-O-C_6H_5$	20.35	0.383	53.1
3g	$-C_5H_9$	22.81	15.915	1.4
3h	$-(CH_2)_2-CH(CH_3)_2$	27.34	14.13	1.9

[a]The selectivity index is the selectivity for the MAO-B isoform and is given as the ratio of IC_{50}(MAO-A)/IC_{50}(MAO-B).

Table 4.8 A comparison of the IC_{50} values for the inhibition of MAO-A by the 8-thiocaffeines with the IC_{50} values of the 8-benzyloxycaffeines. The homologues compared with each other bears similar side chains at C-8 of the caffeine ring.

Compared Compounds	Human MAO-A IC_{50} (µM)	
	8-benzyloxycaffeine	8-thiocaffeine
3a with **4a**	75.19	215.290
3b with **4b**	13.755	8.224
3c with **4c**	15.925	20.537
3d with **4d**	1.337	2.76
3e with **4e**	1.304	2.61
3f with **4h**	20.35	15.493
3g with **4j**	22.81	9.40
3h with **4l**	27.34	15.163

When comparing the IC_{50} values for the inhibition of MAO-A of the 8-thiocaffeine analogues with those of the 8-benzyloxycaffeine analogues, it may be concluded that the abilities of thiocaffeines and the oxycaffeines to inhibit MAO-A are approximately equivalent, but that the most potent compounds in the benzyloxycaffeine series (**3d** and **3e**) were approximately twice as potent as their 8-thiocaffeine counterparts. Both the thiocaffeines and the oxycaffeines are moderate to weak inhibitors of human MAO-A. Interestingly, halogen substitution enhances the MAO-A inhibition activities of both the thiocaffeines and the oxycaffeines. For example, the thiocaffeines and the oxycaffeines bearing halogens (**3d,e** and **4d,e**) are the most potent MAO-A inhibitors among the compounds listed in table 4.8.

Table 4.9 A comparison of the IC_{50} values for the inhibition of MAO-B of the 8-thiocaffeines with the IC_{50} values of the 8-benzyloxycaffeines. The homologues compared with each other bears similar side chains at C-8 of the caffeine ring.

Compared Compounds	Human MAO-B IC_{50} (μM)	
	8-benzyloxycaffeine	8-thiocaffeine
3a with **4a**	10.705	33.207
3b with **4b**	2.99	1.863
3c with **4c**	2.943	0.223
3d with **4d**	0.065	0.192
3e with **4e**	0.062	0.16
3f with **4h**	0.383	0.332
3g with **4j**	15.915	20.863
3h with **4l**	14.13	2.620

When comparing the IC_{50} values for the inhibition of MAO-B of the 8-thiocaffeine analogues with those of the 8-oxycaffeine analogues, it may be concluded that the abilities of thiocaffeines and the oxycaffeines to inhibit MAO-B are similar. Among both the thiocaffeines and the oxycaffeines are compounds that are exceptionally potent inhibitors of human MAO-B. Most notably the thiocaffeines and the oxycaffeines bearing halogens (**3d, e** and **4d, e**) on the C-8 phenyl ring are the most potent MAO-B inhibitors within these series. The halogen containing oxycaffeines (**3d** and **3e**) were however found to be more potent than the halogen containing thiocaffeines (**4d** and **4e**). For example, oxycaffeines **3d** en **3e** were approximately 2.77 fold

more potent than the corresponding thiocaffeienes **4d** en **4e**. On the other hand the thiocaffeine analogue bearing a phenylethyl side chain at C-8 (**4c**, IC_{50} = 0.223 µM) was significantly more potent than the oxycaffeine analogues bearing a phenylethyl side chain at C-8 (**3c**, IC_{50} = 2.943 µM). Similarly, the thiocaffeine analogue bearing an aliphatic side chain at C-8 (**4l**, IC_{50} = 2.620 µM) was significantly more potent than the oxycaffeine bearing a phenylethyl side chain at C-8 (**3h**, IC_{50} = 14.13 µM). In general it may be concluded that while the most potent MAO-B inhibitors among the compounds listed in table 4.9 were oxycaffeines (**3d** and **3e**), there were also potent inhibitors among the thiocaffeine analogues. Similar to the oxycaffeines, the thiocaffeins may also be considered as promising lead compounds for the design of potent MAO-B inhibitors. With the appropriate substitution pattern and C-8 side chain, the MAO-B inhibition potencies of the thiocaffeines may approach those of the more potent oxycaffeines.

4.4 Time-dependent studies

4.4.1 Introduction

Also known as reversibility studies, time-dependent studies evaluate whether an inhibitor binds covalently (irreversible) or non-covalently (reversible) to an enzyme. For the time-dependent studies, an assay was used in which the enzyme activity measurements are based on the extent to which kynuramine is oxidized to 4-HQ by the MAO isoforms (Novaroli *et al*., 2005) (Figure 4.4). The inhibitor and the enzyme (MAO-A or ï B) were combined and incubated for different periods of time (0, 15, 30, 60 minutes). The substrate (kynuramine) was subsequently added and the reaction mixtures were incubated for a further 15 min. The MAO-catalysed 4-HQ formation was measured fluorometrically at excitation and emission wavelengths of 310 nm and 400 nm, respectively. An inhibitor is reversible if the amount of 4-HQ generated by MAO over the 4 time periods remains unchanged.

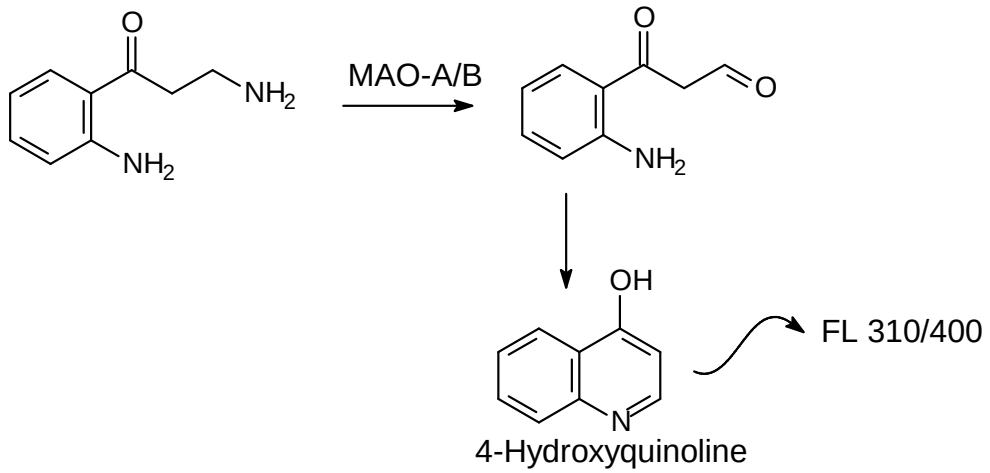

Figure 4.4 Reaction scheme for the oxidation of kynuramine to 4-hydroxyquinoline by MAO-A and -B.

4.4.2 Method

The respective MAO preparations were preincubated for periods of 0, 15, 30, 60 min at 37 °C with compound **4e** at concentrations of 0.32 ε M and 5.22 ε M (approximately 2 fold the measured IC_{50} value) for human MAO-B and human MAO-A, respectively. For this purpose, concentrations of 0.03 mg/mL of both human MAO-A and ï B were used. The incubations were carried out in potassium phosphate buffer (100 mM, pH 7.4, made isotonic with KCl). A final concentration of 45 ε M kynuramine for human MAO-A and 30 ε M kynuramine for human MAO-B were then incubated with the preincubated enzyme preparations at 37 °C for 15 min. The final volumes of these incubations were 500 ε l and the final concentration of compound **4e** was 0.16 ε M and 2.61 ε M, respectively. The final concentrations of the enzyme preparations were 0.015 mg/ml human MAO-A and ï B. The reactions with the recombinant human enzymes were terminated by the addition of 400 ε l NaOH (2 M). A volume of 1000 ε l distilled water was subsequently added to the incubations. The rates of formation of 4-HQ were measured at excitation and emission wavelengths of 310 nm and 400 nm, respectively. Quantitative estimations of 4-HQ were made by means of a linear calibration curve ranging from 0.0469ï 1.5 µM of authentic 4-HQ. Each calibration standard was prepared to a final volume of 500 µl in potassium phosphate buffer and also contained 400 µl NaOH (2 N) and 1000 µl distilled water. All measurements were carried out in triplicate and are expressed as mean ± SD.

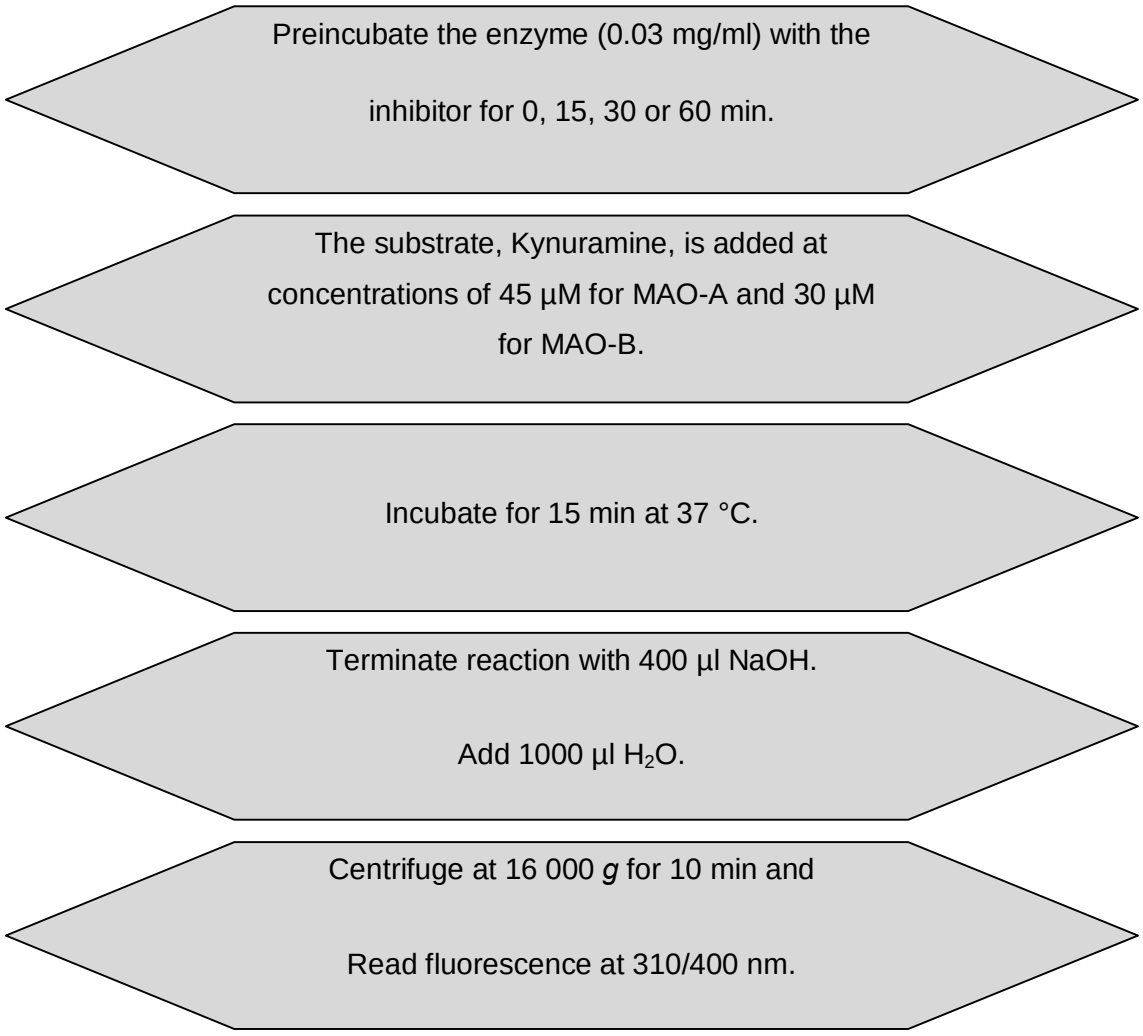

Figure 4.5 An overview of protocol followed to determine the time-dependence of inhibition of MAO.

4.4.3 Results

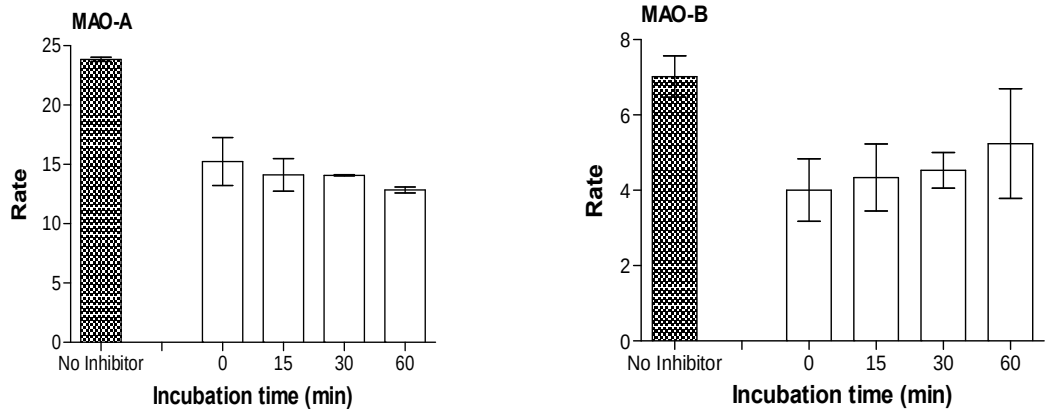

Figure 4.6 Time-dependent inhibition of recombinant human MAO-A and recombinant human MAO-B by compound **4e**. The enzymes were preincubated for various periods of time (0ï 60 min) with compound **4e** at concentrations of 5.22 µM and 0.32 µM, respectively. The concentrations of the enzyme substrate, kynuramine, were 45 and 30 µM for the studies with MAO-A and MAO-B, respectively. The catalytic rates are expressed as nmoles 4-hydroxyquinoline formed/min/mg protein.

As shown in figure 4.6, there is no time-dependent reduction in the rates of MAO-A and ï B catalysed oxidation of kynuramine when compound **4e** is preincubated with the MAO-A and ï B, for various periods of time. From this result it may be concluded that the inhibition of MAO-A and ï B is reversible, at least for the time period (60 min) and at the inhibitor concentrations (2 × IC_{50}) evaluated.

4.5 Mode of inhibition - Construction of Lineweaver-Burke plots

4.5.1 Introduction

Using a set of Lineweaverï Burk plots, the mode of inhibition may be examined. For this purpose, an assay with the same principles as the assay used for IC_{50} value determinations was employed. With this procedure the MAO-A and ï B catalysed formation of 4-HQ from kynuramine was measured in the presence of one selected inhibitor (**4e**) (Novaroli *et al*., 2005) (Figure 4.7). Lineweaverï Burk plots were constructed by plotting the initial rates of MAO

oxidation at four different substrate concentrations in the absence and presence of three different concentrations of the inhibitors. As enzyme source, recombinant human MAO-A and -B were used.

4.5.2 Method

Compound **4e,** at concentrations of 0, 1.305, 2.61 and 5.22 ε M for MAO-A and 0, 0.04, 0.08 and 0.16 ε M for MAO-B, was selected as inhibitor. The selection of **4e** was based on the finding that this compound proved to be the most potent inhibitor of MAO-A and ï B among the test compounds. Kynuramine (at 15, 30, 60 and 90 ε M) served as substrate. The 16 different incubations (500 µl), containing the different substrate and inhibitor concentrations, were pre-warmed for 15 minutes at 37 °C and human MAO-A or -B (0.015 mg/ml) was added. After 20 minutes of incubation, the reactions were terminated with the addition of 400 µl NaOH (2 N) and 1000 µl distilled water. The amount of fluorescence, which represents the amount of 4-HQ formed, was measured fluorometrically at excitation and emission wavelengths of 310 nm and 400 nm, respectively. Quantitative estimations of 4-HQ were made by means of a linear calibration curve ranging from 0.0469ï 1.5 µM. Each calibration standard was prepared to a final volume of 500 µl in potassium phosphate buffer and also contained 400 µl NaOH (2 N) and 1000 µl distilled water. Linear regression analysis was performed using the SigmaPlot® software package (Systat Software® Inc.).

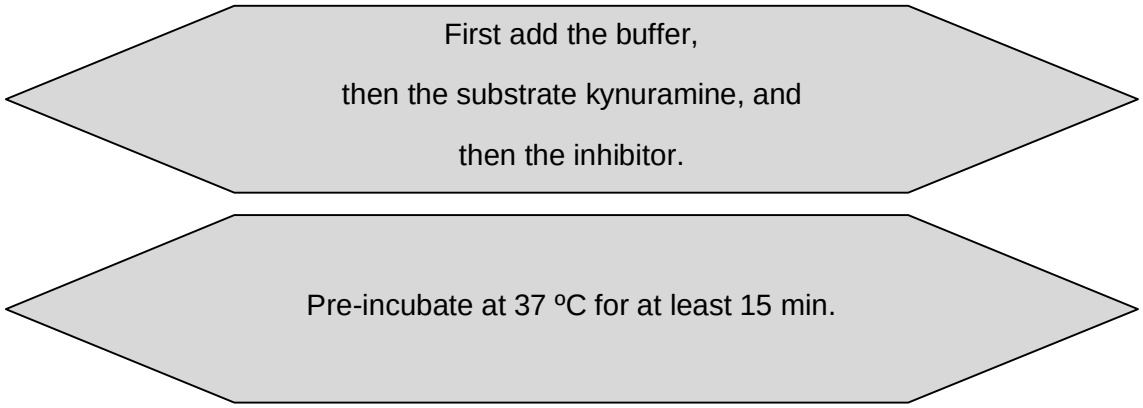

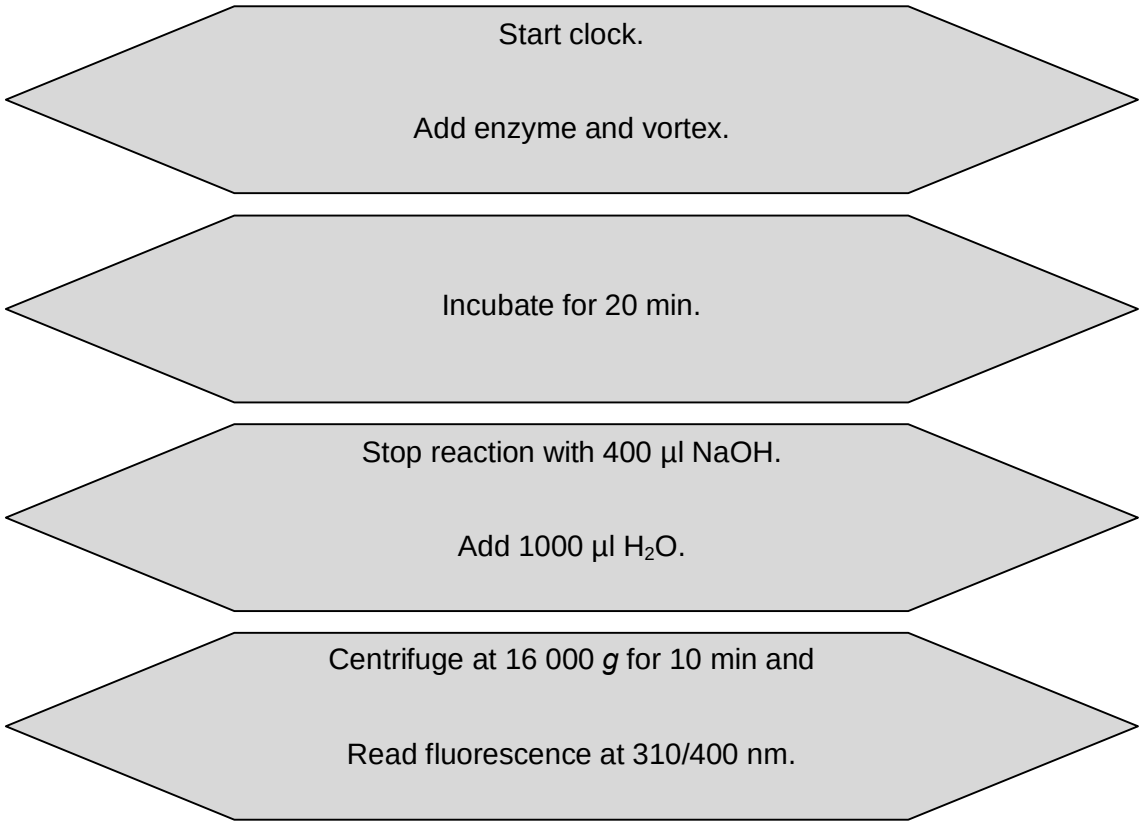

Figure 4.7 An overview of protocol followed to construct Lineweaver-Burk plots for the inhibition of MAO.

As can be seen from figure 4.8, the Lineweaver-Burk plots for both MAO-A and ï B intersect on the y-axis. This is indicative that the inhibitor is a competitive inhibitor of both human MAO-A and -B.

4.5.3 Results – Lineweaver-Burk plots

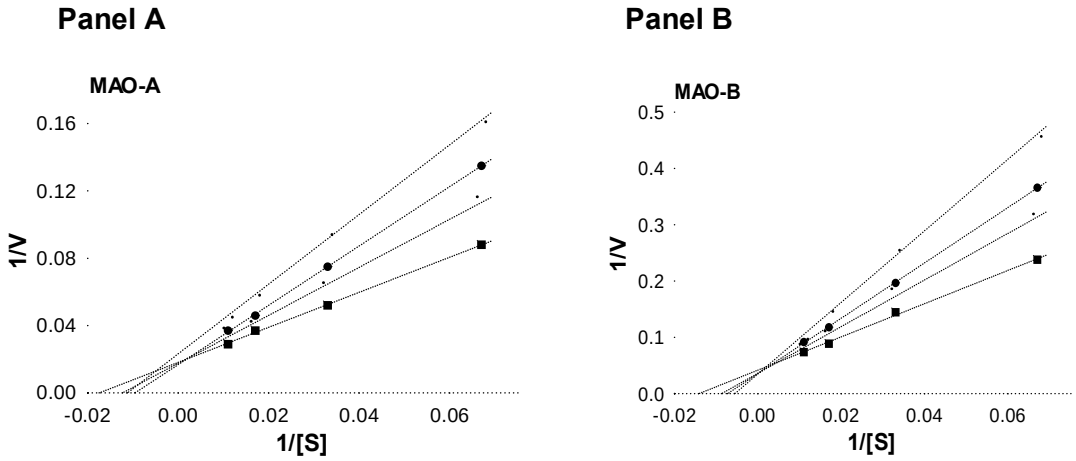

Figure 4.8 Lineweaver-Burk plots of the recombinant human MAO-A and -B catalyzed oxidation of kynuramine in the absence (filled squares) and presence of various concentrations of compound **4e**. For the studies with MAO-A the concentrations of compound **4e** were: 1.305 µM (open squares), 2.61 µM (filled circles) and 5.22 µM (open circles). For the studies with MAO-B the concentrations of compound **4e** were: 0.04 µM (open squares), 0.08 µM (filled circles) and 0.16 µM (open circles). The rates (V) are expressed as nmol product formed/min/mg protein.

4.6. Molecular modeling

4.6.1 Background

The development and discovery of new drugs for therapeutic application can be done by designing ligands for a specific receptor target. This is done by way of structural and computational chemistry. Molecular docking is the process of computationally fitting a ligand to a receptor or enzyme.

Docking studies are not only employed to identify new drugs, but can be used to examine the interaction between the active site of an enzyme and the docked inhibitor. Due to an increasing availability of high resolution structural data on enzymes and other protein receptors, docking studies are becoming an integral part of drug discovery (Knegtel *et al.,* 1997). In combination

with SAR studies, docking studies can be used to identify critical structural features of inhibitors for optimal activity towards a specific enzyme. In this study one inhibitor, compound **4e**, was docked into the active site of MAO-B.

4.6.2 Method

The molecular docking studies were carried out with the Windows® based Discovery Studio® 1.7 modeling software. The inhibitor (**4e**) was drawn in Discovery Studio® and prepared for docking with the "Prepare Ligands" protocol within Discovery Studio®. The MAO-B (2V5Z.pdb) enzyme model was obtained from Brookhaven Protein Data Bank. This structure contains safinamide as cocrystallized ligand. After the enzyme was prepared with the "Clean Protein" function it was typed with the CHARMm forcefield. A series of three minimizations were carried out with the enzyme model while the backbone was constrained. The first minimization was a steepest descent minimization, followed by the conjugate gradient and adopted Newton-Rapheson (NR) minimizations. During the minimization, the implicit distance-dependent dielectrics solvent model was used with the dielectric constant set to 4. Existing ligands were erased from the enzyme and the backbone constraints removed. The binding site was identified within the enzyme before the ligand was docked using the "Ligandfit" protocol. Following the docking. *in situ* ligand minimization employing the "Smart Minimizer" algorithm was used to refine the positions of the docked ligands. Ten possible docking poses were calculated for the inhibitor (**4e**).

4.6.3 Results and discussion

It was shown that **4e** binds to MAO-B with the caffeine moiety oriented towards the FAD co-factor while the C-8 sulfanyl side chain protrudes into the entrance cavity (Fig 4.9). This is a similar orientation to that of CSC, a potent inhibitor of MAO-B. The Ile-199 residue, which acts as a gate, is in an open conformation. Hydrogen bonding occurs between the carbonyl oxygen at C-6 of the inhibitor (**4e**) and the HOH-1155 molecule. A ´ -interaction also occurred between the inhibitor (**4e**) and the residue Tyr-398. These interactions between the caffeine ring and the substrate cavity may, to a large degree, explain the high binding affinities of several caffeine analogues to the MAO-B active site. Also of importance are the interactions of the C-8 side chain with the entrance cavity. Since the entrance cavity is a hydrophobic environment, the C-8

side chain is stabilized here via Van der Waals interactions. These interactions are considered to be important for the binding of C-8 substituted caffeine analogues to MAO-B, since caffeine, which does not contain a C-8 substituent, is a weak MAO-B inhibitor. The bromine substitution on the phenyl ring of the C-8 substituent enhances MAO-B inhibition potency by possibly enhancing dipole interactions with the entrance cavity.

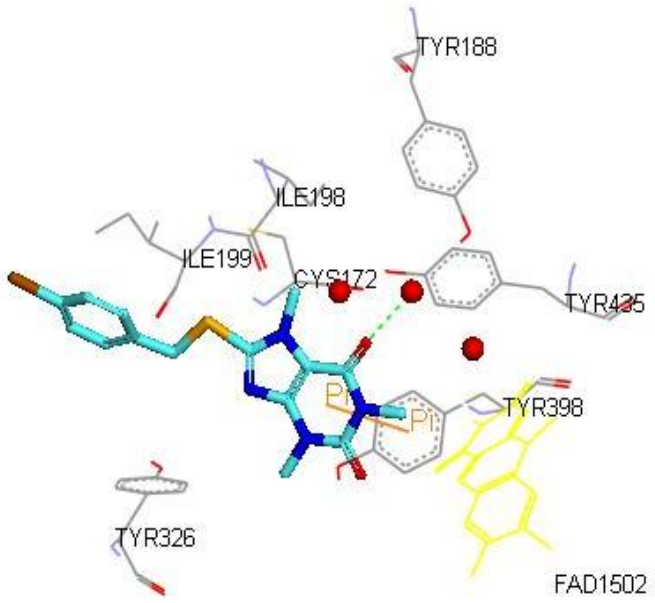

Fig. 4.9 An illustration of **4e** docked within MAO-B. The inhibitor is displayed in cyan, the FAD co-factor in yellow and hydrogen bonds in green. The red spheres represent water molecules.

4.7 Conclusion

This chapter demonstrates that 8-thiocaffeine analogues are inhibitors of MAO-A and ï B. The inhibitors display moderately potent inhibition activities towards human MAO-A with IC_{50} values ranging from 2.61 µM to 215.3 µM. The 8-thiocaffeine analogues were found to exhibit selectivity for the MAO-B isoenzyme. Among the test compounds, several highly potent inhibitors were identified. The most potent inhibitor was 8-{[(4-bromophenyl)methyl]sulfanyl}caffeine (**4e**) with an IC_{50} value of 0.16 µM towards human MAO-B. This study also shows that the selected analogue (**4e**), binds reversibly to MAO-A and ï B, and that the mode of MAO-B inhibition is competitive. From the structure-activity relationships

the following three observations may be considered particularly valuable for the design of thiocaffeine derived MAO-B inhibitors:

- The phenylethyl substituent at C-8 yields compounds with potent MAO-B inhibition activity.
- The phenoxyethyl substituent at C-8 yields compounds with potent MAO-B inhibition activity.
- Substitution on the phenyl ring of the C-8 side chain of 8-thiocaffeine analogues with halogens (Cl, Br and F) enhances the MAO-B inhibition potencies.

When comparing the inhibition potencies of the 8-thiocaffeine derivatives with those of the 8-benzyloxycaffeine analogues it may be concluded that, while the most potent MAO-B inhibitors are among the oxycaffeines, the thiocaffeines also represents a promising candidate class of compounds for the design of potent MAO-B inhibitors.

Chapter 5

Summary

In the current study, twelve C-8-substituted alkyl- and arylthiocaffeine analogues (**4a-l**) were synthesized and evaluated as inhibitors of recombinant human MAO-A and ï B. Both MAO-A and ï B are of pharmacological importance, since these enzymes are responsible for the metabolism of monoamine neurotransmitters in the brain. MAO-A is responsible for the oxidation of serotonin and noradrenalin and inhibitors of this enzyme are frequently used to treat depressive illness. MAO-B is the major dopamine metabolizing enzyme in the brain and inhibitors of this enzyme are used in the treatment of neurodegenerative diseases such as PD. MAO-B inhibitors may possess neuroprotective properties in PD by reducing the formation of potentially neurotoxic by-products, hydrogen peroxide and dopaldehyde, that are associated with the oxidation of dopamine. In addition, MAO-B inhibitors may also provide symptomatic relief, especially when combined with L-dopa, since they prevent the metabolism of dopamine and thereby may conserve the dopamine supply in the brain.

The lead compound for the design of new MAO-B inhibitors in the current study was caffeine. Although caffeine is a weak MAO-B inhibitor, substitution at C-8, with a variety of substituents has been shown to enhance the MAO-B inhibition potency of caffeine by several orders of magnitude. Of particular importance to this study is the observation that substitution of caffeine with a benzyloxy substituent at C-8 yields compounds which inhibit MAO-B with exceptional potencies (Strydom *et al*., 2010). Studies in our laboratory have shown that a variety of C-8-substituted benzyloxy side chains enhance the MAO-B inhibition potency of caffeine. The benzyloxy substituent therefore appears to be useful for enhancing the MAO-B inhibition potency of caffeine. In fact, a recent study has indicated that a relatively wide variety of C-8 alkyloxy substituents enhance the MAO-B inhibition potency of caffeine (Strydom *et al*., 2010). The current study investigated whether alkylthio substituents possess similar biological properties compared to alkyloxy substituents with respect to the enhancement of the MAO-B inhibition potency of caffeine. For this purpose this study examined if C-8 substitution of

caffeine with a variety of alkylthio substituents also enhances caffeine`s MAO-B inhibition potency to a similar degree than that observed with the alkyloxy substituents (Strydom *et al*., 2010). Twelve C-8-substituted alkyl- and arylthiocaffeine analogues (**4a-l**) were synthesized and evaluated as inhibitors of recombinant human MAO-A and ï B. The MAO-A and ï B inhibition potencies of the 8-thiocaffeine analogues were subsequently compared to that of the previously studied 8-alkyl- and aryloxycaffeine analogues.

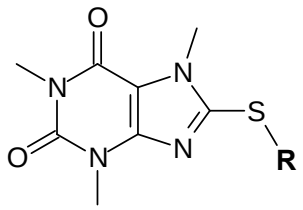

Compound	R	Compound	R
4a	C_6H_5	**4g**	$-CH_2-(4-OCH_3-C_6H_4)$
4b	$-CH_2-C_6H_5$	**4h**	$-(CH_2)_2-O-C_6H_5$
4c	$-(CH_2)_2-C_6H_5$	**4i**	$-C_6H_{11}$
4d	$-CH_2-(4-Cl-C_6H_4)$	**4j**	$-C_5H_9$
4e	$-CH_2-(4-Br-C_6H_4)$	**4k**	-2-Naphthalenyl
4f	$-CH_2-(4-F-C_6H_4)$	**4l**	$-(CH_2)_2-CH(CH_3)_2$

Chemistry: Twelve C-8-substituted alkyl- and arylthiocaffeine analogues (**4a-l**) were successfully synthesized by reacting 8-chlorocaffeine with the appropriate alkyl- and arylthiol derivatives in the presence of water, sodium hydroxide and ethanol. All of the thiol starting materials were commercially available. The structures of the target inhibitors were verified by NMR and MS analysis. Both the ^{1}H NMR and ^{13}C NMR spectra corresponded with the proposed structures and the expected exact masses were also recorded for each compound. HPLC analysis revealed a single peak for almost all the compounds analyzed, which indicates a high degree of purity for each compound.

MAO inhibition studies: The 8-thiocaffeine analogues were evaluated as inhibitors of recombinant human MAO-A and ï B. The recombinant human enzymes were commercially

available. A fluorometric assay was employed to measure the inhibition potencies of the test compounds, and the activities were expressed as the IC_{50} values. The MAO activity measurements were based on measuring the amount of 4-HQ that is produced when the MAO-A/B mixed substrate, kynyramine, is oxidized by the MAO enzymes. Since 4-HQ is fluorescent, the concentrations of the generated 4-HQ were measured with a fluorescence spectrophotometer at an excitation wavelength of 310 nm and an emission wavelength of 400 nm.

IC_{50} values: The results showed that, while the 8-thiocaffeine analogues also inhibited MAO-A, they were MAO-B selective inhibitors. The following observations are noteworthy:

- Among all of the thiocaffeine inhibitors, **4e** was the most potent MAO-B inhibitor with an IC_{50} value of 0.16 µM. This inhibitor also exhibited a high degree of selectivity towards MAO-B with a SI value of 16.3.
- Compound **4c** exhibited the highest degree of selectivity for MAO-B with a SI value of 92.1.
- Extending the length of the C-8 chain of the 8-thiocaffeine analogues resulted in an increase in MAO-B inhibition potency.
- Substitution on the phenyl ring of the C-8 substituent of the 8-thiocaffeine analogues with halogens (Cl, Br and F) enhances the MAO-B inhibition potencies.
- Replacing the C-8 phenyl ring of compound **4a** with saturated cyclopentyl and cyclohexyl rings, as well as a naphthalenyl ring and an aliphatic side chain yielded improved MAO-B inhibition potencies compared to **4a**.
- The phenoxyethyl substituted homologue (**4h**) was also found to be a potent MAO-B inhibitor with an IC_{50} value of 0.332 µM. These findings provide further evidence that increasing the chain length of the C-8 side chain, with oxygen in the chain like in this case, enhances the MAO-B inhibition potency of the 8-thiocaffeine analogues.

Time-dependency and mode of inhibition: The time-dependency of inhibition of both MAO-A and ï B by a selected 8-thiocaffeine analogue was evaluated. The results showed that compound **4e**, when preincubated with the MAO-A and ï B enzymes, respectively, did not reduce the catalytic rates of MAO-A and ï B in a time dependent manner. From this result it was concluded that the inhibition of MAO-A and ï B is reversible. For the inhibition of MAO-A and ï B by compound **4e**, sets of Lineweaverï Burk plots were constructed in order to determine the mode of inhibition. The results showed that the Lineweaver-Burk plots intersected on the y-axis which indicates that this inhibitor is a competitive inhibitor of both MAO-A and -B.

Future recommendations: Based on the high MAO-B inhibition potencies of some of the thiocaffeine derivatives, this study recommends that further studies be carried out to optimize the MAO inhibition activities of these compounds. The following observations may guide the design of novel thiocaffiene derivatives with improved MAO-B inhibition potencies:

- the phenylethyl substituted analogue (**4c**) was an exceptionally potent MAO-B inhibitor.
- the phenoxyethyl substituted homologue (**4h**) was also found to be a very potent MAO-B inhibitor.
- substitution on the phenyl ring of the C-8 side chain of the 8-thiocaffeine analogues with halogens (Cl, Br and F) enhances the MAO-B inhibition potencies.

This study therefore recommends that phenylethyl and phenoxyethyl substituted thiocaffeine derivatives which contain halogens on the phenyl ring be synthesized and evaluated as MAO inhibitors. Such structures may be particularly potent MAO-B inhibitors. Examples of such structures are given in table 5.1.

Table 5.1 Recommended thiocaffeine analogues for future studies.

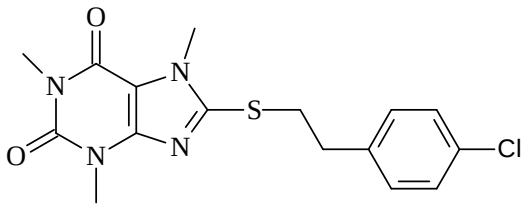	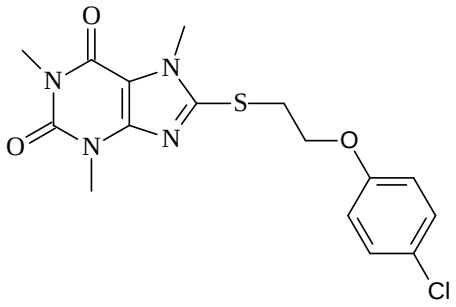
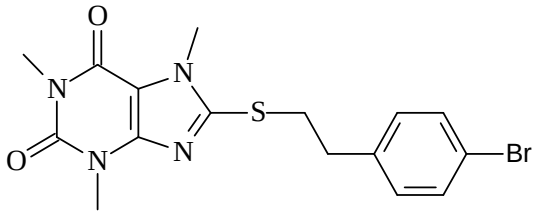	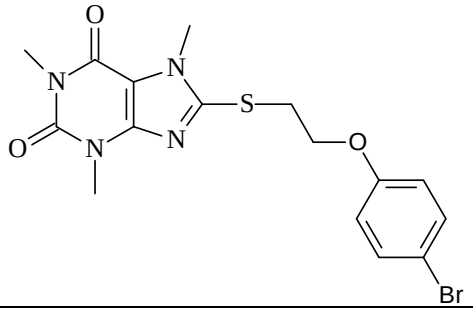

Molecular docking: Using molecular modeling it was shown that the caffeine ring of the 8-thiocaffeine analogue **4e** binds in close proximity to the FAD cofactor in the substrate cavity of MAO-B. Here it forms hydrogen bond and ´ -interactions. The C-8 side chain extends into the entrance cavity of the enzyme where it may play an important role in the stabilization of the inhibitor within the active site of MAO-B.

Bibliography

Akao, Y., Youdim, M.B., Davis, B.A., Naoi, M., & Rabey, J.M. (2001). Rasagiline mesylate, a new MAO-B inhibitor for the treatment of Parkinsonôs disease: a double-blind study as adjunctive therapy to L-dopa. *Journal of neurochemistry,* 78:727-735.

Ascherio, A., Chen, H., Schwarzschild, M.A., Zhang, S.M., Colditz, G.A., & Speizer, F.E. (2003). Caffeine, postmenopausal estrogen, and risk of Parkinson's disease. *Neurology*, 60:790-795.

Athanassiadou, A., Voutsinas, G., Psiouri, L., Leroy, E., Polymeropoulos, M.H., Ilias, A., & Maniatis, G.M. (1999). Genetic analysis of families with Parkinsonôs disease that carry the Ala53thr mutation in the gene encoding alpha-synuclein. *American journal of human genetics,* 65:555-558.

Auluck, P.K., Chan, H.Y., Trojanowski, J.Q., Lee, V.M.Y., & Bonini, N.M. (2002). Chaperone suppression of alpha-synuclein toxicity in a Drosophila model for Parkinson's disease. *Science,* 295:865-868.

Bach, A.W., Lan, N.C., Johnson, D.L., Abell, C.W., Bembenek, M.E., Kwan, S.W., Seeburg, P.H., & Shih, J.C. (1988) cDNA cloning of human liver monoamine oxidase A and B: molecular basis of differences in enzymatic properties. *Proceedings of the national academy of sciences of the United States of America*, 85:4934ï 4938.

Bernheimer, H., Birkmayer, W., Hornykiewicz, O., Jellinger, K., & Seitelberger, F. (1973). Brain dopamine and the syndromes of Parkinson and Huntington. Clinical, morphological and neurochemical correlations. *Journal of neurology science,* 20:415-455.

Betarbet, R., Sherer, T.B., MacKenzie, G., Garcia-Osuna, M., Panov, A.V. & Greenamyre, J.T. (2000). Chronic systemic pesticide exposure reproduces features of Parkinson's disease. *Nature Neuroscience,* 3:1301ï 1306.

Binda, C., Newton-Vinson, P., Hubálek F., Edmondson, D.E., & Mattevi, A. (2001). Structure of human monoamine oxidase B, a drug target for the treatment of neurological disorders. *Nature structural biology,* 9:22-26.

Binda, C., Wang, J., Pisani, L., Caccia, C., Carotti, A., Salvati, P., Edmondson, D.E., & Mattevi, A. (2007). Structures of human monoamine oxidase B complexes with selective noncovalent inhibitors: Safinamide and coumarin analogs. *Journal of medical chemistry,* 50:5848-5852.

Bové, J., Marin, C., Bonastre, M., & Tolosa, E. (2002). Adenosine A_{2a} antagonism reverses levodopa-induced motor alterations in hemiparkinsonian rats. *Synapse,* 46:251-257.

Bové, J., Prou, D., Perier, C., & Przedborski, S. (2005). Toxin-induced models of Parkinsonôs disease. *Journal of the American society for experimental neurotherapeutics,* 2:484-494.

Brooks, W.J., Jarvis, M.F., & Wagner, G.C. (1989). Astrocytes as a primary locus for the conversion of MPTP into MPP^+. *Journal of neural transmission,* 76:1-12.

Burke, WJ. (2003). 3,4-Dihydroxyphenylacetaldehyde: a potential target for neuroprotective therapy in Parkinson's disease. *Current drug targets for CNS neurology disorders*, 2:143-148.

Burns, R.S., LeWitt, P., Ebert, M.H., Pakkenberg, H., & Kopin, I.J. (1985). The clinical syndrome of striatal dopamine deficiency; parkinsonism induced by MPTP. *New England journal of medicine,* 312:1418-1421.

Cantuti-Castelvetri, I., Shukkitt-Hale, B., & Joseph, J.A. (2003). Dopamine neurotoxicity: age-dependent behavioral and histological effects. *Neurobiology of aging,* 24:697-706.

Cleeter, M.W., Cooper, J.M., & Schapira, A.H. (1992). Irreversible inhibition of mitochondrial complex I by 1-methyl-4-phenylpyridinium: evidence for free radical involvement. *Journal of neurochemistry,* 58:786-789.

Collins, G.G.S., Sandler, M., Williams, E.D., & Youdim, M.B.H. (1970). Multiple forms of human brain mitochondrial monoamine oxidase. *Nature,* 225:817-820.

Colzi, A., Dâagostini, F., Cesura, A.M., Borroni, E., & Da Prada, M. (1993). MAO-A inhibitors and dopamine metabolism in rat caudatus: evidence that an increased cytosolic level of dopamine displaces reversible MAO-A inhibitors *in vivo. Journal of pharmacology and experimental therapeutics*, 265:103-111.

Cumming, P., Munk, O.L., & Doudet, D. (2001). Loss of metabolites from monkey striatum during PET with FDOPA. *Synapse,* 41:212ï 218.

Cumming, R.G., Thomas, M., Szonyi, G., Salkeld, G., OÖNeill, L., Westbury, C., & Frampton, G. (1999). Home visits by an occupational therapist for assessment and modification of environmental hazards: a randomized trial of falls prevention. *Journal of the American geriatrics society*, 47:1397ï 1402.

Damier, P., Hirsch, E.C., Agid, Y., & Graybiel, A.M. (1999). The substantia nigra of the human brain, II. Patterns of loss of dopamine-containing neurons in Parkinsonôs disease. *Brain,* 122:1437-1448.

Dauer, W., & Przedborski, S. (2003). Parkinsonôs Disease: mechanisms and models. *Neuron,* 39:889-909.

Davidson, J.R. (2003). Pharmacotherapy of social phobia. *Acta psychiatrica Scandinavica,* 417:65-71.

Day, B.J., Patel, M., Calavetta, L., Chang, L.Y., & Stamler, J.S. (1999). A mechanism of paraquat toxicity involving nitric oxide synthase. *Proceedings of the national academy of sciences of the United States of America,* 96:12760-12765.

De Colibus, L., Li, M., Binda, C., Lustig, A., Edmondson, D.E., & Mattevi, A. (2005). Three-dimensional structure of human monoamine oxidase A: relation to the structures of rat MAO-

A and human MAO-B. *Proceedings of the national academy of sciences of the United States of America,* 102:12684-12689.

Deleu, D., Northway, M.G., & Hanssens, Y. (2004). Clinical pharmacokinetic and pharmacodynamic properties of drugs used in the treatment of Parkinsonôs disease. *Clinical pharmacokinetics,* 41:261-309.

Edmondson, D.E., Mattevi, A., Binda, C., Li, M., & Hubálek, F. (2004). Structure and mechanism of monoamine oxidase. *Current medicinal chemistry,* 11:1983-1993.

Elbaz, A., &Tranchant, C. (2007). Epidemiologic studies of environmental exposures in Parkinsonôs disease. *Journal of neurology science,* 262:37-44.

Esposito, E., Di Matteo, A., Benigno, M., Pierucci, M., Crescimanno, G., & Di Giovanni, G. (2007). Non-steroidal anti-inflammatory drugs in Parkinsonôs disease. *Experimental neurology,* 205:295-312.

Fahn, S., Oakes, D., Shoulson, I., Kieburtz, K., Rudolph, A., Lang, A., Olanow, C.W., Tanner, C., & Marek, K. (2004). L-dopa and the progression of Parkinsonôs disease. *New England journal of medicine,* 351:2498-2508.

Faull, R.L., & Laverty, R. (1969). Changes in dopamine levels in the corpus striatum following lesions in the substantia nigra. *Experimental neurology*, 23:332-340.

Ferger, B., Teismann, P., & Mierau, J. (2000). The dopamine agonist pramipexole scavenges hydroxyl free radicals induced by striatal application of 6-hydroxydopamine in rats: an *in vivo* microdialysis study. *Brain research,* 883:216-223.

Fernandez, H.H., & Chen, J.J. (2007). Monoamine oxidase-B inhibition in the treatment of Parkinsonôs disease. *Pharmacotherapy,* 27:174S-185S.

Finberg, J.P., Lamensdorf, I., Weinstock, M., Schwartz, M., & Youdim, M.B. (1999). Pharmacology of rasagiline (*N*-propargyl-1*R*-aminoindan). *Advanced neurology,* 80:495-499.

Finberg, J.P., Tenne, M., & Youdim, M.B. (1981). Tyramine antagonistic properties of AGN 1135, an irreversible inhibitor of monoamine oxidase type B. *British journal for pharmacology*, 73:65-74.

Finberg, J.P., Wang, J., Bankiewicz, K., Harvey-White, J., Kopin, I.J., & Goldsteen, D.S. (1998). Increased striatal dopamine production from L-dopa following selective inhibition of monoamine oxidase B by R(+)-*N*-propargyl-1-aminoindan (rasagiline) in the monkey. *Journal of neural transmission,* 52:279-285.

Fischer, E., & Reese, L. (1883). 8-Chlorocaffeine. *Liebigs annalen der chemie*, 221:336.

Giasson, B.I., Duda, J.E., Murray, I.V., Chen, Q., Souza, J.M., Hurtig, H.I., Ischiropoulos, H., Trojanowski, J.Q., & Lee, V.M. (2000). Oxidative damage linked to neurodegeneration by selective alpha-synuclein nitration in synucleinopathy lesions. *Science*, 290:985-989.

Green, A.R., Mitchell, B.D., Tordoff, A.F., & Youdim, M.B. (1977). Evidence for dopamine deamination by both type A and type B monoamine oxidase in rat brain *in vivo* and for the degree if inhibition of enzyme necessary for increased functional activity of dopamine and 5-hydroxytryptamine. *British journal of pharmacology,* 60:343-349.

Grunblatt, E., Mandel, S., Jacob-Hirsch, J., Zeligson, S., Amariglo, N., Rechavi, G., Li, J., Ravid, R., Roggendorf, W., Riederer, P., & Youdim, M.B. (2004). Gene expression profiling of parkinsonian substantia nigra pars compacta; alterations in ubiquitin-proteasome, heat shock protein, iron and oxidative stress regulated proteins, cell adhesion/cellular matrix and vesicle trafficking genes. *Journal of neural transmission*, 111:1543-1573.

Haefely, W., Burkard, W.P., Cesura, A.M., Kettler, R., Lorez, H.P., Martin, J.R., Richards, J.G., Scherschlicht, R., & Da Prada, M. (1992). Biochemistry and pharmacology of moclobemide, a prototype RIMA. *Psychopharmacology*, 106:S6-S14.

Hardy, J. (2005). Expression of normal sequence pathogenic proteins for neurodegenerative disease contributes to disease risk: ópermissive templatingôas a general mechanism underlying neurodegeneration. *Biochemical society transactions,* 33:578-581.

Hastings, T.G., & Lewis, D.A. (1996). Reactive dopamine metabolites and neurotoxicity: implications for Parkinsonôs disease. *Advances in experimental medicine and biology,* 387:97-106.

Healy, D.G., Falchi, M., O'Sullivan, S.S., Bonifati, V., Durr, A., Bressman, S., Brice, A., Aasly, J., Zabetian, C.P., Goldwurm, S., Ferreira, J.J., Tolosa, E., Kay, D.M., Klein, C., Williams, D.R., Marras, C., Lang, A.E., Wszolek, Z.K., Berciano, J., Schapira, A.H., Lynch, T., Bhatia, K.P., Gasser, T., Lees, A.J., & Wood NW. (2008). Phenotype, genotype and worldwide genetic penetrance of LRRK-2-associated Parkinsonôs disease: a case-control study. *Lancet neurology,* 7:583-590.

Heikkila, R.E., Terleckyj, I., & Sieber, B.A. (1990). Monoamine oxidase and the bioactivation of MPTP and related neurotoxins: relevance to DATATOP. *Journal of neural transmission,* 32:217-227.

Howells, D.W., Porritt, M.J., Wong, J.Y., Batchelor, P.E., Kalnins, R., Hughes, A.J., & Donnan, G.A. (2000). Reduced BDNF mRNA expression in the Parkinsonôs disease substantia nigra. *Experimental neurology,* 166:127-135.

Hubálek, F., Binda, C., Khalil, A., Li, M., Mattevi, A., Castagnoli, N., & Edmondson D.E. (2005). Demonstration of isoleucine 199 as a structural determinant for the selective inhibition of human monoamine oxidase B by specific reversible inhibitors. *The journal of biological chemistry,* 280:15761-15766.

Ikeda, K., Kurokawa, M., Aoyama, S., & Kuwana, Y. (2002). Neuroprotection by adenosine A_{2A} receptor blockade in experimental models of Parkinsonôs disease. *Journal of neurochemistry,* 80:262-270.

Jalkanen, S., & Salmi, M. (2001). Cell surface monoamine oxidase: enzymes in search of a function. *The EMBO journal,* 20:3893-3901.

Javoy, F., Sotelo, C., Herbert, A., & Agid, Y. (1976). Specificity of dopaminergic neuronal degeneration induced by intracerebral injection of 6-hydroxydopamine in the nigrostriatal dopamine system. *Brain research,* 102:210-215.

Johnston, P. (1968). Some observations upon a new inhibitor of monoamine oxidase in brain tissue. *Biochemical pharmacology,* 17:1285-1297.

Kearney, E.B., Salach, J.I., Walker, W.H., Seng, R.L., Kenney, W., Zeszotek, E., & Singer, T.P. (1971). Structure of the covalently bound flavin of monoamine oxidase. *Biochemical and biophysical research communications,* 42:490-496.

Kitada, T., Asakawa, S., Hattori, N., Matsumine, H., Yamamura, Y., Minoshima, S., Yokochi, M., Mizuno, Y., & Shimizu, N. (1998). Mutations in the parkin gene cause autosomal recessive juvenile parkinsonism. *Nature,* 392:605-608.

Klinman, J.P., & Mu, D. (1994). Quinoenzymes in biology. *Proceedings of the national academy of sciences of the United States of America,* 63:299-344.

Knetgel, R.M.A., Kuntz, I.D., & Oshiro, C.M. (1997). Molecular docking to ensembles of protein structures. *Journal of molecular biology,* 266:424-440.

Langston, J.W., Ballard, P., & Irwin, I. (1983). Chronic pakinsonsm in humans due to a product of meperidine-analog synthesis. *Science*, 219:979-980.

Le, W.D., & Jankovic, J. (2001). Are dopamine receptor agonists neuroprotective in Parkinsonôs disease? *Drugs and aging,* 18:389-396.

Lees, A. (2005). Alternatives to L-dopa in the initial treatment of early Parkinsonôs disease. *Drugs and aging,* 22:731-740.

Lees, A.J., Hardy, J., & Revesz, T. (2009). Parkinsonôs disease. *Lancet*, 373:2055-2066.

LeWitt, P.A., & Taylor, D.C. (2008). Protection against parkinsonôs disease progression: clinical experience. *Neurotherapeutics,* 5:210-225.

LeWitt, P.A., Segel, S.A., Mistura, K.L., & Schork, K.L. (1993). Symptomatic anti-parkinsonism effects of monoamine oxidase-B inhibition: comparison of selegiline and lazabemide. *Clinical neuropharmacology,* 16:332-337.

Liou, H.H., Tsai, M.C., Chen, C.J., Jeng, J.S., Chang, Y.C., Chen, S.Y., & Chen, R.C. (1997). Environmental risk factors and Parkinsonôs disease: a case-control study in Taiwan. *Neurology,* 48:1583-1588.

Long, L.M. (1947). 8-R-Thio- and 8-R-sulfonylcaffeine derivatives. *Journal of the American chemical society,* 69:2939-2940.

Luthman, J., Fredriksson, A., Sundstrom, E., Jonsson, G., & Archer, T. (1989). Selective lesion of central dopamine or noradrenaline neuron systems in the neonatal rat: motor behavior and monoamine alterations at adult stage. *Behavioural brain research*, 33:267-277.

Lyles, G.A. (1996). Mammalian plasma and tissue-bound semicarbazide-sensitive amine oxidases: biochemical, pharmacological and toxicological aspects. *Journal of biochemistry and cellular biology,* 28:259-274.

Ma, J., Yoshimura, M., Yamashita, E., Nakagawa, A., Ito, A., & Tsukihara, T. (2004). Structure of rat monoamine oxidase A and its specific recognitions for substrates and inhibitors. *Journal of molecular biology,* 338: 103-114.

Mandel, S., Grünblatt, E., Riederer, P., Gerlach, M., Levites, Y., & Youdim, M.B.H. (2003). Neuroprotective strategies in Parkinsonôs disease: an update on progress. *Central nervous system drugs,* 17:729-762.

Mandell, S., Weinreb, O., Amit, T., & Youdim, M.B. (2005). Mechanism of neuroprotective action of the anti-parkinson drug rasagiline and its derivatives. *Brain research reviews,* 48:379-387.

Manning-Bog, A.B., McCormack, A.L., Li, J., Uversky, V.N., Fink, A.L., & Di Monte, D.A. (2002). The herbicide paraquat causes upregulation and aggregation of alpha-synuclein in mice: paraquat and alpha-synuclein. *Journal of biological chemistry,* 277:1641-1644.

Maroney, A.C., Glicksman, M.A., Basma, A.N., Walton, K.M., Knight, E. Jr., Murphy, C.A., Bartlett, B.A., Finn, J.P., Angeles, T., Matsuda, Y., Neff, N.T., & Dionne, C.A. (1998). Motor neuron apoptosis is inflicted by CEP-1347 (KT7515), a novel inhibitor of the JNK signalling pathway. *Journal of neuroscience,* 18:104-111.

Mason, R.P., Olmstead, E.G., & Jacob, R.F. (2000). Antioxidant activity of the monoamine oxidase B inhibitor lazabemide. *Biochemical pharmacology,* 60:709-716.

Miller, J.R., Edmondson, D.E., & Grissom, C.B. (1995). Mechanistic probes of monoamine oxidase B catalysis: Rapid-scan stopped flow and magnetic field independence of the reductive half-reaction. *Journal of the American chemical society*, 117:7830-7831.

Mu, D., Janes, S.M., Smith, A.J., Brown, D.E., Dooley, D.M., & Klinman, J.P. (1992). Tyrosine codon corresponds to topa quinine at the active site of copper amine oxidases. *Journal of biological chemistry,* 267:7979-7982.

Nagatsu, T. (1997). Isoquinoline neurotoxins in the brain and Parkinsonôs disease. *Neuroscience research,* 29:99-111.

Newton Vinson, P., Hubalek, F., & Edmondson, D.E. (2000) High-level expression of human liver monoamine oxidase B in Pichia pastoris. *Protein expression and purification*, 20:334-345.

Nicotra, A., Pierucci, F., Parvez, H., & Senatori, O. (2004). Monoamine oxidase expression during development and aging. *Neurotoxicology*, 25:155-165.

Novaroli, L., Reist, M., Favre, E., Carotti, A., Catto, M., & Carrupt, P.A. (2005). Human recombinant monoamine oxidase B as reliable and efýcient enzyme source for inhibitor screening. *Bioorganic & medicinal chemistry*, 13:6212ï 6217.

Olanow, C.W., Jenner, P., & Brooks, D. (1998). Dopamine agonist and neuroprotection in Parkinsonôs disease. *Annals of neurology,* 44:S167-S174.

Olanow, C.W., Anthony, A., Schapira, LeWitt, P.A., Kieburtz, K., Sauer, D., Olivieri, G., Pohlmann, H., & Hubble, J. (2006). TCH346 as a neuroprotective drug in Parkinsonôs disease: a double-blind, randomised, controlled trial. *Lancet neurology,* 5:1013-1020.

Olanow, C.W., Watts, R.L., & Koller, W.C. (2001). An algorithm (decision tree) for the management of Parkinsonôs disease: treatment guidelines. *Neurology,* 56 (Suppl 5):S1-88.

Parkinsonôs study group. (1989). DATATOP: a multicenter controlled clinical trial in early Parkinsonôs disease. *Archives of neurology,* 46:1052-1060.

Parkinsonôs study group. (1993). Effects of tocopherol and deprenyl on the progression of disability in early Parkinsonôs disease. *New English journal of medicine,* 328:176-183.

Parkinsonôs study group. (1994). A controlled trial of lazabemide in L-dopa-treated Parkinsonôs disease. *Archives of neurology,* 51:342-347.

Parkinsonôs study group. (1996). Effect of lazabemide on the progression of disability in early Parkinsonôs disease. *Annals of neurology,* 40:99-107.

Pretorius, J., Malan, S.F., Castagnoli, N., Jr., Bergh, J.J., & Petzer, J.P. (2008). Dual inhibition of monoamine oxidase B and antagonism of the adenosine A(2A) receptor by (E,E)-8-(4-phenylbutadien-1-yl)caffeine analogues. *Bioorganic & medical chemistry,* 16:8676-8684.

Przedborksi, S. (2004). Pathogenesis of nigral cell death in Parkinson's disease. *Parkinson's and related disorders,* 11:S3-S7.

Przedborski, S., Kostic, V., Jaskson-Lewis, V., Naini, A.B., Simonetti,S., Fahn, S., Carlson, E., Epstein, C.J., & Cadet, J.L. (1992). Transgenic mice with increased Cu/Zn-superoxide dismutase activity are resistant to N-methyl-4-phenyl-1,2,3,6-tetrahydropyridine-induced neurotoxicity. *Journal of neuroscience,* 12:1658-1667.

Przedborski, S., Tieu, K., Perier, C., & Vila, M. (2004). MPTP as a mitochondrial neurotoxic model of Parkinson's disease. *Journal of bioenergetics and biomembranes,* 36:375-379.

Ramsay, R.R. (1991). Kinetic mechanism of monoamine oxidase A. *Biochemistry,* 30:4624-4629.

Ransom, B.R., Kunis, D.M., Irwin, I., & Langston, J.W. (1987). Astrocytes convert the parkinsonism inducing neurotoxin, MPTP, to its active metabolite. *Neuroscience letters,* 75:323-328.

Rascol, O., Olanow, C.W., Brooks, D., Koch, G., Truffinet, P., & Bejuit, R. (2002). A 2-year multicenter placebo-controlled, double blind parallel group study of the effect of rulizole in Parkinson's disease. *Movement disorders,* 17:39.

Riederer, P., & Youdim, M.B. (1986). Monoamine oxidase acitivity and monoamine metabolism in brains of parkinsonian patients treated with selegiline. *Journal of neurochemistry,* 46:1359-1365.

Riederer, P., Danielczyk, W., & Grünblatt, E. (2004). Monoamine oxidase-B inhibition in *Alzheimer's disease. Neurotoxicology, 25:271-277.*

Riederer, P., Sofic, E., Rausch, W.D., Schmidt, B., Reynolds, G.P., Jellinger, K., & Youdim, M.B. (1989). Transition metals, ferritin, glutathione, and ascorbic acid in parkinsonian brains. *Journal of neurochemistry,* 52:515-520.

Rodwell, V.W., & Kennely, P.J. Haperôs Illustrated Biochemistry. 28th Edition, Chapter 8:60-71.

Samii, A., Nutt, J.G., & Ransom, B.R. (2004). Parkinsonôs disease. *Lancet*, 363:1783-1793.

Saura, M.J., Kettler, R., Da Prada, M., & Richards, J.C. (1990). Molecular neuroanatomy of MAO-A and ï B. *Journal of neural transmission,* 32:49-53.

Scherfler, C., Schocke, M.F., Seppi, K., Esterhammer, R., Brenneis, C., Jaschke, W., Wenning, G.K., & Poewe, W. (2006). Voxel-wise analysis of diffusion weighted imaging reveals disruption of the olfactory tract in Parkinsonôs disease. *Brain,* 129:538-542.

Schuler, F., & Casida, J.E. (2001). Functional coupling of PSST and ND1 subunits in NADH: ubiquinone oxidoreductase established by photoaffinity labeling. *Biochimica et biophysica acta,* 1506:79-87.

Selley, M.L. (2005). Simvastatin prevents 1-methyl-4-phenyl-1,2,3,6-tetrahydropyridine-induced striatal dopamine depletion and protein tyrosine nitration in mice. *Brain research,* 1037:1-6.

Shih, J.C., Chen, K., & Ridd, M.J. (1999). Monoamine oxidase: from genes to behavior. *Annual review of neuroscience,* 22:197-217.

Shimizu, K., Ohtaki, K., Matsubara, K., Aoyama, K., Uezono, T., Saito, O., Suno, M., Ogawa, K., Hayase, N., Kimura, K., & Shiono, H. (2001). Carrier-mediated processes in blood-brain barrier penetration and neural uptake of paraquat. *Brain research,* 906:135-142.

Shin, M.H., Jang, J.H., & Surh, Y.J. (2004). Potential roles of NF-əB and ERK1/2 in cytoprotection against oxidative cell death induced by tetrahydropapaveroline. *Free radical biology and medicine,* 36:1185ï 1194.

Shults, C.W., Haas, R.H., & Beal, M.F. (1999). A possible role of coenzyme Q_{10} in the etiology and treatment of Parkinsonôs disease. *Biofactors,* 9:267-272.

Silverman, R.B. (1992) The organic chemistry of enzyme-catalyzed reactions. *Advances in electron transfer chemistry*, 2:177-180.

Singer, T.P., Ramsay, R.R., McKeown, K., Trévor, A., & Castagnoli, N. (1988). Mechanism of the neurotoxicity of 1-methyl-4-phenylpyridinium (MPP^+), the toxic bioactivation product of 1-methyl-4-phenyl-1,2,3,6-tetrahydropyridine (MPTP). *Toxicology,* 49:17-23.

Smeyne, R.J., & Jackson-Lewis, V. (2005). The MPTP model of Parkinsonôs disease. *Molecular brain research,* 134:57-66.

Son, S., Ma, J., Kondou, Y., Yoshimura, M., Yamashita, E., & Tsukihara, T. (2008). Structure of human monoamine oxidase A at 2.2-Å resolution: The control of opening the entry for substrates/inhibitors. *Proceedings of the national academy of sciences of the United States of America*, 105:5739-5744.

Spillantini, M.G., Schmidt, M.L., Lee, V.M., Trojanowski, R., & Goedert, M. (1997). Alpha-synuclein in Lewy bodies. *Nature,* 388:839-840.

Strydom, B., Malan, S.F., Castagnoli, N., Jr., Bergh, J.J., & Petzer, J.P. (2010). Inhibition of monoamine oxidase by 8-benzyloxycaffeine analogues. *Bioorganic & medicinal chemistry,* 18:1018-1028.

Tabor, C.W., Tabor, H., & Rosenthal, S.M. (1954). Purification of amine oxidase from beef plasma. *Journal of biological chemistry,* 208:645-661.

Tanaka, K., Miyazaki, I., Fujita, N., Haque, M.E., Asanuma, M., & Ogawa, N. (2001). Molecular mechanism in activation of glutathione system by ropinirole, a selective dopamine D2 agonist. *Neurochemistry research,* 26:31-36.

Tansey, M.G., McCoy, M.K., & Frank-Cannon, T.C. (2007). Neuroinflammatory mechanisms in Parkinsonôs disease: potential environmental triggers, pathways, and targets for early therapeutic intervention. *Experimental neurology,* 208:1-25.

Tatton, W.G., Chalmers-Redman, R., Brown, D., & Tatton, N. (2003). Apoptosis in Parkinsonôs disease: signals for neuronal degradation. *Annals of neurology,* 53:S61-S70.

Taylor, K.S., Counsell, C.E., Gordon, J.C., & Harris, C.E. (2005). Screening for undiagnosed parkinsonism among older people in general practice. *Age and aging,* 34:501-504.

Twelves, D., Perkins, K.S., & Counsell, C. (2003). Systematic review of incidence studies of Parkinsonôs disease. *Movement Disorders,* 18:19-31.

Ulmschneider, M.B., & Sansom, M.S. (2001). Amino acid distributions in integral membrane protein structures. *Biochimica et biophysica* acta*,* 2:1512-1515.

Ungerstedt, U. (1971). Stereotaxic mapping of the monoamine pathways in the rat brain. *Acta physiologica Scandinavica,* 367:1-48.

Waldmeier, P, Bozyczko-Coyne, D., Williams, M., & Vaught, J.L. (2006). Recent clinical failures in Parkinsonôs disease with apoptosis inhibitors underline the need for a paradigm shift in drug discovery for neurodegenerative diseases. *Biochemical pharmacology,* 72:1197-1206.

Walker, M.C., & Edmondson, D.E. (1994). Structure-activity relationships in the oxidation of benzylamine analogs by bovine liver mitochondrial monoamine oxidase B. *Biochemistry,* 33:7088ï 7098.

Wang, S.X., Nakamura, N., Mure, M., Klinman, J.P., & Sanders-Loehr, J. (1997). Characterization of the native lysine tyrosylquinone cofactor in lysyl oxidase by Raman spectroscopy. *Journal of biological chemistry,* 272:28841-28844.

Warrick, J.M., Chan, H.Y., Gray-Board, G.L., Chai, Y., Paulson, H.L., & Bonini, N.M. (1999). Suppression of polyglutamine-mediated neurodegeneration in Drosophila by the molecular chaperone HSP70. *Nature genetics,* 23:425-428.

Williams, D.R., Hadded, A., al-Din, A.S., Wreikat, A.L., & Lees, A.J. (2005). Kufor Rakeb disease: autosomal recessive L-dopa responsive Parkinsonism with pyramidal degeneration, supranuclear gaze palsy and dementia. *Movement disorders,* 20:1264-1271.

Wu, D.C., Jackson-Lewis, V., Vila, M., Tieu, K., Teismann, P., Vadseth, C., Choi, D.K., Ischiropoulos, H., & Przedborski, S. (2002). Blockade of microglial activation is neuroprotective in the 1-methyl-4-phenyl-1,2,3,6-tetrahydropyridine mouse model of Parkinsonôs disease. *Journal of neuroscience,* 22:1763-1771.

Yacoubian, T.A., & Standaert, D.G. (2009). Targets for neuroprotection in Parkinsonôs disease. *Biochimica et biophysica acta,* 1792:676-687.

Yamada, M., & Yasuhara, H. (2004). Clinical pharmacology of MAO inhibitors: safety and future. *Neurotoxicology,* 25:215-21.

Yamada, M., & Yasuhara, H. (2004). Clinical pharmacology of MAO inhibitors: Safety and future. *Neurotoxicology,* 25:215-221.

Youdim, M.B.H., & Weinstock, M. (2004). Therapeutic applications of selective and non-selective inhibitors of monoamine oxidase A and B that do not cause significant tyramine potentiation. *Neurotoxicology,* 25:243-250.

Youdim, M.B.H., Banerjee, D.K., Kelner, K., Offutt, L., & Pollard, H.B. (1989). Steroid regulation of monoamine oxidase activity in the adrenal medulla. *Federation of American societies for experimental biology journal*, 3:1753ï 1759

Youdim, M.B.H., Finberg, J.P., & Tipton, K.F. (1988). Monoamine oxidase. *Advances in experimental pharmacology,* 2:119-192.

Youdim, M.B.H., & Bakhle, Y.S. (2006). Monoamine oxidase: isoforms and inhibitors in Parkinsonôs disease and depressive illness. *British journal of pharmacology,* 147:S287-S296.

Youdim, M.B.H., Collins, G.G.S., Sandler, M., Bevan-Jones, A.B., Pare, C.M., & Nicholson, W.J. (1972). Human brain monoamine oxidase, multiple forms and selective inhibitors. *Nature,* 236:225-228.

Youdim, M.B.H., Edmondson, D., & Tipton, K.F. (2006). The therapeutic potential of monoamine oxidase inhibitors. *Neuroscience,* 7:295-309.

Zecca, L., Youdim, M.B., Riederer, P Connor, J.R., & Crichton, R.R. (2004). Iron, brain ageing and neurodegenerative disorders. *Nature reviews neuroscience,* 5:863-873.

Zhou, M., Diwu, Z., Panchuk-Voloshina, N., & Haugland, R.P. (1997). A stable nonfluorescent derivative of resorufin for the fluorometric determination of trace hydrogen peroxide applications in detecting the activity of phagocyte NADPH oxidase and other oxidases. *Analytical biochemistry,* 253:162-168.

Zhu, Q., Chen, K., & Shih, J. (1994). Bidirectional promoter of human monoamine oxidase A (MAO A) controlled by transcription factor Sp1. *Journal of neuroscience*, 14:7393ï 7403.

Zisook, S.E. (1985). Clinical overview of monoamine oxidase inhibitors. *Psychosomatics,* 26:240ï 251.

Addendum

List of ^{1}H and ^{13}C spectrums:

^{1}H NMR

8-(Phenylsulfanyl)caffeine

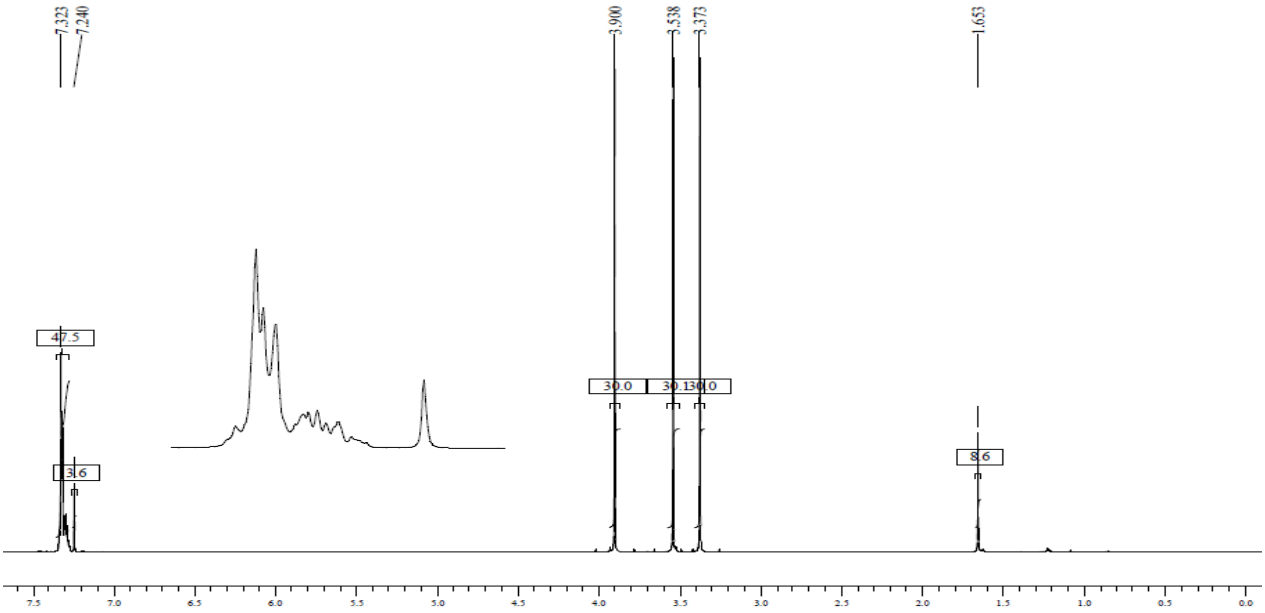

^{13}C NMR

8-(Phenylsulfanyl)caffeine

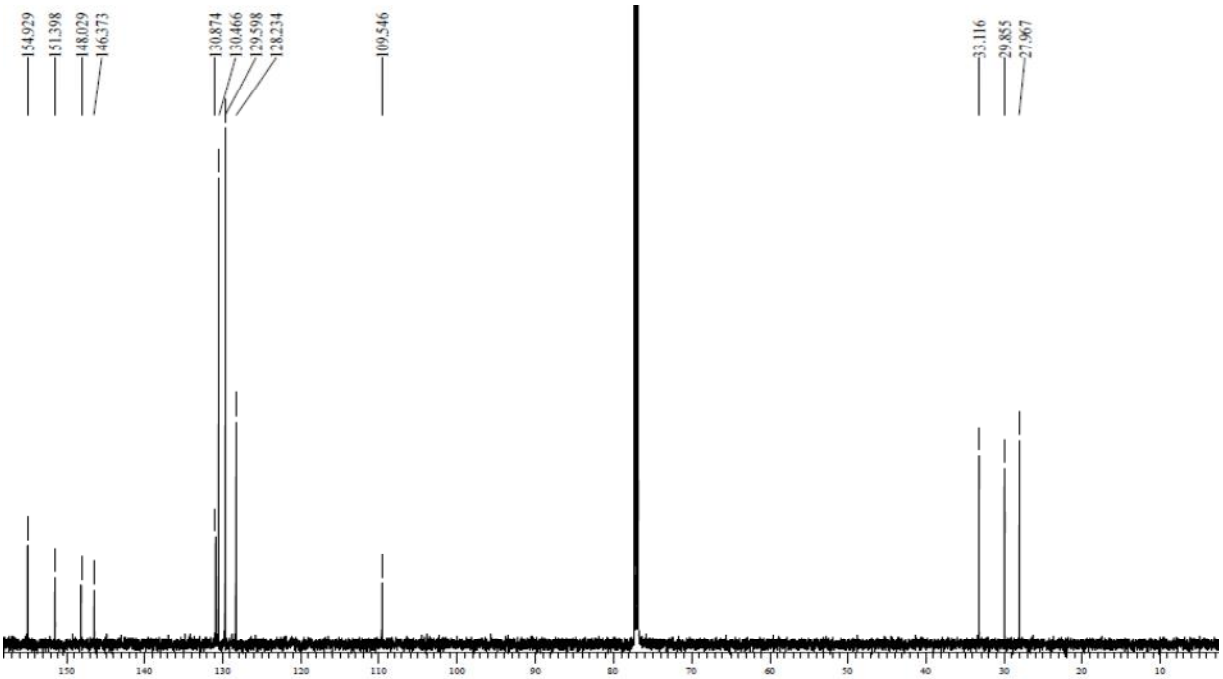

^{1}H NMR

8-(Benzylsulfanyl)caffeine

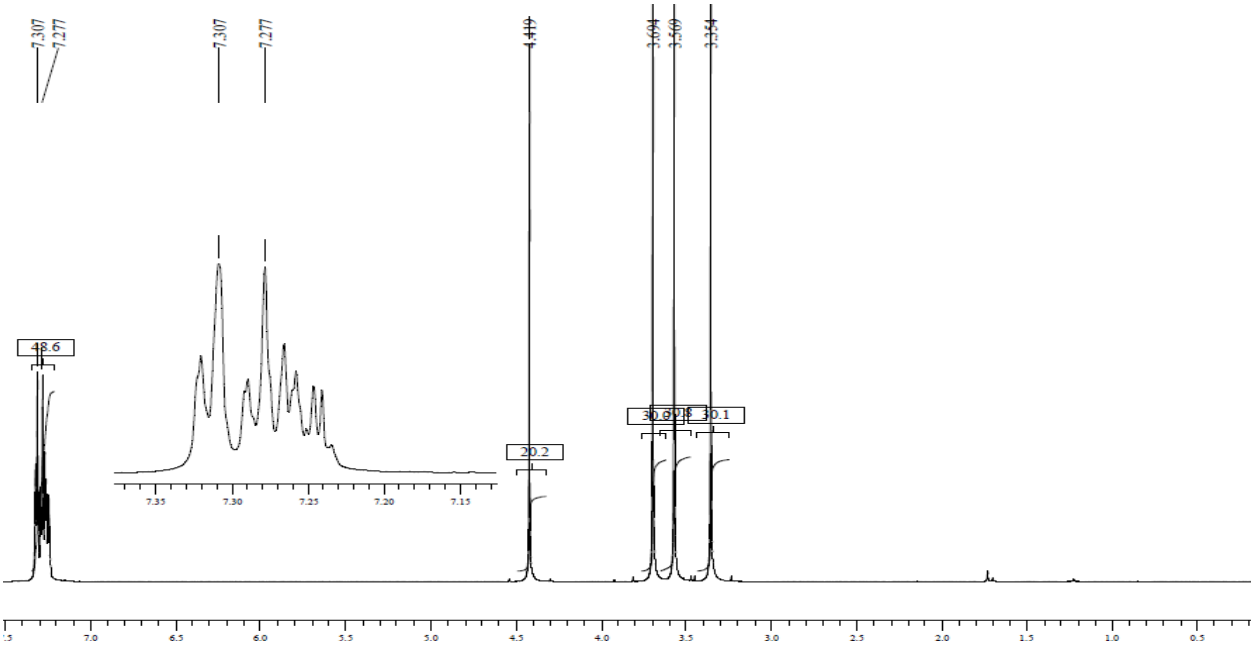

^{13}C NMR

8-(Benzylsulfanyl)caffeine

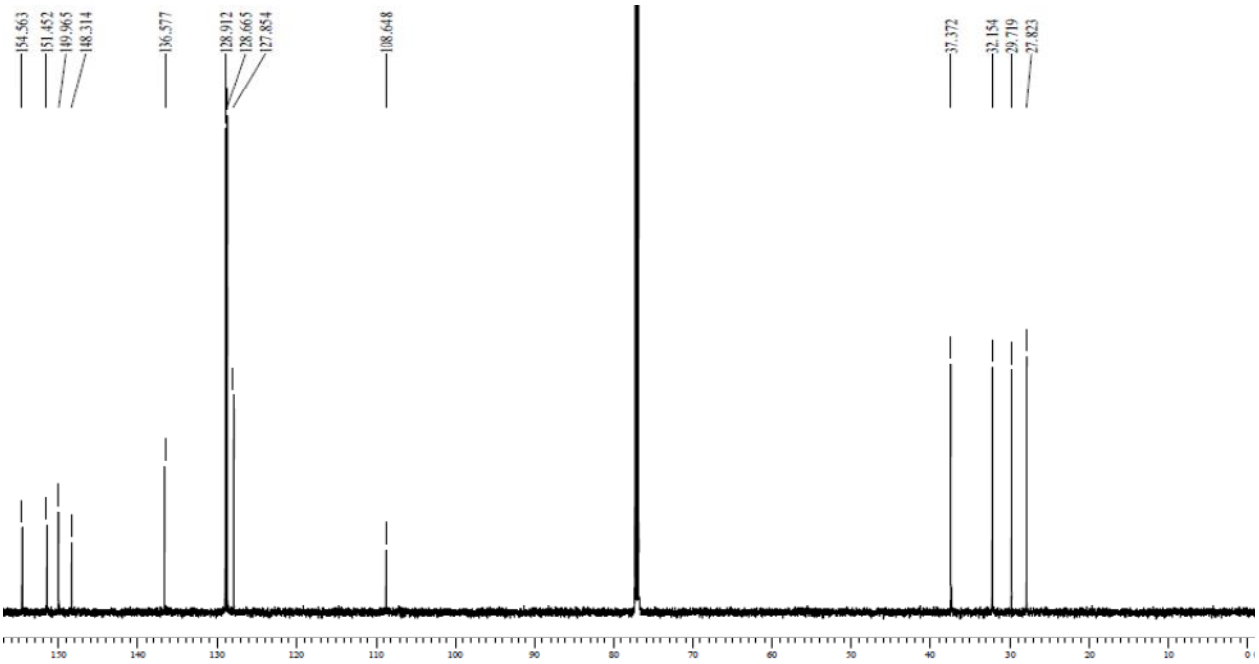

^{1}H NMR

8-[(2-Phenylethyl)sulfanyl]caffeine

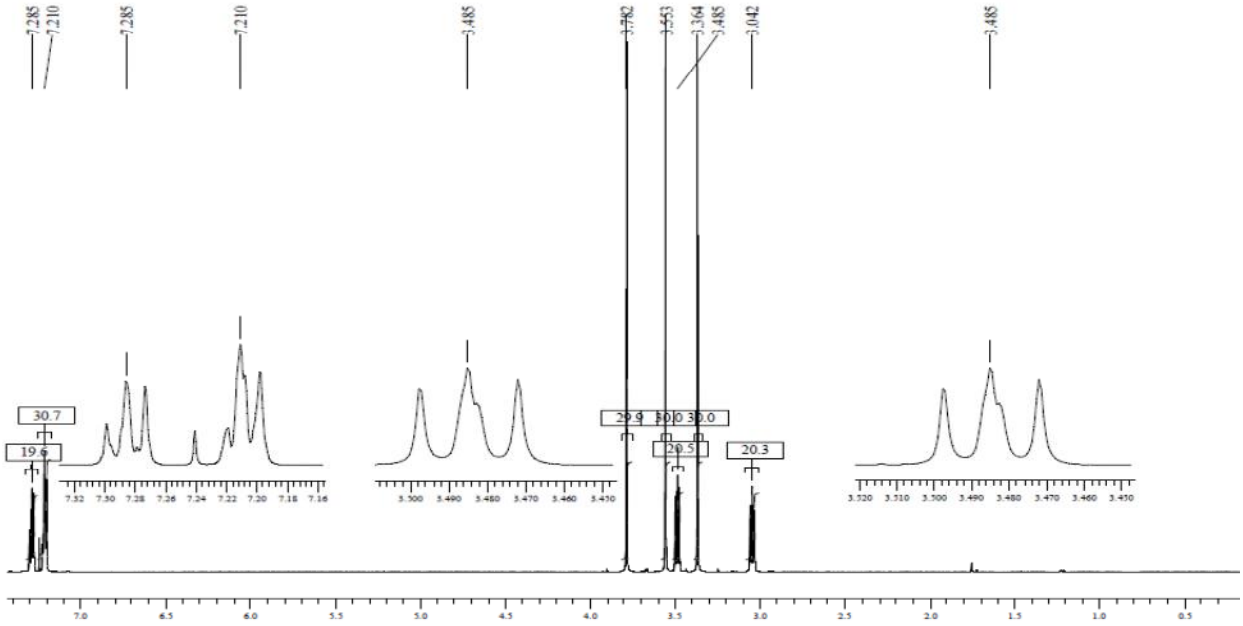

^{13}C NMR

8-[(2-Phenylethyl)sulfanyl]caffeine

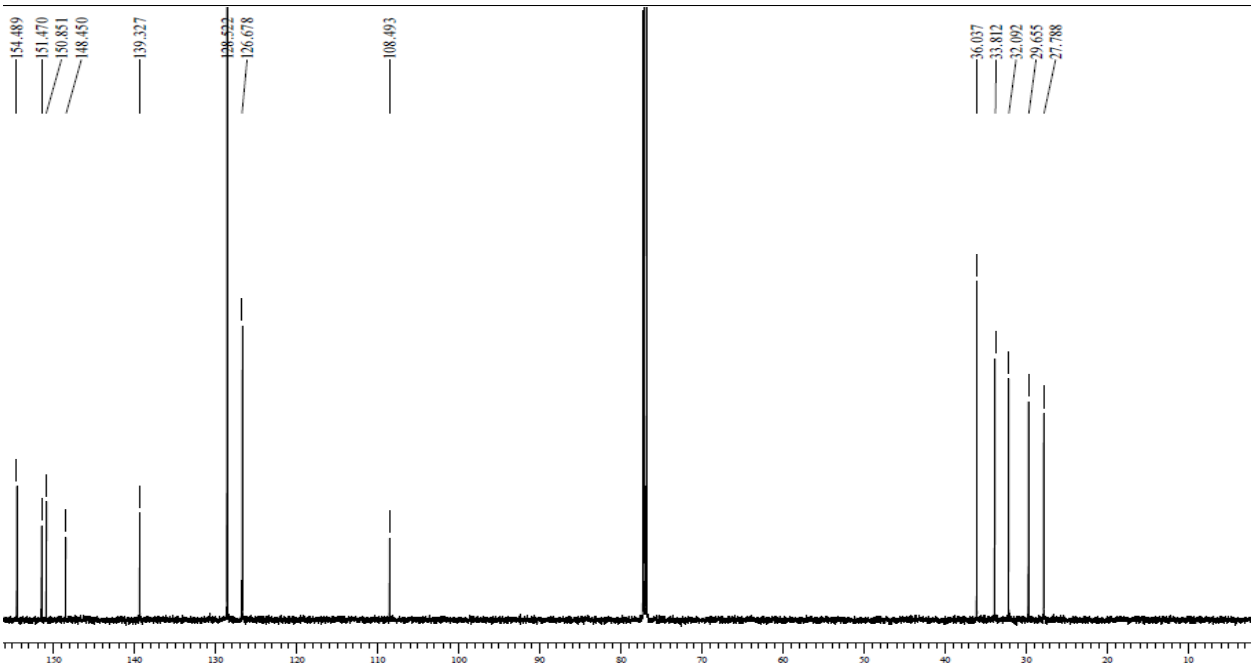

^{1}H NMR

8-{[(4-Chlorophenyl)methyl]sulfanyl}caffeine

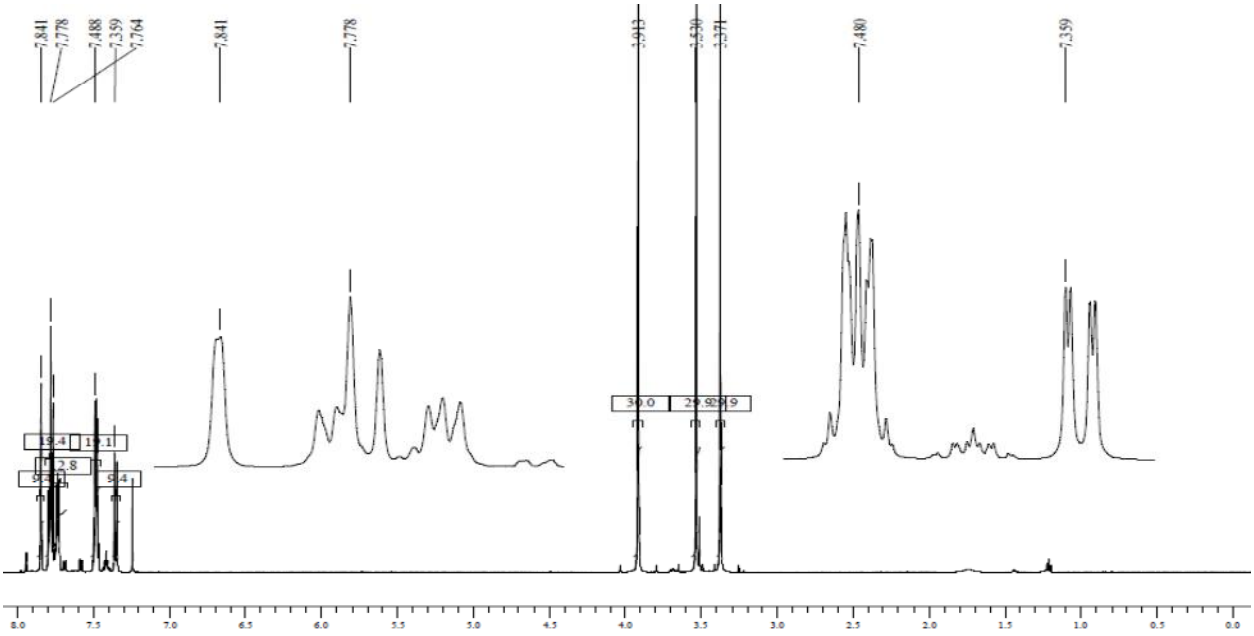

^{13}C NMR

8-{[(4-Chlorophenyl)methyl]sulfanyl}caffeine

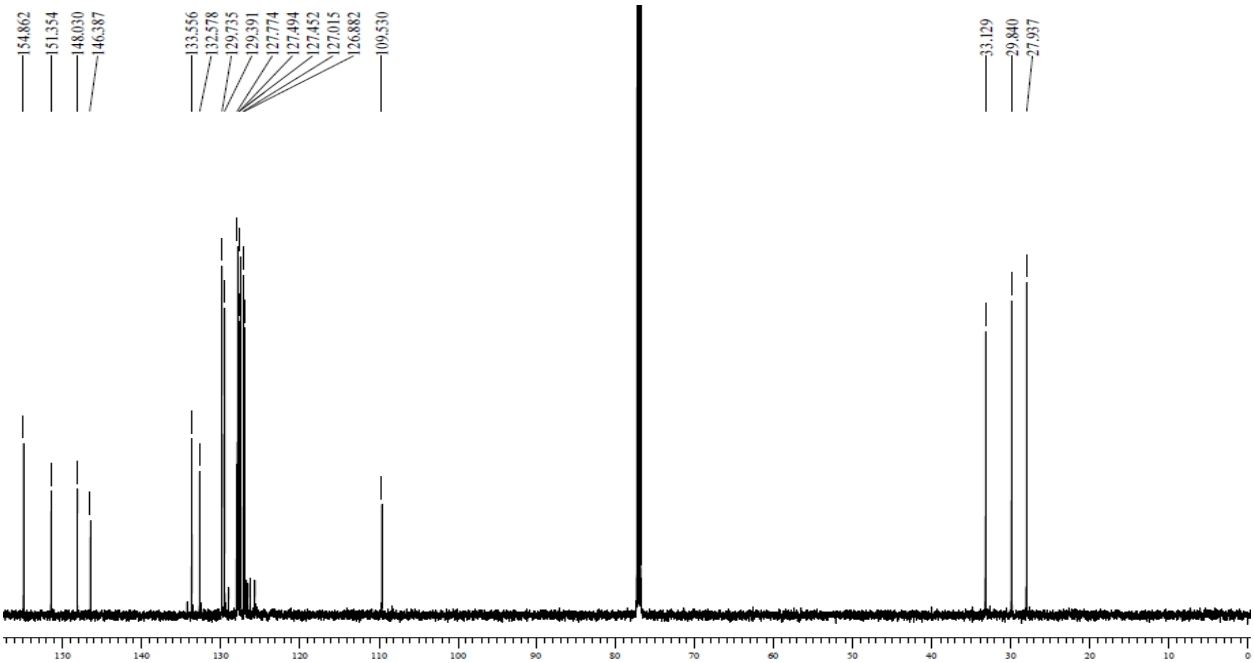

^{1}H NMR

8-{[(4-Bromophenyl)methyl]sulfanyl}caffeine

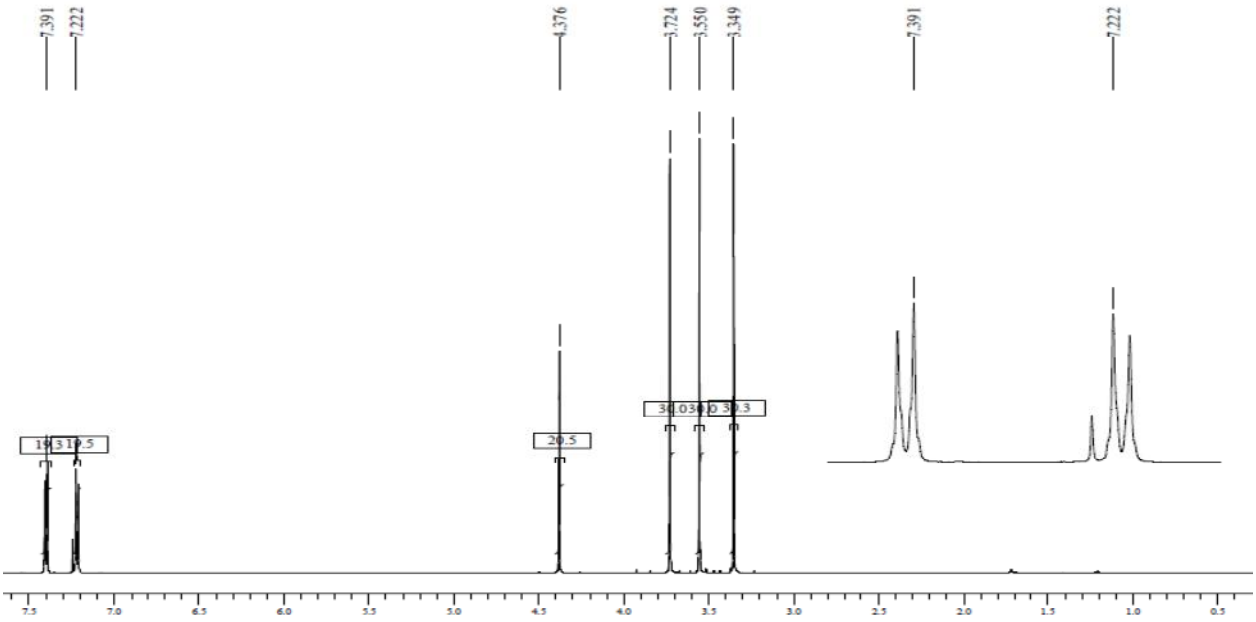

^{13}C NMR

8-{[(4-Bromophenyl)methyl]sulfanyl}caffeine

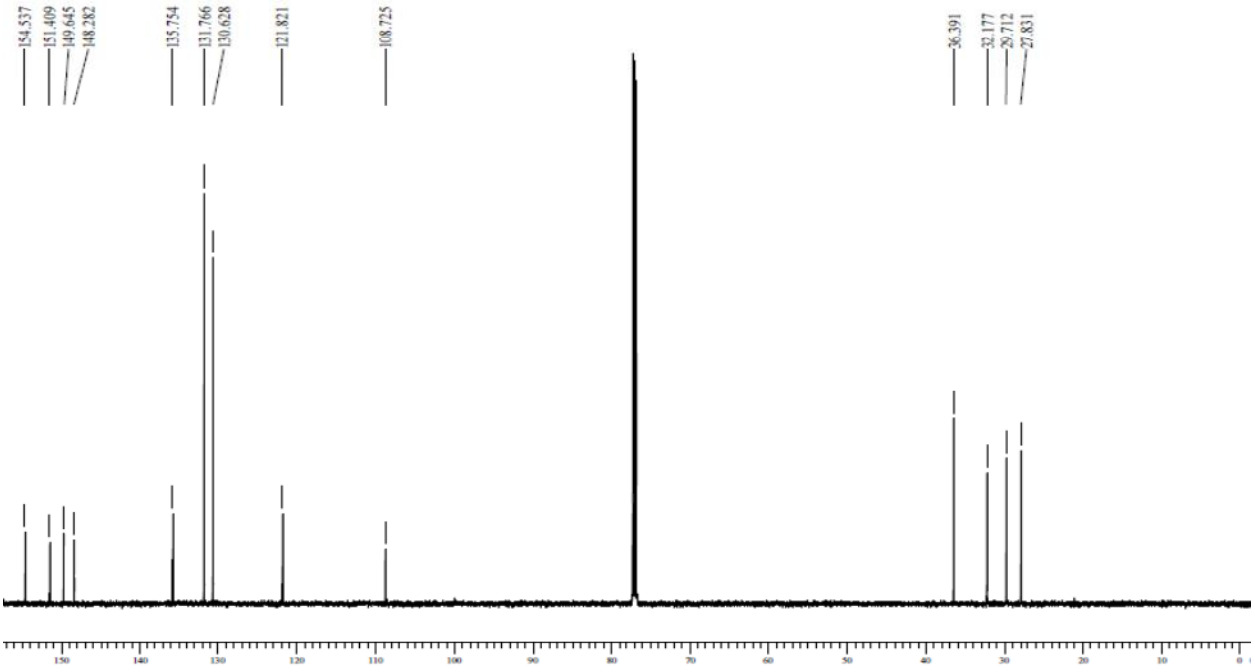

^{1}H NMR

8-{[(4-Fluorophenyl)methyl]sulfanyl}caffeine

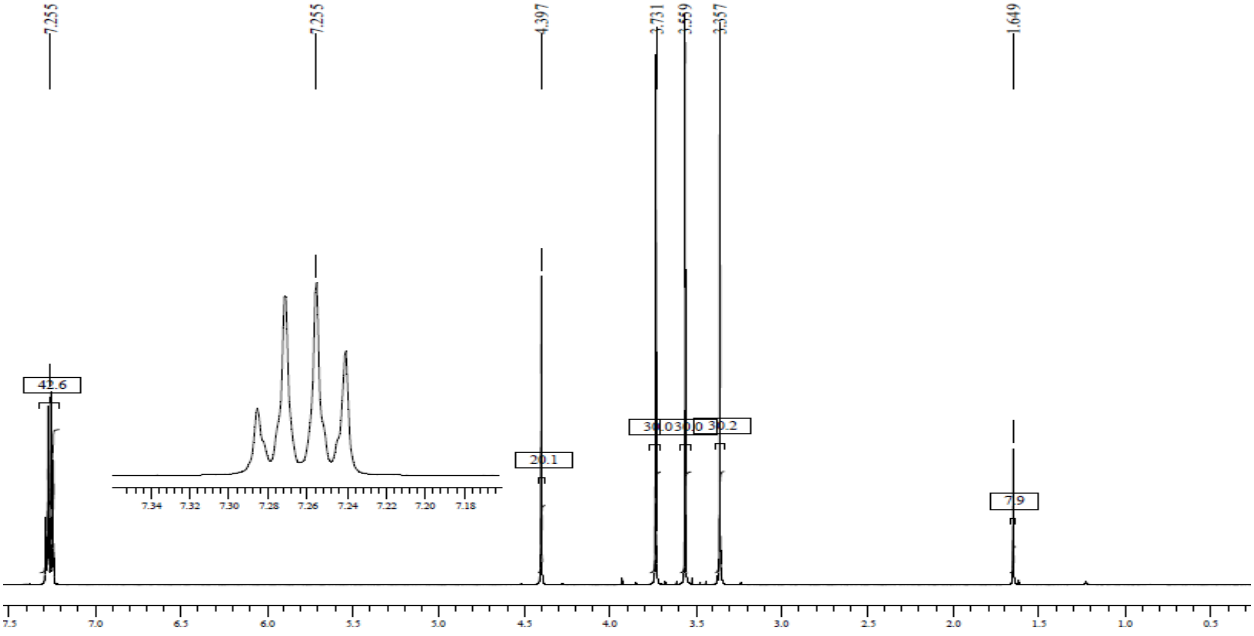

^{13}C NMR

8-{[(4-Fluorophenyl)methyl]sulfanyl}caffeine

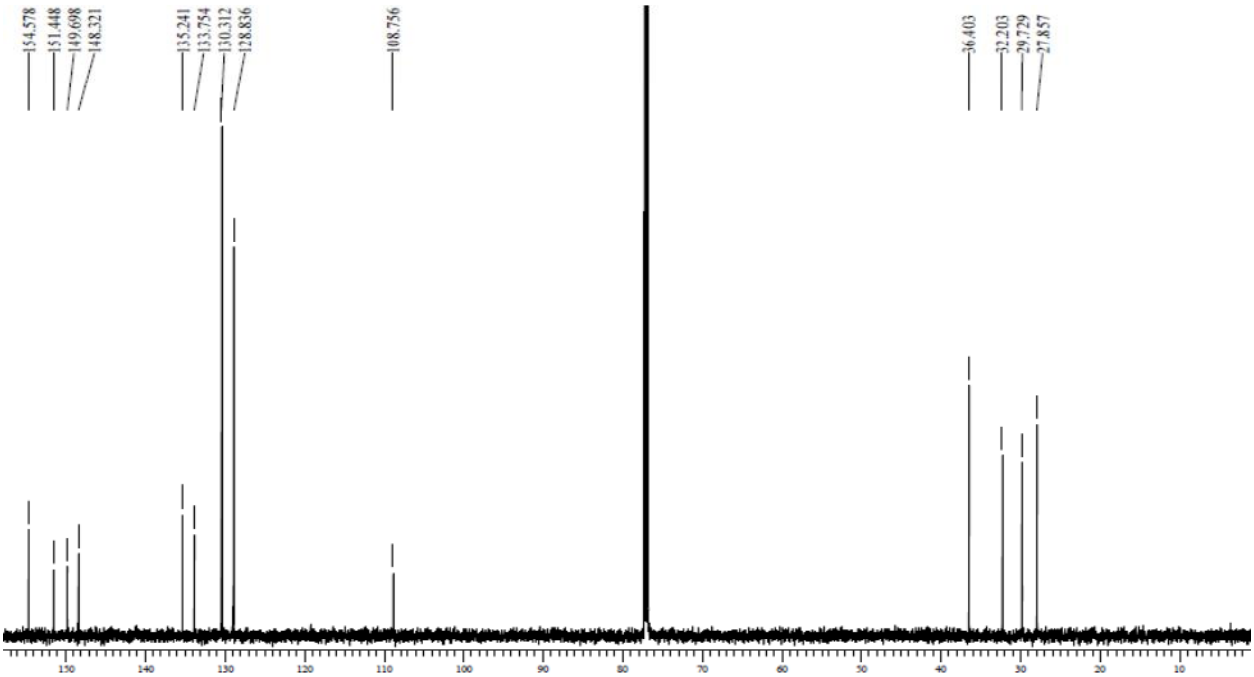

^{1}H NMR

8-{[(4-Methoxyphenyl)methyl]sulfanyl}caffeine

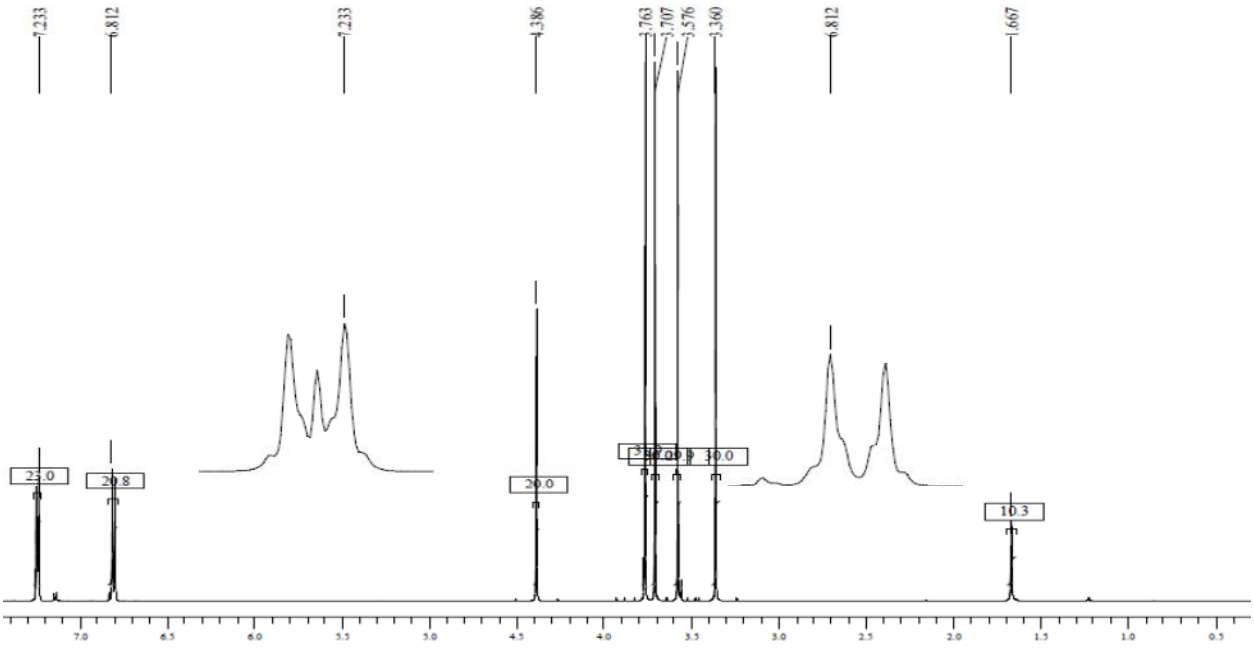

^{13}C NMR

8-{[(4-Methoxyphenyl)methyl]sulfanyl}caffeine

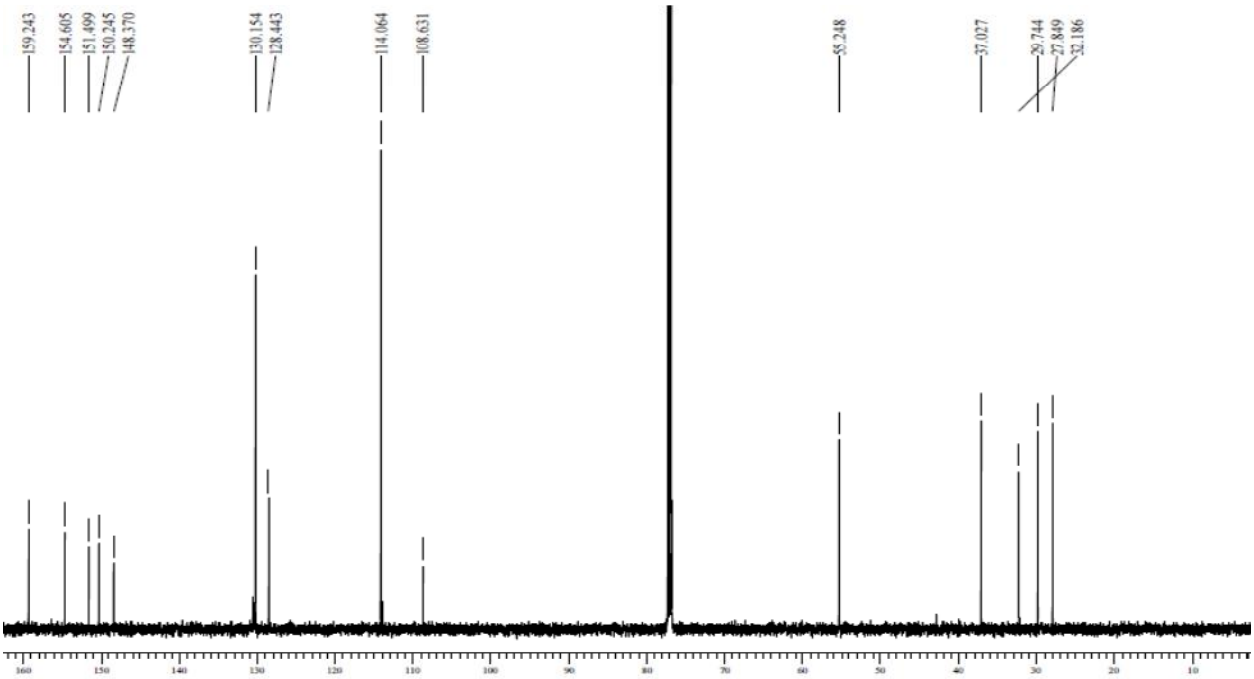

^{1}H NMR

8-[(2-Phenoxyethyl)sulfanyl]caffeine

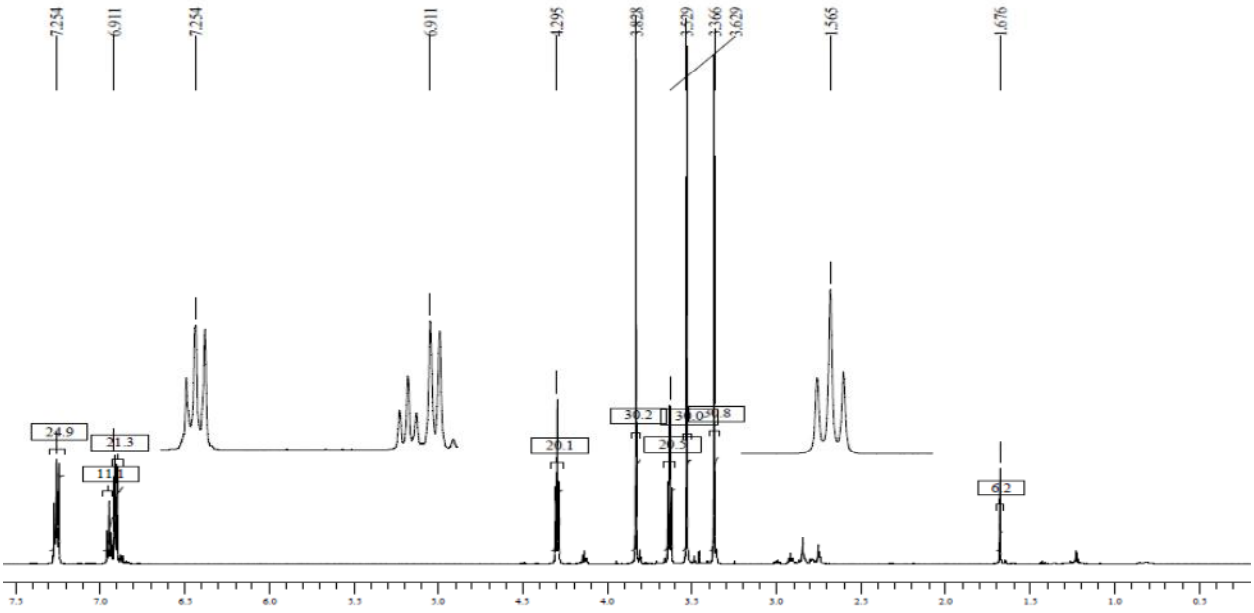

^{13}C NMR

8-[(2-Phenoxyethyl)sulfanyl]caffeine

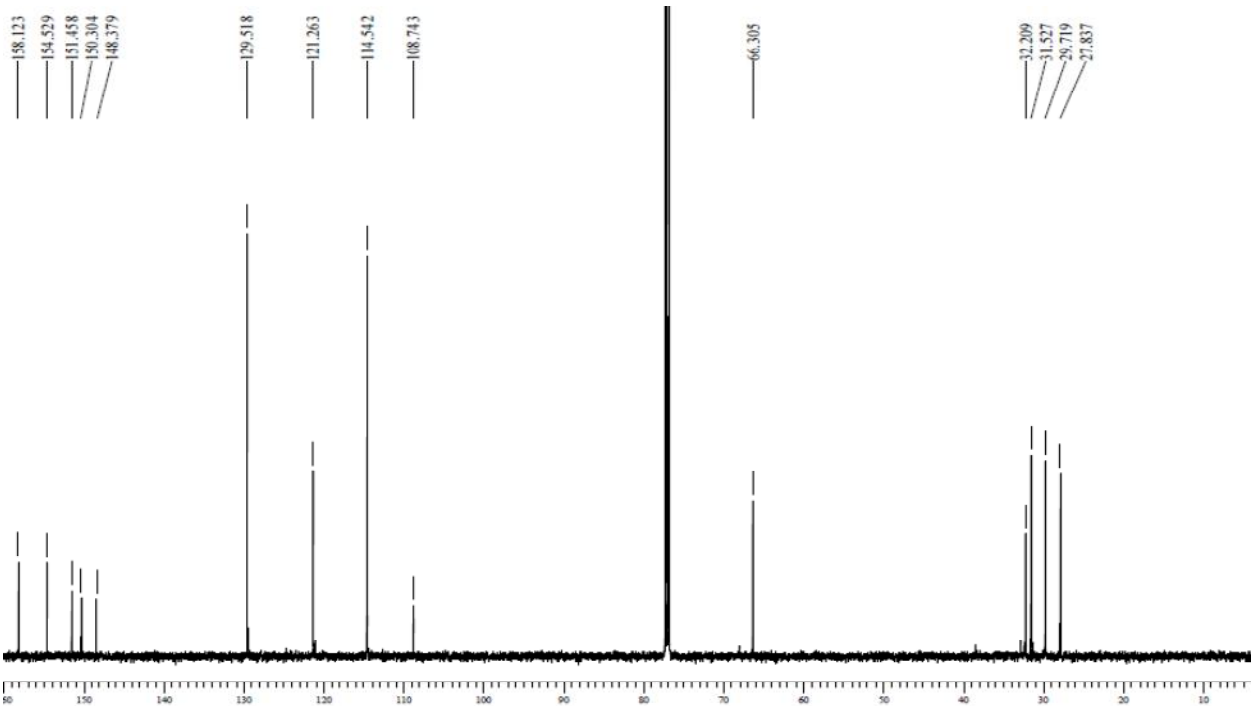

^{1}H NMR

8-(Cyclohexylsulfanyl)caffeine

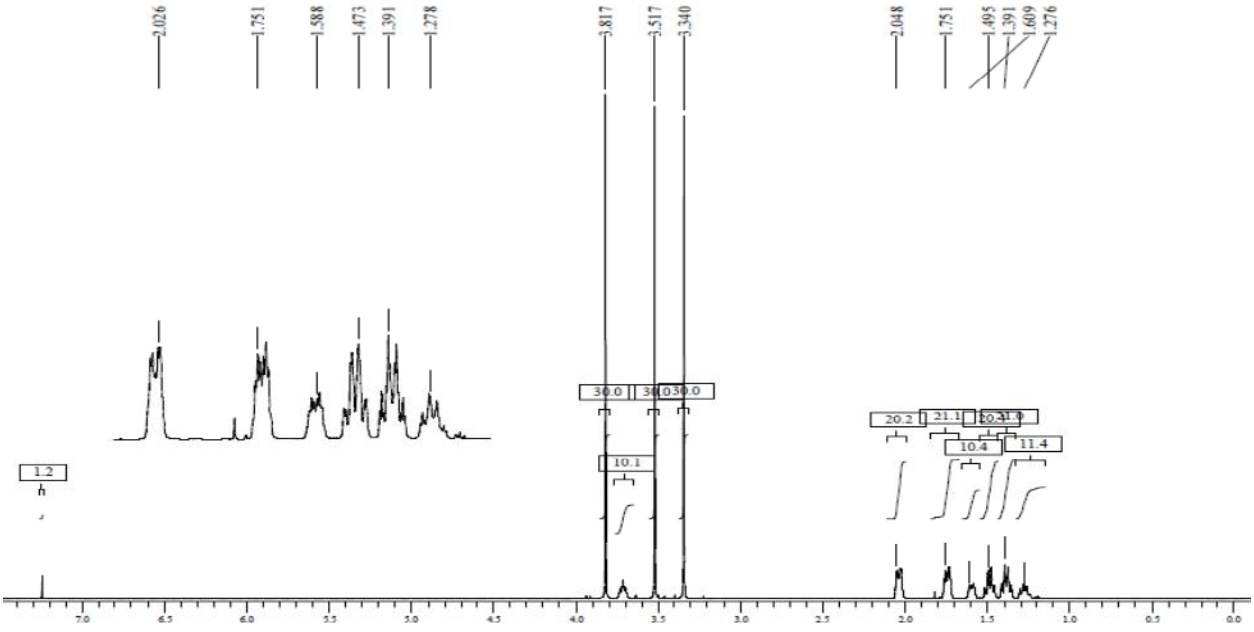

^{13}C NMR

8-(Cyclohexylsulfanyl)caffeine

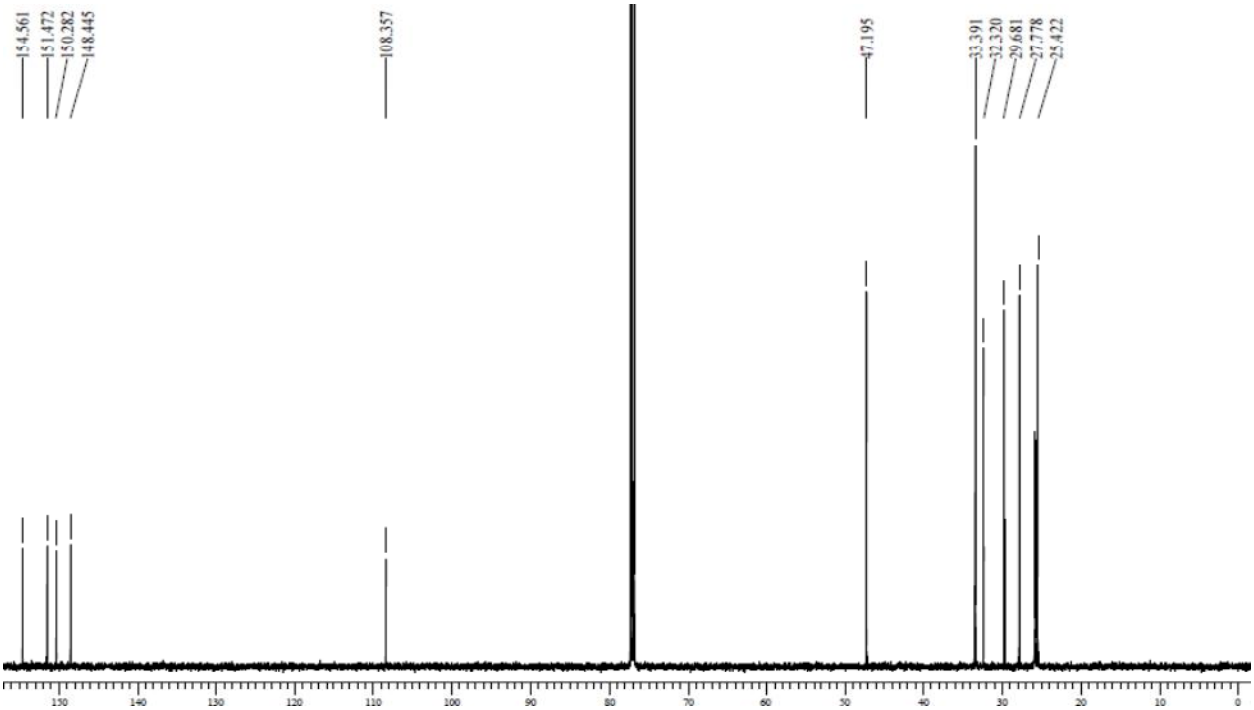

^{1}H NMR

8-(Cyclopentylsulfanyl)caffeine

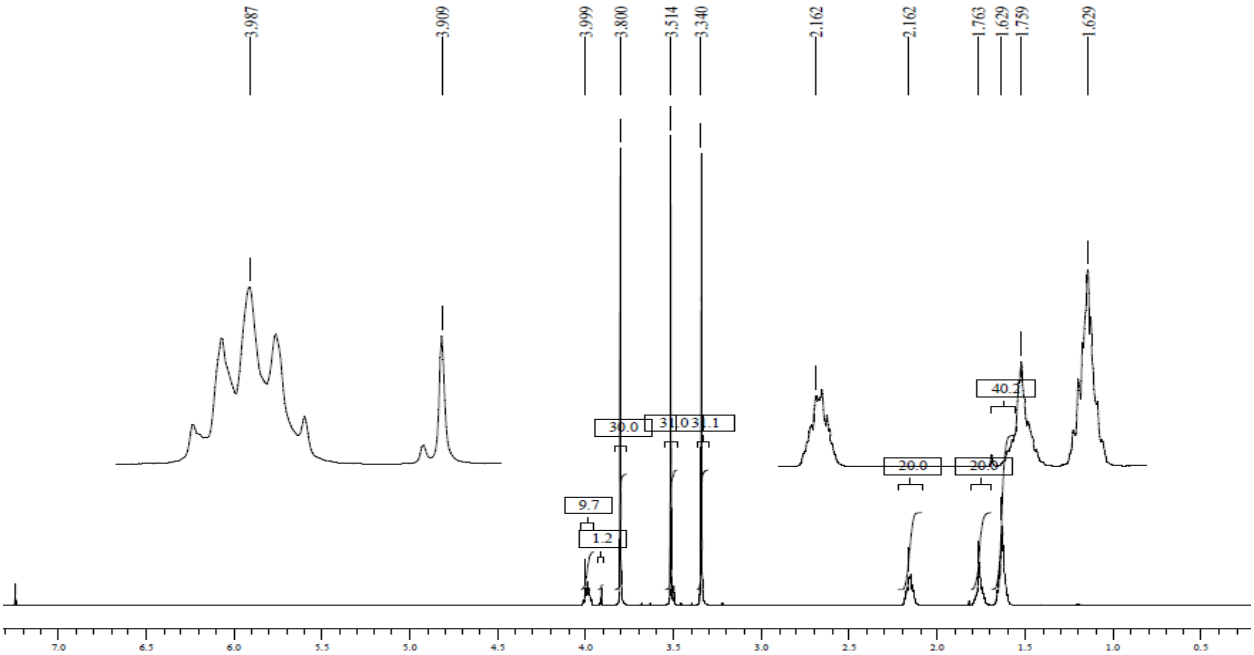

^{13}C NMR

8-(Cyclopentylsulfanyl)caffeine

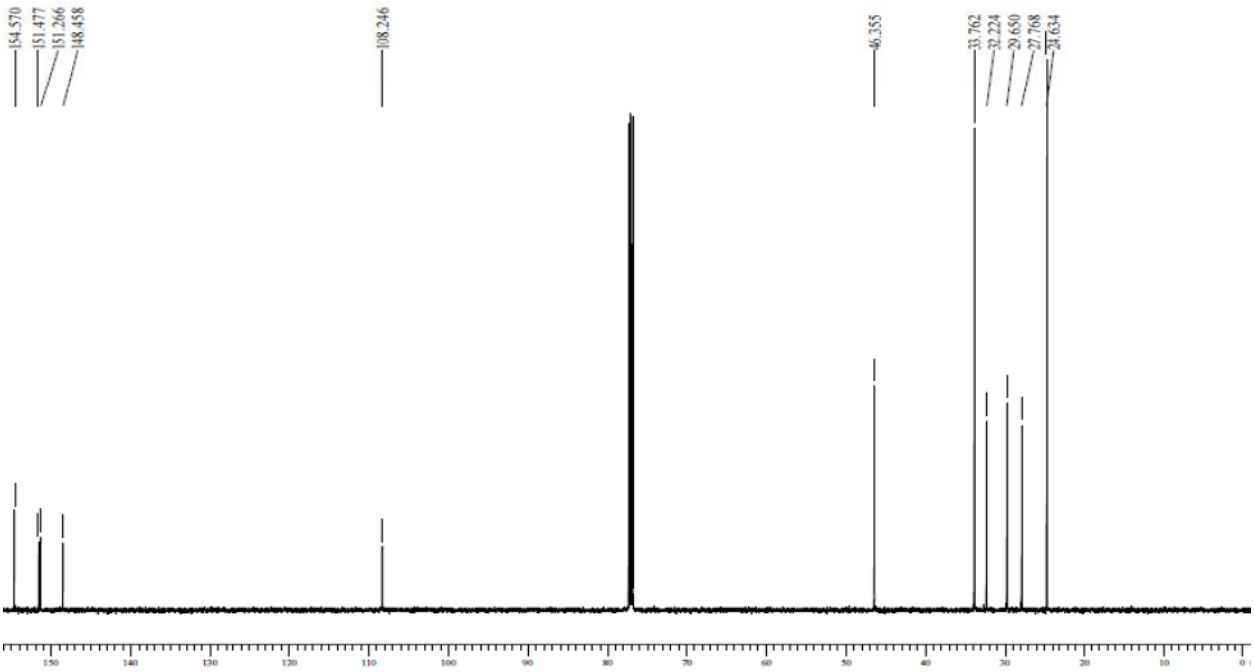

^{1}H NMR

8-(Naphthalen-2-ylsulfanyl)caffeine

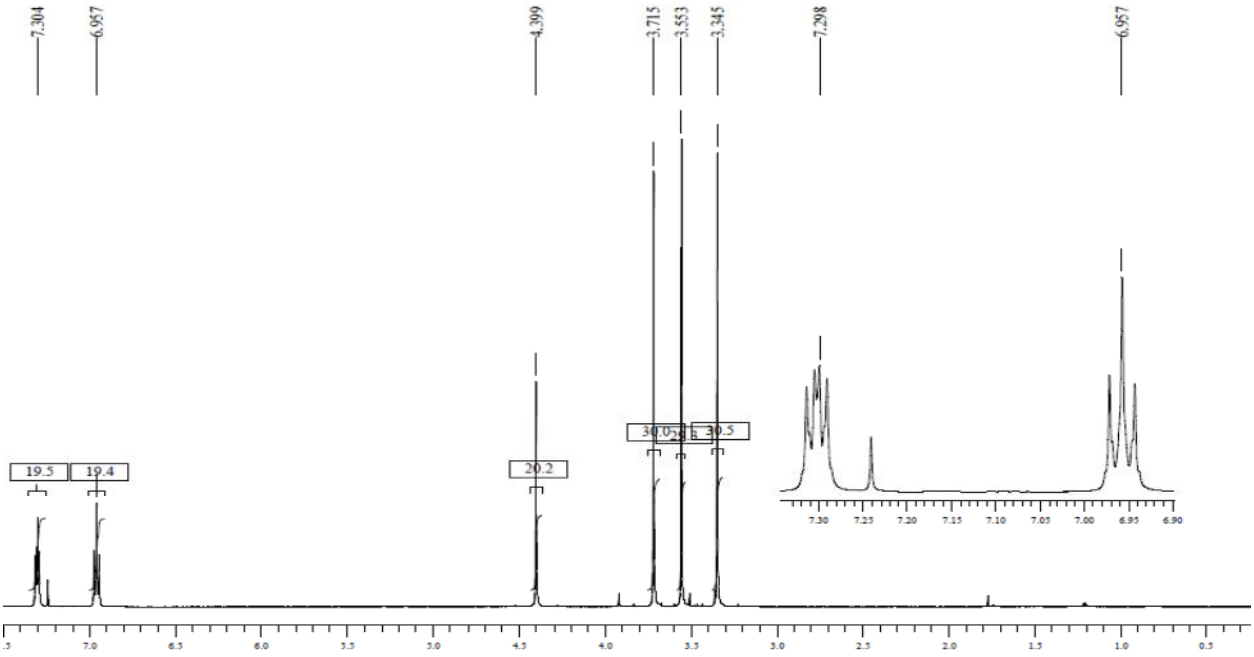

^{13}C NMR

8-(Naphthalen-2-ylsulfanyl)caffeine

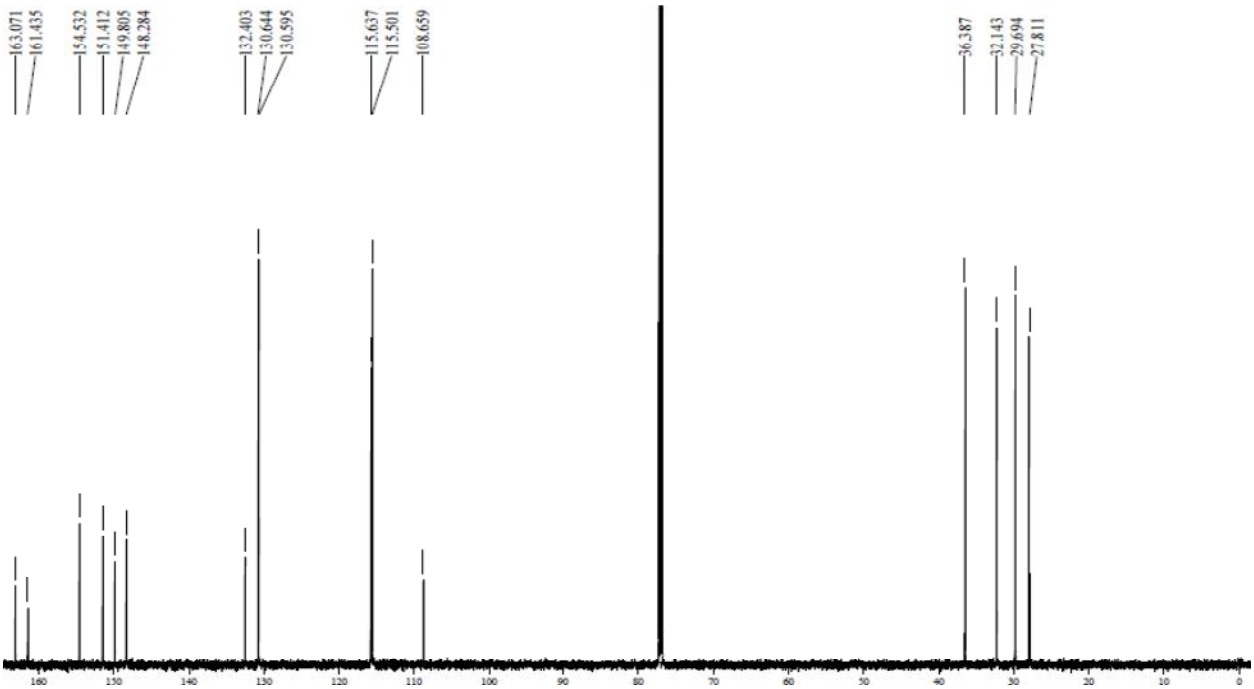

^{1}H NMR

8-[(3-Methylbutyl)sulfanyl]caffeine

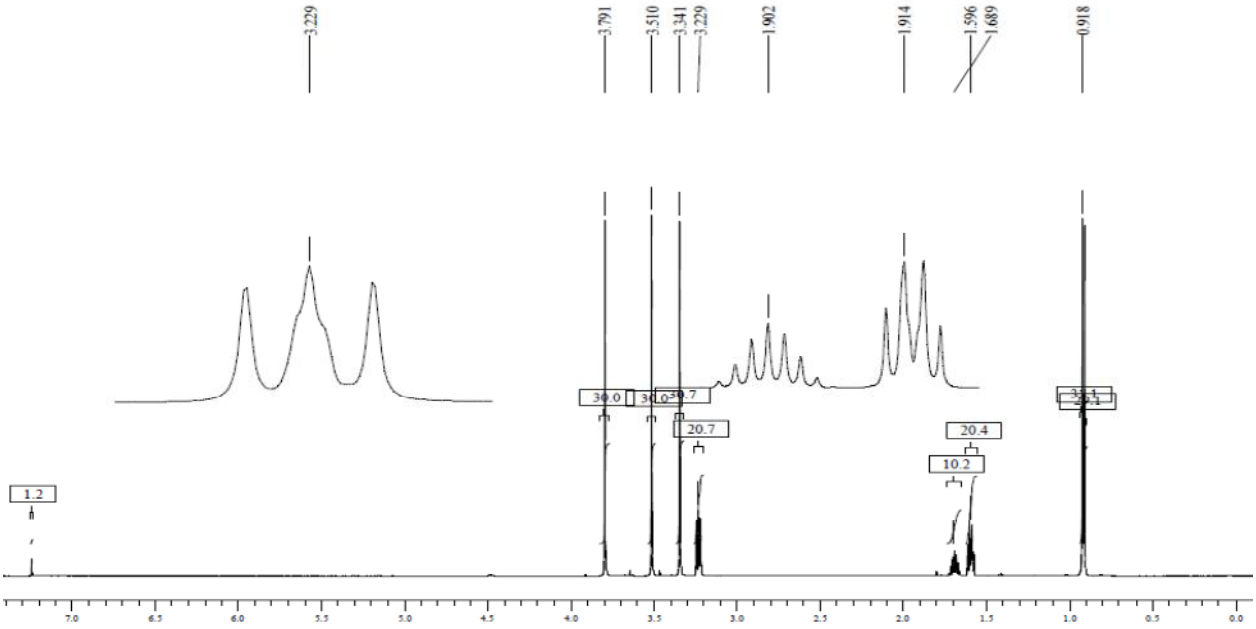

^{13}C NMR

8-[(3-Methylbutyl)sulfanyl]caffeine

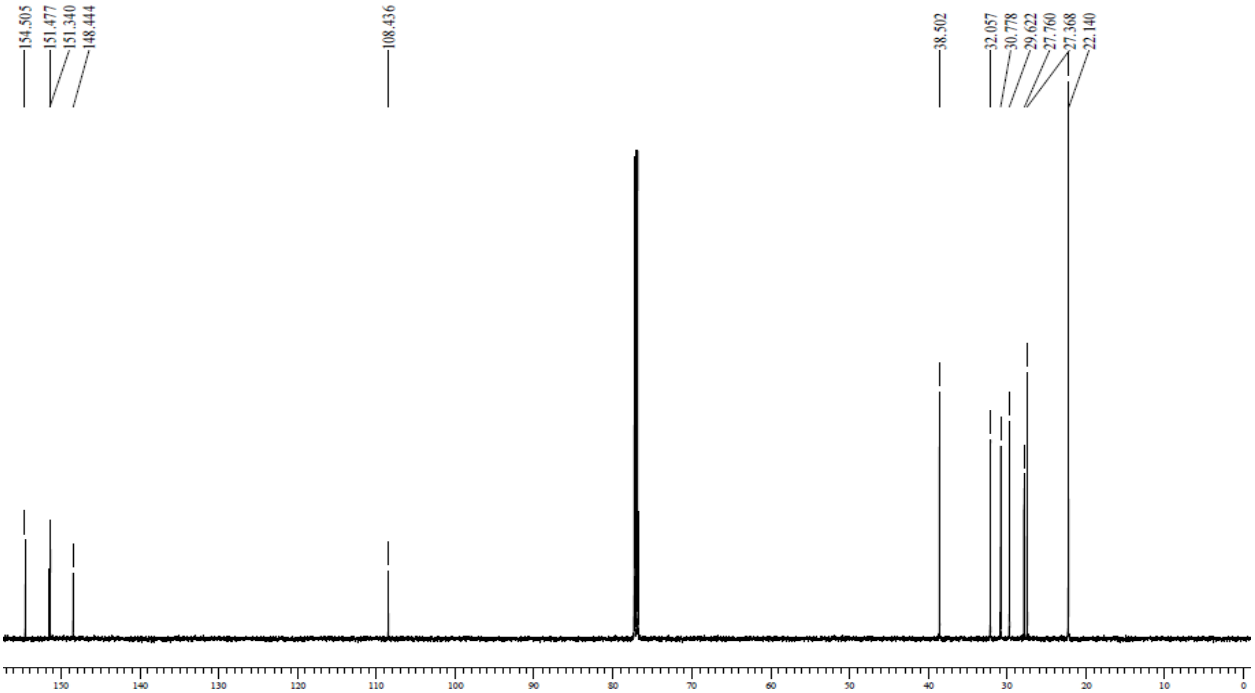

HPLC chromatograms

8-(Phenylsulfanyl)caffeine

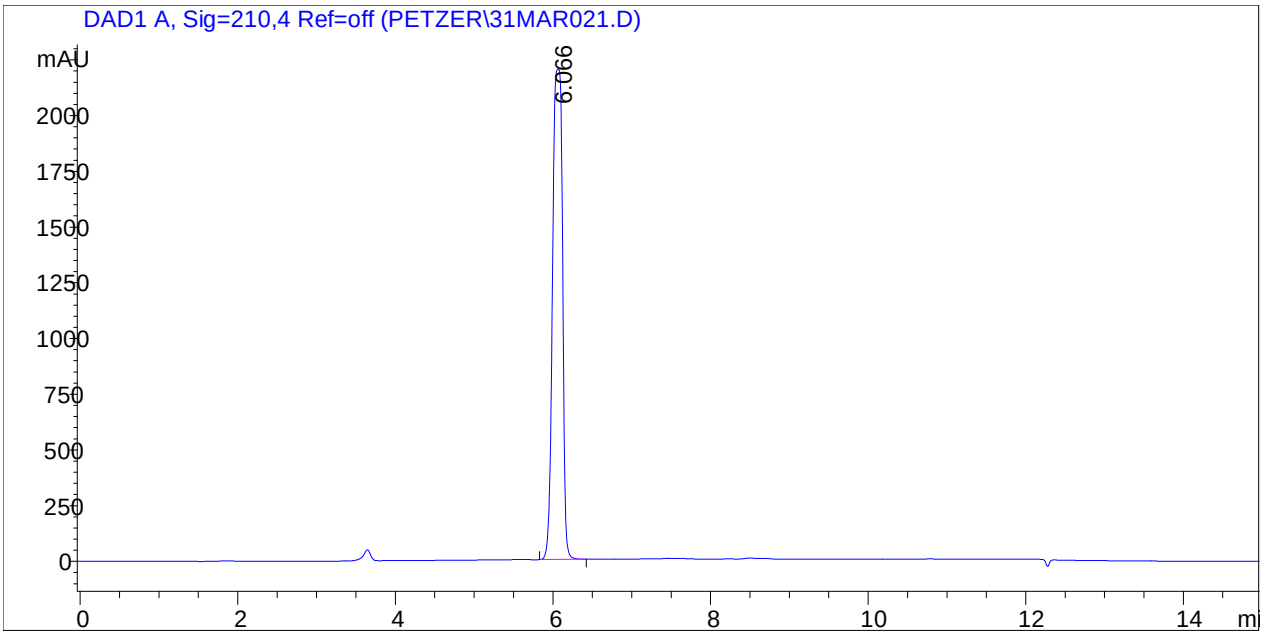

8-(Benzylsulfanyl)caffeine

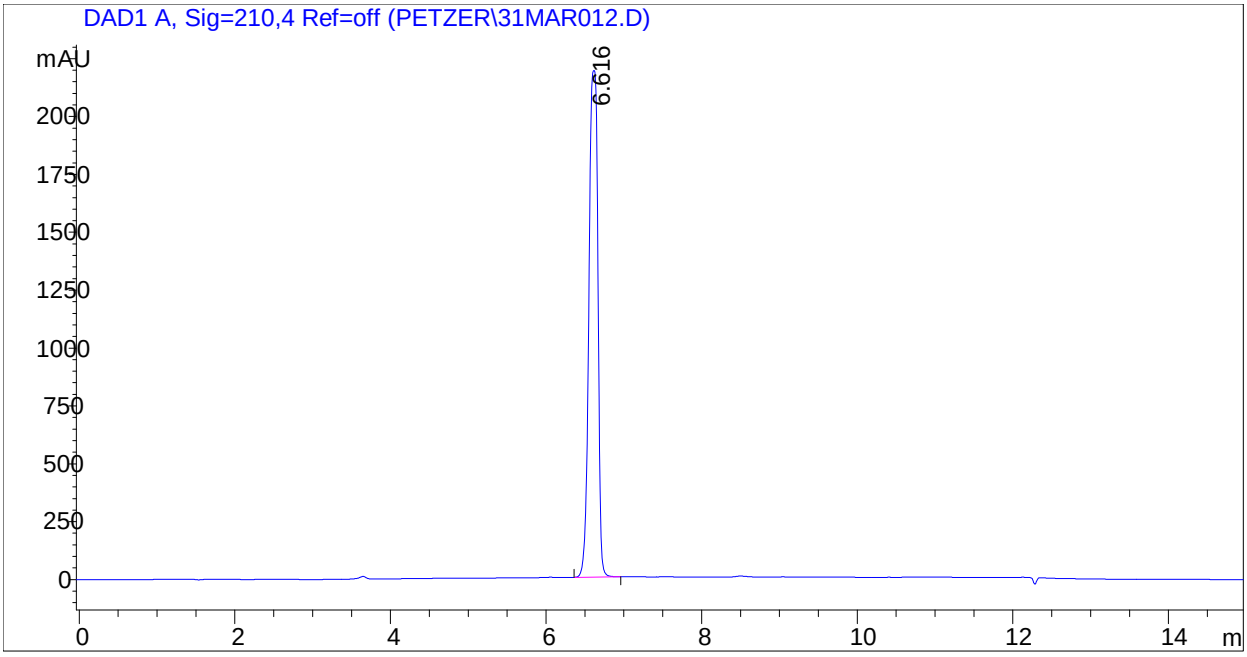

8-[(2-Phenylethyl)sulfanyl]caffeine

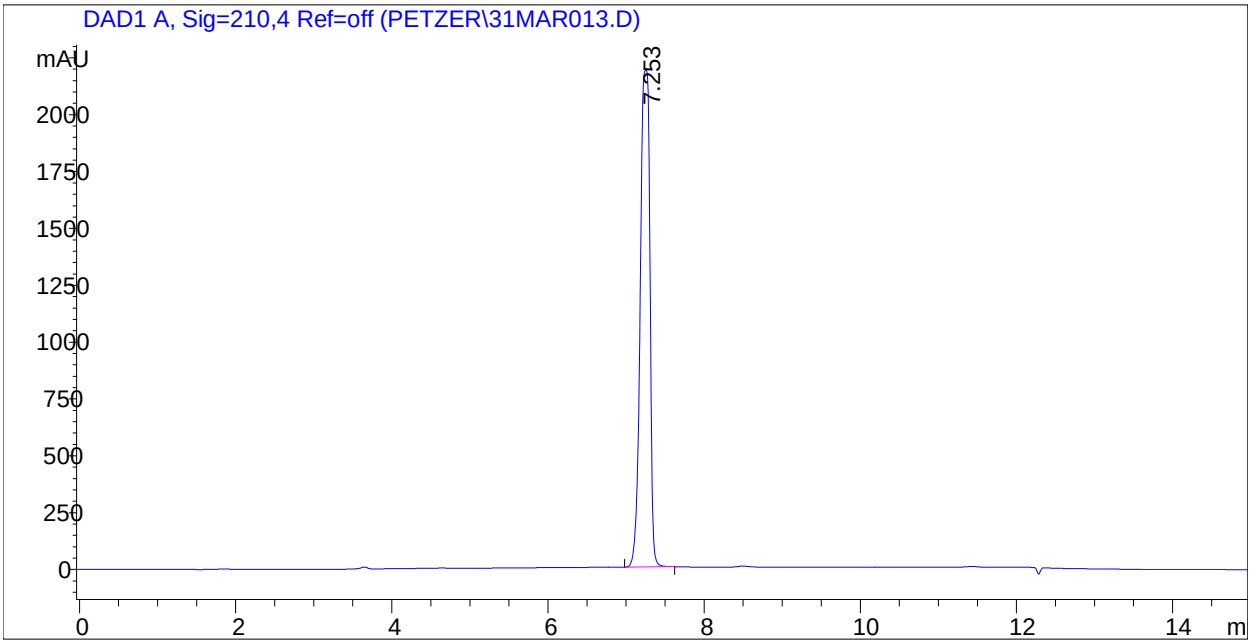

8-{[(4-Chlorophenyl)methyl]sulfanyl}caffeine

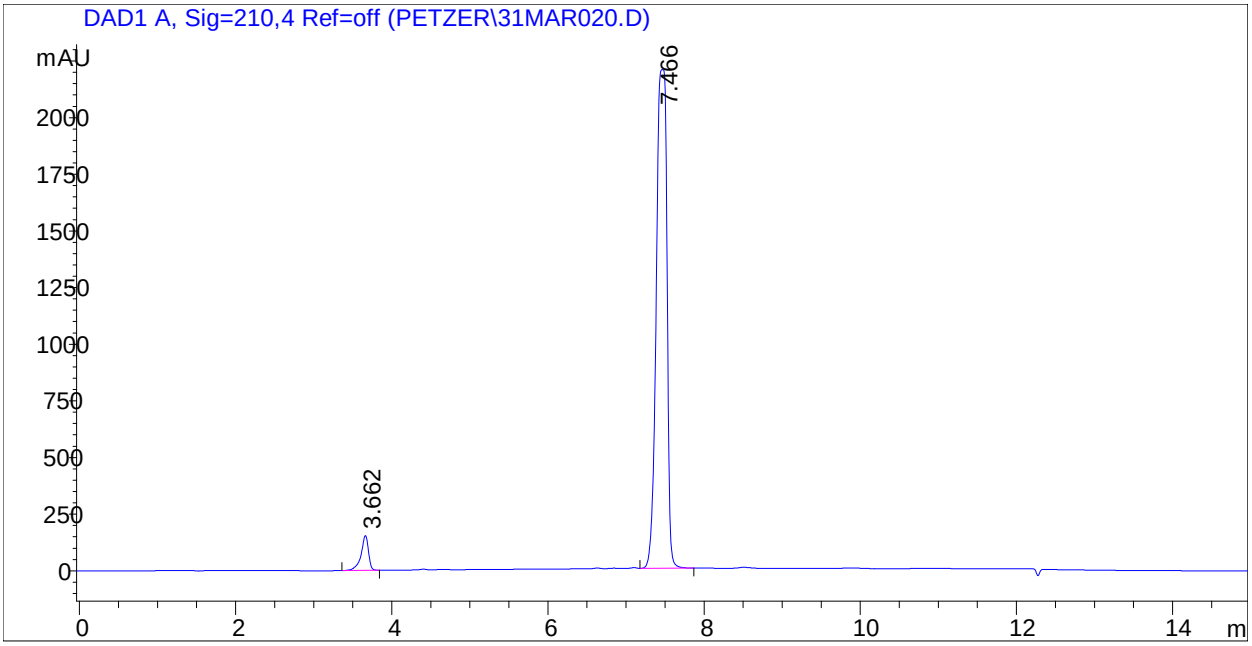

8-{[(4-Bromophenyl)methyl]sulfanyl}caffeine

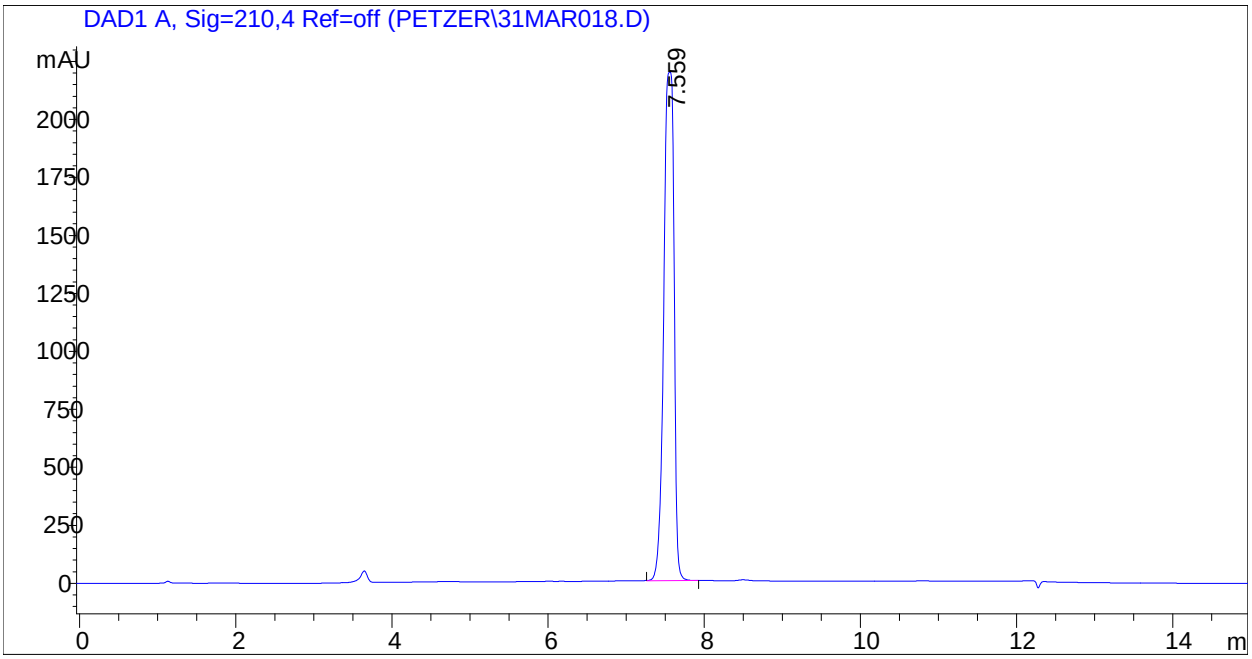

8-{[(4-Fluorophenyl)methyl]sulfanyl}caffeine

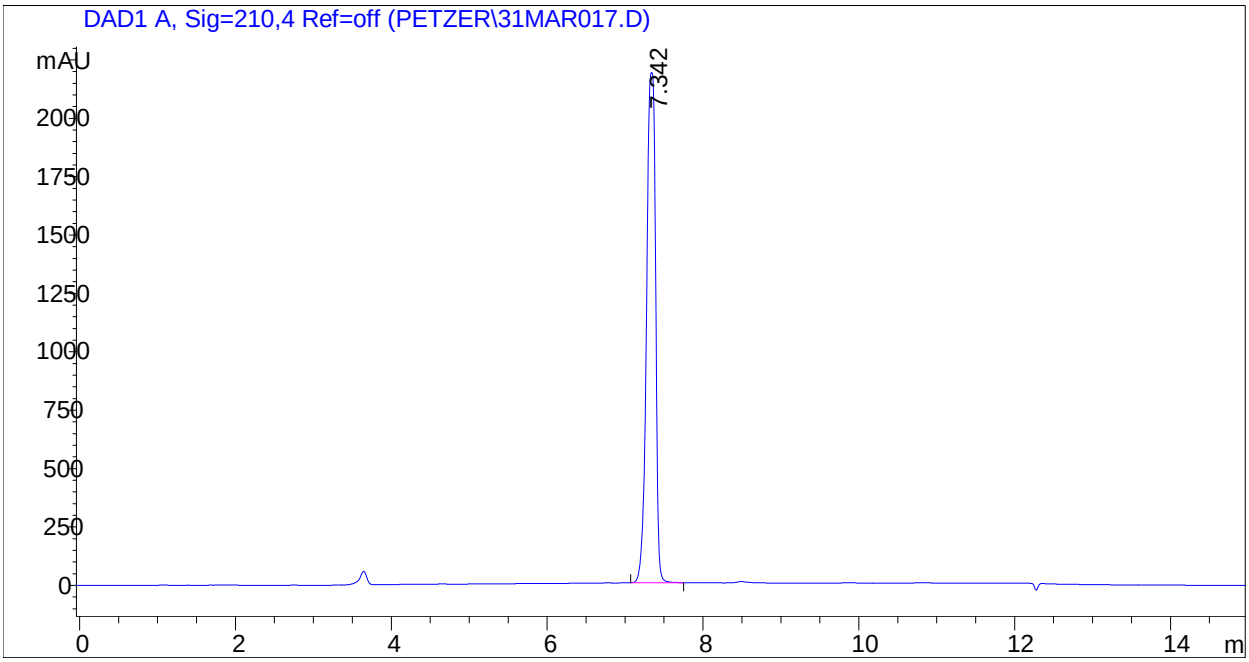

8-{[(4-Methoxyphenyl)methyl]sulfanyl}caffeine

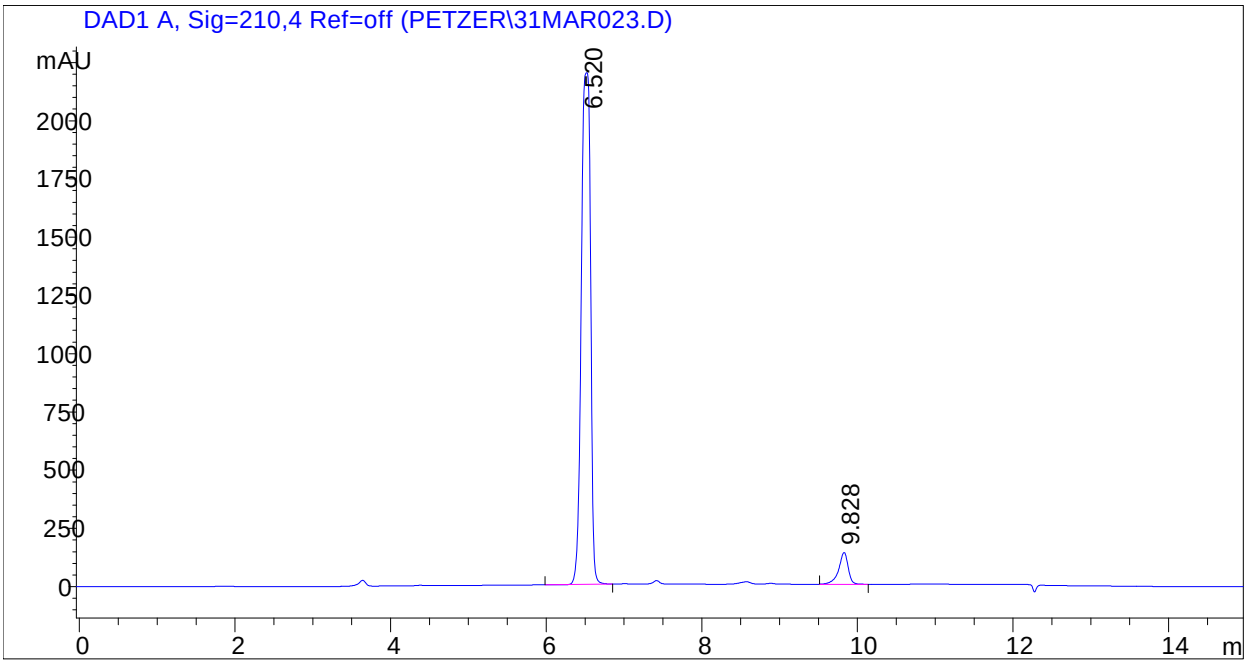

8-[(2-Phenoxyethyl)sulfanyl]caffeine

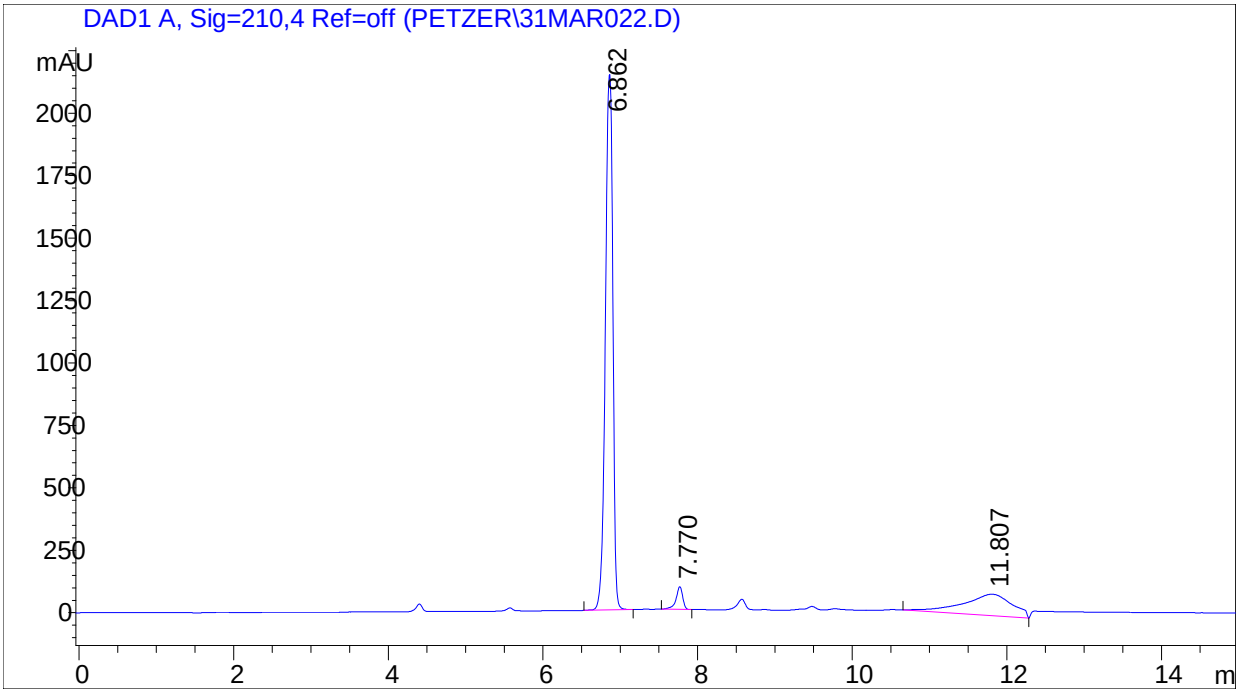

8-(Cyclohexylsulfanyl)caffeine

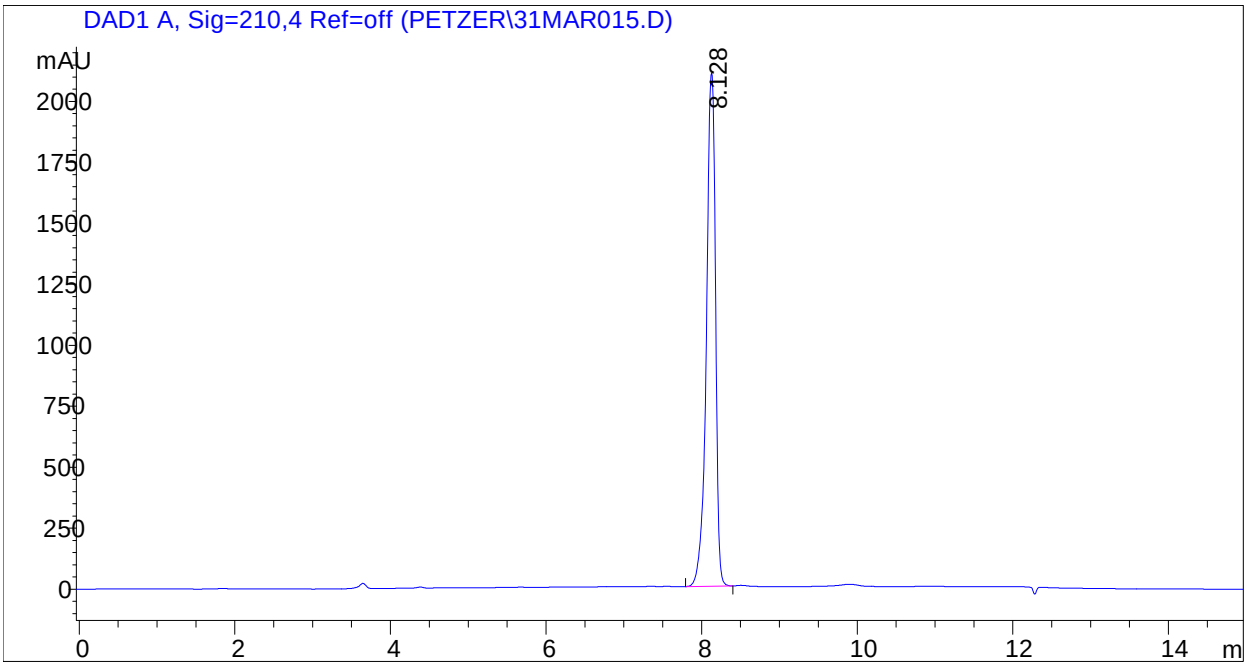

8-(Cyclopentylsulfanyl)caffeine

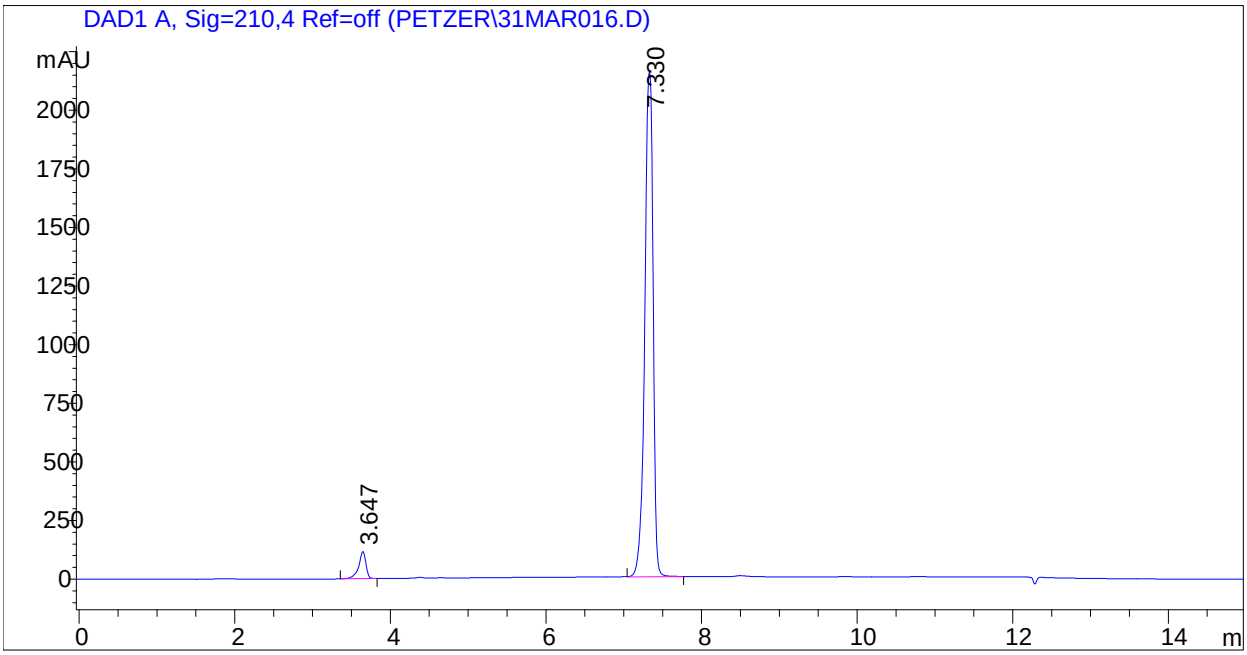

8-(Naphthalen-2-ylsulfanyl)caffeine

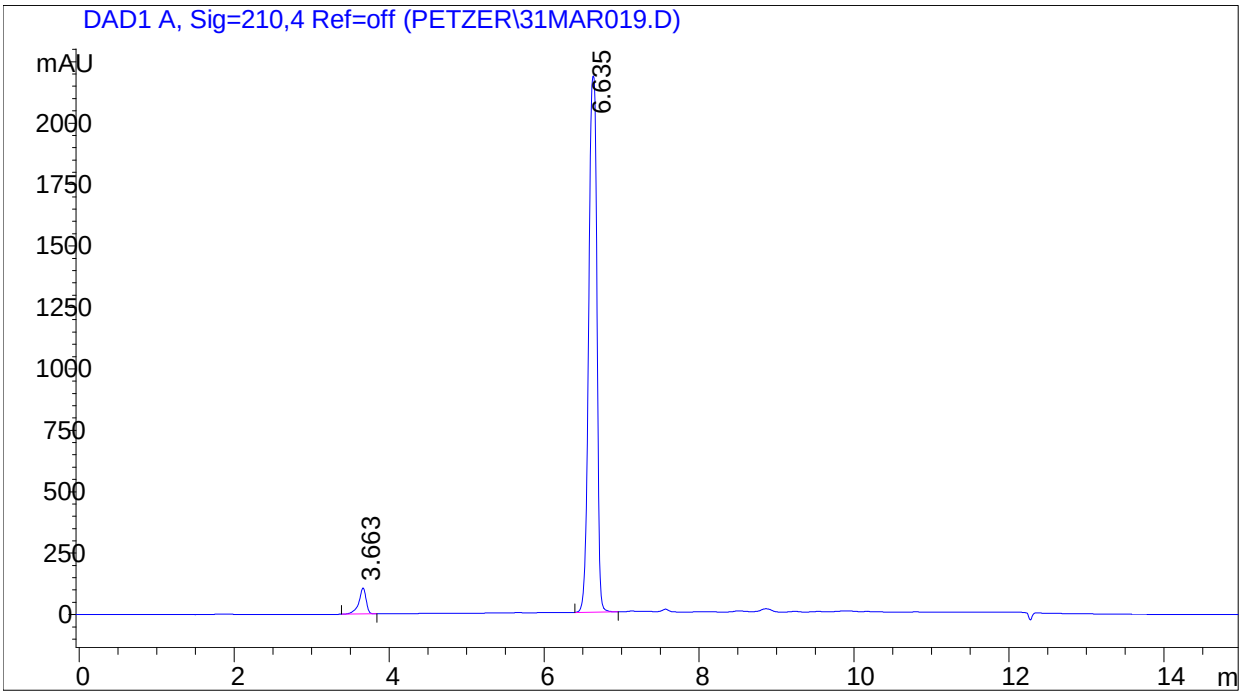

8-[(3-Methylbutyl)sulfanyl]caffeine

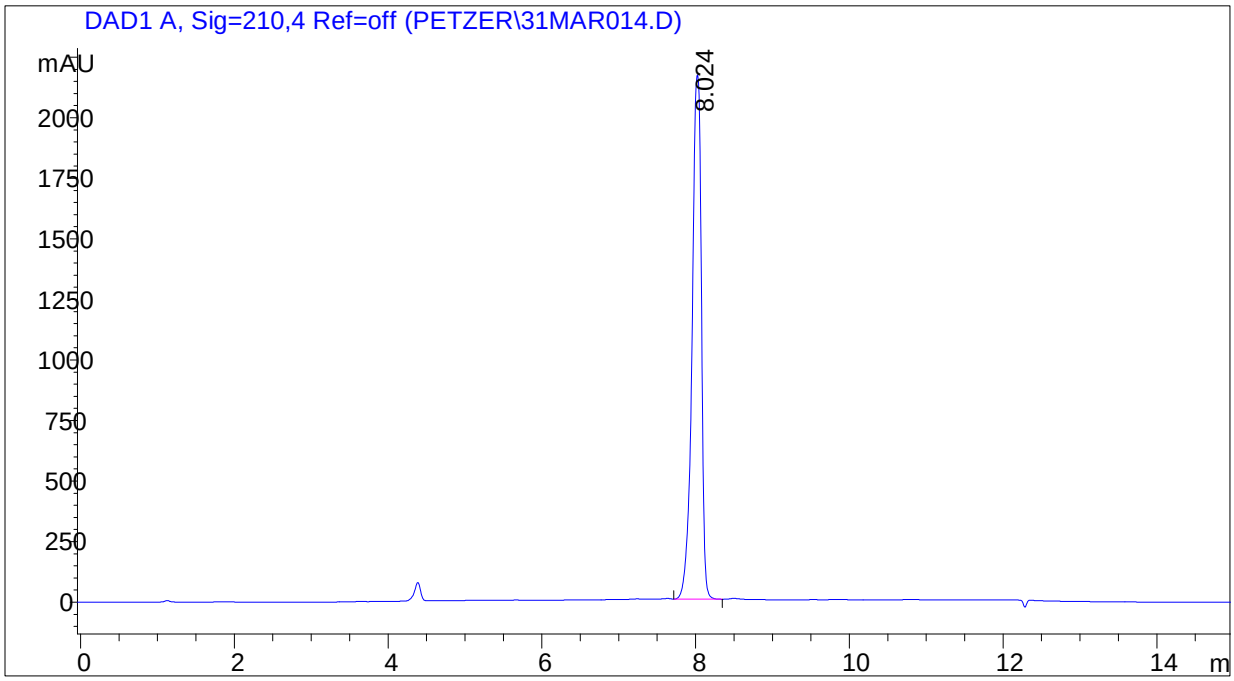

MS spectra

8-(Phenylsulfanyl)caffeine

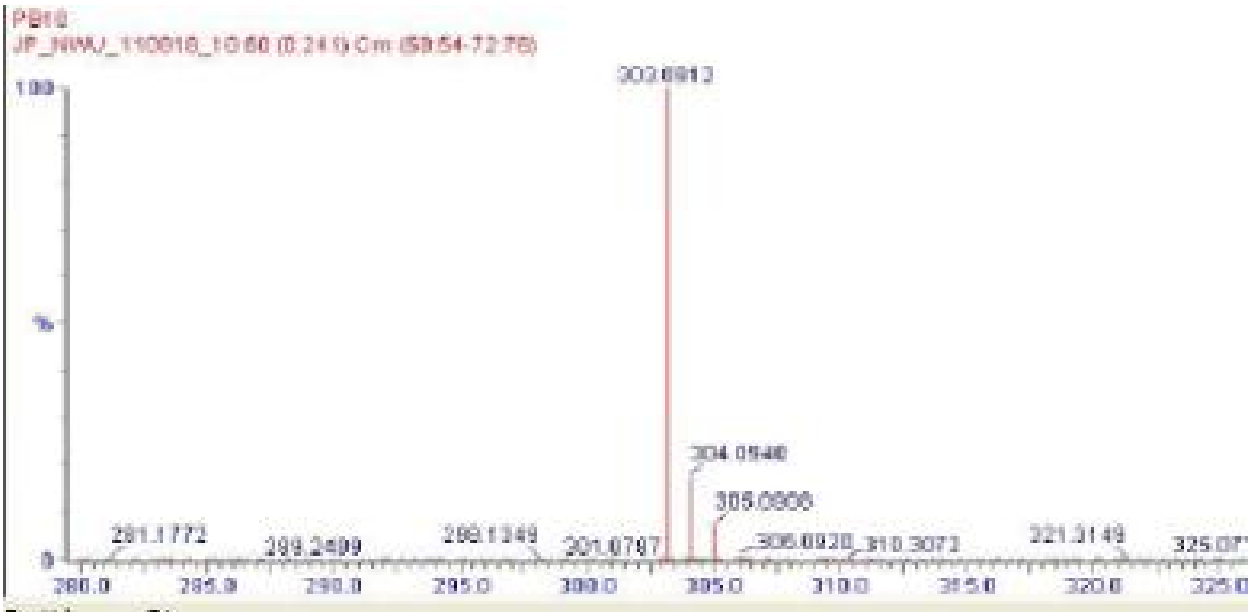

8-(Benzylsulfanyl)caffeine

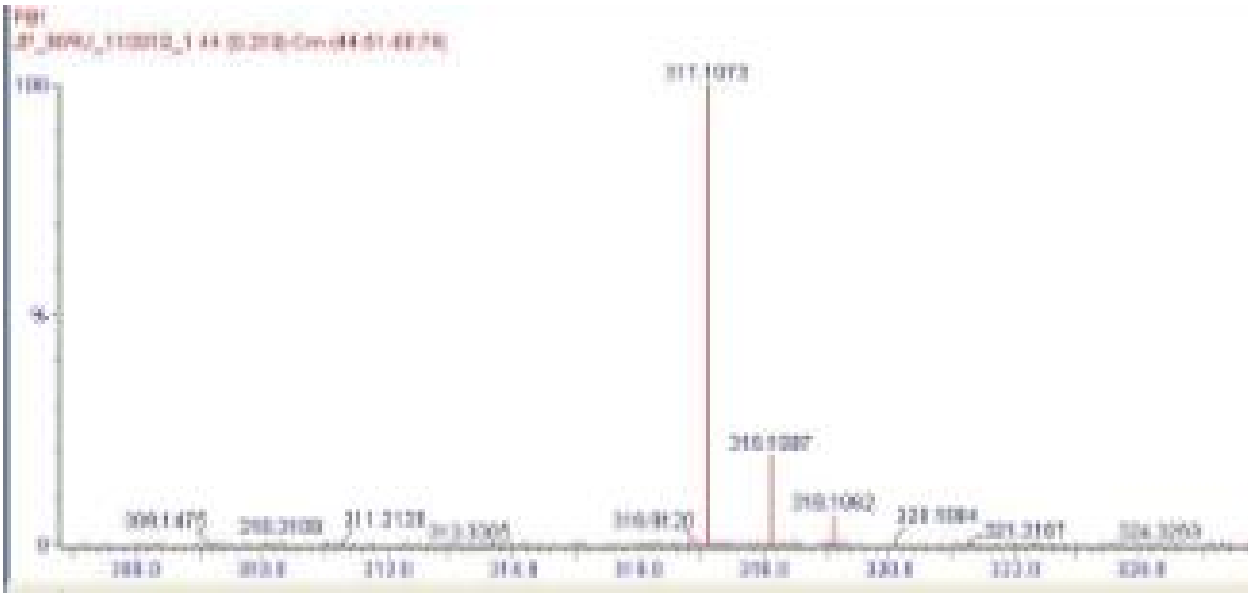

8-[(2-Phenylethyl)sulfanyl]caffeine

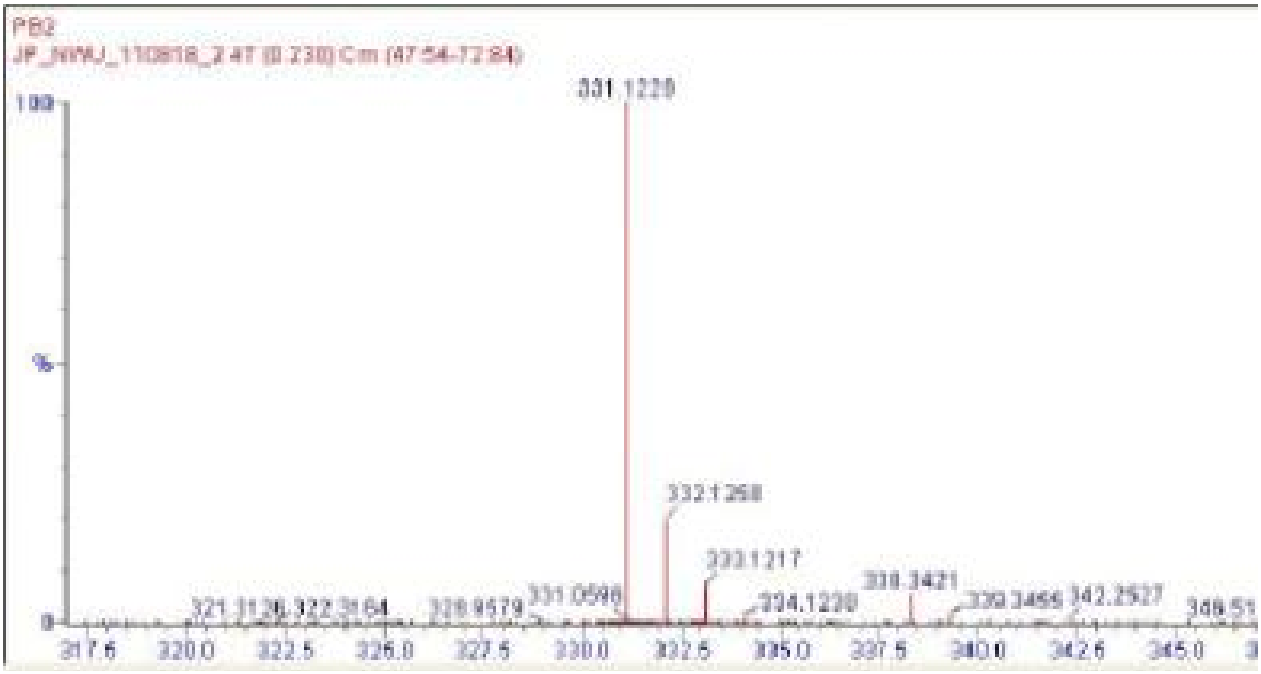

8-{[(4-Chlorophenyl)methyl]sulfanyl}caffeine

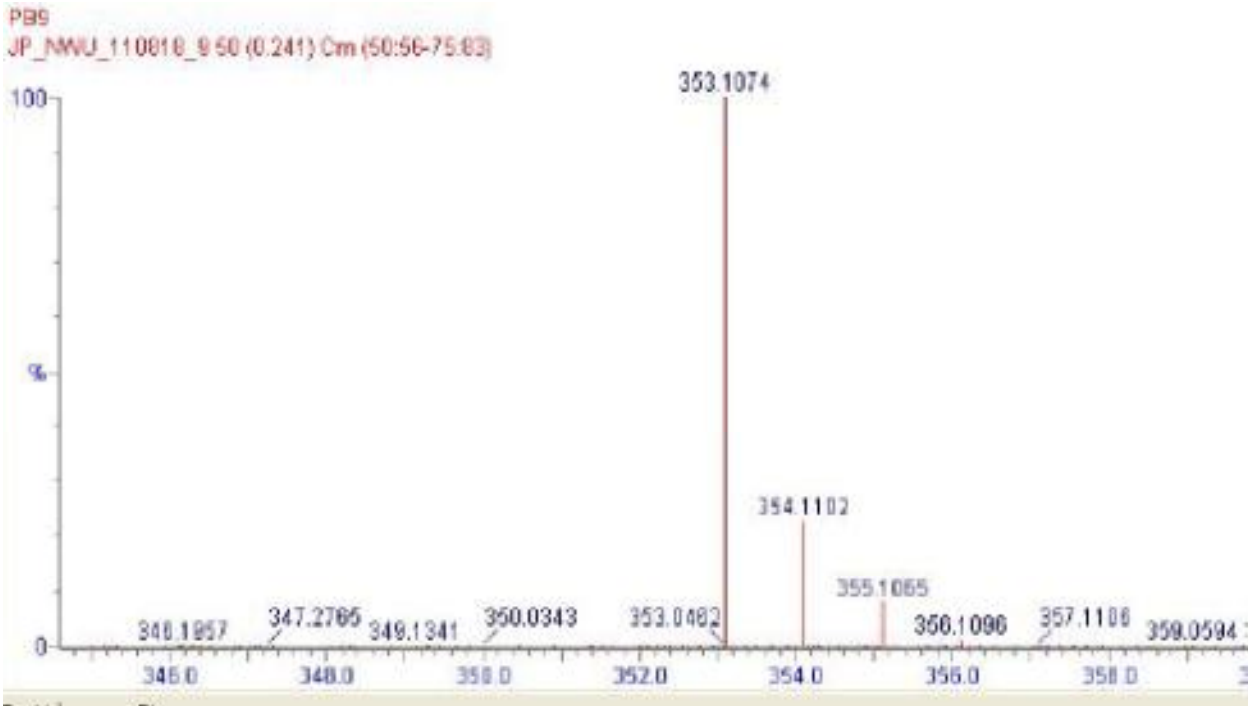

8-{[(4-Bromophenyl)methyl]sulfanyl}caffeine

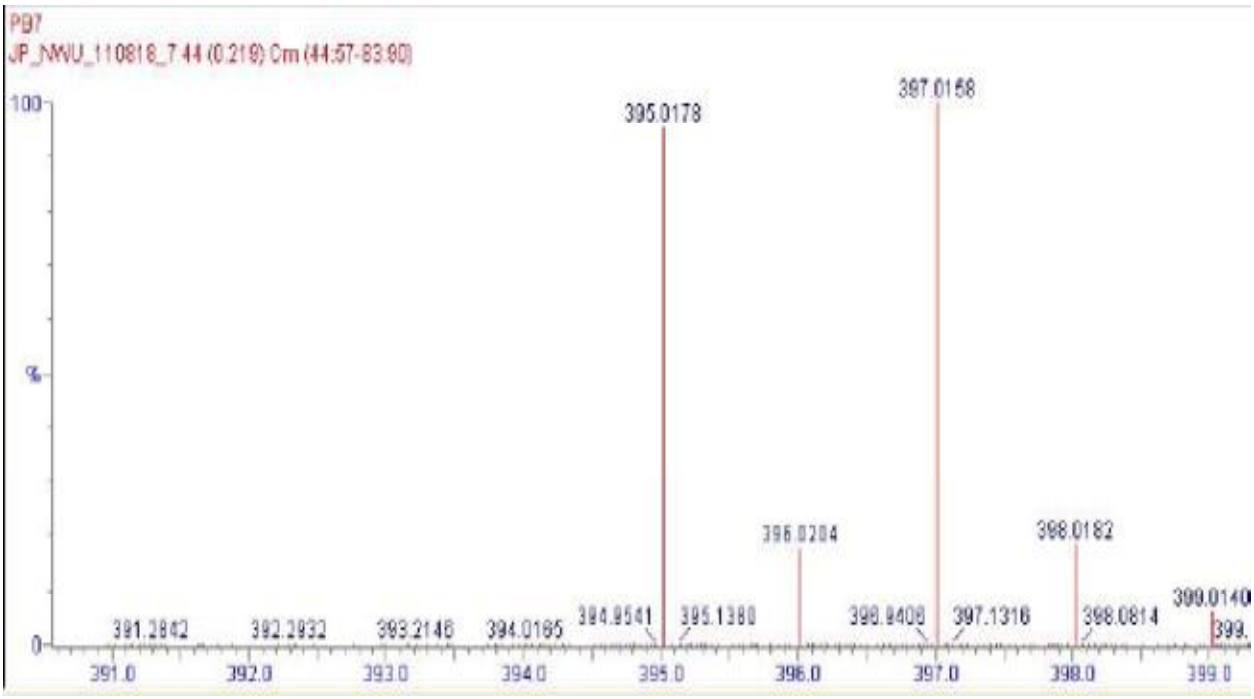

8-{[(4-Fluorophenyl)methyl]sulfanyl}caffeine

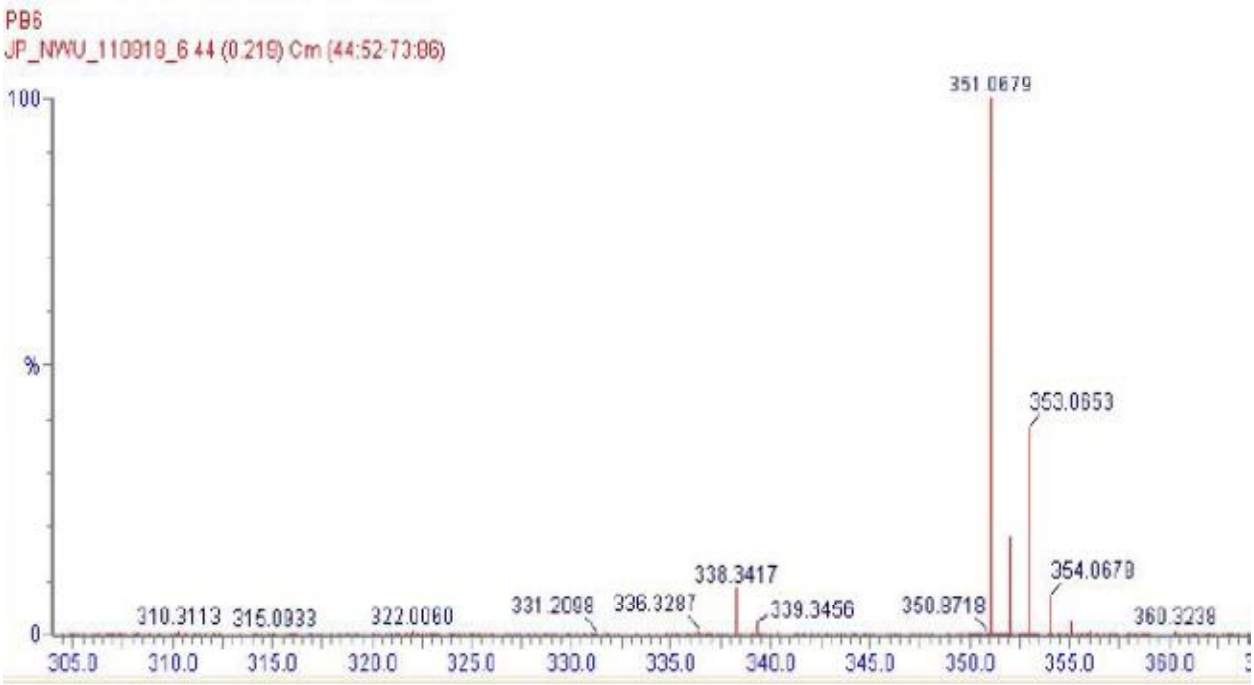

8-{[(4-Methoxyphenyl)methyl]sulfanyl}caffeine

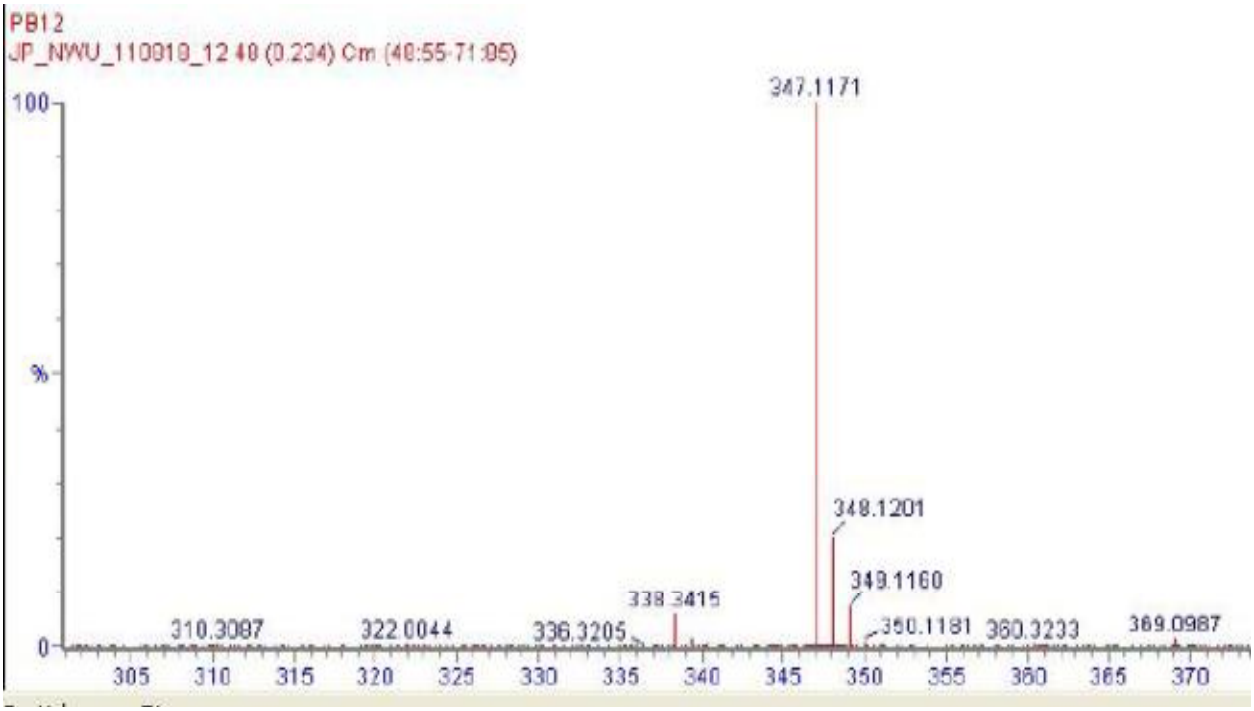

8-[(2-Phenoxyethyl)sulfanyl]caffeine

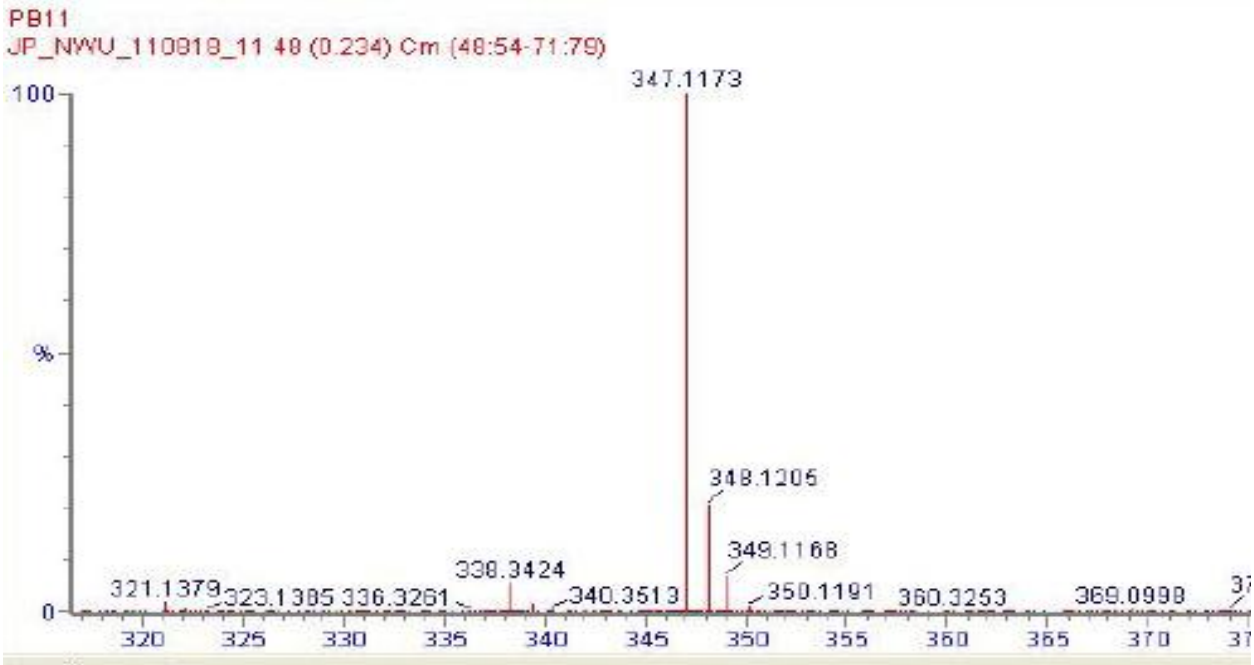

8-(Cyclohexylsulfanyl)caffeine

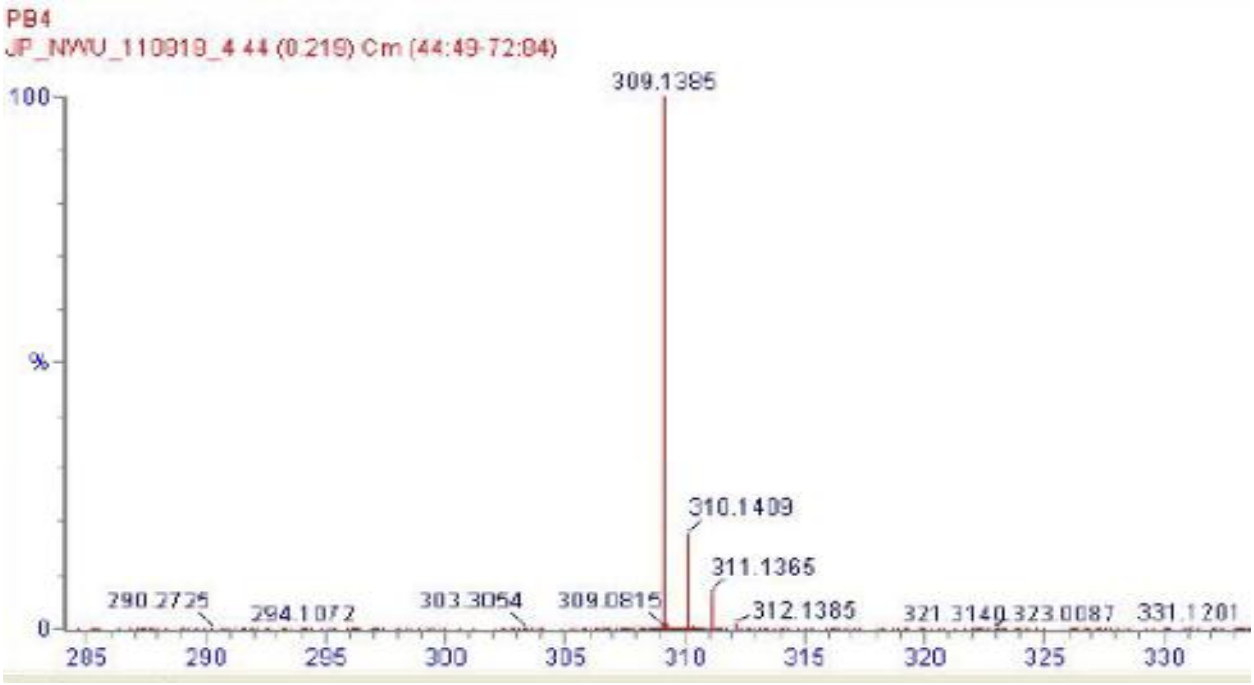

8-(Cyclopentylsulfanyl)caffeine

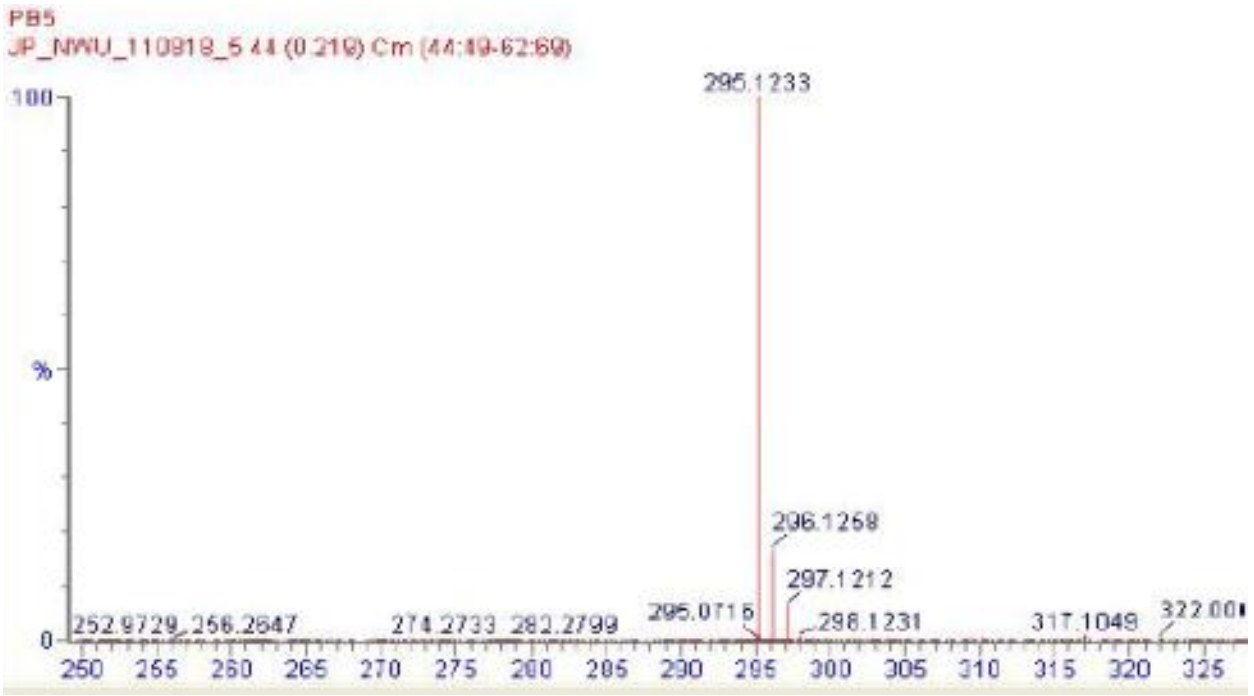

8-(Naphthalen-2-ylsulfanyl)caffeine

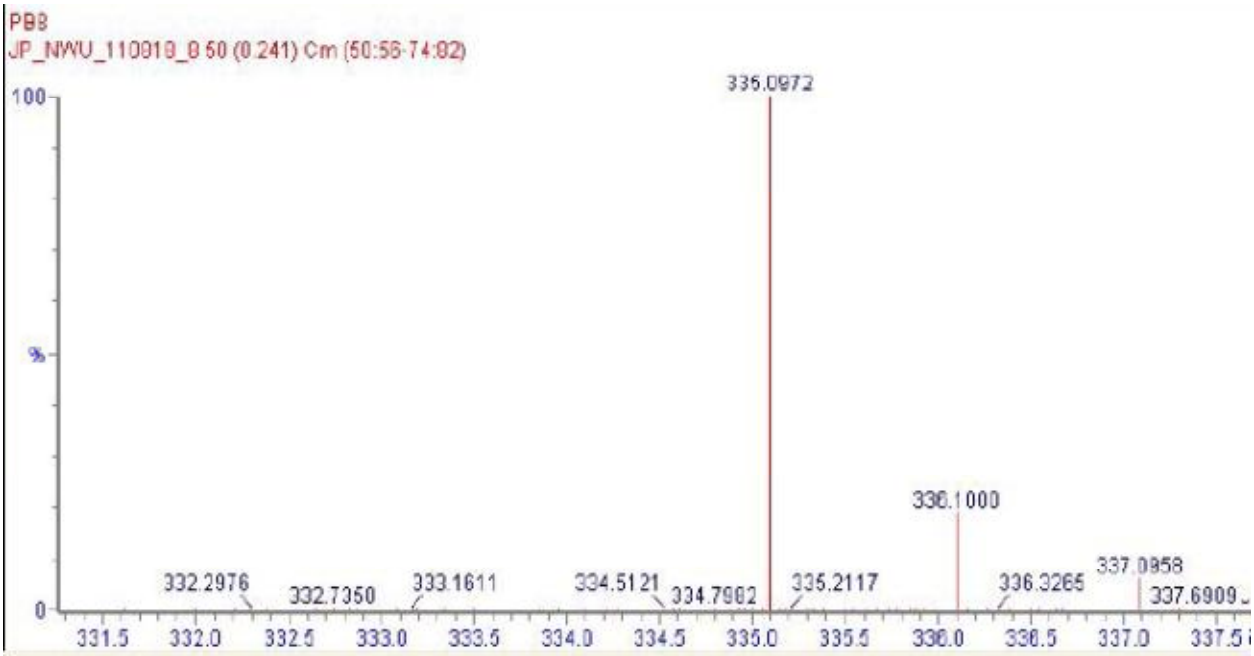

8-[(3-Methylbutyl)sulfanyl]caffeine

Concept article

The research conducted in this project was included as part of a paper published in Bioorganic & Medicinal Chemistry. See article below.

Thio- and aminocaffeine analogues as inhibitors of human monoamine oxidase

Hermanus P. Booysen,[a] Christina Moraal,[a] Gisella Terre Blanche,[a] Anél Petzer,[b] Jacobus J. Bergh,[a] and Jacobus P. Petzer[a,*]

[a] *Pharmaceutical Chemistry, School of Pharmacy, North-West University, Private Bag X6001, Potchefstroom, 2520, South Africa*

[b] *Unit for Drug Research and Development, School of Pharmacy, North-West University, Private Bag X6001, Potchefstroom, 2520, South Africa*

Abstract: In a recent study it was shown that 8-benzyloxycaffeine analogues act as potent reversible inhibitors of human monoamine oxidase (MAO) A and B. Although the benzyloxy side chain appears to be particularly favorable for enhancing the MAO inhibition potency of caffeine, a variety of other C8 oxy substituents of caffeine also lead to potent MAO inhibition. In an attempt to discover additional C8 substituents of caffeine that lead to potent MAO inhibition and to explore the importance of the ether oxygen for the MAO inhibition properties of C8 oxy-substituted caffeines, a series of 8-sulfanyl- and 8-aminocaffeine analogues were synthesized and their human MAO-A and -B inhibition potencies were compared to those of the 8-oxycaffeines. The results document that the sulfanylcaffeine analogues are reversible competitive MAO-B inhibitors with potencies comparable to those of the oxycaffeines. The most potent inhibitor, 8-{[(4-bromophenyl)methyl]sulfanyl}caffeine, exhibited an IC_{50} value of 0.167 µM towards MAO-B. While the sulfanylcaffeine analogues also exhibit affinities for MAO-A, they display in general a high degree of MAO-B selectivity. The aminocaffeine analogues, in contrast, proved to be weak MAO inhibitors with a number of analogues exhibiting no binding to the MAO-A and -B isozymes. The results of this study are discussed with reference to possible binding orientations of selected caffeine analogues within the active site cavities of MAO-A and -B. MAO-B selective sulfanylcaffeine derived inhibitors may act as lead compounds for the design of antiparkinsonian therapies.

Keywords: Monoamine oxidase; Reversible inhibition; Caffeine; Sulfanylcaffeine; Thiocaffeine; Aminocaffeine.

*Corresponding author. Tel.: +27 18 2992206; fax: +27 18 2994243;

e-mail: jacques.petzer@nwu.ac.za.

1. Introduction

The monoamine oxidases (MAO) A and B are mitochondrial bound flavin adenine dinucleotide (FAD) enzymes which catalyze the Ŭ-carbon oxidation of a variety of aminyl substrates.[1] Human MAO-A and ï B consist of 529 and 520 amino acids, respectively, and the FAD is covalently bound to a cysteinyl residue in both enzymes (Cys-406 and Cys-397 in MAO-A and ï B, respectively). While MAO-A and ï B are products of separate genes they share approximately 70% amino acid sequence identity.[2] The X-ray crystallographic structures of MAO-A and ï B indicate that the amino acid residues comprising the active sites and their relative geometries are similar with only 6 of the 16 active site amino acid residues differing between the 2 enzymes.[3,4] In spite of these similarities, MAO-A and ï B have different substrate and inhibitor specificities. Most notably, MAO-A metabolizes the neurotransmitters, serotonin and norepinephrine, as well as the dietary amine, tyramine. MAO-B is well known to metabolize extraneous amines such as benzylamine and phenylethylamine. Dopamine is considered to be a substrate for both isozymes.[5]

Since MAO-A and ï B are both involved in the degradation of neurotransmitter amines, inhibitors of these enzymes are employed as drugs in the treatment of several disorders.[5] For example, MAO-A inhibitors block the central oxidation of serotonin by MAO-A and are used as antidepressants. MAO-B inhibitors reduce the MAO-B catalyzed oxidative metabolism of dopamine in the brain and are used in the treatment of Parkinsonôs disease. Of importance is the observation that MAO-B activity and density increase in most brain regions including the basal ganglia with age while MAO-A activity remains unchanged.[6,7] In the aged parkinsonian brain MAO-B is therefore thought to be the principal MAO isozyme responsible for dopamine catabolism. MAO-B inhibitors may conserve dopamine in the basal ganglia and offer a symptomatic benefit in the treatment of Parkinsonôs disease.[8ï10] MAO-B inhibitors are frequently combined with levodopa therapy since inhibitors of this enzyme have been shown to enhance the elevation of dopamine levels derived from levodopa.[11] MAO-B inhibitors may permit a reduction of the dose of levodopa required for a therapeutic effect and therefore the occurrence of levodopa associated side effects.[12] MAO may also play an important role in the neurodegenerative processes associated with Parkinsonôs disease. The oxidation of dopamine by MAO stoichiometrically yields potentially toxic metabolic by-products.[13] For each mole of

dopamine oxidized by MAO, one mole of hydrogen peroxide (which may lead to oxidative damage) and dopaldehyde (which may react with exocyclic amino groups of nucleosides and N-terminal and lysine Ů-amino groups of proteins) are formed.[13] Inhibitors of MAO reduce the MAO-catalyzed metabolism of DA and as a result reduce the formation of these toxic by-products. MAO inhibitors are therefore considered as a potential treatment strategy to slow the progression of Parkinsonôs disease since they may exert neuroprotective effects in the brain.[13]

Based on the therapeutic value of MAO inhibitors the current study aims to discover new reversible inhibitors of the MAO enzymes, particularly the B isozyme. For this purpose caffeine (**1**) serve as lead compound (Fig. 1). Although caffeine is a weak MAO-B inhibitor (K_i = 3.6 mM), substitution at the C8 position with a variety of substituents has been shown to enhance the MAO-B inhibition potency of caffeine to a large degree.[14] In previous studies it was shown that substitution at C8 of caffeine with alkyloxy substituents (**2**) yielded particularly potent MAO-B inhibitors with a number of compounds exhibiting IC_{50} values in the nM range.[15,16] Interestingly these oxycaffeines are also MAO-A inhibitors, a property that may be attributed to the relatively large degree of rotational freedom of the C8 side chain at the carbon-oxygen ether bond. It has been suggested that structures with a relatively larger degree of conformational freedom may be better suited for binding to MAO-A than relatively rigid structures.[15] Based on these promising results the present study investigates the possibility that alkylsulfanyl and alkylamino substituents at C8 of caffeine may similarly enhance the MAO-A and ï B inhibition potency of caffeine. For this purpose, a series of twelve aryl- and alkylsulfanylcaffeine analogues (**3a**ï **l**) and ten aryl- and alkylaminocaffeine analogues (**4a**ï **h**, **5a**ï **b**) were synthesized and evaluated as potential inhibitors of recombinant human MAO-A and ï B (Fig. 2 and Tables 1ï 3).

2. Results

2.1. Chemistry

The aryl- and alkylsulfanylcaffeine analogues (**3a**ï **l**) were synthesized by reacting 8-chlorocaffeine (**6**) with an appropriate thiol reagent (**7**) in the presence of NaOH and employing a mixture of ethanol and water as reaction solvent (Scheme 1).[17] The aryl- and

alkylaminocaffeine analogues (**4a**ï **h**) were similarly prepared by reaction of an appropriate amine reagent (**8**) with 8-chlorocaffeine but with the exception that the addition of base and additional solvent were not required (Scheme 2).[18] Methylation of **4c** and **4e** at the C8 amine to yield aminomethyl caffeine analogues **5a** and **5b**, respectively, were carried out in DMSO using CH_3I as alkylating agent and KOH as base. The structures of all the target compounds were verified by ^1H NMR, ^{13}C NMR and mass spectrometry. The purities of the compounds were estimated by HPLC analysis.

2.2. Inhibition of MAO-A and –B

The MAO inhibition potencies of the sulfanylcaffeine (**3a**ï **l**) and aminocaffeine analogues (**4a**ï **h**, **5a**ï **b**) were examined by employing the recombinant human MAO-A and ï B enzymes as enzyme sources.[19] The mixed MAO-A/B substrate, kynuramine, was used as substrate for the inhibition studies of both MAO-A and ï B. Kynuramine displays similar K_m values towards the two enzymes with values of 16.1 µM and 22.7 µM for MAO-A and ï B, respectively.[15] The MAO-catalyzed oxidation of kynuramine yields 4-hydroxyquinoline, a fluorescent compound which is readily measured in basic solutions at excitation and emission wavelengths of 310 nm and 400 nm, respectively. Neither the substrate nor the test inhibitors fluoresce under these conditions, or quench the fluorescence of 4-hydroxyquinoline. The inhibition potencies of the sulfanylcaffeine and aminocaffeine analogues are expressed as the IC_{50} values, which were determined from sigmoidal dose-response curves constructed in triplicate from 6 different inhibitor concentrations spanning at least 3 orders of magnitude.

*2.2.1. MAO inhibition by sulfanylcaffeine analogues (**3a**–**l**)*

The MAO inhibition potencies of the sulfanylcaffeine analogues (**3a**ï **l**) are presented in table 1. As shown by the selectivity index (SI) values, the sulfanylcaffeine analogues are selective inhibitors of MAO-B. The only exceptions are **3k** which displays slight selectivity for the MAO-A isozyme and **3l** which is essentially nonselective. 8-(Phenylsulfanyl)caffeine (**3a**) which displays slight selectivity for MAO-B, was found to be a relatively weak inhibitor of both MAO-A and ï B. Extension of the C8 side chain by one methylene unit to yield the benzylsulfanyl homologue **3b**

(IC_{50} = 1.86 µM) enhances the MAO-B inhibition potency 17-fold compared to **3a** (IC_{50} = 33.2 µM). A further increase in the length of the C8 side chain yields even more potent MAO-B inhibitors. For example, compounds **3c** and **3d**, the phenylethylsulfanyl and phenoxyethylsulfanyl homologues exhibited IC_{50} values of 0.223 µM and 0.332 µM, respectively. While the extension of the C8 side chain of **3a** (IC_{50} = 56.4 µM) by one methylene unit to yield **3b** (IC_{50} = 8.22 µM) also results in improved MAO-A inhibition, further increasing the length of the C8 side chain does not result in a further enhancement of inhibition activity. For example, **3c** (IC_{50} = 20.5 µM) and **3d** (IC_{50} = 15.5 µM) are weaker MAO-A inhibitors than the benzylsulfanyl homologue **3b** (IC_{50} = 8.22 µM).

Interestingly, halogen substitution of the phenyl ring of the C8 side chain is also associated with an increase in MAO-B inhibition potency. The benzylsulfanyl substituted caffeine homologues containing chlorine (**3e**; IC_{50} = 0.192 µM), bromine (**3f**; IC_{50} = 0.167 µM) and fluorine (**3g**; IC_{50} = 0.348 µM) on the benzyl phenyl ring were found to be 5ï 11-fold more potent than the corresponding unsubstituted homologue **3b** (IC_{50} = 1.86 µM). Methoxy substitution of the phenyl ring of 8-(benzylsulfanyl)caffeine, in contrast, is associated with a loss of both MAO-A and ï B inhibition activity. Halogen substitution of 8-(benzylsulfanyl)caffeine (**3b**) also enhances MAO-A inhibition potency, although by a lesser degree compared to MAO-B. The homologues containing chlorine (**3e**; IC_{50} = 2.77 µM), bromine (**3f**; IC_{50} =2.62 µM) and fluorine (**3g**; IC_{50} = 4.80 µM) on the benzyl phenyl ring are 1.7ï 3-fold more potent than the corresponding unsubstituted homologue **3b** (IC_{50} = 8.22 µM).

The results document that compound **3i**, the sulfanylcaffeine analogue containing a branched alkyl side chain at C8, is also a relatively good MAO-B inhibitor with an IC_{50} value of 2.62 µM. In fact, **3i** is approximately 12-fold more potent as an MAO-B inhibitor than was 8-(phenylsulfanyl)caffeine (**3a**) which contains a C8 phenylsulfanyl side chain. This result demonstrates that a ring system in the C8 side chain is not an absolute requirement for MAO-B inhibition by sulfanylcaffeine analogues. In accordance with this view, compound **3i** also proved to be more potent as a MAO-B inhibitor than the sulfanylcaffeine analogues containing cyclohexyl (**3j**), cyclopentyl (**3k**) and napthalenyl (**3l**) C8 side chains. Interestingly the

sulfanylcaffeine analogues containing cyclohexyl (**3j**), cyclopentyl (**3k**) and napthalenyl (**3l**) C8 side chains were more potent inhibitors of both MAO-A and ï B than the phenyl substituted analogue **3a**. This result suggests that, with the appropriate structural modification, these moieties may be suitable for the future design of sulfanylcaffeine derived MAO inhibitors. An example of such a structural modification would be the extension of the length of the C8 side chain. Based on the observations that the naphthalenyl substituted sulfanylcaffeine analogue **3l** is 15- and 9-fold more potent as a MAO-A and ï B inhibitor, respectively, than the phenyl substituted sulfanylcaffeine analogue **3a** and that **3l** is a nonselective inhibitor, the naphthalenyl moiety may be particularly suited for the design of sulfanylcaffeine derived mixed MAO-A/B inhibitors.

*2.2.2. MAO inhibition by aminocaffeine analogues (**4a**–**h**, **5a**–**b**)*

The MAO inhibition potencies of the aminocaffeine analogues **4a**ï **h** are presented in tables 2 and 3. The data show that these compounds were relatively weak inhibitors of both MAO-A and ï B with IC_{50} values ranging from 5.78ï 45.2 µM and 9.60ï 24.4 µM for the inhibition of MAO-A and ï B, respectively. In fact, several of the compounds exhibited no binding to the MAO-A and ï B isozymes. Even homologues containing extended C8 side chains such as **4d** (-NH-$(CH_2)_3$-C_6H_5) and **4e** (-NH-$(CH_2)_4$-C_6H_5) did not exhibit potent MAO inhibition. Similarly, homologue **4g** which contains a halogen on the phenyl ring of the C8 side chain was found to be a relatively weak MAO inhibitor. These results demonstrate that, in contrast to the sulfanylcaffeine analogues, extension of the length of the C8 side chain and halogen substitution do not lead to potent MAO-B inhibition by the aminocaffeine analogues. Compared to the sulfanylcaffeine analogues, the aminocaffeine analogues are therefore weak MAO-B inhibitors. For example, sulfanylcaffeine analogue **3c** (IC_{50} = 0.223 µM) is 78-fold more potent as an MAO-B inhibitor than its corresponding aminocaffeine homologue **4c** (IC_{50} = 17.6 µM).

To investigate the possibility of enhancing the MAO inhibition potencies of the aminocaffeines, selected analogues, **4c** and **4e**, were methylated at the C8 amine to yield compounds **5a** and **5b**, respectively. While methylation improved the MAO-B inhibition potency of **4e** by approximately 3-fold, MAO-A inhibition activity was slightly reduced. Methylation of **4c** did not

result in a significant improvement of MAO-B inhibition potency and led to a reduction in MAO-A inhibition. Compared to the sulfanylcaffeine analogues, the aminocaffeine analogues are also weak MAO-B inhibitors. For example, sulfanylcaffeine analogue **3c** (IC_{50} = 0.223 µM) is 75-fold more potent than its aminomethylcaffeine homologue **5a** (IC_{50} = 16.8 µM). It is noteworthy that the most potent MAO-B inhibitor among the aminocaffeine analogues was the C8 methylated derivative **5b** with an IC_{50} value of 2.97 µM. It can therefore be concluded that while methylation of the C8 amine of aminocaffeine analogues may result in enhanced MAO-B inhibition potency, the resulting compounds remain relatively weak inhibitors compared to the sulfanylcaffeine analogues.

2.3. Reversibility of MAO-A and –B inhibition

Based on the nature of the interactions with the MAO enzymes, inhibitors may be classified as reversible or irreversible. Irreversible inhibitors normally form covalent interactions with the enzymes while reversible inhibitors bind via intermolecular interactions. While irreversible inhibitors of MAO have been clinically used for many years, this mode of inhibition may be associated with certain shortcomings.[20] These include a slow and variable recovery of enzyme activity following withdrawal of the irreversible inhibitor.[21] The turnover rate for the biosynthesis of MAO-B in the human brain may be as much as 40 days.[22] In contrast, enzyme activity is regained relatively quickly following withdrawal of a reversible inhibitor, once the inhibitor is cleared from the tissues. Based on these observations, the reversibility of MAO-A and ï B inhibition by the sulfanylcaffeine and aminocaffeine analogues was examined. For this purpose the time-dependency of the inhibition of MAO-A and ï B, respectively, by sulfanylcaffeine analogue **3f** was measured. The time-dependency of the inhibition of MAO-A and ï B by aminocaffiene analogues **4g** and **5b**, respectively, was also examined. While irreversible inhibitors would lead to a time-dependent reduction of enzyme activity, the degree of enzyme inhibition in the presence of a reversible MAO inhibitor remains unchanged irrespective of the time for which the inhibitor is incubated with the enzyme.[23]

The test inhibitors, at concentrations of approximately 2-fold their measured IC_{50} values for the inhibition of the respective MAO enzymes, were preincubated with recombinant human MAO-A

or ï B for time periods of 0, 15, 30 and 60 min. Following these preincubations the residual MAO catalytic activities were measured after the addition of the substrate, kynuramine. The results of these reversibility studies are presented in figures 3 and 4. The graphs show that when **3f** and **4g** are preincubated with MAO-A and **3f** and **5b** are preincubated with MAO-B there are no time-dependent reductions of MAO-A and ï B catalytic activities. Even after a period of 60 min the test compounds do not reduce the MAO catalytic rates. These results suggest that the test caffeines are not time-dependent inhibitors of MAO-A and ï B and interact reversibly, at least for the time period (0ï 60 min) and at the inhibitor concentrations (2 × IC_{50}) evaluated.

This study also examined the possibility that **3f** may act as a competitive inhibitor of human MAO-A and ï B. For this purpose, sets of Lineweaverï Burk plots were constructed for the inhibition of these enzymes by **3f**. The initial catalytic rates of MAO-A or ï B were measured in the absence and presence of three different concentrations of **3f**. These measurements were carried out using four different concentrations of the substrate, kynuramine (15ï 90 µM). The Lineweaverï Burk plots obtained from these experiments are shown in figure 5. The graphs show that the Lineweaverï Burk plots constructed for the inhibition of MAO-A and ï B are linear and intersect at the y-axis. This indicates that the inhibition of the MAO enzymes by **3f** is competitive. This result is further support that **3f** is a reversible MAO inhibitor.

2.4. Molecular modeling

The results of the MAO inhibition studies shows that among the sulfanylcaffeine analogues evaluated here, several compounds act as potent reversible inhibitors of MAO-B with IC_{50} values in the nM range. Interestingly, extension of the length of the C8 side chain leads to enhanced MAO-B inhibition potency. While the sulfanylcaffeine analogues are also MAO-A inhibitors, they display, for the most part, selectivity for the MAO-B isozyme. In contrast to the sulfanylcaffeine analogues, the aminocaffeine analogues were found to be weak MAO-B inhibitors with many analogues exhibiting no binding to either MAO-A or B. To provide additional insight, the predicted binding modes of selected analogues (**3a**ï **c** and **4c**) in the active site cavities of MAO-A and ï B were examined using molecular docking.

The docking studies were carried out using the LigandFit application of the Discovery Studio modeling software (Accelrys) according to a previously reported protocol.[23] As enzyme models, the three-dimensional structures of human MAO-A cocrystallized with harmine (PDB entry: 2Z5X)[3] and human MAO-B cocrystallized with safinamide (PDB entry: 2V5Z)[4] were selected. The enzyme models were prepared by calculating the protonation states of the ionizable residues and adding the hydrogen atoms accordingly. After the valences of the FAD cofactor and cocrystallized ligands were corrected, hydrogen atoms were added and the models were subjected to an energy minimization cascade while the protein backbone was constrained. For the purpose of the docking, only the crystal waters which are reported to be conserved and non-displaceable were retained (see Experimental).[3,4]

The best ranked docking solution for the binding of the selected analogues (**3a**ï **c** and **4c**) to MAO-B shows one prevailing orientation for all of the inhibitors. As shown by the binding orientation of **3c**, the caffeine ring binds within the substrate cavity of MAO-B, in close proximity to the FAD cofactor (Fig. 6). This places the carbonyl oxygen at C2 of the caffeine ring 3.4 Å from the flavin N5 and the carbonyl oxygen at C6 within hydrogen bond distance to the phenolic hydrogen of Tyr-435. The caffeine ring also forms a potential ´ ï ´ interaction with the aromatic ring of Tyr-398. The region defined by the flavin isoalloxazine ring, Tyr-398 and Tyr-435 is the only polar space of the MAO-B active site and is also the site where amine catalysis occurs.[24] In the MAO-B model selected for these studies, the side chain of Ile-199 is rotated into an alternative conformation to allow for the fusion of the substrate and entrance cavities.[25] This rotation of the Ile-199 side chain from the active site cavity is essential for relatively large inhibitors, such as safinamide and C8 substituted caffeine derivatives, to be able to bind to MAO-B. As a result the phenylethyl C8 side chain of **3c** is allowed to extend into the hydrophobic entrance cavity where it may be stabilized via Van der Waals interactions. As expected, the relatively shorter phenyl (**3a**) and benzyl (**3b**) C8 side chains of sulfanylcaffeine homologues **3a** and **3b** do not extend as deep into the MAO-B entrance cavity as the side chain of **3c**, and may therefore undergo interactions with the entrance cavity to a lesser extent compared to **3c** (Fig. 7). Despite the similar binding orientations of **3a** and **3b** within the MAO-B active site, **3b** was found to be a 17-fold more potent inhibitor. Since **3b** protrudes only slightly

deeper (by ~1.2 Å) into the entrance cavity compared to **3a**, this result suggest that a relatively small enhancement of the space occupied by an inhibitor in the entrance cavity leads to a large increase in binding affinity. Another possible explanation may be that the larger degree of conformational freedom afforded by the longer C8 side chain of **3b** may facilitate improved interaction with the entrance cavity. The view that interaction with the entrance cavity is essential for high affinity inhibitor binding is supported by the observation that caffeine is a weak MAO-B inhibitor.[14] Lacking a C8 side chain, caffeine is expected to bind only within the substrate cavity and is unable to interact with the entrance cavity. The lower MAO-B inhibition potencies of **3a** and **3b** compared to compound **3c** may thus be explained by weaker interaction with the entrance cavity.

Interestingly the aminocaffeine analogue **4c** adopts a similar binding mode to that described above for **3c** and as a result forms similar interactions with the MAO-B active site (Fig. 8). The only additional interaction that may occur between **4c** and MAO-B is a potential hydrogen bond between the C8 amine and the phenolic group of Tyr-326. The results of the MAO inhibition studies however documents that the aminocaffeine analogues are weak MAO-B inhibitors with **4c** being 78-fold weaker than the corresponding sulfanylcaffeine homologue **3c**. The docking studies therefore suggest that differing binding orientations cannot account for the apparent loss of MAO-B inhibition activity of the aminocaffeine analogues.

The predicted binding orientation of **3c** within the active site of MAO-A is similar to the binding orientation observed in MAO-B with the caffeine ring bound in close proximity to the FAD cofactor and the C8 side chain extending towards the entrance of the active site (Fig. 9). Interestingly, the caffeine ring is rotated by ~180 ºC compared to the binding orientation adopted in the MAO-B active site. This dissimilarity in binding orientations in the MAO-A and ï B active sites has also been observed in docking studies with 8-benzyloxycaffeine analogues.[15] As a result of the flipped orientation of the caffeine ring, the C2 carbonyl oxygen is within hydrogen bond distance of the phenolic hydrogen of Tyr-444 and two active site waters. Also, the caffeine ring of **3c** binds more distant from Tyr-407 (~4.3 Å) in MAO-A than from the corresponding residue, Tyr-398 (~3.6 Å), in MAO-B. For this reason, a ´ ï ´ interaction similar to that observed

between the caffeine ring and Tyr-398 in MAO-B, is not observed between **3c** and the MAO-A active site. This may represent a possible reason for the finding that sulfanylcaffeine analogues are in general more potent MAO-B inhibitors than MAO-A inhibitors. Also noteworthy is the observation that, in the MAO-A active site, the C8 side chain of **3c** is bent at the CH_2-S thioether bond from the plane of the caffeine ring while in the MAO-B active site, the side chain of **3c** exhibits a modest deviation from the plane of the caffeine ring (Fig. 10). The differing binding orientations adopted by C8 substituted caffeine derivatives in MAO-A and ï B may, for the most part, be attributed to steric hindrance caused by the aromatic moieties of Phe-208 in MAO-A and Tyr-326 in MAO-B. As illustrated in figure 11A, the binding orientation and position of **3c** in the MAO-B active site cannot be reproduced in MAO-A because this would result in structural overlap with the phenyl ring of Phe-208. In MAO-B, the amino acid residue that occupies the same position as Phe-208 in MAO-A is Ile-199. In MAO-B the side chain of Ile-199 may rotate out of the active site cavity to allow for the observed binding pose of **3c**.[25] Similarly, the binding orientation and position of **3c** in the MAO-A active site cannot be reproduced in MAO-B because of structural overlap with of Tyr-326 (Fig. 11B). In MAO-A, the amino acid residue that occupies the analogous position as Tyr-398 in MAO-B is Ile-335. The relatively smaller side chain of Ile-335 compared to the aromatic ring of Tyr-398, does not sterically prevent the observed binding orientation of **3c** in the MAO-A active site.[3]

3. Discussion

Based on previous reports that oxycaffeine analogues are MAO inhibitors,[15,16] the present study investigated the possibility that C8 substituted sulfanylcaffeine and aminocaffeine analogues may also act as inhibitors of human MAO-A and ï B. The results demonstrated that several of the sulfanylcaffeine analogues act as potent MAO-B inhibitors and that the inhibition is reversible. For example, the bromine substituted sulfanylcaffeine analogue **3f** was the most potent MAO-B inhibitor with an IC_{50} value of 0.167 µM. The relatively high MAO-B inhibition potencies of the sulfanylcaffeine analogues may be evaluated by comparison of the IC_{50} value of **3f** (IC_{50} = 0.167 µM.) with the reversible inhibitor safinamide, which binds to MAO-B with an IC_{50} value of 0.08 µM.[4] While the sulfanylcaffeine analogues are also MAO-A inhibitors, they are for the most part selective for the MAO-B isoform. Modeling studies predict that the sulfanylcaffeine analogues adopt dissimilar binding modes in the MAO-A and ï B active site

cavities, respectively. Compared to the predicted orientation in MAO-B, the caffeine ring is flipped by approximately 180 º in the MAO-A active site which results in differing interactions of the caffeine ring with the polar regions of the MAO-A and ï B substrate cavities. The alternative binding orientation of the caffeine ring in MAO-A may be less optimal for the formation of stabilizing polar interactions compared to the binding orientation adopted in MAO-B and may explain, at least in part, the lower binding affinities of the sulfanylcaffeine analogues to MAO-A.[15] Interestingly, modeling studies suggest that the C8 side chain of the sulfanylcaffeine analogue **3c** is bent to a high degree from the plane of the caffeine ring at the CH_2-S thioether bond while in the MAO-B active site, the C8 side chain displays only a modest deviation from the plane of the caffeine moiety. The ability of the C8 side chain to adopt a bent orientation may be an important requirement for the inhibition of MAO-A. Rigid C8 substituted caffeine analogues such as (E)-8-(3-chlorostyryl)caffeine (CSC) (Fig. 12) are not MAO-A inhibitors while displaying high affinity binding to MAO-B.[26] The observation that CSC does not bind to MAO-A may be explained by its low degree of flexibility and inability to adopt a bent orientation similar to that observed for **3c** in the MAO-A active site.

The notion that the C8 side chains of the caffeine analogues are important structural features for MAO-A and ï B inhibition is supported by the observation that caffeine is a weak MAO inhibitor.[14] Modeling shows that, in the MAO-B active site, the C8 side chains of the sulfanylcaffeine analogues may extend into the hydrophobic entrance cavity where they are stabilized by Van der Waals interactions. Since extension of the C8 chain length results in enhanced MAO-B inhibition potency it may be concluded that longer C8 side chains form more productive interactions with the MAO-B entrance cavity, which thus leads to more potent enzyme inhibition. Halogen substitution on the phenyl ring of the C8 side chain also leads to a significant enhancement of MAO-B inhibition. This result may be explained by the possibility that halogen substitution may further improve Van der Waals and dipole interactions between the MAO-B entrance cavity and the C8 side chain. While it is not clear why methoxy substitution of 8-(benzylsulfanyl)caffeine leads to a loss of both MAO-A and ï B inhibition potency, this result is in accordance with the findings of a previous study which showed that MAO-B inhibition potencies of a series of benzyloxycaffeine analogues correlate with the electronegativity of substituents on the phenyl ring of the C8 side chain and that electron-withdrawing groups enhance MAO-B inhibition potency.[15] Interestingly, this study shows that C8 side chains that do

not contain phenyl rings are also suitable for MAO inhibition. Examples of sulfanylcaffeine analogues containing such side chains are the 3-methylbutyl (**3i**), cyclohexyl (**3j**), cyclopentyl (**3k**) and napthalenyl (**3l**) substituted homologues.

One of the most significant findings of this study is that the aminocaffeine analogues are weak MAO inhibitors with most homologues displaying no inhibition. The predicted binding orientation and interactions of aminocaffeine analogue **4c** in the MAO-B active site is similar to the orientation of sulfanylcaffeine analogue **3c**. In fact **4c** displays an additional hydrogen bond interaction with Tyr-326. In spite of these predictions **4c** is approximately 78-fold weaker as a MAO-B inhibitor compared to **3c**. Even methylation of the C8 amines to yield tertiary amines does not produce inhibitors with similar potencies to those of the sulfanylcaffeine analogues. While the reasons for this behavior is not clear, differing ionization states of the sulfanylcaffeine and aminocaffeine analogues do not explain the difference in binding affinities to the MAO enzymes, since both the sulfanylcaffeine and aminocaffeine analogues are expected to be uncharged in the buffer used for the inhibition studies (pH 7.4). Also, it is unlikely that aminocaffeines are excluded from entering the access channel leading to the active site cavity since aminyl substrates are thought to be deprotonated prior to entering the MAO active sites.[24]

In conclusion, the sulfanylcaffeine analogues exhibit similar MAO-B inhibition potencies to those of the previously reported oxycaffeine analogues with various homologues from both series exhibiting IC_{50} values in the nM range.[15,16] The attachment of substituents at C8 of caffeine via a thioether linkage therefore enhances MAO-B inhibition activity to a similar extent compared to attachment via an oxyether. In contrast, C8 substituted aminocaffeines are not suitable for MAO inhibition. Based on the potent MAO-B inhibition properties of the sulfanylcaffeine analogues, they may be considered as lead compounds for the development of reversible MAO-B inhibitors.

4. Experimental section

4.1. Chemicals and instrumentation

Unless otherwise noted, all starting materials were obtained from Sigma-Aldrich and were used without purification. Proton (^{1}H) and carbon (^{13}C) NMR spectra were recorded on a Bruker Avance III 600 spectrometer at frequencies of 600 MHz and 150 MHz, respectively. All NMR measurements were conducted in $CDCl_3$ and DMSO-d_6 and the chemical shifts are reported in parts per million (ŭ) downfield from the signal of tetramethylsilane added to the deuterated solvent. Spin multiplicities are given as s (singlet), d (doublet), dd (doublet of doublets), t (triplet), q (quartet), qn (quintet), sept (septet) or m (multiplet). High resolution mass spectra (HRMS) were obtained on a Waters Synapt G2 instrument in electrospray ionization (ESI) mode. The HRMS spectrum of **4a** was recorded on a DFS high resolution magnetic sector mass spectrometer (Thermo Electron Corporation) in atmospheric pressure chemical ionization (APCI) mode. Melting points (mp) were measured with a Stuart SMP10 melting point apparatus and are uncorrected. The purity of the synthesized compounds were determined via HPLC analyses which were conducted with an Agilent 1100 HPLC system equipped with a quaternary gradient pump and an Agilent 1100 series diode array detector (see Supplementary Material). HPLC grade acetonitrile (Merck) and Milli-Q water (Millipore) were used for the chromatography. For fluorescence spectrophotometry, a Varian Cary Eclipse fluorescence spectrophotometer was employed. Microsomes from insect cells containing recombinant human MAO-A and ï B (5 mg/mL) and kynuramine.2HBr were obtained from Sigma-Aldrich.

4.2. Synthesis of C8-substituted thiocaffeine analogues (**3a**ï **l**)

A solution of NaOH (4 mmol) in 3.5 mL water and 7 mL ethanol was cooled in an ice bath and the appropriate thiol (4 mmol) was added. The reaction mixture was stirred and 8-chlorocaffeine (4 mmol) was added in a single portion to yield a suspension. The reaction was heated under reflux for 60 min and then cooled on ice. The white precipitate was collected by filtration and washed with 30 mL ethanol. The product was recrystallized from 30 mL ethanol at room temperature and the crystals were washed with 30 mL ethanol.[17]

4.2.1. **8-(Phenylsulfanyl)caffeine (3a)**

The title compound was prepared from thiophenol in a yield of 65.1%: mp 149 °C (ethanol). ^{1}H NMR (Bruker Avance III 600, $CDCl_3$) δ 3.37 (s, 3H), 3.54 (s, 3H), 3.90 (s, 3H), 7.32 (m, 5H); ^{13}C NMR (Bruker Avance III 600, $CDCl_3$) δ 28.0, 29.9, 33.1, 109.5, 128.2, 129.6, 130.5, 130.9, 146.4, 148.0, 151.4, 154.9; ESI-HRMS *m*/*z*: calcd for $C_{14}H_{15}N_4O_2S$ (MH^+), 303.0916, found 303.0912; Purity (HPLC): 98%.

4.2.2. **8-(Benzylsulfanyl)caffeine (3b)**

The title compound was prepared from benzyl mercaptan in a yield of 59%: mp 149 °C (ethanol). ^{1}H NMR (Bruker Avance III 600, $CDCl_3$) δ 3.35 (s, 3H), 3.57 (s, 3H), 3.69 (s, 3H), 4.42 (s, 2H), 7.27 (m, 3H), 7.31 (m, 2H); ^{13}C NMR (Bruker Avance III 600, $CDCl_3$) δ 27.8, 29.7, 32.2, 37.4, 108.7, 127.9, 128.7, 128.9, 136.6, 148.3, 150.0, 151.5, 154.6; ESI-HRMS *m*/*z*: calcd for $C_{15}H_{17}O_2N_4S$, 317.1072 (MH^+), found 317.1073; Purity (HPLC): 99%.

4.2.3. **8-[(2-Phenylethyl)sulfanyl]caffeine (3c)**

The title compound was prepared from phenylethyl mercaptan in a yield of 22.9%: mp 95 °C (ethanol). ^{1}H NMR (Bruker Avance III 600, $CDCl_3$) δ 3.04 (t, 2H, J = 7.9 Hz), 3.36 (s, 3H), 3.49 (t, 2H, J ï 7.9 Hz), 3.55 (s, 3H), 3.78 (s, 3H), 7.21 (m, 3H), 7.29 (m, 2H); ^{13}C NMR (Bruker Avance III 600, $CDCl_3$) δ 27.8, 29.7, 32.1, 33.8, 36.0, 108.5, 126.7, 128.5, 139.3, 148.5, 150.9, 151.5, 154.5; ESI-HRMS *m*/*z*: calcd for $C_{16}H_{19}N_4O_2S$, 331.1229 (MH^+), found 331.1229; Purity (HPLC): 99%.

4.2.4. **8-[(2-Phenoxyethyl)sulfanyl]caffeine (3d)**

The title compound was prepared from 2-phenoxyethanethiol in a yield of 43.9%: mp 114 °C (ethanol). ^{1}H NMR (Bruker Avance III 600, $CDCl_3$) δ 3.37 (s, 3H), 3.53 (s, 3H), 3.63 (t, 2H, J = 6.4 Hz), 3.83 (s, 3H), 4.30 (t, 2H, J = 6.4 Hz), 6.91 (d, 2H, J = 8.3 Hz), 6.94 (t, 1H, J = 7.2 Hz), 7.25 (m, 2H); ^{13}C NMR (Bruker Avance III 600, $CDCl_3$) δ 27.8, 29.7, 31.5, 32.2, 66.3, 108.7,

114.5, 121.3, 129.5, 148.4, 150.3, 151.5, 154.5, 158.1; ESI-HRMS *m*/*z*: calcd for $C_{16}H_{19}N_4O_3S$ (MH^+), 347.1176, found 347.1173; Purity (HPLC): 95%.

4.2.5. **8-{[(4-Chlorophenyl)methyl]sulfanyl}caffeine (3e)**

The title compound was prepared from 4-chlorobenzyl mercaptan in a yield of 85.6%: mp 169 °C (ethanol). ^{1}H NMR (Bruker Avance III 600, $CDCl_3$) *δ* 3.36 (s, 3H), 3.56 (s, 3H), 3.73 (s, 3H), 4.40 (s, 2H), 7.26 (m, 4H); ^{13}C NMR (Bruker Avance III 600, $CDCl_3$) *δ* 27.9, 29.7, 32.2, 36.4, 108.8, 128.8, 130.3, 133.8, 135.2, 148.3, 149.7, 151.5, 154.6; ESI-HRMS *m*/*z*: calcd for $C_{15}H_{16}ClN_4O_2S$ (MH^+), 351.0682, found 351.0679; Purity (HPLC): 97%.

4.2.6. **8-{[(4-Bromophenyl)methyl]sulfanyl}caffeine (3f)**

The title compound was prepared from 4-bromobenzyl mercaptan in a yield of 82.0%: mp 166 °C (ethanol). ^{1}H NMR (Bruker Avance III 600, $CDCl_3$) *δ* 3.35 (s, 3H), 3.55 (s, 3H), 3.72 (s, 3H), 4.38 (s, 2H), 7.21 (d, 2H, J = 8.3 Hz), 7.40 (d, 2H, J = 8.3 Hz); ^{13}C NMR (Bruker Avance III 600, $CDCl_3$) *δ* 27.8, 29.7, 32.2, 36.4, 108.7, 121.8, 130.6, 131.8, 135.8, 148.3, 149.6, 151.4, 154.5; ESI-HRMS *m*/*z*: calcd for $C_{15}H_{16}BrN_4O_2S$ (MH^+), 395.0177, found 395.0178; Purity (HPLC): 98%.

4.2.7. **8-{[(4-Fluorophenyl)methyl]sulfanyl}caffeine (3g)**

The title compound was prepared from 4-fluorobenzyl mercaptan in a yield of 71.6%: mp 175 °C (ethanol). ^{1}H NMR (Bruker Avance III 600, $CDCl_3$) *δ* 3.35 (s, 3H), 3.55 (s, 3H), 3.72 (s, 3H), 4.40 (s, 2H), 6.96 (t, 2H, J = 8.3 Hz), 7.30 (q, 2H, J = 5.3 Hz); ^{13}C NMR (Bruker Avance III 600, $CDCl_3$) *δ* 27.8, 29.7, 32.1, 36.4, 108.7, 115.6 (d), 130.6 (d), 132.4 (d), 148.3, 149.8, 151.4, 154.5, 161.4, 163.1; ESI-HRMS *m*/*z*: calcd for $C_{15}H_{16}FN_4O_2S$ (MH^+), 335.0976, found 335.0972; Purity (HPLC): 95%.

4.2.8. **8-{[(4-Methoxyphenyl)methyl]sulfanyl}caffeine (3h)**

The title compound was prepared from 4-methoxybenzyl mercaptan in a yield of 90.5%: mp 159 °C (ethanol). ^{1}H NMR (Bruker Avance III 600, $CDCl_3$) δ 3.36 (s, 3H), 3.58 (s, 3H), 3.71 (s, 3H), 3.76 (s, 3H), 4.39 (s, 2H), 6.80 (d, 2H, J = 8.7 Hz), 7.24 (d, 2H, J = 8.7 Hz); ^{13}C NMR (Bruker Avance III 600, $CDCl_3$) δ 27.8, 29.7, 32.1, 37.0, 55.3, 108.6, 114.1, 128.4, 130.2, 148.4, 150.2, 151.5, 154.6, 159.2; ESI-HRMS *m*/*z*: calcd for $C_{16}H_{19}N_4O_3S$ (MH^+), 347.1176, found 347.1171; Purity (HPLC): 94%.

4.2.9. **8-[(3-Methylbutyl)sulfanyl]caffeine (3i)**

The title compound was prepared from 3-methyl-1-butanethiol in a yield of 35.3%: mp 79 °C (ethanol). ^{1}H NMR (Bruker Avance III 600, $CDCl_3$) δ 0.91 (d, 6H, J = 6.8 Hz), 1.59 (q, 2H, J = 7.9 Hz), 1.69 (sept, 1H, J = 6.8 Hz), 3.23 (t, 2H, J = 7.5 Hz), 3.34 (s, 3H), 3.51 (s, 3H), 3.79 (s, 3H); ^{13}C NMR (Bruker Avance III 600, $CDCl_3$) δ 22.1, 27.4, 27.8, 29.6, 30.8, 32.1, 38.5, 108.4, 148.4, 151.3, 151.5, 154.5; ESI-HRMS *m*/*z*: calcd for $C_{13}H_{21}N_4O_2S$ (MH^+), 297.1385, found 297.1382; Purity (HPLC): 97%.

4.2.10. **8-(Cyclohexylsulfanyl)caffeine (3j)**

The title compound was prepared from cyclohexanethiol in a yield of 37.2%: mp 133 °C (ethanol). ^{1}H NMR (Bruker Avance III 600, $CDCl_3$) δ 1.28 (m, 1H), 1.38 (m, 2H), 1.48 (m, 2H), 1.58 (m, 1H), 1.74 (m, 2H), 2.03 (m, 2H), 3.34 (s, 3H), 3.52 (s, 3H), 3.71 (m, 1H), 3.82 (s, 3H); ^{13}C NMR (Bruker Avance III 600, $CDCl_3$) δ 25.4, 25.8, 27.8, 29.7, 32.3, 33.4, 47.2, 108.4, 148.4, 150.3, 151.5, 154.6; ESI-HRMS *m*/*z*: calcd for $C_{14}H_{21}N_4O_2S$ (MH^+), 309.1385, found 309.1385; Purity (HPLC): 99%.

4.2.11. **8-(Cyclopentylsulfanyl)caffeine (3k)**

The title compound was prepared from cyclopentanethiol in a yield of 60.9%: mp 135 °C (ethanol). ^{1}H NMR (Bruker Avance III 600, $CDCl_3$) δ 1.63 (m, 4H), 1.76 (m, 2H), 2.15 (m, 2H),

3.34 (s, 3H), 3.51 (s, 3H), 3.80 (s, 3H), 3.99 (qn, 1H); ^{13}C NMR (Bruker Avance III 600, $CDCl_3$) δ 24.6, 27.8, 29.7, 32.2, 33.8, 46.4, 108.2, 148.5, 151.3, 151.5, 154.6; ESI-HRMS *m*/*z*: calcd for $C_{13}H_{19}N_4O_2S$ (MH^+), 295.1229, found 295.1233; Purity (HPLC): 95%.

4.2.12. **8-(Naphthalen-2-ylsulfanyl)caffeine (3l)**

The title compound was prepared from 2-naphthalenethiol in a yield of 87.7%: mp 175 °C (ethanol). ^{1}H NMR (Bruker Avance III 600, $CDCl_3$) δ 3.37 (s, 3H), 3.53 (s, 3H), 3.91 (s, 3H), 7.35 (dd, 1H, J = 1.9, 8.3 Hz), 7.48 (m, 2H), 7.73 (m, 1H), 7.78 (m, 2H), 7.84 (s, 1H); ^{13}C NMR (Bruker Avance III 600, $CDCl_3$) δ 27.9, 29.8, 33.1, 109.5, 126.9, 127.0, 127.4, 127.5, 127.8, 127.9, 129.4, 129.7, 132.6, 133.6, 146.4, 148.0, 151.4, 154.9; ESI-HRMS *m*/*z*: calcd for $C_{18}H_{17}N_4O_2S$ (MH^+), 353.1072, found 353.1074; Purity (HPLC): 94%.

4.3. Synthesis of C8-substituted aminocaffeine analogues (4a–h)

A mixture of 8-chlorocaffeine (2 mmol) and the appropriate amine (10 mmol) was heated under reflux (175ï 180 ºC) for 3 hours. The reaction was cooled to room temperature and treated with 50 mL acetic acid (5%). The resulting suspension was stirred for 15 min at room temperature and the precipitate was collected by filtration. The product was dried at 60 ºC and recrystallized twice from ethanol (30 mL) at 0 ºC.[18]

4.3.1. **8-(Phenylamino)caffeine (4a)**

The title compound was prepared from aniline and 8-chlorocaffeine in a yield of 24.2%: mp 164ï 265 °C (ethanol). ^{1}H NMR (Bruker Avance III 600, DMSO-d_6) δ 3.15 (s, 3H), 3.35 (s, 3H), 3.74 (s, 3H), 6.96 (t, 1H, J = 7.5 Hz), 7.29 (t, 2H, J = 7.5 Hz), 7.67 (d, 2H, J = 8.3 Hz), 9.07 (s, 1H); ^{13}H NMR (Bruker Avance III 600, DMSO-d_6) δ 27.3, 29.4, 30.5, 102.0, 118.1, 121.7, 128.7, 140.0, 147.2, 149.3, 150.9, 153.3; APCI-HRMS *m*/*z*: calcd for $C_{14}H_{15}N_5O_2$ (M^+), 285.1226, found 285.1230; Purity (HPLC): 98%.

4.3.2. **8-(Benzylamino)caffeine (4b)**

The title compound was prepared from benzylamine and 8-chlorocaffeine in a yield of 74.0%: mp 230 °C (ethanol). ^{1}H NMR (Bruker Avance III 600, DMSO-d_6) δ 3.14 (s, 3H), 3.35 (s, 3H), 3.58 (s, 3H), 4.53 (d, 2H, J = 5.6 Hz), 7.23 (t, 1H, J = 7.5 Hz), 7.32 (t, 2H, J = 7.5 Hz), 7.36 (d, 2H, J = 7.5 Hz), 7.56 (t, 1H, J = 5.6 Hz); ^{13}H NMR (Bruker Avance III 600, DMSO-d_6) δ 27.1, 29.2, 29.8, 45.7, 102.0, 126.9, 127.4, 128.3, 139.6, 148.2, 150.9, 152.9, 154.0; ESI-HRMS *m*/*z*: calcd for $C_{15}H_{18}N_5O_2$ (MH^+), 300.1460, found 300.1459; Purity (HPLC): 99%.

4.3.3. **8-[(2-Phenylethyl)amino]caffeine (4c)**

The title compound was prepared from 2-phenylethylamine and 8-chlorocaffeine in a yield of 68.3%: mp 221 °C (ethanol). ^{1}H NMR (Bruker Avance III 600, DMSO-d_6) δ 2.88 (t, 2H, J = 7.2 Hz), 3.14 (s, 3H), 3.32 (s, 3H), 3.49 (m, 2H), 3.51 (s, 3H), 7.11 (t, 1H, J = 5.3 Hz), 7.19 (t, 1H, J = 7.2 Hz), 7.22 (d, 2H, J = 7.5 Hz), 7.29 (t, 2H, J = 7.5 Hz); ^{13}H NMR (Bruker Avance III 600, DMSO-d_6) δ 27.1, 29.2, 29.7, 35.3, 44.1, 101.8, 126.1, 128.3, 128.7, 139.4, 148.3, 150.9, 152.9, 153.9; ESI-HRMS *m*/*z*: calcd for $C_{16}H_{20}N_5O_2$ (MH^+), 314.1617, found 314.1621; Purity (HPLC): 99%.

4.3.4. **8-[(3-Phenylpropyl)amino]caffeine (4d)**

The title compound was prepared from 3-phenylpropylamine and 8-chlorocaffeine in a yield of 76.8%: mp 204ï 205 °C (ethanol). ^{1}H NMR (Bruker Avance III 600, DMSO-d_6) δ 1.88 (qn, 2H, 7.5 Hz), 2.64 (t, 2H, J = 7.5 Hz), 3.13 (s, 3H), 3.30 (s, 3H), 3. 32 (m, 2H), 3.52 (s, 3H), 6.98 (t, 1H, J = 5.3 Hz), 7.16 (t, 1H, J = 7.2 Hz), 7.22 (d, 2H, J = 7.5 Hz), 7.26 (t, 2H, J = 7.5 Hz); ^{13}H NMR (Bruker Avance III 600, DMSO-d_6) δ 27.1, 29.2, 29.7, 30.8, 32.3, 42.0, 101.8, 125.7, 128.2, 128.3, 141.7, 148.3, 150.9, 152.8, 154.1; ESI-HRMS *m*/*z*: calcd for $C_{17}H_{22}N_5O_2$ (MH^+), 328.1773, found 328.1774; Purity (HPLC): 99%.

4.3.5. **8-[(4-Phenylbutyl)amino]caffeine (4e)**

The title compound was prepared from 4-phenylbutylamine and 8-chlorocaffeine in a yield of 63.0%: mp 179ï 180 °C (ethanol). ^{1}H NMR (Bruker Avance III 600, DMSO-d_6) δ 1.59 (m, 4H), 2.60 (t, 2H, J = 7.2 Hz), 3.13 (s, 3H), 3.30 (s, 3H), 3.32 (m, 2H), 3.51 (s, 3H), 6.94 (t, 1H, J = 5.6 Hz), 7.14 (t, 1H, J = 7.2 Hz), 7.18 (d, 2H, J = 7.2 Hz), 7.25 (t, 2H, J = 7.2 Hz); ^{13}C NMR (Bruker Avance III 600, DMSO-d_6) δ 27.1, 28.2, 28.8, 29.2, 29.7, 34.8, 42.2, 101.7, 125.6, 128.2, 128.3, 142.1, 148.3, 150.9, 152.8, 154.1; ESI-HRMS *m*/*z*: calcd for $C_{18}H_{24}N_5O_2$ (MH^+), 342.1930, found 342.1929; Purity (HPLC): 99%.

4.3.6. **8-{[2-(Pyridin-2-yl)ethyl]amino}caffeine (4f)**

The title compound was prepared from 2-(2-pyridyl)ethylamine and 8-chlorocaffeine in a yield of 20.4%: mp 196ï 197 °C (ethanol). ^{1}H NMR (Bruker Avance III 600, DMSO-d_6) δ 3.03 (t, 2H, J = 7.2 Hz), 3.13 (s, 3H), 3.31 (s, 3H), 3.50 (s, 3H), 3.65 (q, 2H, 6.7 Hz), 7.10 (t, 1H, J = 5.6 Hz), 7.20 (t, 1H, J = 5.6 Hz), 7.26 (d, 1H, J = 7.5 Hz), 7.69 (t, 1H, J = 7.5 Hz), 8.49 (d, 1H, J = 4.1 Hz); ^{13}C NMR (Bruker Avance III 600, DMSO-d_6) δ 27.1, 29.2, 29.7, 37.5, 42.4, 101.8, 121.5, 123.2, 136.4, 148.3, 149.0, 150.9, 152.8, 153.9, 159.1; ESI-HRMS *m*/*z*: calcd for $C_{15}H_{19}N_6O_2$ (MH^+), 315.1569, found 315.1570; Purity (HPLC): 98%.

4.3.7. **8-{[2-(3-Chlorophenyl)ethyl]amino}caffeine (4g)**

The title compound was prepared from 2-(3-chlorophenyl)ethanamine and 8-chlorocaffeine in a yield of 48.5%: mp 111ï 113 °C (ethanol). ^{1}H NMR (Bruker Avance III 600, DMSO-d_6) δ 2.88 (t, 2H, J = 7.2 Hz), 3.13 (s, 3H), 3.32 (s, 3H), 3.50 (s, 3H), 3.52 (m, 2H), 7.10 (t, 1H, J = 5.6 Hz), 7.18 (d, 1H, J = 7.5 Hz), 7.24 (d, 1H, J = 8.3 Hz), 7.29 (d, 1H, J = 7.5 Hz), 7.31 (s, 1H); ^{13}C NMR (Bruker Avance III 600, DMSO-d_6) δ 27.1, 29.2, 29.7, 34.8, 43.7, 101.8, 126.1, 127.5, 128.6, 130.1, 132.9, 142.0, 148.3, 150.9, 152.8, 153.8; ESI-HRMS *m*/*z*: calcd for $C_{16}H_{19}N_5O_2Cl$ (MH^+), 348.1227, found 348.1225; Purity (HPLC): 98%.

4.3.8. **8-(Cyclopentylamino)caffeine (4h)**

The title compound was prepared from cyclopentylamine and 8-chlorocaffeine in a yield of 38.6%: mp 217ï 218 °C (ethanol). ^{1}H NMR (Bruker Avance III 600, DMSO-d_6) δ 1.52 (m, 4H), 1.68 (m, 2H), 1,93 (m, 2H), 3.13 (s, 3H), 3.31 (s, 3H), 3.53 (s, 3H), 4.10 (m, 1H), 6.76 (d, 1H, J = 7.2 Hz); ^{13}H NMR (Bruker Avance III 600, DMSO-d_6) δ 23.4, 27.1, 29.2, 29.8, 32.4, 54.2, 101.7, 148.3, 150.9, 152.8, 153.8; ESI-HRMS *m*/*z*: calcd for $C_{13}H_{20}N_5O_2$ (MH^+), 278.1617, found 278.1612; Purity (HPLC): 96%.

4.4. Methylation of the C8-substituted aminocaffeine analogues (5a–b)

Potassium hydroxide (0.05 g) was powderized and suspended in 5 mL DMSO. The resulting mixture was stirred for 30 min at room temperature and the aminocaffeine analogue (3 mmol) dissolved in DMSO (5 mL) was added. The reaction was heated to 40 ºC (in order for the aminocaffeine analogue to remain in solution) and iodomethane (0.8 mmol) was added. Stirring of the reaction was continued and another portion of iodomethane (0.8 mmol) was added every 20 min until silica gel TLC (petroleum ether/ ethyl actetate 30:70) indicated completion of the reaction. The pH of the reaction was also continually measured, and when acidic (pH paper), another portion of potassium hydroxide (0.05 g) was added. Upon completion, the reaction was cooled to room temperature and water (250 mL) was added. The resulting solution was incubated for several days at 4 ºC and the formed crystals were collected by filtration.

4.4.1. **8-[Methyl(2-phenylethyl)amino]caffeine (5a)**

The title compound was prepared from 8-[(2-phenylethyl)amino]caffeine (**4c**) and iodomethane in a yield of 57.7%: mp 103 °C (ethanol). ^{1}H NMR (Bruker Avance III 600, DMSO-d_6) δ 2.88 (t, 2H, J = 7.5 Hz), 2.98 (s, 3H), 3.16 (s, 3H), 3.33 (s, 3H), 3.47 (t, 2H, J = 7.5 Hz), 3.59 (s, 3H), 7.18 (m, 1H), 7.25 (m, 4H); ^{13}C NMR (Bruker Avance III 600, DMSO-d_6) δ 27.3, 29.3, 32.5, 33.0, 38.6, 54.5, 103.8, 126.1, 128.3, 128.8, 139.0, 147.1, 150.9, 153.5, 156.6; ESI-HRMS *m*/*z*: calcd for $C_{17}H_{22}N_5O_2$ (MH^+), 328.1774, found 328.1734; Purity (HPLC): 99%.

4.4.2. **8-[Methyl(4-phenylbutyl)amino]caffeine (5b)**

The title compound was prepared from 8-[(4-phenylbutyl)amino]caffeine (**4e**) and iodomethane in a yield of 49.9%: mp 114 °C (ethanol). ^{1}H NMR (Bruker Avance III 600, DMSO-d_6) *δ* 1.57 (m, 4H), 2.57 (t, 2H, J = 7.15 Hz), 2.90 (s, 3H), 3.16 (s, 3H), 3.26 (t, 2H, J = 7.15 Hz), 3.32 (s, 3H), 3.65 (s, 3H), 7.15 (m, 3H), 7.24 (t, 2H, J = 7.91 Hz); ^{13}C NMR (Bruker Avance III 600, DMSO-d_6) *δ* 26.3, 27.3, 27.9, 29.3, 32.6, 34.7, 38.4, 52.5, 103.8, 125.7, 128.2, 128.2, 142.0, 147.1, 150.9, 153.5, 156.9; ESI-HRMS *m*/*z*: calcd for $C_{19}H_{26}N_5O_2$ (MH^+), 356.2087, found 356.2088; Purity (HPLC): 98%.

4.5. IC_{50} determinations for the inhibition of human MAO

Microsomal preparations form insect cells containing recombinant human MAO-A and ï B (5 mg/mL) served as enzyme sources and all enzymatic reactions were conducted in potassium phosphate buffer (100 mM, pH 7.4, made isotonic with KCl) to a final volume of 500 µL.[19] The reactions contained the MAO-A/B mixed substrate, kynuramine, at concentrations of 45 µM and 30 µM for the incubations with MAO-A and ï B, respectively, various concentrations of the test inhibitor (0ï 100 µM) and the MAO enzymes (0.0075 mg/mL). The enzyme activities employed for the IC_{50} value determinations were 24ï 28 nmoles 4-hydroxyquinoline formed/min/mg protein for MAO-A and 6ï 8 nmoles 4-hydroxyquinoline formed/min/mg protein for MAO-B. Stock solutions of the test inhibitors were prepared in DMSO and added to the reactions to yield a final concentration of 4% (v/v) DMSO. The enzyme reactions were incubated at 37 °C for 20 minutes and then terminated with the addition of 400 µL NaOH (2 N) and 1000 µL distilled water. After centrifugation at 16,000 *g* for 10 min, the fluorescence of the MAO generated 4-hydroxyquinoline in the supernatant fractions were measured ($ə_{ex}$ = 310 nm, $ə_{em}$ = 400 nm). To determine the concentrations of 4-hydroxyquinoline, a linear calibration curve was constructed from solutions of 4-hydroxyquinoline (0.047ï 1.50 µM) in potassium phosphate buffer. The calibration standards were prepared to a volume of 500 µL and contained 4% DMSO, 400 µL NaOH (2 N) and 1000 µL distilled water. The initial rate of MAO catalysis was plotted versus the logarithm of the inhibitor concentration to obtain a sigmoidal doseï response curve. Each curve was constructed from 6 different inhibitor concentrations spanning at least 3 orders of a magnitude. These data were fitted to the one site competition model incorporated into the

GraphPad Prism software and the IC_{50} values were determined in triplicate and are expressed as mean ± standard deviation (SD).

4.6. Time-dependent inhibition studies

The reversibility of MAO inhibition was examined by determining the time-dependence of inhibition of three selected inhibitors, **3f**, **4g** and **5b**. The selected inhibitors were preincubated in potassium phosphate buffer (100 mM, pH 7.4, made isotonic with KCl) with MAO-A and ï B (0.015ï 0.03 mg/mL) for periods of 0, 15, 30, 60 min at 37 ºC. The concentrations of the inhibitors used were two-fold their measured IC_{50} values for the inhibition of the respective MAO enzymes and were: 5.22 µM (**3f**) and 11.56 µM (**4g**) for the studies with MAO-A, and 0.32 µM (**3f**) and 5.94 µM (**5b**) for the studies with MAO-B. To compensate for a potential time-dependent loss of enzyme activity, the enzyme preincubations were firstly incubated at 37 ºC and the inhibitors were subsequently added at different time points. These time points were selected as to ensure that all enzyme preparations were preheated at 37 ºC for exactly 60 min, irrespective of the time period (0ï 60 min) for which the enzyme preparations were preincubated in the presence of the test inhibitor. These reactions were diluted 2-fold by the addition of kynuramine at concentrations of 45 µM and 30 µM for the incubations with MAO-A and ï B, respectively, and the resulting reactions (500 µL final volume) were incubated at 37 °C for a further 15 minutes. The final enzyme concentration in these reactions was 0.0075ï 0.015 mg/mL and the concentrations of the selected inhibitors were approximately equal to their IC_{50} values for the inhibition of the respective isozymes. The reactions were terminated with the addition of 400 µL NaOH (2 N) and 1000 µL distilled water and the rates of MAO catalyzed generation of 4-hydroxyquinoline were measured and calculated as described above. All measurements were carried out in triplicate and are expressed as mean ± SD.[23]

4.7. Construction of Lineweaver-Burk plots

A set consisting of four Lineweaverï Burk plots were constructed for the inhibition of MAO-A and ï B by the selected inhibitor **3f**. One plot was constructed in the absence of inhibitor while three plots were constructed in the presence of three different concentrations of **3f** each. These

concentrations were 1.31ï 5.22 µM and 0.04ï 0.16 µM for the inhibition studies with MAO-A and ï B, respectively. Four different kynuramine concentrations (15ï 90 µM) were employed for each plot and the concentrations of recombinant human MAO-A and ï B used were 0.015 mg/mL. The initial MAO catalytic rates were measured as described above. Linear regression analysis was performed using GraphPad Prism.[23]

4.8. Molecular modeling studies

The modeling studies were carried out with the Windows based Discovery Studio 1.7 molecular modeling software (Accelrys).[23,27] For this purpose the crystallographic structures of MAO-A co-crystallized with harmine (PDB code: 2Z5X)[3] and MAO-B co-crystallized with safinamide (PDB code: 2V5Z)[4] were obtained from the Brookhaven Protein Data Bank (www.rcsb.org/pdb). The protonation states of the ionizable amino acids residues were calculated at pH 7.4 and hydrogen atoms were added to the receptor models. The valences of the FAD cofactors (oxidized state) and co-crystallized ligands were corrected and hydrogen atoms were added according to the appropriate protonation states at pH 7.4. The structures were typed automatically with the Momany and Rone CHARMm forcefield, the backbone of the protein was constrained and the structures were subjected to a three step energy minimization. The first step was a steepest descent minimization which was followed by conjugate gradient minimization. For both protocols the termination criteria was set to a maximum of 2500 steps or a minimum value of 0.1 for the root mean square of the energy gradient. The final step was an adopted basis Newton-Rapheson minimization and the termination criteria was set to a maximum of 5000 steps or a minimum value for the root mean square of the energy gradient of 0.01. For these minimization steps the implicit generalized Born solvation model with simple switching was employed with the dielectric constant set to 4. For both the MAO-A and ï B models, the crystal water molecules were removed with the exception of 3 active site waters in each model. The X-ray crystallographic structures of MAO-B shows that three active site water molecules (HOH 1155, 1170 and 1351; A-chain) are conserved, all located in the vicinity of the FAD cofactor.[4] In the MAO-A model, the crystal waters HOH 710, 718 and 739 which occupies the analogous positions in the MAO-A active site compared to those cited above for MAO-B, were retained. The co-crystallized ligands and the backbone constraints were subsequently removed from the models and the binding sites were identified by a flood-filling algorithm. The

structures of **3a**ï **c** and **4c** were constructed within Discovery Studio, their hydrogen atoms were added according to the appropriate protonation states at pH 7.4. The geometries of the ligands were briefly optimized in Discovery Studio using a fast Dreiding-like forcefield (1000 iterations) and the atom potential types and partial charges were assigned with the Momany and Rone CHARMm forcefield. Docking of the ligands was carried out with the LigandFit application of Discovery Studio and the docking solutions were refined using the Smart Minimizer algorithm. The parameters for the docking runs were set to their default values, ten possible binding solutions were computed for each docked ligand and the best-ranked binding conformation of each ligand was determined according to the DockScore values. The illustrations were prepared in PyMOL.[28] It is interesting to note that among the 10 best ranked binding orientations, there were orientations which exhibited a reversed binding mode with the caffeine ring directed towards the entrance of the MAO-A and ï B active sites while the C8 sulfanyl and amino side chains project towards the FAD cofactor. Based on the low DockScore values these orientations were however deemed unlikely.

Acknowledgements

The NMR spectra were recorded by André Joubert of the SASOL Centre for Chemistry, North-West University while the MS spectra were recorded by the Mass Spectrometry Service, University of the Witwatersrand and the Mass Spectrometry Unit, Stellenbosch University. This work was supported by grants from the National Research Foundation and the Medical Research Council, South Africa.

References

1. Binda, C.; Newton-Vinson, P.; Hubálek, F.; Edmondson, D. E.; Mattevi, A. *Nat. Struct. Biol.* **2002**, *9*, 22.
2. Shih, J. C.; Chen, K.; Ridd, M. J.; *Annu. Rev. Neurosci*. **1999**, *22*, 197.
3. Son, S. ï Y.; Ma, J.; Kondou, Y.; Yoshimura, M.; Yamashita, E.; Tsukihara, T. *Proc. Natl. Acad. Sci. U.S.A*. **2008**, *105*, 5739.
4. Binda, C.; Wang, J.; Pisani, L.; Caccia, C.; Carotti, A.; Salvati, P.; Edmondson, D. E.; Mattevi, A. *J. Med. Chem*. **2007**, *50*, 5848.

5. Youdim, M. B. H.; Edmondson, D.; Tipton, K. F. *Nat. Rev. Neurosci*. **2006**, *7*, 295.
6. Nicotra, A.; Pierucci, F.; Parvez, H.; Senatori, O. *Neurotoxicology*. **2004**, *25*, 155.
7. Fowler, J. S.; Volkow, N. D.; Wang, G. J.; Logan, J.; Pappas, N.; Shea, C.; MacGregor, R. *Neurobiol. Aging*. **1997**, *18*, 431.
8. Youdim, M. B. H.; Collins, G. G. S.; Sandler, M.; Bevan-Jones, A. B.; Pare, C. M.; Nicholson, W. J. *Nature*. **1972**, *236*, 225.
9. Collins, G. G. S.; Sandler, M.; Williams, E. D.; Youdim, M. B. H. *Nature*. **1970,** *225*, 817.
10. Di Monte, D. A.; DeLanney, L. E.; Irwin, I.; Royland, J. E.; Chan, P.; Jakowec, M. W.; Langston, J. W. *Brain. Res*. **1996**, *738*, 53.
11. Finberg, J. P.; Wang, J.; Bankiewich, K.; Harvey-White, J; Kopin, I. J.; Goldstein, D. S. *J. Neural Transm. Suppl*. **1998**, *52*, 279.
12. Fernandez, H. H.; Chen, J. J. *Pharmacotherapy*. **2007**, *27*, 174S.
13. Youdim, M. B. H.; Bakhle, Y. S. *Br. J. Pharmacol*. **2006**, *147*, S287.
14. Van der Walt, E. M.; Milczek, E. M.; Malan, S. F.; Edmondson, D. E.; Castagnoli, N., Jr.; Bergh, J. J.; Petzer, J. P. *Bioorg. Med. Chem. Lett*. **2009**, *19*, 2509.
15. Strydom, B.; Malan, S. F.; Castagnoli, N.; Bergh, J. J.; Petzer, J. P. *Bioorg. Med. Chem*. **2010**, *18*, 1018.
16. Strydom, B.; Bergh, J. J.; Petzer, J. P. *Eur. J. Med. Chem*. **2011**, *46*, 3474.
17. Long, L. M. *J. Am. Chem. Soc*. **1947**, *69*, 2939.
18. Cramer, L. *Chem. Ber*. **1894**, *27*, 3089.
19. Novaroli, L.; Reist, M.; Favre, E.; Carotti, A.; Catto, M.; Carrupt, P. A. *Bioorg. Med. Chem*. **2005**, *13*, 6212.
20. Prins, L. H. A.; Petzer, J. P.; Malan, S. F. *Eur. J. Med. Chem*. **2010**, *45*, 4458.
21. Tipton, K.F.; Boyce, S.; O'Sullivan, J.; Davey, G. P.; Healy, J. *Curr. Med. Chem*. **2004**, *11*, 1965.
22. Fowler, J. S.; Volkow, N. D.; Logan, J.; Wang, G.; MacGregor, R. R.; Schlyer, D.; Wolf, A. P.; Pappas, N.; Alexoff, D.; Shea, C.; Dorflinger, E.; Kruchowy, L.; Yoo, K.; Fazzini, E.; Patlak, C. *Synaps*. **1994**, *18*, 86.
23. Manley-King, C. I.; Bergh, J. J.; Petzer, J. P. *Bioorg. Med. Chem*. **2011**, *19*, 261.
24. Binda, C.; Mattevi, A.; Edmondson, D. E.; *J. Biol. Chem*. **2002**, *277*, 23973.
25. Hubálek, F.; Binda, C.; Khalil, A.; Li, M.; Mattevi, A.; Castagnoli, N., Jr.; Edmondson, D. E. *J. Biol. Chem.* **2005**, *280*, 15761.
26. Vlok, N.; Malan, S. F.; Castagnoli, N., Jr.; Bergh, J. J.; Petzer, J. P. *Bioorg. Med. Chem.* **2006**, *14*, 3512.
27. Accelrys Discovery Studio 1.7, Accelrys Software Inc., San Diego, CA, USA. 2006, http://www.accelrys.com.

28. DeLano, W. L. The PyMOL Molecular Graphics System. DeLano Scientific, San Carlos, USA, 2002.

Table 1. The IC_{50} values for the inhibition of recombinant human MAO-A and ï B by compounds **3a**ï **l**

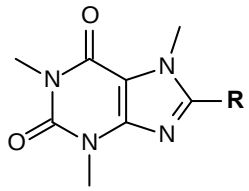

		IC_{50} (µM)[a]		
	R	MAO-A	MAO-B	SI[b]
3a	-S-C_6H_5	56.4 ± 12.9	33.2 ± 3.41	1.7
3b	-S-CH_2-C_6H_5	8.22 ± 1.13	1.86 ± 0.034	4.4
3c	-S-$(CH_2)_2$-C_6H_5	20.5 ± 4.49	0.223 ± 0.010	91.9
3d	-S-$(CH_2)_2$-O-C_6H_5	15.5 ± 2.17	0.332 ± 0.033	46.7
3e	-S-CH_2-(4-Cl-C_6H_4)	2.77 ± 0.570	0.192 ± 0.025	14.4
3f	-S-CH_2-(4-Br-C_6H_4)	2.62 ± 0.104	0.167 ± 0.020	15.7
3g	-S-CH_2-(4-F-C_6H_4)	4.80 ± 0.584	0.348 ± 0.036	13.8
3h	-S-CH_2-(4-CH_3O-C_6H_4)	ï [c]	ï [c]	ï
3i	-S-$(CH_2)_2$-$CH(CH_3)_2$	15.2 ± 4.09	2.62 ± 0.546	5.8
3j	-S-C_6H_{11}	24.4 ± 8.76	13.1 ± 3.49	1.9
3k	-S-C_5H_9	9.40 ± 0.572	20.9 ± 3.11	0.4
3l	-S-2-Naphthalenyl	3.60 ± 0.291	3.60 ± 1.10	1.0

[a] All values are expressed as the mean ± SD of triplicate determinations.

[b] The selectivity index is the selectivity for the MAO-B isoform and is given as the ratio of IC_{50}(MAO-A)/IC_{50}(MAO-B).

[c]No inhibition observed at a maximum concentration of 100 µM of the test inhibitor.

Table 2. The IC_{50} values for the inhibition of recombinant human MAO-A and ï B by compounds **4a**ï **h**

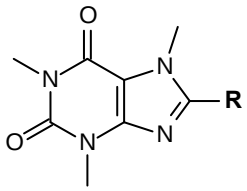

		IC_{50} (µM)[a]		
	R	MAO-A	MAO-B	SI[b]
4a	-NH-C_6H_5	ï [c]	ï [c]	ï
4b	-NH-CH_2-C_6H_5	ï [c]	ï [c]	ï
4c	-NH-$(CH_2)_2$-C_6H_5	45.2 ± 9.19	17.6 ± 2.48	2.6
4d	-NH-$(CH_2)_3$-C_6H_5	ï [c]	ï [c]	ï
4e	-NH-$(CH_2)_4$-C_6H_5	30.9 ± 6.74	9.60 ± 0.759	3.2
4f	-NH-$(CH_2)_2$-(pyridin-2-yl)	ï [c]	19.4 ± 5.07	ï
4g	-NH-$(CH_2)_2$-(3-ClC_6H_4)	5.78 ± 0.411	24.4 ± 18.0	0.2
4h	-NH-C_5H_9	ï [c]	ï [c]	ï

[a] All values are expressed as the mean ± SD of triplicate determinations.

[b] The selectivity index is the selectivity for the MAO-B isoform and is given as the ratio of IC_{50}(MAO-A)/IC_{50}(MAO-B).

[c]No inhibition observed at a maximum concentration of 100 µM of the test inhibitor.

Table 3. The IC_{50} values for the inhibition of recombinant human MAO-A and ï B by compounds **5a**ï **b**

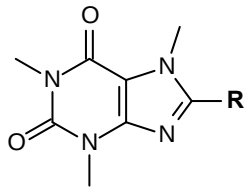

		IC_{50} (μM)[a]		
	R	MAO-A	MAO-B	SI[b]
5a	-(NCH_3)-$(CH_2)_2$-C_6H_5	107 ± 9.85	16.8 ± 6.83	6.4
5b	-(NCH_3)-$(CH_2)_4$-C_6H_5	37.7 ± 6.40	2.97 ± 0.536	12.7

[a] All values are expressed as the mean ± SD of triplicate determinations.

[b] The selectivity index is the selectivity for the MAO-B isoform and is given as the ratio of IC_{50}(MAO-A)/IC_{50}(MAO-B).

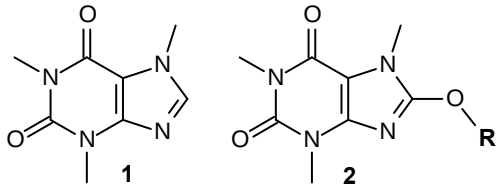

Figure 1. The structures of caffeine (**1**) and oxycaffeine analogues (**2**).

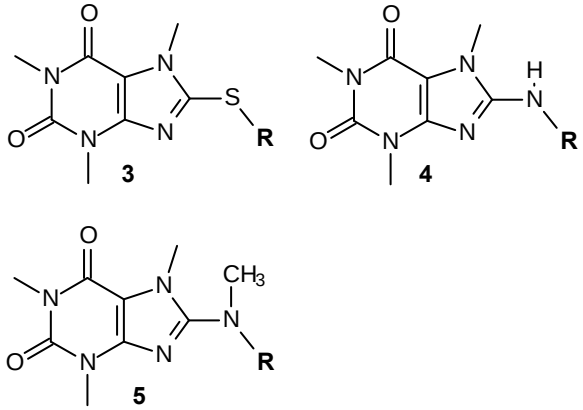

Figure 2. The structures of sulfanylcaffeine analogues (**3**), aminocaffeine analogues (**4**) and aminomethylcaffeine analogues (**5**).

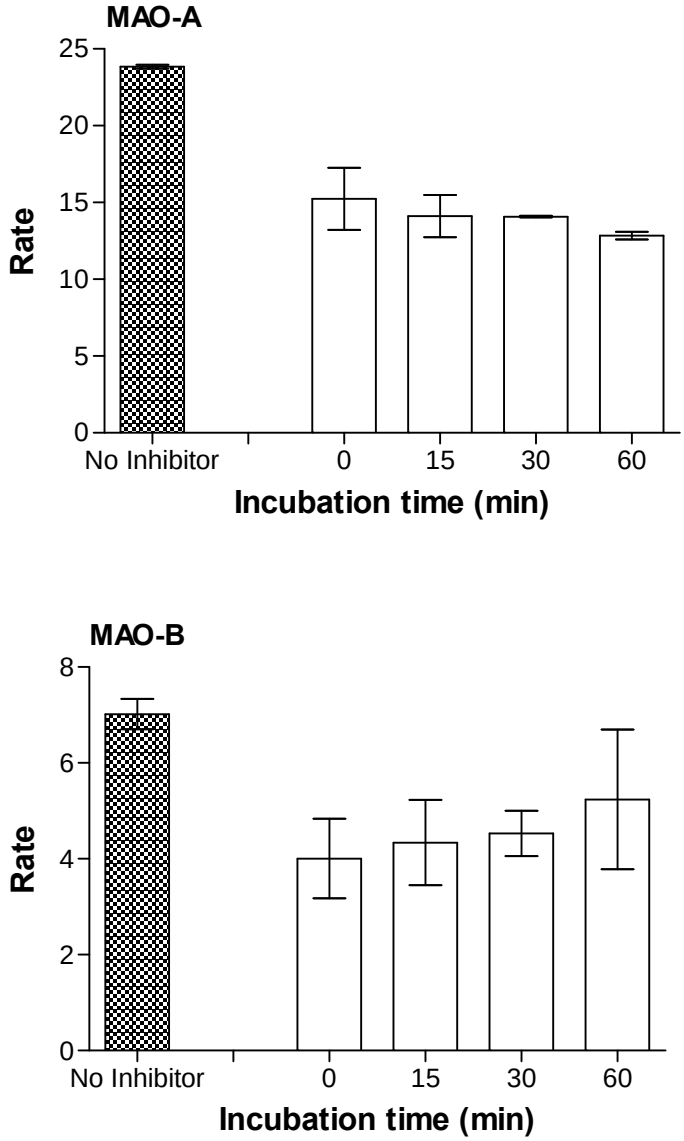

Figure 3. Time-dependent inhibition of recombinant human MAO-A and ï B by **3f**. The enzymes were preincubated for various periods of time (0ï 60 min) with **3f** at concentrations of 5.22 µM and 0.32 µM for MAO-A and ï B, respectively. The concentrations of the enzyme substrate, kynuramine, were 45 and 30 µM for the studies with MAO-A and MAO-B, respectively, and the enzyme concentrations were 0.015 mg/mL. The catalytic rates are expressed as nmoles 4-hydroxyquinoline formed/min/mg protein.

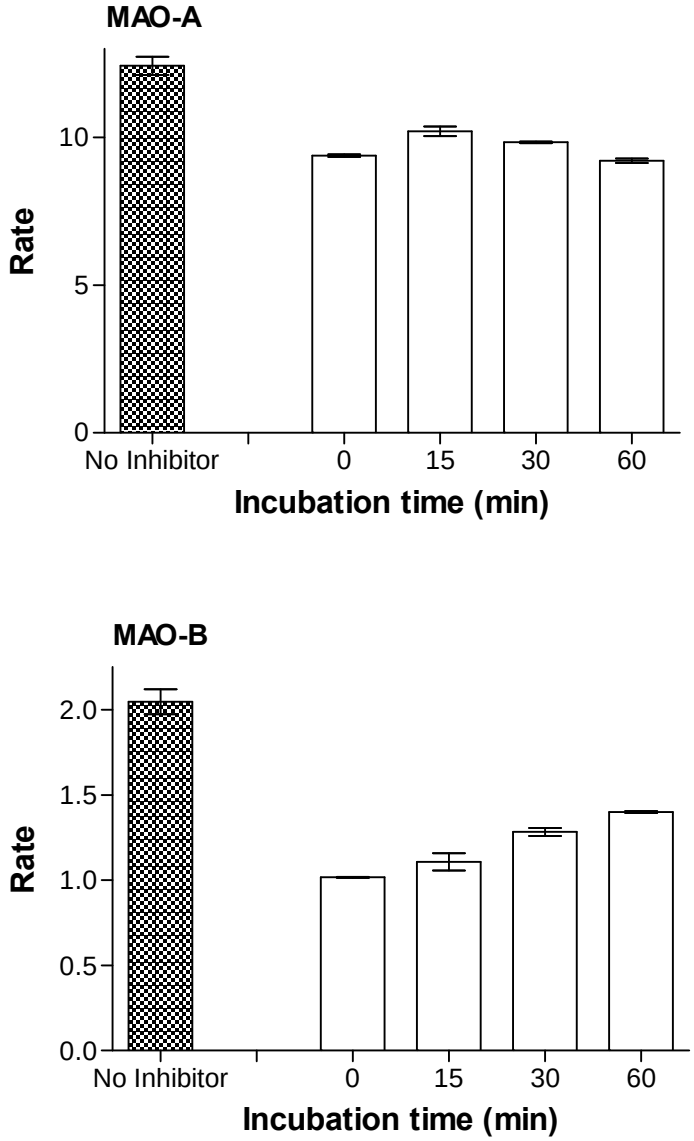

Figure 4. Time-dependent inhibition of recombinant human MAO-A and ï B by **4g** and **5b**, respectively. The enzymes were preincubated for various periods of time (0ï 60 min) with **4g** (MAO-A) and **5b** (MAO-B) at concentrations of 11.56 µM and 5.94 µM, respectively. The concentrations of the enzyme substrate, kynuramine, were 45 and 30 µM for the studies with MAO-A and MAO-B, respectively, and the enzyme concentrations were 0.0075 mg/mL. The catalytic rates are expressed as nmoles 4-hydroxyquinoline formed/min/mg protein.

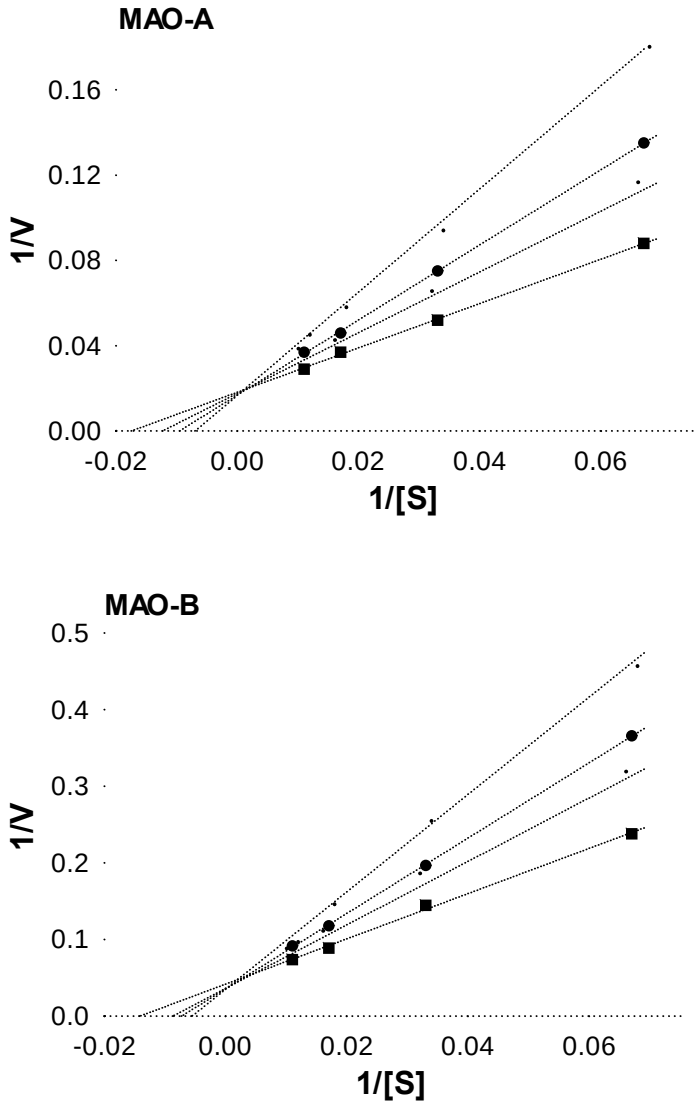

Figure 5. Lineweaver-Burk plots of the recombinant human MAO-A and ï B catalyzed oxidation of kynuramine in the absence (filled squares) and presence of various concentrations of **3f**. For the studies with MAO-A the concentrations of **3f** were: 1.31 µM (open squares), 2.61 µM (filled circles), 5.22 µM (open circles). For the studies with MAO-B the concentrations of **3f** were: 0.04 µM (open squares), 0.08 µM (filled circles), 0.16 µM (open circles).The rates (V) are expressed as nmol product formed/min/mg protein.

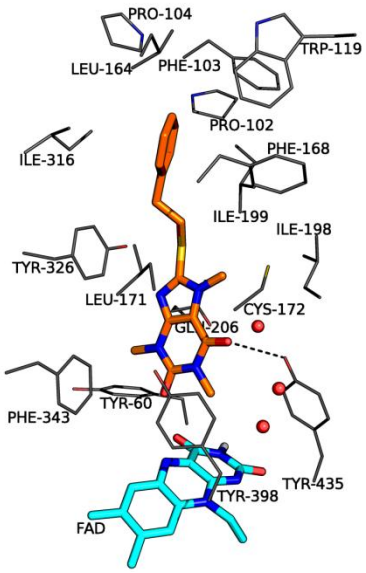

Figure 6. The predicted binding orientation of **3c** (orange) in the MAO-B active site.

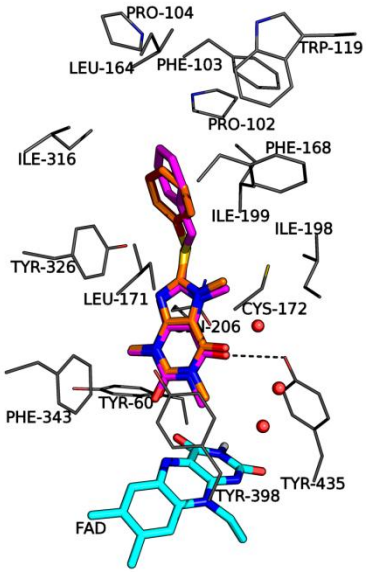

Figure 7. The predicted binding orientations of **3a** (orange) and **3b** (magenta) in the MAO-B active site.

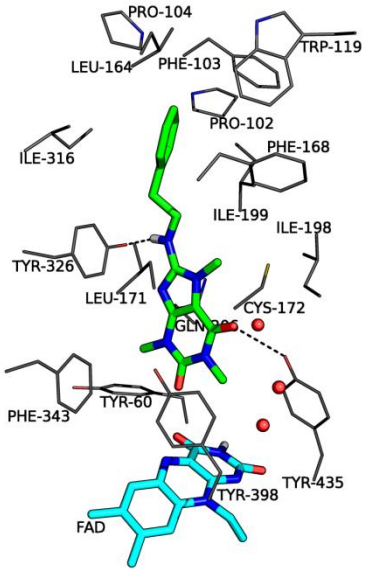

Figure 8. The predicted binding orientation of **4c** (green) in the MAO-B active site.

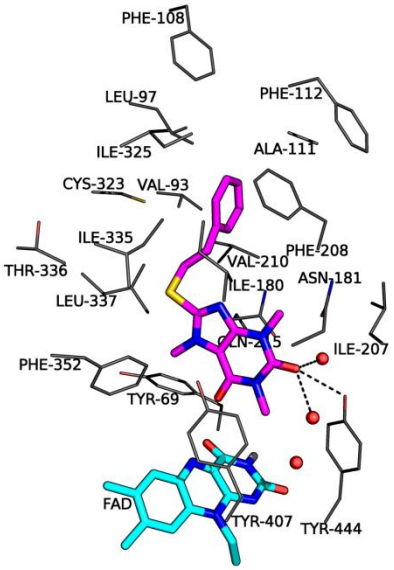

Figure 9. The predicted binding orientation of **3c** (magenta) in the MAO-A active site.

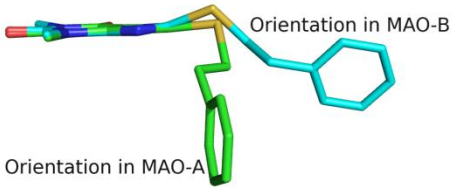

Figure 10. The predicted binding orientations of **3c** within the active sites of MAO-A (green) and MAO-B (cyan) with the caffeine moieties of the respective orientations overlaid.

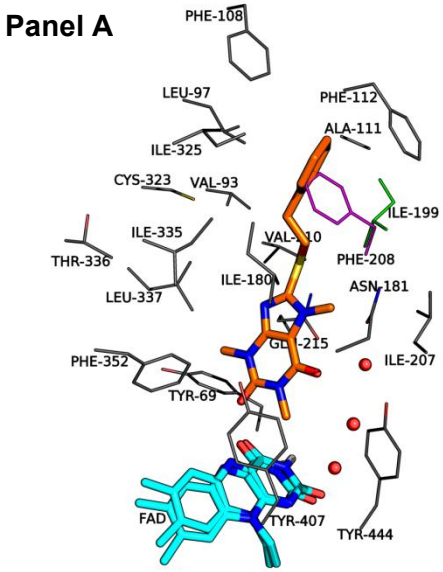

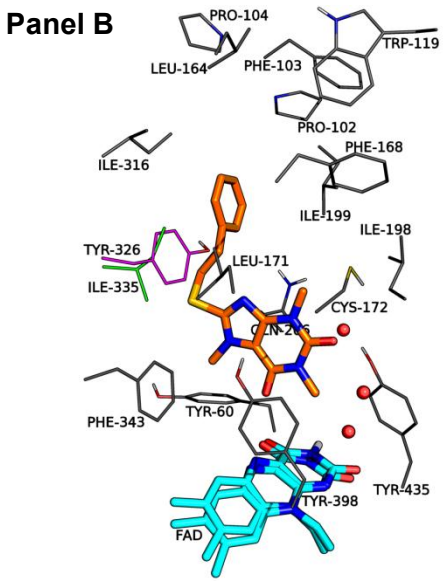

Figure 11. Illustrations of the overlaid active sites of human MAO-A and ï B. Panel A: The predicted binding orientation of **3c** as docked within the active site of MAO-B is shown in the MAO-A active site. The active site residues of MAO-A are displayed in gray with Phe-208 in magenta while residue Ile-199 in MAO-B is displayed in green. Panel B: The predicted binding orientation of **3c** as docked within the active site of MAO-A is shown in the MAO-B active site. The active site residues of MAO-B are displayed in gray with Tyr-326 in magenta while residue Ile-325 in MAO-A is displayed in green.

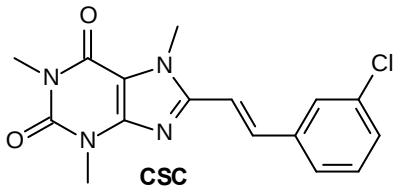

Figure 12. The structure of (E)-8-(3-chlorostyryl)caffeine (CSC).

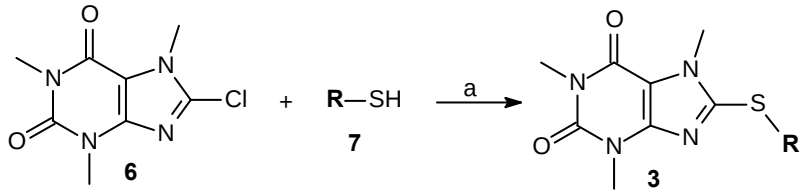

Scheme 1. Synthetic pathway to sulfanylcaffeine analogues (**3**). Reagents and conditions: (a) NaOH, H_2O/ethanol, reflux.

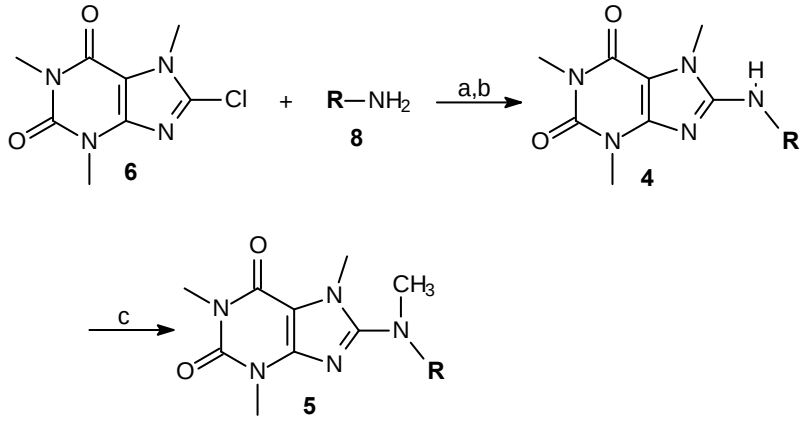

Scheme 2. Synthetic pathway to aminocaffeine analogues (**4** and **5**). Reagents and conditions: (a) reflux; (b) acetic acid; (c) KOH, DMSO, CH_3I.

Acknowledgements

- To my Heavenly Father, thank you for all the blessings and unconditional love.
- Prof. J.P. Petzer, thank you for all your knowledge and wisdom.
- Prof. J.J. Bergh, thank you for all your advice and guidance.
- Mari and Walter, thank you for all your love and support during all the good and difficult times.
- To all my friends, thank you for all the good times and fond memories.